

# **UNIVERSIDAD DE CÓRDOBA**

**Programa de doctorado:** Química Fina

**Título de la tesis (español e inglés):**

**SÍNTESIS DE NANOPARTICULAS ASISTIDA POR MICROONDAS  
EN CONDICIONES BATCH**

**MICROWAVE-ASSISTED SYNTHESIS OF NANOCATALYSTS IN  
BATCH CONDITIONS**

**Director/Directores:**

Rafael Luque Álvarez de Sotomayor

Alina M. Balu Balu

**Autor de la tesis:**

Alessio Zuliani

**Fecha de depósito tesis en el Idep: 14 de noviembre de 2019**

TITULO: *MICROWAVE-ASSISTED SYNTHESIS OF NANOCATALYSTS IN  
BATCH CONDITIONS*

AUTOR: *Alessio Zuliani*

---

© Edita: UCOPress. 2020  
Campus de Rabanales  
Ctra. Nacional IV, Km. 396 A  
14071 Córdoba

[https://www.uco.es/ucopress/index.php/es/  
ucopress@uco.es](https://www.uco.es/ucopress/index.php/es/ucopress@uco.es)

---



**TÍTULO DE LA TESIS:**

**MICROWAVE-ASSISTED SYNTHESIS OF NANOCATALYSTS IN BATCH CONDITIONS**

**SÍNTESIS DE NANOPARTICULAS ASISTIDA POR MICROONDAS EN CONDICIONES BATCH**

**DOCTORANDO/A:**

**ALESSIO ZULIANI**

**INFORME RAZONADO DEL/DE LOS DIRECTOR/ES DE LA TESIS**

(se hará mención a la evolución y desarrollo de la tesis, así como a trabajos y publicaciones derivados de la misma).

La presente Memoria de Tesis Doctoral ha sido desarrollada por D. Alessio Zuliani en el marco del proyecto europeo COSMIC (European Training Network for Continuous Sonication and Microwave Reactors) MSCA-ETN-H2020 (Grant Agreement 721290). El objetivo general del proyecto COSMIC ha sido el desarrollo de tecnologías para la transición desde la química industrial tradicional a los métodos de procesos intensificados, a través de la aplicación de nuevas fuentes energéticas alternativas, en concreto el uso de la irradiación mediante ultrasonidos y microondas.

En este aspecto, el empleo de las microondas permite el desarrollo de reacciones a gran velocidad, minimizando o suprimiendo las reacciones secundarias. Además, las tecnologías de síntesis a través de la irradiación con microondas permiten el calentamiento de las reacciones sin gradientes térmicos y con una elevada eficiencia energética. Explotando estos fundamentos de las técnicas microondas, en la presente Tesis Doctoral, se ha llevado a cabo la síntesis de nuevos nano materiales basados en Ni, Ag, Au y Cu, que posteriormente han sido caracterizados con diferentes técnicas y han sido empleados en algunas reacciones catalizadas heterogéneamente de gran interés (incluyendo fotoquímica, síntesis de compuestos de química fina y síntesis de biocombustibles). Además, como objetivo específico de un futuro escalado a nivel industrial, las síntesis de los nuevos materiales, así como las diferentes aplicaciones han sido específicamente investigadas mediante procesos (simples, altamente reproducibles y rápidos) de bajo impacto ambiental.

Como resultado principal de las investigaciones realizadas y demostrando la calidad de estas, se han publicados tres artículos, con D. Alessio Zuliani como primero autor, en revistas del primer cuartil (Q1) del "Journal Citations Reports". Además, el trabajo derivado de la presente Tesis Doctoral ha sido publicado en otros artículos, incluyendo dos reviews, cinco artículos experimentales y un capítulo de un libro. Siendo el intercambio y la comunicación puntos fundamentales del proyecto COSMIC, D. Alessio Zuliani ha conseguido realizar tres estancias en el extranjero (dos meses en KU Leuven-Bélgica, un mes en Microinnova GmbH-Austria y tres meses en la Universidad de Turin-Italia y ha participado a ocho (8) conferencias internacionales.

Las publicaciones incluidas como compendio de la presente Tesis Doctoral son:

**Título:** Microwave-assisted valorization of pig bristles: towards visible light photocatalytic chalcocite composites

**Autores (p.o. de firma):** A. Zuliani, M.J. Muñoz-Batista, R. Luque

**Revista (año vol.,pág.):** Green Chemistry, 2018, 20, 3001-3007

**Base de Datos Internacional o Nacional (caso de CC.JJ., CC.SS. Y Humanidades) en las que está indexada:** SCI

**Área temática en la Base de Datos de referencia:** Chemistry, multidisciplinary / Green & Sustainable Science & Technology

**Índice de impacto de la revista en el año de publicación del Artículo:** (2018) 9.405

**Lugar que ocupa/Nº de revistas del Área temática:** 20/172 (Q1) / 2/35 (Q1)

**Título:** Heterogeneously Catalyzed Synthesis of Imidazolones via Cycloisomerizations of Propargylic Ureas Using Ag and Au/Al SBA-15 Systems

**Autores (p.o. de firma):** A. Zuliani, P. Ranjan, R. Luque, E. V. Van der Eycken

**Revista (año vol.,pág.):** ACS Sustainable Chemistry & Engineering, 2019, 7 (5), 5568-5575

**Base de Datos Internacional o Nacional (caso de CC.JJ., CC.SS. Y Humanidades) en las que está indexada:** SCI

**Área temática en la Base de Datos de referencia:** Chemistry, multidisciplinary / Green & Sustainable Science & Technology

**Índice de impacto de la revista en el año de publicación del Artículo:** (año de publicación 2019, todavía privo de índice de impacto, el índice de impacto se refiere al 2018) 6.970

**Lugar que ocupa/Nº de revistas del Área temática:** 26/172 (Q1) / 5/35 (Q1)

**Título:** Efficient and Environmentally Friendly Microwave-Assisted Synthesis of Catalytically Active Magnetic Metallic Ni Nanoparticles

**Autores (p.o. de firma):** A. Zuliani, A. M. Balu, R. Luque

**Revista (año vol.,pág.):** ACS Sustainable Chemistry & Engineering, 2017, 5 (12), 11584-11587

**Base de Datos Internacional o Nacional (caso de CC.JJ., CC.SS. Y Humanidades) en las que está indexada:** SCI

**Área temática en la Base de Datos de referencia:** Chemistry, multidisciplinary / Green & Sustainable Science & Technology

**Índice de impacto de la revista en el año de publicación del Artículo:** (2017) 6.140

**Lugar que ocupa/Nº de revistas del Área temática:** 29/171 (Q1) / 5/33 (Q1)

Por todo ello, se autoriza la presentación de la tesis doctoral.

Córdoba, 8 de Noviembre de 2019

Firma del/de los director/es

Fdo.: Rafael Luque Álvarez de Sotomayor

Fdo.: Alina M. Balu Balu





*“...On bended knee is no way to be free  
Lifting up an empty cup I ask silently  
That all my destinations will accept the one that's me  
So I can breathe...”*

*Eddie Vedder, Guaranteed 2007*

*Alla mia sposa Camilla,  
al nostro angioletto  
e a Gioele.*







Departamento de Química Orgánica  
Facultad de Ciencias  
Universidad de Córdoba  
*Grupo FQM-383*



## Doctoral Thesis

# MICROWAVE-ASSISTED SYNTHESIS OF NANOCATALYSTS IN BATCH CONDITIONS



### Supervisors

Prof. Rafael Luque Álvarez de Sotomayor

Prof. Alina M. Balu Balu

### PhD Candidate

Alessio Zuliani





This project has received funding from the European Union's EU  
Framework Programme for Research and Innovation Horizon 2020  
under Grant Agreement  
No 721290





# Contents



<b>Preface</b> .....	<b>1</b>
<b>Introduction</b> .....	<b>9</b>
A glance at the PhD Project .....	11
<b>Microwave Chemistry and Nanomaterials</b> .....	<b>17</b>
A frequencies story: the evolution of microwave technology .....	21
On the wave: basic physical principles of micro(electromagnetic)waves .....	24
<i>Generating microwaves</i> .....	24
<i>Microwave heating</i> .....	31
<i>Dielectric properties</i> .....	33
<i>Microwave thermal effects</i> .....	35
Small, smaller and smallest: (state of) the art of nanocatalysis .....	37
<i>The power of light: some of the last achievements in photochemistry</i> .....	39
<i>Until perfection: recent studies in the synthesis of fine chemical</i> .....	41
<i>Full throttle: "Advances in nanocatalysts design for biofuels production"</i> .....	43
<b>Hypothesis and Objectives</b> .....	<b>85</b>
<b>Results and Discussion</b> .....	<b>93</b>
Microwave-assisted valorization of pig bristles: towards visible light photocatalytic chalcocite composites .....	95
<i>Supporting Information</i> .....	113
Heterogeneously catalyzed synthesis of imidazolones <i>via</i> cycloisomerizations of propargylic ureas using Ag and Au/Al SBA-15 systems .....	117
<i>Supporting Information</i> .....	138
Efficient and environmentally friendly microwave-assisted synthesis of catalytically active magnetic metallic Ni nanoparticles .....	141
<i>Supporting Information</i> .....	152
<b>Conclusions and perspectives</b> .....	<b>157</b>

<b>Summary .....</b>	<b>161</b>
English .....	163
Spanish .....	167
<b>Index of Quality .....</b>	<b>171</b>
<b>Achievements .....</b>	<b>177</b>
<i>Publications</i> .....	179
<i>Other dissemination/communication activities</i> .....	180
<i>Congress participation</i> .....	180
<i>Secondments</i> .....	181
<b>Acknowledgments .....</b>	<b>183</b>
<b>Annex I: Materials and Methods .....</b>	<b>189</b>
Characterization .....	191
<i>XRD</i> .....	191
<i>Surface area and porosity measurements (BET)</i> .....	194
<i>SEM-EDS and TEM</i> .....	197
<i>GC and GC-MS</i> .....	199
<i>UV-Vis</i> .....	200
<i>NMR</i> .....	201
Microwave-assisted methods .....	203
Pro II software .....	205
Photocatalytic activity .....	205
<b>Annex II: Articles Permissions .....</b>	<b>207</b>





# Preface



The PhD thesis herein described has been funded with a Marie Skłodowska-Curie Actions (MSCAs) award. MSCAs were established in 1996 by the European Commission as tools to fund research in the European Research Area (ERA).<sup>1</sup> MSCAs offer fellowships for all phases of researchers' careers (PhDs or early stage researchers), encouraging international, interdisciplinary and intersectoral mobility. Through MSCAs, different organizations (universities, companies as well as academic and non-academic research centres) can host brilliant foreign researcher (who has lived less than 12 months in the hosting country in the last 3 years before starting the action), creating networking and partnerships with the principal institutions in the EU and all over the World. The Actions responds to innovative and actual challenges of the modern World in different fields (from natural science to history and marketing), being among the highest attractive grants in Europe. Since 1996, more than 100,000 researchers have been awarded with a MSCAs fellowship.<sup>2</sup>

MSCAs are dedicated to Marie Skłodowska-Curie, one of the most talented scientist of Europe. Born in Warsaw (Poland) as Maria Skłodowska on the 7<sup>th</sup> of November 1867 from a married couple of teachers, Maria proved to be an enthusiastic kid and was an excellent student at school. She loved learning and studying. Lamentably, women weren't allowed to attend University at that time in Poland. Therefore, Maria decided to study abroad, but she needed money. In 1885 she made a deal with her sister Bronya. Maria would have worked to help paying Bronya's medical studies. In turn, when Bronya was a doctor, she would have paid for Maria's education. After six years working as governess, and after Bronya got her degree, in 1891 Marie (as she signed herself at the registration at the University) became a student at the Sorbonne University in Paris, being one of the 23 women of around 1,800 total undergraduates. In 1893 she obtained a degree in Physics and just after one year she got a degree also in Maths. In 1894 she met Pierre Curie, a scientist and college professor and she married him one year later. In 1897 Marie Curie gave birth to Irene, her first daughter, and in the same year she started studying uranium, coining the term "radioactive" to define any substance "giving off" or "spreading" rays. She also started studying a mineral named "pitchblende", which she found to be much more radioactive than pure uranium. In 1898 Marie and Pierre isolated polonium, but still they were sure that there was another radioactive element in pitchblende. In fact, in 1902 they isolated radium. In 1903 Marie and Pierre Curie received

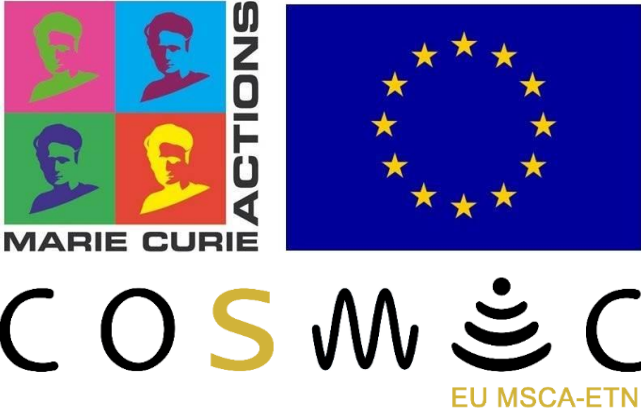
together the Nobel Prize for Physics. A few months later, in 1904, Marie Curie gave birth to her second daughter, Eve. A couple of years later, Pierre died in an accident. Despite the shock for her loss, Marie continued working and studying. As a result, Marie Curie was awarded with the Nobel Prize for Chemistry in 1911, being the first person, and the only woman, awarded with two Nobel prizes (followed by only other three persons, up to date). In her last decade of life, her health was rapidly failing due to the exposition to radiations (still not known to be harming) and she was diagnosed with leukaemia. Marie Skłodowska-Curie died on the 4<sup>th</sup> of July 1934, at the age of 66.<sup>3</sup>

The PhD thesis here described has been elaborated as outcome of one of the fifteen individual projects belonging to the MSCA EU-H2020 COSMIC, the European Training Network (ETN) for Continuous Sonication and Microwave Reactors (Grant Agreement No 721290).<sup>4</sup> More in details, the COSMIC Project, a four years project started in October 2016, aimed to provide support and trainings to the chemical industry in the transition from batch to intensified processes. This transition has been proved to be essential in order to stop the decline of the European share of the global chemical market (from ~31 % in 1996 to ~15 % in 2015) and the employment of the EU citizens in this sector (collapsed from 1.60 million in 1996 to 1.15 million in 2013).<sup>5, 6</sup>

The intensification of the chemical processes, though the development of competitive technologies, could in fact overpass the lower-labour-cost markets in the emerging global economies (*e.g.*, Asia and the Near East), and give a boost to the EU chemicals production.<sup>7</sup> Remarkably, nowadays the technologies in the chemical sector tend to be batch-type, combined with mechanical mixing and conduction-based heat transfer, inherently leading to serious drawbacks including: excessive energy consumption (limiting the heat transfer into the reactor as well as the mass transfer of undesired by-products from the bulk and the consumption of excessive amounts of energy); variable product quality (influencing the rate and the yield of the chemical reactions and leading to increased by-product formation and/or reductions in selectivity); limited scale-up; poor efficiency; high emissions and limited flexibility.<sup>8</sup> Furthermore, the operations with large volumes requires extra unit processes that must be scaled throughout the entire plant assembly, resulting in a huge land-usage footprint and increased emissions of waste heat, greenhouse gases and volatile organic compounds (VOCs, mostly due to purification and cleaning operations).<sup>9</sup>

The propose of COSMIC consisted in the development of innovative processes bringing together three advanced areas in the field of process technology: flow chemistry, millifluidics and alternative energy sources, *i.e.* microwaves (MWs) and ultrasounds (US). Ultrasound and microwaves have been chosen as the alternative energy sources due to their different, but complementary, actions: while US affects mass transfer and mixing, microwaves affect heat transfer.<sup>10</sup> These non-conventional, non-contact energy sources create the possibility for new process as a result of the additional actuation of the chemical reactions *via* intensified mass and heat transfer, mixing and/or reaction activation. Some examples include the use of ultrasound to prevent clogging where the chemistry involves solids,<sup>11</sup> as well as the use of microwaves to focus on the heat transfer on metal-containing catalytic particles.<sup>12</sup> In the past decade, these alternative energy sources have been pointed as key methods with the potential to intensify chemicals synthesis in terms of energy and resource efficiency.<sup>13-16</sup> However, despite their great potential, only a few relevant applications (in term of possible industrial applicability) have been demonstrated so far.<sup>17-20</sup> COSMIC focused on the synthesis of organic molecules and nanoparticles for use in organic synthesis, catalyst preparation and health applications, through microwave and ultrasound assisted techniques, aiming to the potential industrial applicability. A truly innovative challenge in the field. The PhD thesis here presented specifically aimed at the application of microwaves to the synthesis of heterogeneous catalysts and particles in the size range of nanometres. Remarkably, some of the prepared catalysts were used by other researchers in the network of COSMIC. Specifically, the nanocatalysts were also employed in organic synthesis reactions carried out using ultrasound and microwaves, in both batch and flow conditions.

The COSMIC Project brought together a networking of institutes from seven EU countries, including seven Universities and four companies. Specifically, KU Leuven (Belgium), the UCL (London), the University of Turin (Italy), the University of Cordoba (Spain), the University of Zaragoza (Spain), the University of Göttingen (Germany) and the Universitat Politècnica de València (Spain) were the involved academic institutes. Arkema (France), Weber Ultrasonics (Belgium) Microinnova GmbH (Austria) and MEAM (Belgium) were the involved companies. A total of fifteen high-potential ESRs (Early Stage Researchers) of eight different nationalities were trained during COSMIC ETN, developing fifteen different projects.



1. <https://ec.europa.eu/research/mariecurieactions/>
2. [https://ec.europa.eu/research/mariecurieactions/news/marie-sklodowska-curie-actions-award-one-hundred-thousandth-fellowship\\_en](https://ec.europa.eu/research/mariecurieactions/news/marie-sklodowska-curie-actions-award-one-hundred-thousandth-fellowship_en)
3. Venezia, M., *Marie Curie: Scientist Who Made Glowing Discoveries*. Scholastic: New York, 2009.
4. <https://cosmic-etn.eu>
5. [https://ec.europa.eu/growth/sectors/chemicals\\_nl](https://ec.europa.eu/growth/sectors/chemicals_nl)
6. <https://www.chemlandscape.cefic.org/country/eu/>
7. Grutzner, T.; Schnider, C.; Zollinger, D.; Seyfang, B. C.; Kunzle, N., Reducing Time to Market by Innovative Development and Production Strategies. *Chemical Engineering & Technology* **2016**, *39* (10), 1835-1844.
8. Calabrese, G. S.; Pissavini, S., From Batch to Continuous Flow Processing in Chemicals Manufacturing. *Aiche Journal* **2011**, *57* (4), 828-834.
9. Klemes, J.; Huisingh, D., Economic use of renewable resources, LCA, cleaner batch processes and minimising emissions and wastewater. *Journal of Cleaner Production* **2008**, *16* (2), 159-163.
10. Peng, Y. Q.; Song, G. H.; Dou, R. L., Surface cleaning under combined microwave and ultrasound irradiation: flash synthesis of 4H-pyrano 2,3-c pyrazoles in aqueous media. *Green Chemistry* **2006**, *8* (6), 573-575.
11. Zhang, L.; Geng, M.; Teng, P.; Zhao, D.; Lu, X.; Li, J. X., Ultrasound-promoted intramolecular direct arylation in a capillary flow microreactor. *Ultrasonics Sonochemistry* **2012**, *19* (2), 250-256.
12. Mishra, R. R.; Sharma, A. K., Microwave-material interaction phenomena: Heating mechanisms, challenges and opportunities in material processing. *Composites Part a-Applied Science and Manufacturing* **2016**, *81*, 78-97.
13. Baxendale, I. R.; Hayward, J. J.; Ley, S. V., Microwave reactions under continuous flow conditions. *Combinatorial Chemistry & High Throughput Screening* **2007**, *10* (10), 802-836.
14. Meullemiestre, A.; Breil, C.; Abert-Vian, M.; Chemat, F., Microwave, ultrasound, thermal treatments, and bead milling as intensification techniques for extraction of lipids from oleaginous *Yarrowia lipolytica* yeast for a biojetfuel application. *Bioresource Technology* **2016**, *211*, 190-199.
15. Kumar, V.; Nigam, K. D. P., Process intensification in green synthesis. *Green Processing and Synthesis* **2012**, *1* (1), 79-107.
16. Cintas, P.; Tagliapietra, S.; Gaudino, E. C.; Palmisano, G.; Cravotto, G., Glycerol: a solvent and a building block of choice for microwave and ultrasound irradiation procedures. *Green Chemistry* **2014**, *16* (3), 1056-1065.
17. Leonelli, C.; Mason, T. J., Microwave and ultrasonic processing: Now a realistic option for industry. *Chemical Engineering and Processing-Process Intensification* **2010**, *49* (9), 885-900.
18. Cintas, P.; Mantegna, S.; Gaudino, E. C.; Cravotto, G., A new pilot flow reactor for high-intensity ultrasound irradiation. Application to the synthesis of biodiesel. *Ultrasonics Sonochemistry* **2010**, *17* (6), 985-989.
19. Lehmann, H.; LaVecchia, L., Scale-Up of Organic Reactions in a Pharmaceutical Kilo-Lab Using a Commercial Microwave Reactor. *Organic Process Research & Development* **2010**, *14* (3), 650-656.
20. Beneroso, D.; Monti, T.; Kostas, E. T.; Robinson, J., Microwave pyrolysis of biomass for bio-oil production: Scalable processing concepts. *Chemical Engineering Journal* **2017**, *316*, 481-498.







# Introduction



## A glance at the PhD Project

The PhD thesis here presented focuses on the development of novel methods for the preparation of nanodimensional catalysts through microwave irradiation in batch conditions. While the utilization of microwaves responded to the necessity of the process intensification in the chemical industry, the nanocatalysts were selected due to their unique heterogeneous-homogeneous characteristics.

According to Colin Ramshaw, Process intensification (PI) is definable as a methodology for making significant reductions in equipment size, energy consumption and waste generation while increasing cleanness and safety of a given production goal.<sup>1,2</sup> Furthermore, PI decreases the manufacturing costs, therefore enhancing, due to lower production expenses, the market attractiveness of the final products.<sup>3-6</sup> As a consequence, the development of techniques for the PI is strategically of primary importance for chemical companies.<sup>7</sup>

One winning tool for the PI is the exploitation of microwave technologies.<sup>8,9</sup> More in details, thanks to the deep studies aimed at exploring the mechanism of actions of microwaves over different materials, microwave-assisted techniques have spread from the original application as simple alternative heating method in our kitchens, to a large variety of innovative processes. These include, for example, the extraction of natural compounds, the synthesis of composites and nanodimensional materials, and catalytic reactions.<sup>10-13</sup>

The use of microwaves for the preparation of nanocatalysts has particularly emerged for the rapid and clean characteristics in contrast with conventional heating treatments.<sup>14-17</sup>

Nanocatalysts, therefore catalysts having nanodimensional size (1-100 nm\*),<sup>18-</sup><sup>21</sup> have been used in catalysis since the 19<sup>th</sup> century.<sup>22</sup> Being at the frontier between

---

\* Establish an unambiguous definition of nanoparticles may be somehow controversial. In general, the literature reports as "nanoparticle" a substance having at least one dimension between 1 and 100 nm, or "on the order of ~100 nm". According to the EU Commission, "Nanomaterial" means: "A natural, incidental or manufactured material containing particles, in an unbound state or as an aggregate or as an agglomerate and where, for 50 % or more of the particles in the number size distribution, one or more external dimensions is in the size range 1 nm - 100 nm". Also the International Organization for Standardization (ISO) gave a similar definition, indicating

homogeneous and heterogeneous systems, nanodimensional catalysts bring together high efficiency and selectivity with recovery and recyclability characteristics.<sup>23, 24</sup> Most diffused methods for the preparation of nanocatalysts comprise the use of a metal precursor, usually a salt, an oxidizing or reducing agents (e.g. NaBH<sub>4</sub>), a stabilizer (PVP, ethylene glycol, etc.) and, in most of the cases, a supporting material (oxides, zeolites, charcoal, polymers, etc.).<sup>25</sup> Nanocatalysts have been successfully employed in cross-coupling reactions, oxidations, hydrogenations, electron-transfer reactions, electrochemical cells, and numerous others applications.<sup>26-34</sup>

As outcome of the PhD thesis, three published research articles demonstrated the efficacy of microwave-assisted techniques for the preparation of catalytically active nanoparticles. The first paper describes the MW-assisted preparation of photocatalytically active copper sulphides nanoparticles-carbon composite. The novel compound was used to achieve the photodegradation of methyl red, a common pollutant dye, under visible light irradiation. The second article shows the microwave-assisted preparation of gold and silver nanoparticles supported over mesoporous silica (AISBA-15) in comparison with the same material prepared *via* a mechanochemical approach. The nanocatalysts were used to catalyse the microwave-assisted cyclization of propargyl ureas, an important reaction for the fine chemical industry. The third article discloses the preparation of pure nickel nanoparticles *via* a quick and environmentally friendly microwave-assisted technique. The so-produced particles were employed in the microwave-assisted hydrogenolysis of benzylphenylether (BPE), a lignin structure compound, as model reaction for bio-combustible production.

In order to contextualize these research articles, the first chapter of the Thesis reports fundamental concepts and last achievements of microwave chemistry and nanocatalysis. More in details, the first part of the chapter describes notions of microwave chemistry. The second part of the chapter discusses recent works on nanocatalysis, with special attention to the fields of applications reported in the research articles. Specifically, an overview of recent progresses of nanocatalysis in photochemistry,

---

as "nanoparticle" "a nano-object with all three external dimensions in the nanoscale, which is approximately 1 to 100 nm". However, some other research articles, defined as "nanoparticles" materials having at least one dimension below 1 µm. As a result, the wider definition of nanoparticles as "a substance in the 1-1,000 nm order", published in the book "*Nanoparticles' Promises and Risks*" edited by Springer (2014, Basel) may be also accepted.

synthesis of fine chemical and biofuels production is reported. In order to highlight the importance of nanocatalysts for the production of biofuel, this last argument is described with a comprehensive minireview.<sup>†35, 36</sup>

---

<sup>†</sup> According to the production volumes of a petroleum refinery, it should be mentioned that the ideal biorefinery must direct ~95% of production to biofuels, and only ~5% to fine chemical products. Therefore, nanocatalysts for biofuel production are of particular interest and deserve a deeper discussion.

1. Ramshaw, C., Process intensification and Green Chemistry. *Green Chemistry* **1999**, *1* (1), 15-17.
2. Reay, D.; Ramshaw, C.; Harvey, A., Process Intensification: Engineering for Efficiency, Sustainability and Flexibility. *Process Intensification: Engineering for Efficiency, Sustainability and Flexibility* **2008**, 1-444.
3. Green, A., Process intensification: the key to survival in global markets? *Chemistry & Industry* **1998**, (5), 168-172.
4. Charpentier, J. C., In the frame of globalization and sustainability, process intensification, a path to the future of chemical and process engineering (molecules into money). *Chemical Engineering Journal* **2007**, *134* (1-3), 84-92.
5. Charpentier, J. C., Among the trends for a modern chemical engineering, the third paradigm: The time and length multiscale approach as an efficient tool for process intensification and product design and engineering. *Chemical Engineering Research & Design* **2010**, *88* (3A), 248-254.
6. Ott, D.; Kralisch, D.; Dencic, I.; Hessel, V.; Laribi, Y.; Perrichon, P. D.; Berguerand, C.; Kiwi-Minsker, L.; Loeb, P., Life Cycle Analysis within Pharmaceutical Process Optimization and Intensification: Case Study of Active Pharmaceutical Ingredient Production. *Chemsuschem* **2014**, *7* (12), 3521-3533.
7. Becht, S.; Franke, R.; Geisselmann, A.; Hahn, H., An industrial view of process intensification. *Chemical Engineering and Processing-Process Intensification* **2009**, *48* (1), 329-332.
8. Kumar, V.; Nigam, K. D. P., Process intensification in green synthesis. *Green Processing and Synthesis* **2012**, *1* (1), 79-107.
9. Martin, A.; Navarrete, A., Microwave-assisted process intensification techniques. *Current Opinion in Green and Sustainable Chemistry* **2018**, *11*, 70-75.
10. Lidstrom, P.; Tierney, J.; Wathey, B.; Westman, J., Microwave assisted organic synthesis - a review. *Tetrahedron* **2001**, *57* (45), 9225-9283.
11. Kappe, C. O.; Stadler, A., Microwaves in Organic and Medicinal Chemistry. *Microwaves in Organic and Medicinal Chemistry* **2005**, *52*, 1-409.
12. Kappe, C. O., Microwave dielectric heating in synthetic organic chemistry. *Chemical Society Reviews* **2008**, *37* (6), 1127-1139.
13. Kokel, A.; Schafer, C.; Torok, B., Application of microwave-assisted heterogeneous catalysis in sustainable synthesis design. *Green Chemistry* **2017**, *19* (16), 3729-3751.
14. Amin, R. S.; Elzatahry, A. A.; El-Khatib, K. M.; Youssef, M. E., Nanocatalysts Prepared by Microwave and Impregnation Methods for Fuel Cell Application. *International Journal of Electrochemical Science* **2011**, *6* (10), 4572-4580.
15. Alosfur, F. K. M.; Jumali, M. H. H.; Radiman, S.; Ridha, N. J.; Yarmo, M. A.; Umar, A. A., Modified microwave method for the synthesis of visible light-responsive TiO<sub>2</sub>/MWCNTs nanocatalysts. *Nanoscale Research Letters* **2013**, *8*.
16. Joseph, S.; Mathew, B., Microwave assisted facile green synthesis of silver and gold nanocatalysts using the leaf extract of *Aerva lanata*. *Spectrochimica Acta Part A-Molecular and Biomolecular Spectroscopy* **2015**, *136*, 1371-1379.
17. Li, A. Y.; Kaushik, M.; Li, C. J.; Moores, A., Microwave-Assisted Synthesis of Magnetic Carboxymethyl Cellulose-Embedded Ag-Fe<sub>3</sub>O<sub>4</sub> Nanocatalysts for Selective Carbonyl Hydrogenation. *ACS Sustainable Chemistry & Engineering* **2016**, *4* (3), 965-973.
18. Strambeanu, N.; Demetrovici, L.; Dragos, D.; Lungu, M., Nanoparticles: Definition, Classification and General Physical Properties. In *Nanoparticles' Promises and Risks: Characterization, Manipulation, and Potential Hazards to Humanity and the Environment*, Lungu, M.; Neculae, A.; Bunoiu, M.; Biris, C., Eds. Springer International Publishing: Cham, **2015**; pp 3-8.

19. Calzolari, L.; Gilliland, D.; Rossi, F., Measuring nanoparticles size distribution in food and consumer products: a review. *Food Additives and Contaminants Part A-Chemistry Analysis Control Exposure & Risk Assessment* **2012**, *29* (8), 1183-1193.
20. Wagner, S.; Gondikas, A.; Neubauer, E.; Hofmann, T.; von der Kammer, F., Spot the Difference: Engineered and Natural Nanoparticles in the Environment-Release, Behavior, and Fate. *Angewandte Chemie-International Edition* **2014**, *53* (46), 12398-12419.
21. [https://ec.europa.eu/environment/chemicals/nanotech/faq/definition\\_en.htm](https://ec.europa.eu/environment/chemicals/nanotech/faq/definition_en.htm)
22. Rampino, L. D.; Nord, F. F., Preparation of palladium and platinum synthetic high polymer catalysts and the relationship between particle size and rate of hydrogenation. *Journal of the American Chemical Society* **1941**, *63*, 2745-2749.
23. Astruc, D.; Lu, F.; Aranzaes, J. R., Nanoparticles as recyclable catalysts: The frontier between homogeneous and heterogeneous catalysis. *Angewandte Chemie-International Edition* **2005**, *44* (48), 7852-7872.
24. Somorjai, G. A.; Frei, H.; Park, J. Y., Advancing the Frontiers in Nanocatalysis, Biointerfaces, and Renewable Energy Conversion by Innovations of Surface Techniques. *Journal of the American Chemical Society* **2009**, *131* (46), 16589-16605.
25. Polshettiwar, V.; Asefa, T., *Nanocatalysis Synthesis and Applications*. John Wiley & Sons, Inc.: **2013**.
26. Zhang, Q.; Fan, W.; Gao, L., Anatase TiO<sub>2</sub> nanoparticles immobilized on ZnO tetrapods as a highly efficient and easily recyclable photocatalyst. *Applied Catalysis B-Environmental* **2007**, *76* (1-2), 168-173.
27. Ding, L.; Hao, C.; Xue, Y.; Ju, H., A bio-inspired support of gold nanoparticles-chitosan nanocomposites gel for immobilization and electrochemical study of K562 leukemia cells. *Biomacromolecules* **2007**, *8* (4), 1341-1346.
28. Li, Y.; Somorjai, G. A., *Nanoscale Advances in Catalysis and Energy Applications*. *Nano Letters* **2010**, *10* (7), 2289-2295.
29. Yang, C.; Wu, J.; Hou, Y., Fe<sub>3</sub>O<sub>4</sub> nanostructures: synthesis, growth mechanism, properties and applications. *Chemical Communications* **2011**, *47* (18), 5130-5141.
30. Wang, T.; Zhu, H.; Zhuo, J.; Zhu, Z.; Papakonstantinou, P.; Lubarsky, G.; Lin, J.; Li, M., Biosensor Based on Ultrasmall MoS<sub>2</sub> Nanoparticles for Electrochemical Detection of H<sub>2</sub>O<sub>2</sub> Released by Cells at the Nanomolar Level. *Analytical Chemistry* **2013**, *85* (21), 10289-10295.
31. Dong, Z.; Le, X.; Li, X.; Zhang, W.; Dong, C.; Ma, J., Silver nanoparticles immobilized on fibrous nanosilica as highly efficient and recyclable heterogeneous catalyst for reduction of 4-nitrophenol and 2-nitroaniline. *Applied Catalysis B-Environmental* **2014**, *158*, 129-135.
32. Zhang, Y.; Xiao, J.; Sun, Y.; Wang, L.; Dong, X.; Ren, J.; He, W.; Xiao, F., Flexible nanohybrid microelectrode based on carbon fiber wrapped by gold nanoparticles decorated nitrogen doped carbon nanotube arrays: In situ electrochemical detection in live cancer cells. *Biosensors & Bioelectronics* **2018**, *100*, 453-461.
33. Muthukumar, H.; Mohammed, S. N.; Chandrasekaran, N.; Sekar, A. D.; Pugazhendhi, A.; Matheswaran, M., Effect of iron doped Zinc oxide nanoparticles coating in the anode on current generation in microbial electrochemical cells. *International Journal of Hydrogen Energy* **2019**, *44* (4), 2407-2416.
34. Didehban, K.; Vessally, E.; Hosseinian, A.; Edjlali, L.; Khosroshahi, E. S., Nanocatalysts for C-Se cross-coupling reactions. *Rsc Advances* **2018**, *8* (1), 291-301.
35. Kamm, B.; Kamm, M., Principles of biorefineries. *Applied Microbiology and Biotechnology* **2004**, *64* (2), 137-145.
36. Calvino-Casilda, V.; López-Peinado, A. J.; Martín-Aranda, R. M.; Pérez Mayoral, E., *Nanocatalysis Applications and Technologies*, Taylor & Francis Group: Boca Raton, **2019**.







# **Microwave Chemistry and Nanomaterials**



In 2000 the topic “nanoparticles” appeared in 1,935 records, while in 2018 it was found in more than 75,000 works.<sup>1</sup> This rapid growth of interest has encouraged the development of efficient, innovative, sometimes also sophisticated,<sup>2-5</sup> and environmentally friendly,<sup>6-9</sup> processes for the preparation of nanodimensional systems.<sup>10-18</sup> These numerous synthetic strategies can be divided into two main categories: top-down and bottom-up. With the approach top-down, an external force (grinding, ultrasounds, *etc.*) is applied to a solid which is smashed into smaller particles. On the other hand, with the approach bottom-up, atoms pass through atomic transformations or molecular condensations in order to produce nanoparticles (*e.g.* chemical or physical vapour deposition, thermal decomposition, sol-gel methods).<sup>19, 20</sup> In general, a process, or a tool, for the synthesis of nanoparticles, requires to satisfy a sequence of conditions, including:

- The control of particles aggregation/agglomeration
- The control of the purity of the material
- The stabilization of the physical properties of the nanoparticles
- The control of the reproducibility of the synthesis
- The control of particles size and shape and size distribution
- High mass production, scale-up and low cost

The enhancement of all these characteristics *via* the process intensification is highly attractive, as it can remuneratively respond to the incremental demand of the nanoparticles market.

Featuring reduced reaction times, minimized (or suppressed) side reactions, enhanced yields and selectivity as well as highly reproducibility, microwave-assisted techniques have emerged as outstanding tools for the process intensification.<sup>21-24</sup> In addition, several works have demonstrated the possibility to apply microwave techniques to eco-friendly processes, fulfilling ethical and legislative requests.<sup>25, 26</sup> When applied to the synthesis of nanoparticles, microwave techniques could lead to the preparation of uniform particle sizes thanks to uniform nuclear growth. On the contrary, conventional heating techniques normally implies thermal gradients throughout the bulk media (already itself an issue in scaling-up the process) affecting the nucleation of the particles and the growth rates, therefore lowering the quality of the nanoparticles.<sup>27-29</sup> Microwave

heating can also prevent the formation of a metalling coating on the reactor walls, avoiding tedious cleaning procedures.<sup>30</sup>

## A frequencies story: the evolution of microwave technology

When J. C. Maxwell published the “Treatise on Electricity and Magnetism” in 1873, establishing the mathematic principles of electromagnetism, the Scientific Community was so excited and looked forward to finding practical applications of the new theory. The enthusiasm was so high, that when Maxwell died (1879), the famous physician H. Von Helmholtz sponsored a prize for the first experimental evidence of Maxwell’s predictions. Nine years later, at the Technische Hochschule in Karlsruhe (Germany), T. Hertz could produce (and detect) microwaves (frequencies close to GHz), winning the challenge.<sup>‡</sup> Hertz used a basic transmitter equipped with a Ruhmkorff coil as high-voltage pulses generator. The coil generated a spark discharge within straight wire connections. As detector, Hertz used a ring antenna with a spark gap. When the antenna was detecting sufficient voltage, it produced visible spark, proving microwaves transmission, as illustrated in Figure 1.<sup>31</sup>

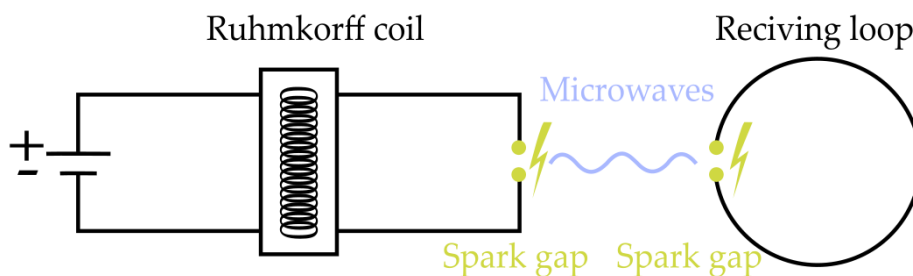


**Figure 1.** Illustration of Hertz’s experiment for the production and detection of microwaves.

Despite the importance of Hertz’s experiment, the milestone of microwaves history could be traced back to some decades later, when the magnetron, the standard generator of microwaves, was created. The term “magnetron” firstly appeared in the journal “Physical Review” in 1921, describing a vacuum tube rectifier made of two cylinders (described in the next section).<sup>32</sup> Despite visionary, the device was still too

<sup>‡</sup> According to the bibliography (Lee, T.H., *Planar Microwave Engineering*, Cambridge University Press: Cambridge, 2019), O. Lodge published his experiments proving Maxwell’s theory one month before Hertz. However, Lodge was not that lucky, and his effort was recognized only after years.

pioneering, being unstable and not very efficient. In addition, even if it could theoretically produce microwaves, it was created to investigate the behaviour of electrons between the cathode and anode in the presence of a magnetic field. Years later, the British developed the air defence system called “Chain Home”, a superior radar designed to operate at higher frequencies than standard ones, theoretically microwaves. Unfortunately, the lack of technology, in terms of both power sources and detectors, limited the operativity to high frequency range - HF (around 22 MHz incremented up to 55 MHz), and it was impossible to produce microwave radiation.<sup>33</sup> On the 21<sup>st</sup> of February 1940 at the University of Birmingham, H. Booth and J. Randall could achieve the first microwave frequency radar transmission thanks to a cavity magnetron tube (operating at 3 GHz and 500 W). A few months later, they were able to bring a radar prototype in the US, in order to reach an agreement for an industrial development. By the end of 1940, the Massachusetts Institute of Technology (MIT) funded the Radiation Laboratory, which produced more than forty prototypes within a few months of activity. Due to World War II events, despite microwave heating capability was recognized since the beginning,<sup>5</sup> communication and navigation applications for military purposes had the priority. All these efforts were well paid, as microwave radars strongly helped the Allies fighting against the Nazis, especially the Royal Air Force against the Luftwaffe. When WWII was over, Raytheon Company, a US defence contractor, published the first patent on microwave heating (1945). Not surprising, Raytheon was one of the mayor producer of magnetrons during WWII.

A couple of years later, Raytheon launched on the market the “Radarange”, the first airline microwave oven, capable of “cooking an hamburger in 30 seconds”. In 1950, again at Raytheon, P. L. Spencer developed the first domestic microwave oven prototype. A few years later, in 1965, hundreds of patents were filled on various aspects of microwave ovens (*e.g.* packaging, processes, design and techniques). Finally, during the 70’s and the 80’s, the domestic use of microwave oven spread globally, and is nowadays one of the most common electric device in our kitchens.<sup>34</sup>

---

<sup>5</sup> An anecdote/legend says that P.L. Spencer (from Raytheon) firstly noticed the microwave heating effect when a chocolate bar started melting in his pocket, while he was working nearby an active magnetron (another version substitute the chocolate bar with popcorn).

The application of microwave heating at industrial level was firstly investigated at the Department of Food Technology of the MIT. Curiously, it was the domestic use of microwaves that inspired their industrial applications. Initially, some experiments were run in order to demonstrate the possibility of microwave-assisted coffee roasting and bleaching of vegetables operating with high volumes. However, it was again at Raytheon that the first pilot plant for microwave freeze-drying was successfully started. Lately, in the beginning of 1960, Cryodry Corporation (USA) introduced to the US and European market the first industrial microwave system operating at 915 MHz. The system was studied for the final drying of potatoes during the preparation of chips. A few years later, Raytheon and Litton Industries Atherton sold systems operating at higher frequency, specifically 2459 MHz (5-10 kW). Nowadays, the market is full of professional equipment for industrial microwave-heating applications, especially for the food industry (baking, potato processing, precooking of bacon, pasta drying, *etc.*).<sup>35, 36</sup>

The first use of MWs in chemical R&D could be tracked back to the end of the 60's, in the field of polymer synthesis (drying and polymerization of an epoxy resin). A few years later, in 1972, the microwave-assisted calcination and sintering of ceramics was demonstrated. Sequentially, some studies about fundamental and application studies of microwave inorganic chemistry were published.<sup>37</sup> Finally, in 1986, R. Gedye and R. J. Giguere published two pioneering works about the use of microwave in organic synthesis.<sup>38, 39</sup> Notably, at the beginning, the application of microwaves in Chemistry increased slowly and gradually. The turning point of microwave Chemistry happened around 2000, when the number of publication started to rapidly increase, mostly due to the availability of commercial microwaves devices intended for laboratory investigation.<sup>40</sup> The new devices in fact allowed scientist to abandon domestic oven for upgraded equipment where they can control, and record, microwave output power, temperature and pressure, making microwave chemical experiments easily reproducibles.<sup>41-43</sup>

## **On the wave: basic physical principles of micro(electro-magnetic)waves**

### ***Generating microwaves***

The first magnetron was built by A. W. Hull modifying a well-known vacuum tube rectifier. At the end of XIX century, vacuum tube rectifiers were widely used to rectify alternative current, by exploiting the principles of thermionic emission (emission of electrons of a heated up material). This phenomenon of thermionic emission is quite evident in conductive materials (above all the metals) where the surface band of lightly bound electrons can easily carry current. In fact, when enough energy is applied to the surface of a conductive material, the electrons (on the surface) can be expelled. Considering the application of thermal energy, the thermionic emission could happen when a semiconductor material is heated up, *e.g.* though Joule heating, to the temperature where the average thermal energy approaches the work function. If this phenomenon occurs to filament in a vacuum tube, as shown in Figure 2-A, the tube will be filled of electrons. If two wires connected to the terminals of a battery are placed into the vacuum tube with some space between them, as shown in Figure 2-B, current could flow thanks to these electrons. Additionally, if the negative terminal of the battery is placed on the metal source of free electrons, as shown in Figure 2-C, the current will flow, but if the current is inverted (Figure 2-D), no current will flow (unless the current is extremely high). This because the electric field produced by the battery setup will attract electrons back into the filament. As a result, when the vacuum tube is applied to an alternative current source, it will act as rectifier.<sup>44</sup>

A simple improvement of this type of vacuum tube rectifier can be done by adding a conductive mesh between the filament and the anode. As a result, the current flow can be reduced, increased, or completely stopped by the additional electric field of the conductive mesh. Basically, this modified device, called triode, lets the vacuum tube rectifier work as an oscillator and amplifier.



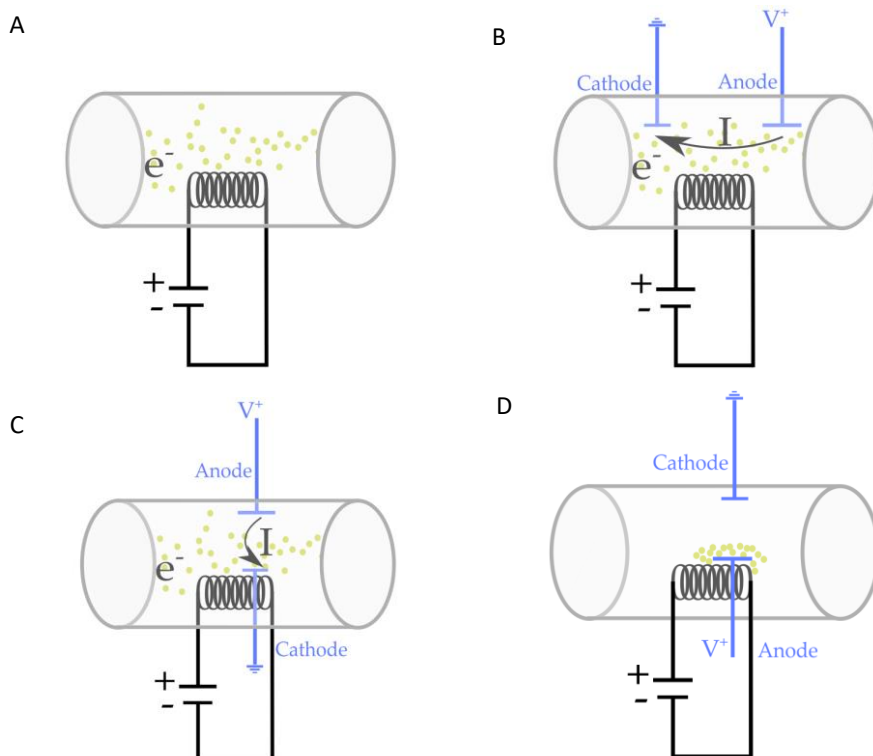


**Figure 2.** Illustrations of vacuum tube: A) filled with electrons; B) allowing the passage of electrons; C) cathode mounted on the filament; D) inverted current of case C.

Hull modified a vacuum tube triode in order to investigate the behaviour of electrons between the cathode and anode in the presence of a magnetic field. More in details, he used a thin cylinder containing the electron source filament connected to the negative terminal of a battery. He enclosed the cylinder with a coaxial cylindrical plate, connected to the positive terminal of the battery. Finally, he surrounded the cylindrical plate with a winding, capable to generate a magnetic field, with field lines lined up (approximately) with the cylinders. Finally, he placed the all setup in a vacuum tube, building the Hull's magnetron (Figure 3). In a Hull's magnetron, when electrons are generated, and tend to flow from the inner cylinder to the external cylinder, they are influenced by the magnetic field generated by the winding.<sup>45</sup>

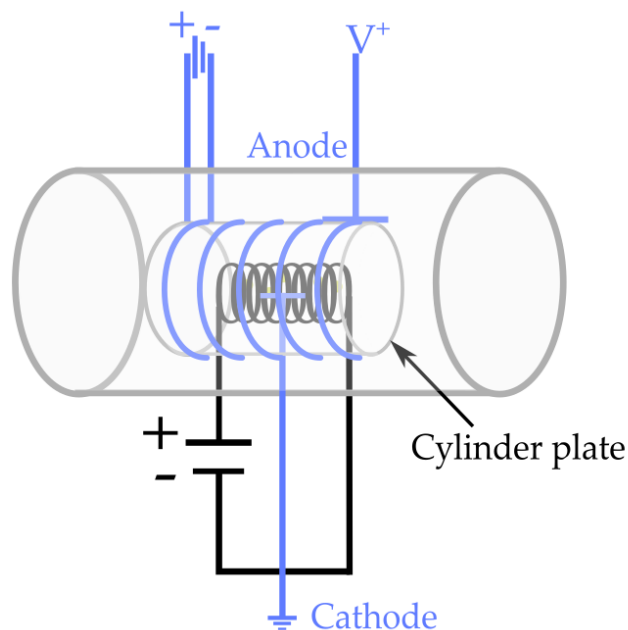


**Figure 3.** Schematic representation of Hull's magnetron.

Remarkably, a charge moving through a magnetic field, experience the Lorentz Force:

$$F = q(v \times B)**$$

As a consequence, the electrons are attracted to the cylindrical plate though curved paths, and are accelerated in the electric and magnetic field.<sup>46</sup> Eventually, if a really high magnetic field is applied the electrons are curved back to the filament. The specific magnetic field strength where this phenomenon is observed, it's called the Hull cut-off field. More in details, when the magnetic field applied is lower than the Hull cut-off field, the electrons emitted from the filament are able to reach the anode (Figure 4-A). On the other hand, when the magnetic field applied is higher that the Hull cut-off field, the electrons are curved back (Figure 4-B).

\*\*  $v$  is the charge's velocity vector and  $B$  is the local magnetic field vector.

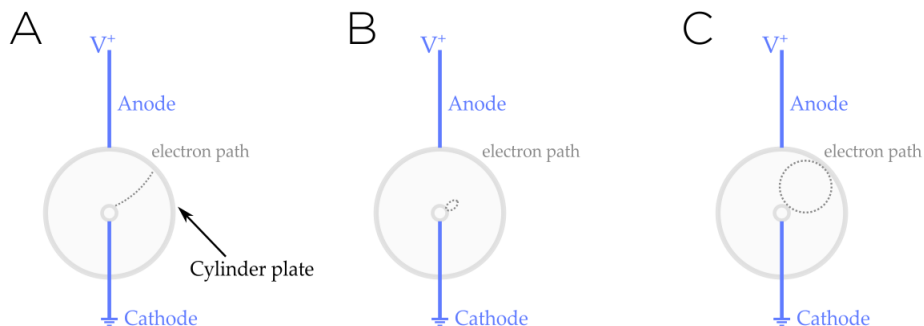


**Figure 4.** Electron paths in the Hull's magnetron applying A) low; B) high; C) medium (critical) magnetic field.

Interesting, when the magnetic field equals the Hull cut-off field, some of the electrons slightly miss the anode, and fly past in a circular trajectory (Figure 4-C). Thanks to Lorentz magnetic force, these circulating electrons are accelerating, but their speed doesn't change significantly. In addition, these electrons don't gain energy (magnetic fields can't do work) but they change direction. This constant acceleration of the electrons trapped in circular electromagnetic orbits within the tube radiates energy away in the form of electromagnetic waves. Many different frequencies are emitted, but a peak occurs at the cyclotron frequency of the electrons, that is their frequency travelling around the circle. As a consequence, by modulating the shape of the magnetron, it is possible to define the wavelength of the emitted electromagnetic waves. More in details, magnetrons allow high power and high frequency emissions, up to dozens of GHz. Considering the electromagnetic spectrum, microwaves are placed between IR and radiofrequencies. More in details, microwaves are electromagnetic waves having wavelengths ranging from 1 cm and 1 m with frequencies between 300 GHz and 300 MHz, and moving at the speed of light (Figure 5). Remarkably, microwaves have low energy photons are incapable of breaking chemical bonds (*i.e.* no DNA damages can occur).<sup>47-49</sup>

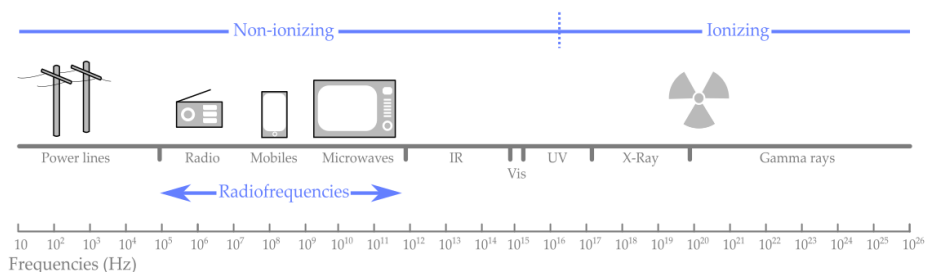


**Figure 5.** Electromagnetic radiations frequencies and their classification.

It is important to mention that the use of frequencies has been established reserving some frequencies for Industrial, Scientific and Mediacal (ISM) purposes in order to not interfere with communication frequencies. The globally used frequencies for ISM purposes are 2.45, 5.8 and 24 GHz, while additional frequencies are established by each country.

The Hull’s magnetron is unfortunately very unstable and poorly efficient. Cavity magnetron are better alternatives to fully exploit microwaves.†† The simplest cavity magnetron, is a Hull magnetron with a special anode full of specially sized cutout chambers, called resonating cavities, illustrated in Figure 6-A.<sup>50</sup> When the magnetron is connected to alternative current, electrons curve outward from the filament in the sub-cut-off magnetic field (usually produced by two permanent ring magnets) and strike the anode. When they strike the anode, the electrons are deposited, generating a negative charge. As a result, each of the resonant cavities forms a sort of LC (tank circuit in which an inductor L and a capacitor C are connected in parallel, Figure 6-B) oscillator circuit: the curved surface acts as a single-loop "inductor" and the cutout connecting the cavities to the main chamber serves as a parallel-plate “capacitor”. In other words, the electrons impacting the cavity-ridden anode serve to "drive" the LC oscillations and the electromagnetic waves.

†† Other microwaves generator include the semiconductors microwaves generator, less common and here not described.<sup>49</sup>

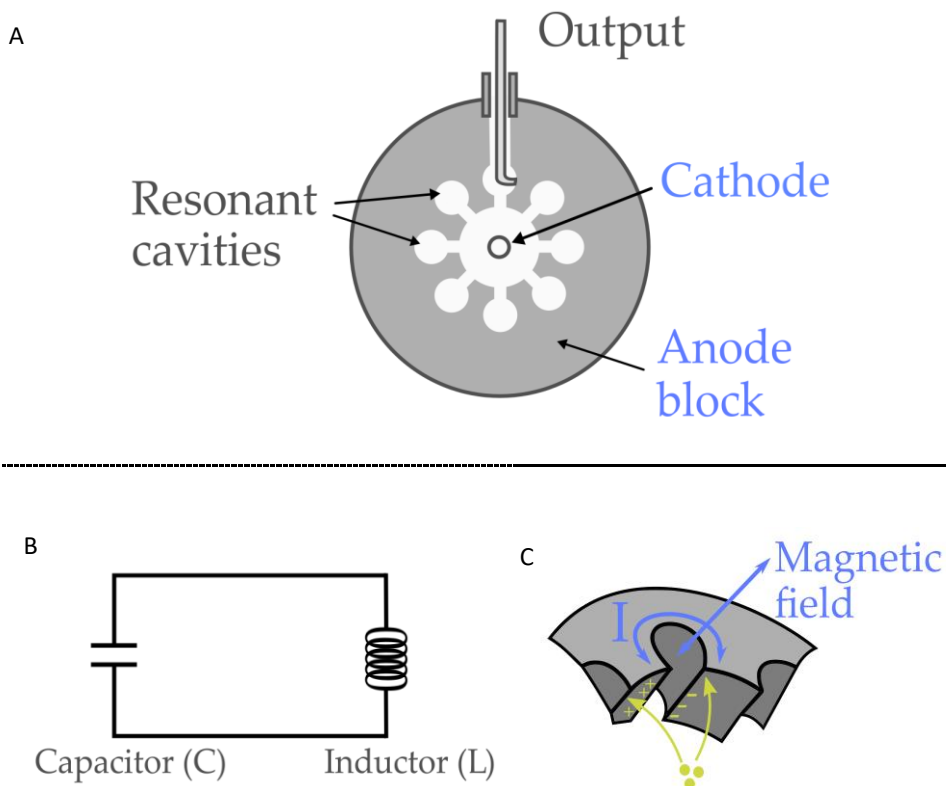


**Figure 6.** A) Section of a cavity magnetron; B) scheme of a LC circuit; C) illustration of the LC circuit produced in each cavity of the magnetron.

The result is that, when electrons deposit charge on the ends of the cavities, electrical oscillations are initiated in the resonant cavities (Figure 6-C). The results of these oscillations are radio frequency electromagnetic waves. The frequency values depend on the inductance/capacitance of the LC oscillators, which in turn depends on the physical dimensions of the cavities.

Microwaves are transmitted from the generator to the target thanks to a metal tube waveguide. The cross-sectional size of the tube varies according to the frequency of the applied radiation, as illustrated in Figure 7. Specifically, the waveguide transmits the microwave radiation at multiples of  $\frac{1}{2}$  waves such that the microwaves are in a resonance state.

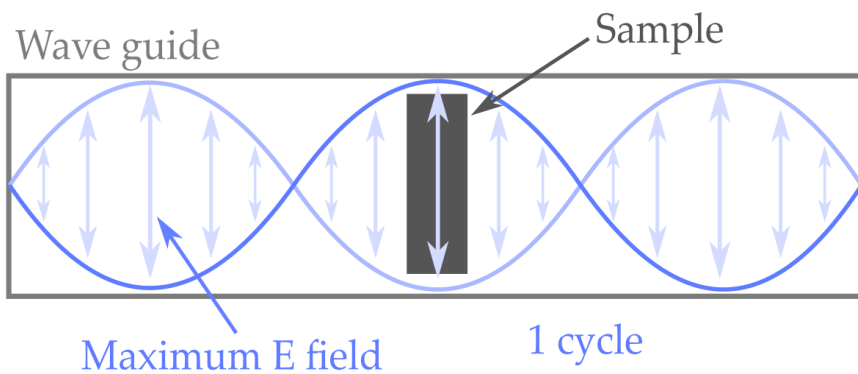


**Figure 7.** Section of a waveguide.

For alternating electric field distributed in the interior of waveguide, the electric charges (plus and minus) interchange at the upper and lower ends of the waveguide. In order to exploit as much as possible the microwave radiation, samples are placed in maximum electric field zones.

## Microwave heating

Microwaves can interact with materials in different ways. For example, when they interact with electrical conductors, *e.g.* most of the metals, they are reflected. When they interact with materials having low dielectric loss characteristics ( $\tan \delta < 0.01$ , explained below) such as quartz or Teflon, they are not (or almost not) affected and are transmitted. Finally, when they interact with dielectric materials ( $\tan \delta$  between 0.05 - 1, see below), the microwaves are adsorbed.<sup>51</sup>

According to C. O. Kappe, D. Dallinger and S. S. Murphree,<sup>52</sup> microwave heating is generated by three different phenomena.<sup>\*\*</sup> The first two are related to the electric component of the microwaves while the last related to the magnetic field of the microwaves:

- Dipolar polarization
- Ionic conduction
- Magnetic (loss) heating

When substances having dipole moments are subjected to an oscillating electric field, they tend to realign following it. During this process, some energy, in the form of heat, is lost due to molecular frictions and dielectric losses. The amount of energy dissipated depends on the ability of the dipoles to align with the frequency of the applied field: if the dipoles don't have time to realign, *i.e.* for high frequencies, or reorient too quickly, *i.e.* low frequencies, no energy is dissipated and no heating occur. The frequency of 2.45 GHz,<sup>55</sup> that is the operative frequency of most of the commercial microwaves, gives the dipoles enough time to align in the field but not enough time to follow the altering field precisely. Consequently, when the dipoles reorient to the electric field, the field has already changed, generating a phase difference between the orientation of the field and the orientation of the dipoles. This cause energy to be lost from the dipole by molecular

---

<sup>\*\*</sup> According to S. Horikoshi and N. Serpone, microwave heating is generated also by three phenomena, called dielectric heating, Joule heating and magnetic loss heating. Importantly, despite called with other different name, the concepts expressed are mosly the same.

<sup>55</sup> The interaction between microwave radiation and dielectrics occur when the frequency of the radiation is close to the frequency of the rotational relaxation process.

friction and collisions, turning kinetic energy into thermal energy, generating dielectric heating.

Ionic conduction occurs when dissolved charged particles, *e.g.* ions, oscillate following the alternated electric field, colliding with neighbouring molecules and atoms. As a result, they create agitation or motion, *i.e.* kinetic energy, thus heat. In terms of heat generation, ionic conduction is stronger than dipolar polarization.

Finally, magnetic losses occur in the microwave region for some metal oxides (*e.g.* magnetite) and some magnetic materials and is generated by the magnetic field component of microwaves (basically, is the selective heating of the magnetic materials, explained in next section). This behaviour is exploited by adding metal oxides having high magnetic losses as impurities to solids having low dielectric loss. Also, it is possible to exploit the magnetic loss using metal oxides as catalysts, thanks to the rapid induction heating.<sup>53</sup>

The microwave-heating efficiency depends on the material state and density: the higher the dispersion of the molecules of the irradiated material, the lower the influence of the electric field (*e.g.*, liquid water can be easily heated up, while vapour cannot). Furthermore, highly regular lattice structures (*e.g.*, ice) having strong interactions of atoms, will not resonate with the frequencies in the microwave range.<sup>\*\*\*</sup>

---

<sup>\*\*\*</sup> A famous experiment to prove this effect consists in heat in a microwave corns in an ice bowl: the corns will pop while the bowl will not melt, due to the strong hydrogen interaction (H-O) in the ice structure.



## Dielectric properties

The microwave-heating characteristics of a material depend on different dielectric properties. The first dielectric property is the permittivity,  $\epsilon$ , which indicates the ability of a material to be polarized by an electric field. The ratio between the permittivity and the permittivity in vacuum gives the dielectric constant,  $\epsilon'$ , that can also be a function of the applied frequency. Another property, is the dielectric loss factor,  $\epsilon''$ , which indicates, in the case of microwaves irradiation, the portion of the energy of an alternating electrical field in a dielectric medium that is converted into heat.  $\epsilon''$  is calculated as sum of dielectric heating and Joule-heating. Therefore,  $\epsilon''$  is a good indicator of the heating efficiency of the microwave irradiation. Remarkably, losses of electric conduction in solids tend to be enhanced by defects in the materials, which reduce the energy needed to generate electrons and holes in the CB and VB. Despite poorly practical for laboratory experiments (due to limitations in the use of frequencies, as explained in previous section), both  $\epsilon'$  and  $\epsilon''$  depend on the frequency: if  $\epsilon'$  tends to increase increasing the frequency (after a plateau up to 2.45 GHz,  $\epsilon''$  slightly increases up to 20 GHz and sequentially decreases.<sup>†††</sup> Also  $\epsilon'$  and  $\epsilon''$  are influenced by the temperature: usually, while  $\epsilon'$  diminishes,  $\epsilon''$  increases. This means that the adsorption of microwaves, expect for some inorganic/polymeric materials,<sup>54</sup> normally decreases by increasing the temperature. If on the one hand this seems inconvenient, as microwave heating at high temperature may be compromised, on the other hand it sets a safety standpoint, avoiding danger runaway reactions.

$\epsilon'$  and  $\epsilon''$  are combined to calculate the loss angle (or loss tangent),  $\tan \delta = \epsilon'' / \epsilon'$ . The loss angle gives in a unique value the measure of the resistance of a molecule. In other words, it's the rate of heating against the ease of polarization, or more easily, it's the ability of a substance to convert electromagnetic energy into heat at a given frequency and temperature.

---

<sup>†††</sup> The 2.45 GHz has been selected for kitchen microwaves in order to not have the maximum  $\epsilon''$ : in fact, in that conditions, microwaves are highly adsorbed (mostly on the surface) and will not penetrate in food.

A material with high  $\tan \delta$  can efficiently absorb microwaves, and can be rapidly heated. Basing on  $\tan \delta$  values, substances (more frequently solvents) can be divided into three microwave adsorbing classes:<sup>52</sup>

- High adsorbing: having  $\tan \delta > 0.5$  (e.g. ethylene glycol, ethanol, methanol)
- Medium adsorbing: having  $\tan \delta$  0.1-0.5 (e.g. acetic acid, water, 1,2-dichloroethane)
- Low adsorbing: having  $\tan \delta < 0.1$  (e.g. chloroform, acetone, acetonitrile, toluene, hexane)

A fourth category may be represented by compounds without a permanent dipole moment, such as dioxane and benzene, that are more or less microwave transparent. Another important factor that must be considered in microwave-assisted reactions is the penetration depth,  $D_p$ . This property indicates the ability of the radiation to penetrate into the media. Clearly, this property is more important when operating with high volume reactors, while it is less evident in commonly used microwave reactor tubes (having diameter  $\sim 1$  cm).  $D_p$  is reported as a value that denotes the depth at which the power density of the microwaves is reduced to  $1/e$  of its initial value (more or less reduced to 37%).  $D_p$  is influenced by temperature and irradiation frequencies. Normally, non-polar solvents have high  $D_p$  compared to polar solvents (e.g.  $D_p$  of toluene is  $\sim 40$  cm while  $D_p$  of water is  $\sim 1.5$  cm). Additionally, ions tend to decrease the  $D_p$  of a substance, therefore a strong stirring is needed when operating with dissolved ions.<sup>55</sup>

## **Microwave thermal effects**

Generally, heat sources in chemistry are oil bath, electric heater (and electric resistance), gas flame, hot wind and hot water. Therefore, the heating processes occur by convection, conduction and radiation thermal transfers. These processes are clearly slow and inefficient, as they depend on convection currents and thermal conductivities, resulting in higher vessel temperatures compared to those of the solutions. The so-generated thermal gradients, called also wall effects, can affect the kinetics of the reactions, favouring, for example, side reactions or product degradations. Oppositely, microwave-heating (when properly carried out) occurs simultaneously in the whole reaction mixture, thanks to the mass heating phenomena, and the penetration of microwaves through the transparent vessels (*e.g.* Teflon, quartz, borosilicate glass) avoid any wall effects. The specific thermal effects of microwaves can be classified in:

- Effects related to kinetics
- Specific microwaves effect

Regarding the kinetics of reactions, thanks to the rapid heating obtained with microwave irradiation, it is possible to increase the rate of a reaction by several times. Despite some works claimed for years the existence of associated kinetic nonthermal microwaves effects, the scientific community is quite united in the definition of microwave irradiation as a “..thermal process [...] incredibly effective, safe, rapid, and highly reproducible [...] under strictly controlled processing conditions...”.<sup>56-58</sup> As a result no “magic microwave effects” occur. Compared to standard thermal heating procedures, microwave-assisted reactions can be carried out efficiently, rapidly and easily.<sup>59-61</sup> Remarkably, it has to be mentioned that microwave heating will not always favour the desired pathway, for example when unwanted reaction products not seen during a conventionally heated experiment at lower T, are formed in the microwave. As a consequence, the specific reaction conditions should always be strictly controlled.

The peculiar mechanism of microwave heating can generate several specific microwave thermal effects. These include the superheating and the selective heating. The superheating effect can be observed when a microwave-heated solution may have

reached its boiling point but may not boil, being in a metastable state. This phenomenon derives from the absence of nucleation sites (or better absence/low heat of imperfections on the vessel were the nucleation sites can grow) and from the presence of a low solvent-vapour interface area.<sup>62</sup> The selective heating is probably the most important specific microwave-heating effect. It is based on the possibility of selecting the substance to heat by the dielectric losses. For example, by using a low adsorbing solvent, it is possible to selectively heat high adsorbing heterogeneous catalysts (*e.g.* due to magnetic loss) or reagents.<sup>63</sup> The low-adsorbing substances are eventually heated by heat transfer from the heated component. This principle can be also applied to bi- or multiphasic systems (*e.g.* water and chloroform).<sup>64</sup> When this principle is applied to a reaction, microwave heating results in less energy consuming compared with traditional heating techniques, where is necessary to heat all the studied mixture in order to achieve the desired heat transfer.

## Small, smaller and smallest: (state of) the art of nanocatalysis

The continuous effort in the research and development of nanodimensional systems have led to the establishment of an extremely remunerative nanoparticles market.<sup>†††</sup> Nanoparticles in fact exhibit new or enhanced size-dependent properties compared with larger particles of the same material, having captivating commercial applications.

Currently, it is possible to find nanoparticles in everyday products, such as in drugs (*e.g.*, biopolymeric nanoparticles for drug delivery) or in personal care products (*e.g.*, nanogold creams and shampoo) as well as in clothes (*e.g.*, silver nanoparticles as antifungal and antibacterial agents) or in food (*e.g.*, ZnO nanoparticles as food additive).<sup>9</sup>  
65-70

Parallely, also the nanocatalysis field has gained more attention year-by-year.<sup>71</sup>  
<sup>72</sup> In fact, nanocatalysts are extremely attractive as they bring together the recovery characteristics of heterogeneous systems with the activity of homogeneous ones.<sup>73</sup> More in details, if on the one hand homogeneous catalysts show high yields and minimized side reaction and by-products, they must be removed (neutralized) producing waste and being not reusable. On the other hand, heterogeneous systems are easily recovered, but they show strongly reduced catalytic activity compared to homogeneous catalysts. This different catalytic activity is generally caused by mass transfer effects, which are mostly negligible in homogeneous catalysis, where reactants, products, and catalysts are in the same phase. In contrast, heterogeneously catalysed reactions are normally limited by mass transfer or diffusion processes between the phase of the catalysts and the phase of the reactants.

In this context, nanocatalysts are catalysts in the nanometer-size where the mass transfer resistance is diminished by the intrinsic large surface to volume ratios. As a result,

---

<sup>†††</sup> Notably, the industrial preparation of nanoparticles began in the XX century. However, the rapid expansion of this market began in the last two/three decades.

nanocatalysts represent a good match between homogeneous and heterogeneous catalysts.<sup>74 §§§</sup>

---

<sup>§§§</sup> Clearly, the research aims at developing the smaller possible catalytic structures, therefore single-atom catalysts (which are being reported every year in a higher number of articles). Up today, nanocatalysts represent the most studied smaller possible catalytic systems.

### ***The power of light: some of the last achievements in photochemistry***

Among all, the utilization of nanodimensional photocatalytically active materials in photoelectrochemical cells (PEC) as well as for chemicals degradation deserves special attention. In fact these type of applications aim to contrast two of the mayor issues that currently affect our World: the production of energy using non-renewable resources, and the pollution of the environment.<sup>75-77 \*\*\*\*</sup>

Without any doubt, one of the most studied material for photocatalytic applications is titanium dioxide.<sup>78</sup> Currently, the research is focusing on the development of well-structured TiO<sub>2</sub> nanodimensional systems with enhanced photocatalytic activity. For example, TiO<sub>2</sub> nanotubes have been demonstrated to have high catalytic activity, and also a red-shift of the adsorption region can be obtained varying the dimension of the tubes.<sup>79-81</sup> Hybrid structures of multiwalled carbon nanotubes/TiO<sub>2</sub> nanocomposites have been proved to be highly active for the degradation of pharmaceutical waste water.<sup>82</sup> Other interesting titanium dioxide nanostructures include the nanosheets architectures. These structures have been used as a “ground-floor” to build heterostructures with high activity under visible light irradiation.<sup>83, 84</sup> Interesting, also a self-doped heterostructure of Ti<sup>3+</sup>/TiO<sub>2</sub> with mesoporous nanosheets structure has been recently synthesized. The structure exhibited a band gap of 2.87 eV (rutile has 2.98 eV band gap), therefore showed photoactivity in the visible region.<sup>85</sup>

ZnO nanoparticles are other highly studied photocatalytic materials. These structures have been claimed to be valid alternative to TiO<sub>2</sub>,<sup>86</sup> and exhibit good photocatalytic activity especially in chemical degradation reactions (*e.g.* dyes, pesticides, aromatic compounds).<sup>17</sup>

Other compounds include, for example, noble metal-metal oxides hybrid nanostructures,<sup>87</sup> Cu or Al oxide nanoparticles,<sup>88, 89</sup> C<sub>3</sub>N<sub>4</sub>-metal nanocomposites<sup>90, 91</sup> or nanodimensional chalcogenides, such as Cu<sub>2</sub>S.<sup>92, 93</sup> Interesting, in recent years, some of these compounds have been also prepared through microwave-assisted synthesis, such as graphene-CdS/CuS composites,<sup>94</sup> Au/Sn<sub>2</sub>S nanoflowers,<sup>95</sup> or nano-scale BiVO<sub>4</sub> compounds.<sup>96</sup>

---

\*\*\*\* Importantly, other applications are also ethically important. For the purpose of the Thesis, applications in PEC cells and for pollutants degradation were selected as the most relevant.

Considering the fact that these photocatalytic compounds are designed for alternative energy production or general environmental applications, a good practice is to carry out the synthesis following the principles of green chemistry.<sup>97, 98</sup>



### ***Until perfection: recent studies in the synthesis of fine chemical***

In the last years, several research group from all over the World have successfully prepared and tested hundreds of different nanocatalysts for the preparation of fine chemicals.<sup>99-101</sup> The novel systems have been used to catalyse different synthesis, including hydrogenations, oxidations, epoxidations, couplings, and many others.<sup>102-109</sup>

A special mention must be given to nanocatalysts supported over mesoporous materials such as carbon or silica (*e.g.* SBA-15, MCM-41, MCM-48).<sup>110-115</sup> or over biomass/waste derived supporting materials, such as chitosan or cellulose.<sup>116-118</sup> These nano-supported structures are particularly useful in catalysing the synthesis of fine chemicals due to the high stability of the supported nanoparticles (avoiding leaching) and due to the improved recovery characteristics (eventually magnetic) of the catalysts, of primary importance when producing high value materials (no product must be lost in filtration/separation procedures during the removal of the catalysts). For example, very recently, palladium nanoparticles have been supported over a chitosan-Fe<sub>3</sub>O<sub>4</sub> system and used as active catalyst for the Suzuki-Miyaura cross coupling reaction carried out at room temperature. Thanks to the presence of magnetite, the catalysts were easily recovered with the aid of an external magnet.<sup>119</sup> Moreover, a novel structure made of cobalt nanoparticles (nitrogen-doped) supported over mesoporous silica MCM-41 has been recently synthesised and used as efficient catalyst for the selective hydrogenation of nitrocompounds.<sup>120</sup>

Among all the nanodimensional metals, gold nanoparticles have emerged due to their high stability under hard reaction conditions, *i.e.* common reaction conditions in the synthesis of fine chemicals.<sup>15, 121</sup> Supported gold nanoparticles have demonstrated high activity in the low-temperature CO oxidation, cyclohexene hydrogenation, and cyclohexane oxidation,<sup>122</sup> with special attention on green chemistry applications.<sup>123, 124</sup> For example, gold nanoparticles supported over cerium oxide have been used as catalysts for the furfural oxidative esterification.<sup>125</sup> More interesting, gold nanoparticles supported over magnetite have been synthesized using an herbal extract as reducing agent avoiding the use of toxic compound. The catalyst showed good catalytic activity for the reduction of azo compounds.<sup>126</sup>

Despite their high catalytic activity, gold nanoparticles have high production costs. As a result, different valid alternatives have been proposed. Between all, silver nanoparticles have emerged due to cheaper production costs and outstanding catalytic activity.<sup>10,127,128</sup> For example, silver nanoparticles have been recently synthesized through a microwave-assisted method using a leaf extract. The nanoparticles showed good catalytic activity in the reduction of 4-nitrophenol.<sup>129</sup> More recently, silver nanoparticles have been prepared through a biological procedure using essential oils of orange peel as a capping and reducing agent. The so-prepared nanocatalysts showed high performances in A3 coupling reactions.<sup>130</sup>

**Full throttle: “Advances in nanocatalysts design for biofuels production”**

Minireview published in ChemCatChem. Alessio Zuliani, Francisco Ivars and Rafael Luque, 2018, 10, 1968–1981, © 2018 Wiley-VCH Verlag GmbH&Co. KGaA, Weinheim



Reproduced by permission of Wiley, link to publication:  
<https://onlinelibrary.wiley.com/doi/full/10.1002/cctc.201701712>

*Abstract: The exploitation of nanocatalysts, at the boundary between homogeneous and heterogeneous catalysis, offers new efficient ways to produce renewable biofuels in environmentally friendly conditions. Specifically, biodiesel and high density fuels have been chosen as major topics of research for the design of catalytic nanomaterials. As solid-state catalysts, they are recyclable, and their nanometric particle size enables high activities that approach those of homogeneous catalysts. In addition, they offer novel and unique catalytic behaviours not accessible to solids above the nanometer range. Furthermore, the use of magnetically active materials has led to the development of nanocatalysts easily recoverable through the application of magnetic fields. In this Minireview, the latest achievements in the production of advanced biofuels using stable, highly active, cheap and reusable nanocatalysts are described.*

### *1. Introduction*

Biofuels, generally defined as any energy-enriched chemical derived from biomass, represent an alternative to the steadily depleting fossil fuel resources. Indeed, biofuels bring together unique characteristics such as renewability, biodegradability, low toxicity, diversity and an easy and locally controllable availability. Moreover, whereas the combustion processes of fossil fuels produce the majority of CO<sub>2</sub> emissions in the Earth's atmosphere, the combustion of biofuels is considered to be carbon neutral.<sup>131-133</sup> Nevertheless, the production of biofuels has to be responsibly planned and handled since the uncontrolled exploitation of plants as biomass source might lead to massive deforestation or to the consumption of soils used for edible crops. In this way, the eco-friendly and sustainable characteristics of biofuels as energy sources depends on the class and the nature of the biomass employed as feedstock, as well as on the characteristics of the production processes, which include reaction conditions, reagents, the use of catalytic or noncatalytic reactions and the type of catalyst employed.<sup>134, 135</sup>

The most general categorization of biofuels is made in terms of the direct or indirect production of energy. Thus, the first category, that of primary biofuels, refers to organic materials used in an unprocessed form, such as wood fuel or dried animal dung fuel, to produce heat or electricity directly. These primary biofuels were the energy engine of human development until the rise of fossil fuels. Although utilizing primary

biofuels for everyday use is no longer accepted in terms of environmental sustainability, it is still the main source of energy, especially for cooking and heating, in a large number of communities in developing countries.

The second category, that of secondary biofuels, refers to those indirectly obtained from organic material, either of plant or animal origin. Their production requires advanced and efficient conversion technologies from which solid, liquid or gaseous biofuels are produced, depending on the specific characteristics of the process.

The main technologies for biomass conversion can be divided in thermochemical, biochemical and extraction methods. Although the processes for upgrading biomass are also employed to obtain fine-chemical products, in this Minireview we will only focus on biofuel production. Thus, thermochemical processes are the ones attracting major research attention and the most common methodologies for biomass conversion into biofuels, with the broader range of developed technologies.<sup>136</sup> Thermochemical methods can be subdivided into gasification and direct liquefaction methods. Gasification is mainly used to produce syngas (mixture of CO and H<sub>2</sub>, primarily used for methanol or Fischer–Tropsch hydrocarbons synthesis) from biomass conversion at low- (LTG) or high-temperature (HTG) in the presence of oxidant gases (mainly O<sub>2</sub>, CO<sub>2</sub>, steam and air). Direct liquefaction is employed to produce liquid biofuels (*e.g.* biodiesel, bio-methanol, bio-oil) and can be subdivided into hydrothermal and catalytic liquefaction, and pyrolytic methods based on thermal biomass decomposition in absence of oxygen.<sup>137</sup>

On the other hand, biochemical processes involve biomass conversion through fermentation or anaerobic digestion, using live microorganisms or enzymes, to produce liquid or gaseous biofuels.

Finally, the extraction methodology is based on physical methods (sonication, microwaves, bead beating, autoclaving, grinding, osmotic shock, *etc.*) and/or chemical methods in the form of solvent extraction (*e.g.* using ionic liquids, Soxhlet, Bligh and Dyer's or supercritical CO<sub>2</sub> extraction).

Depending on the nature of the biomass feedstock, secondary biofuels are subdivided into three different classes: i) first generation biofuels, obtained from food crops; ii) second generation biofuels, derived from non-food biomass crops, no longer

edible food-derived materials (e.g. wasted oils) as well as agricultural, urban and industrial organic waste; and iii) third generation biofuels, which consist of biofuels derived from microalgae. Figure 8 schematically shows the classification of biofuels into categories and classes.

Third generation biofuels can also be theoretically included in the definition of second generation biofuels, as biomass sources from both generations do not directly compete with the food supply. However, the special characteristics of biofuel production from microalgae, potentially capable of much higher yields (up to 300 times) with lower land requirement than any other feedstock, made them worthy of their own category. The extraordinary photosynthetic efficiency of microalgae (high capacity for CO<sub>2</sub> capture) is mainly responsible for some of their unique characteristics such as high adaptability and fast growth rate (above 50 times faster than land based plants).

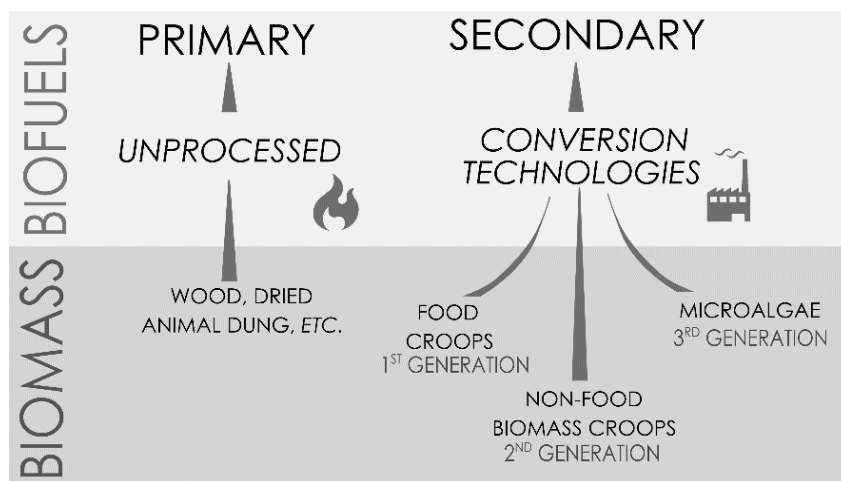


Figure 8. Classification of biofuels.

However, third generation biofuels are more expensive than those from other biomass sources, owing to the high cost caused by the large amount of water, nitrogen and phosphorus (the latter two in terms of fertilizer) required for the microalgae to grow. In addition, the need for fertilizer brings a negative balance of greenhouse gases emissions for the global process once the fertilizer production is considered.<sup>138</sup>

Furthermore, from a strictly logistic view, microalgae cultures need the combination of large cultivation areas, sunlight, water and a source of CO<sub>2</sub> in the same place. Until now, this utopic place does not exist on our planet. Therefore, despite the advantages, third generation biofuels will not become a commercial reality in the short term, and currently they are rather restricted to a small scale.

As to the other biofuel sources, the first generation was the earliest class of secondary biofuels, which was produced using potentially edible biomass feedstock, and therefore considered as not sustainable, because, if massively exploited, it would have a serious impact on the world food supply. In contrast, second generation biofuels uses a more sustainable biomass feedstock in terms of availability, waste recycling potential and with a lower impact of their use on food supply, greenhouse gas emissions, biodiversity and exploitation of agricultural land (linked to food and water supply). However, biomass sources for second generation biofuels used to be more difficult to convert than food feedstocks, owing to their lower reactivity as well as high structural and composition complexity. Nowadays biofuel production is faster, easier and cheaper from highly pure oils and lipids than production from non-food crops and other biomass sources from waste residues. Therefore, first generation biofuels still constitute the majority of biofuels currently manufactured, whereas most of second generation fuels are still at the development stage and not widely available for commercial use.<sup>139, 140</sup>

In most cases, biofuels are still not cost-competitive relative to fossil fuels. Apart from waste-derived biomass, the rest of biomass feedstock can account for up to 60–80% of the total cost of biofuel production, mainly owing to the higher costs of biomass collection and transportation relative to those for fossil fuels extraction and delivery to centralized processing stations.<sup>139,140</sup> Regardless of the economic issue, commercial production and use of biofuels have progressively been scaled up during last decades, mostly because of the prospective threat of fossil fuels shortage along with the challenging international commitments to reduce greenhouse gases emission standards. Accordingly, the research efforts on biofuels technology have been intensified to reduce production costs. The main approach has been to develop more efficient, environmentally friendly and economically viable novel processes, with the aim of moving from the first to the second generation of biofuels.

Some methodologies successfully use homogeneous catalysis to speed reaction rates up, increasing conversion and selectivity, minimizing side reactions and by-products. However, homogeneous catalysts cannot be recovered and reused. They must be neutralized at the end of the reaction, producing vast quantities of undesired waste chemicals that have to be separated, and limiting implementation of continuous downstream processes. Moreover, corrosion is especially favoured in homogeneous catalysis.

Alternatively, heterogeneous catalysis offers, in addition to the aforementioned advantages inherent to a catalytic reaction, the possibility of recycling the solid catalyst and, if using liquid or dissolved biomass, operating processes under continuous flow conditions with reduced corrosion problems in comparison to homogeneously catalyzed reactions. Moreover, the use of solid catalysts opens the chance for multifunctionality, consequently decreasing the number of steps in a biomass upgrading process, towards even higher both energy and cost efficiency.

Nevertheless, mass transfer effects are mostly negligible in homogeneous catalysis, in which reactants, products, and catalysts are in the same phase. In contrast, typical liquid–solid heterogeneously catalyzed reactions for biomass conversion are limited by mass transfer or diffusion processes between the solid phase of catalyst and the liquid phase of reactants, leading to long reaction rates and low efficiency.<sup>141</sup> Therefore, heterogeneous catalysis research has focused on developing solid catalysts in the nanometer-size scale (nanocatalysts), in which mass transfer resistance is minimized by the intrinsic large surface to volume ratios.

Most of the research has focused on developing nanocatalysts for biomass conversion into biodiesel, with a relatively insignificant number of studies on the upgrading of biomass to other liquid biofuels. Accordingly, the aim of this work is to provide an overview of the ultimate advances in nanocatalysts for biodiesel production. In addition, progress in the use of nanocatalysts to produce high density eco-fuels, including those produced from biomass and from plastic waste, will be also summarized.



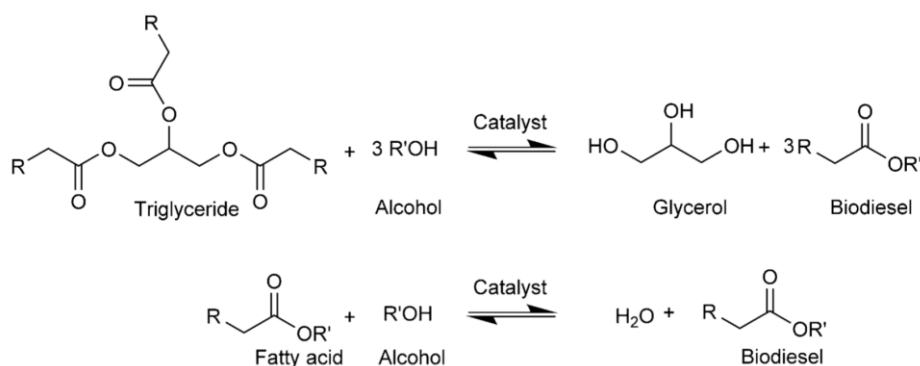
## 2. Biodiesel

The most common biofuels include bio-alcohols, biodiesel, bio-ethers, biogas (mainly a mixture of CH<sub>4</sub> and CO<sub>2</sub>), biosyngas (mixture of CO and H<sub>2</sub>) and high density biofuels.<sup>142</sup> Among them, biodiesel has attracted by far the most attention from the industrial and research sectors, owing to its multiple and well-known advantages.<sup>143</sup> In addition to the benefits related to sustainability such as renewability, biodegradability and low toxicity, biodiesel is fully compatible with conventional diesel fuel engines without any modification.

Biodiesel is composed of mono-alkyl esters of long chain fatty acids (fatty acid alkyl esters, FFAE) derived from natural and renewable lipid feedstock, such as vegetable oil or animal fats. The direct use of oils and fats as diesel is hindered by the high kinematic viscosity of the feedstock and by the deposition of carbon. Hence, oils and fats must be processed to be compatible with existing engines.<sup>134</sup> There are two primary conversion methodologies for producing biodiesels: pyrolysis and transesterification. As introduced above, the pyrolysis is a thermal treatment which needs high temperature and is extremely energy-consuming.<sup>144</sup> Transesterification is the reaction of a fat or oil with an alcohol to form esters and glycerol. The transesterification of TAGs (triacylglycerol) and esterification of FFAs (free fatty acids), illustrated in Scheme 1 and also defined as alcoholysis of plant oils or animal fats, is the most common technology to produce biodiesel.<sup>145</sup>

There are different transesterification processes that can be applied to synthesize biodiesel: (a) base-catalyzed transesterification, (b) acid-catalyzed transesterification, (c) enzyme-catalyzed transesterification, and (d) supercritical alcohol transesterification. The most common method is homogeneously base-catalyzed transesterification, which is significantly faster than any of the other methods (*e.g.* 4000 times faster than homogeneous acid catalysis reaction), in addition to being easier and cheaper.<sup>146-153</sup> Nowadays more than 95% of the world total biodiesel is produced from highly pure edible oil feedstock, consequently increasing food prices and deforestation. On the other hand, non-edible oils have gained attention because of their elevated oil content and the possibility to be grown in territories not suitable for agriculture with reduced cultivation costs. Residual cooking oils are also considered as possible feedstock

for biodiesel production as a result of their low costs, but they are composed mainly of free fatty acids (FFAs), which strongly influence the yield and purity of the biodiesel.<sup>154</sup> Although base-catalyzed transesterification is a simple process, it is very sensitive to the presence of free fatty acids, which leads to undesired saponification reactions of the desired products. Consequently, it requires high cost virgin oil (high grade) as feedstock, highly increasing the production cost as compared to the acid-catalyzed transesterification.



**Scheme 1.** An illustration of transesterification of triglyceride and esterification of free fatty acids.

Nevertheless, regardless of the acid or base reaction mechanism, homogeneous catalysis for biodiesel production has some important limitations, despite its attractive characteristics. Thus, to avoid saponification and hydrolysis of esters, sodium hydroxide is used only with high purity edible oils. On the other hand, sulfuric acid can be used with low-grade feedstock, but it needs longer time of reaction. Finally, the post-reaction treatment required for the removal of the residual catalysts is costly, difficult and generates a large waste water stream. Considering also that the catalysts are consumed during the process, the need for a more promising alternative is straightforward.<sup>134</sup>

Therefore, various types of heterogeneous catalysts have been studied to improve the transesterification of glycerides. These include solid base catalysts, such as hydrotalcites, metal oxides, metallic salts, supported solid bases and alkali-modified zeolites. Unlike homogeneous catalysis, low-quality oils or fats with FFAs and water can

be used with heterogeneous base catalysts, which have been intensively studied over the last decade for transesterification synthesis of biodiesel. However, their catalytic efficiency still needs to be improved. On the other hand, solid acid catalysts, with a longer history than solid bases, are especially suitable for low-quality oil feedstocks with high content of FFAs. Acid catalysts can simultaneously catalyze both esterification and transesterification, showing a much higher tolerance to FFAs and water than basic catalysis, but with less activity. Currently developed solid acid catalysts are cation exchange resins (*i.e.* Amberlyst-15 and NR50), mineral salts (*i.e.* ferric sulfate, zirconium sulfate, aluminum phosphate and zirconium tungsten), supported solid acids, zeolites and heteropolyacid catalysts.<sup>155</sup>

Finally, enzyme-catalyzed transesterification has also been reported as an option because it can avoid saponification, simplifying the purification process and allowing the use of less pure feedstocks such as inedible and waste oils. Enzymes can be used in mild reaction conditions, consuming less energy, and leading to highly pure products even if using high FFAs value feedstock.<sup>156</sup> The consistent price of enzymes calls for the utilization of an immobilizing material to facilitate the recovery of the biocatalyst to amortize the costs over several cycles. Therefore, the integration of a magnetic material makes for an ideal combination.<sup>157</sup> However, long reaction times and low yields, so far, must be significantly improved if they are to be commercially applied feasibly.<sup>143</sup>

### 2.1. Advanced design of nanocatalysts for biodiesel

The research on environmentally friendly and economically viable processes for biomass conversion, moving from first to second generation biofuels, has focused on developing novel heterogeneous catalysts, stable, easy to recycle and with high efficiency and selectivity. As a response to the pressing need for catalyst improvement, especially in production of biodiesel, nanocatalysis has clearly emerged offering unique solutions at the interface between homogeneous and heterogeneous catalysis. In general, the main driving force behind the use of nanocatalysts is their nano-sized solid nature which offers the closest approach to the behaviour of a homogeneous catalyst, with the advantages of recoverability and recyclability.<sup>153, 158, 159</sup> Thus, the high activity of homogeneous systems can be similarly provided by the large specific surface areas intrinsic to solid

catalysts consisting of nanometric size particles. Furthermore, beyond having the advantageous characteristics of both homogenous and heterogeneous systems, nanomaterials open the way to new properties, which also originate from their size. The extent of electronic delocalization in nanometric materials with strong chemical bonding, such as metal nanoparticles, is very sensitive to the particle size. This effect, coupled to structural changes, can lead to size-dependent chemical and physical properties, which cannot be achieved with microscopic particles. The surface reactivity is among these properties, strongly influenced by the atomic coordination at the surface. The latter is controlled not only by nanoparticle size but also by its shape, which determines the atomic-level structure of the outermost exposed planes.<sup>160</sup> In this way, whereas the surface of a spherical nanoparticle exposes a wide variety of atomic environments, a cubic nanoparticle exposes just one type of atomic structure.

In addition to influencing the catalytic activity, the control of the nanoparticle shape leads to the homogeneity of the surface atomic structure, which directly translates into high catalytic selectivity.<sup>161</sup> Therefore, the catalytic properties (activity and selectivity) of nanocatalysts can be tuned by simply changing the shape and size of their active phase.<sup>162</sup> At this point it must be mentioned that nanocatalysts include either nanometer-sized particles or nanopore-separated materials. Metal, alloy or composite nanoparticles can be free or grafted on supports, such as oxides, zeolites or carbonaceous substrates, the latter preferably with high surface area to favour the exposure of the maximum possible surface area of nanoparticles.

Beyond the size and shape of nanoparticles, the acid-base properties, type and content of metal(s) and porosity are key parameters for the catalytic performance of nanocatalysts. Additionally, nanomaterials can be used as supports for enzyme biocatalysis. In that sense, nanocatalysts for biodiesel production are typically classified according to their alkali, acid or enzymatic nature as base, acid, and bio-nanocatalysts, respectively, as illustrated in Figure 9. In general, inorganic nanocatalysts for the synthesis of biodiesel mostly include alkaline earth metal oxides (CaO, MgO),<sup>162-165</sup> hydrotalcites,<sup>166, 167</sup> zeolites,<sup>168, 169</sup> zirconia<sup>170</sup> and sulfated oxides.<sup>171</sup> Most advanced nanocatalysts have been developed to boost the recoverability by exploiting magnetic properties.<sup>172-174</sup> Thus, combination of some of these catalysts with magnetic materials has prompted the evolution of magnetically recoverable nanocatalysts.<sup>175</sup>

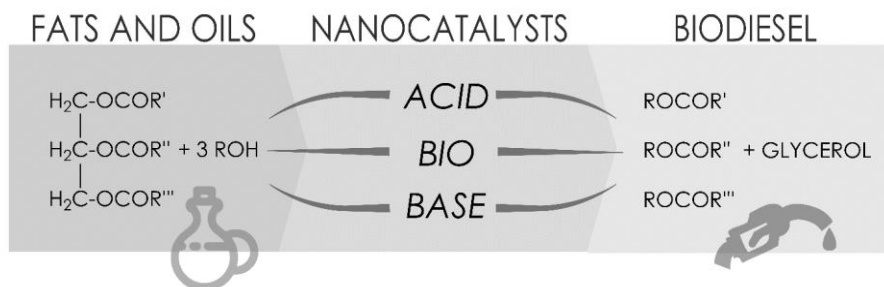


**Figure 9.** Classification of nanocatalysts for the transesterification of triglycerides.

On the other hand, the research on enzyme biocatalysts supported on nanomaterials has opened the doors to new technologies for biofuel productions, especially characterized by milder reaction conditions, avoiding saponification, and requiring simpler product purification.<sup>156</sup> In the last years, enzymes have been proposed in the form of magnetically recoverable nanocatalysts too.<sup>157, 176</sup> Anyway, cost and reaction rates using enzymes must be further improved.<sup>177</sup>

The main drawback to avoid in nanocatalysis is the sintering of nanoparticles. At high temperatures in the reactive environments of many catalytic processes, metal atoms are mobile to the point that important changes in size and shape of metal nanoparticles are induced. Those structural alterations lead to undesirable effects such as inhomogeneity, loss or reversion of selectivity and catalytic deactivation. Therefore, sintering in nanocatalysts, unless prevented, may limit their application to low temperature ranges and short term use. Utilization of ligands or coating materials such as carbon, and inorganic components such as silica, zeolites, polymers and proper metals, has demonstrated to be the best solution to hinder nanoparticle agglomeration.<sup>178</sup> For instance, by coating metal nanoparticles with a mesoporous silica shell, temperatures approaching 1000 K without evidence of sintering and with preservation of the shape and morphology of nanoparticles have been reached.<sup>179</sup> The catalytic activity is not inhibited and reactions are not limited by transport of reactants and products through the mesoporous silica. This porous coating approach can even enhance selectivity by providing additional size and shape selectivity of products depending on how they fit or

are inhibited due to constraints imposed by the pores. The same effect applies to zeolites, which also play an important multifunctional role on the design of nanocatalysts (*i.e.* increasing the thermal and mechanical stability of supported nanoparticles), affecting shape and size product selectivity thanks to their pores, as well as providing tuneable acid-base properties and additional cooperative active sites for multistep reactions.<sup>180</sup>

However, in the case of zeolites, their characteristic microporosity, which offers higher diffusional constraints than mesoporous materials, limits their use to catalyze reactions for biodiesel production because it involves large molecules such as triglycerides. Moreover, zeolites are usually synthesized in crystal sizes within the micrometer range leading to negligible external area surface.

To overcome the accessibility limitations of zeolites, different approaches have been devised such as the synthesis of nanosized zeolite crystals, zeolites with a secondary mesopore network or zeolite composites.<sup>180</sup> Those creative approaches, separately or combined, have allowed the development of new zeolitic materials, the so-called hierarchical zeolites, with enhanced accessibility that is suitable for biomass conversion. As a case in point, nanocrystalline hierarchical zeolites would contain bimodal micro- and mesoporosity, and high external surface area. Therefore, either internal or external active sites can catalyse reactions involving molecules used for biodiesel synthesis such as triglycerides.<sup>180, 181</sup>

All the achievements in the development of advanced nanocatalysts mentioned above have been possible as a result of the combination of deep understanding of surface chemistry and creative use of modern methods for the synthesis of nanostructured materials. This interdisciplinary approach has resulted in well-defined nanocatalysts with an impressive control over their particle size, shape, morphology and thermal stability, which could not have been developed decades ago. To meet the current challenges related to the energy- and cost-efficient conversion of biomass into biofuels, efforts should focus on the detailed understanding of the mechanisms governing the surface catalytic reactions. Such understanding is key to establishing rational strategies for the development of new generations of catalysts with predefined enhanced catalytic performance for the reactions of interest.

## 2.2. Base nanocatalysts

Base nanocatalysts are mainly solids with Brønsted and Lewis basic activity centres that can accept protons from reactants or supply electrons to them. Among the numerous alkali nanocatalysts for biodiesel production, calcium oxides, hydrotalcites and zeolites have received more attention. Above all, calcium oxides have been intensively studied owing to its higher basicity and activity, long catalyst life times, low cost and mild reaction conditions.<sup>182-185</sup> Aiming to increase CaO activity, during the last years the research has focused on the doping of calcium oxide with different compounds such as lithium,<sup>186, 187</sup> potassium fluoride<sup>188-190</sup> and zinc.<sup>191</sup> Recently, a highly active catalyst has been prepared by dropping a solution of potassium carbonate into a solution of commercial CaO.<sup>192</sup> The resulting precipitate was dried and calcined to obtain an activated K-doped calcium oxide with a strongly enhanced activity in the transesterification of *Canola* oil, compared with the pure CaO based catalyst. Thus, a maximum yield of 97.76 % was reached at the low temperature of 338 K with 3 wt% catalyst and a methanol/oil molar ratio of 9:1.

Despite its advantages, the utilization of CaO shows some limitations in the recovery step. During the transesterification process, lattice oxygen species form hydrogen bonds with methanol and glycerin, increasing the viscosity of glycerin and forming solids in suspension with CaO, which is therefore hard to recover.<sup>193</sup>

The magnetic functionalization of calcium-oxide overcomes these limitations. Thus, Zhang *et al.*<sup>194</sup> combined a magnetic material with calcium oxide and a strontium oxide to prepare a magnetic CaO@(Sr<sub>2</sub>Fe<sub>2</sub>O<sub>5</sub>-Fe<sub>2</sub>O<sub>3</sub>)catalyst. The catalyst was synthesized by a simple co-precipitation method. The catalyst was applied to the transesterification of soybean oil into biodiesel, reaching a maximum yield of 94.9 % at 343 K after a 2 h reaction, with methanol/oil molar ratio of 12:1, and 0.5 wt% catalyst. Owing to its magnetic properties, the catalyst was easily recovered after every cycle, showing high efficiency and high stability after five runs. Some hydrotalcites were also successfully employed as catalysts for environmentally benign transesterification processes of vegetable oils. Deng *et al.*<sup>195</sup> prepared a hydrotalcite Mg/Al (3:1) nanocatalyst by a co-precipitation method using urea as precipitating agent, followed by a microwave-hydrothermal treatment. With a charge of 1 wt% catalyst, the transesterification of

*Jatropha* oil reached a yield of 95 % after 1.5 h at 318 K with a methanol/oil molar ratio of 4:1. From a commercial point of view, the properties of the biodiesel were close to those of the German standard (DIN V51606).

Xie *et al.*<sup>196</sup> prepared a functionalized zeolite catalyst by coupling SBA-15 with a guanidine derivative. The hydroxyl group on the SBA allowed the grafting of the guanidine derivative (DCOG), in which the tertiary amine groups acted as active sites for the transesterification of soybean oil. Despite reaching a transesterification yield of 92.6 %, a rather long reaction time (16 h), high catalysts loading (8 wt%), and high methanol/oil ratio (15:1) was required. In any case, DCOG-functionalized SBA-15 showed advantages in terms of easy separation and recovery and high stability in the reutilization. Another magnetic basic nanocatalyst based on  $\text{Na}_2\text{O-SiO}_2/\text{Fe}_3\text{O}_4$  has been recently reported.<sup>195</sup> The catalyst was prepared by loading  $\text{Na}_2\text{SiO}_3$  on commercially available  $\text{Fe}_3\text{O}_4$  nanoparticles, using  $\text{Na}_2\text{O}\cdot 3\text{SiO}_2$  and NaOH as precipitant agents. The catalyst with a Si/Fe molar ratio of 2:5 showed the best catalytic activity in the transesterification of cottonseed oil. The biodiesel yield was strictly related to the methanol/oil molar ratio, with the optimum for a 7:1 ratio providing 99.6 % yield to biodiesel, obtained at 333 K after 100 min reaction time with a 5 wt% catalyst.

### 2.3. Acid nanocatalysts

Acid nanocatalysts usually are less active, but they have much higher tolerance to polar impurities such as FFAs and water, owing to their hydrophobic surface, and therefore are more suitable for low-quality oil feedstocks with high FFAs content. Acid catalysts can simultaneously catalyse the esterification of free fatty acid and the transesterification of triglycerides simultaneously, allowing the use of waste cooking oil as feedstock for biodiesel production.<sup>197, 198</sup> Most attractive acid nanocatalysts recently produced include functionalized magnetic particles, zeolites and zirconia.

Wang *et al.*<sup>199</sup> obtained a magnetic acid catalyst in the form of sulfamic- and sulfonic-acid-functionalized silica-coated crystalline Fe/ $\text{Fe}_3\text{O}_4$  core-shell magnetic nanoparticles (MNPs). These MNPs have demonstrated to be efficient and recoverable catalysts for the biodiesel production from waste cooking oil. As illustrated in Figure 10,



the synthesis of the catalysts consists of three steps: preparation of magnetic nanoparticles, coating with silica and functionalization. The catalysts were tested in the transesterification of glyceryl trioleate and in the esterification of oleic acid in methanol. After 20 hours at 373 K, 88 % and 100 % conversion were obtained with MNPs functionalized with sulfonic acid or sulfamic acid, respectively. The esterification of oleic acid was completed within 4 hours with 100 % of conversion for both catalysts at 343 K in methanol. Whereas the sulfonic-acid-functionalized MNPs showed low reusability, with a conversion drop to 62 % in the fifth run, sulfamic-acid-functionalized MNPs maintained 95 % conversion throughout five reaction cycles.

HUSY, hierarchical H-style ultra-stable Y zeolites, have been studied as highly active catalysts for the transesterification process.<sup>169</sup> However, the high content of acid sites decreases the reusability of the catalysts, thus increasing the production costs. The incorporation of cerium on HUSY zeolite has been proposed as a solution to reduce the number of acid sites on both the external and micropore surface area of the zeolite, increasing the reusability.<sup>200</sup> Ce/HUSY was prepared by calcination of NH<sub>4</sub>USY, followed by impregnation with cerium nitrate solution. Before utilization, the catalyst was activated through calcination at 573 K for 4 h. The transesterification reaction was conducted at 473 K with an ethanol/soybean oil molar ratio of 30:1. Ce/HUSY showed a 99.5 % conversion after the third cycle, as compared to 96.4 % conversion of HUSY.

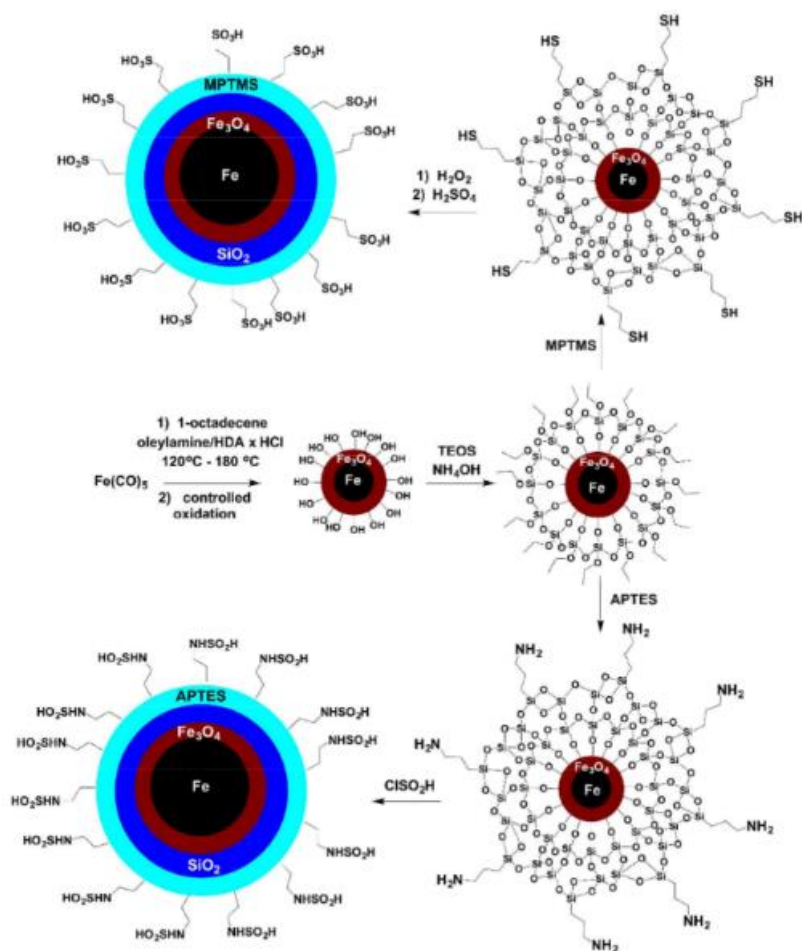


**Figure 10.** Preparation of sulfonic acid functionalized magnetic nanoparticles and sulfamic acid functionalized magnetic nanoparticles. Taken from ref. 199. Copyright (2015), American Chemical Society.

Zirconia nanocatalysts produced by sonochemistry have been recently proposed as catalysts for biodiesel production.<sup>201</sup> The catalysts were synthesized by an ultrasound-assisted impregnation/hydrothermal hybrid method, producing nanoparticles of 1–30 nm supported on MCM-41. The performance of the catalyst was investigated in the biodiesel production from sunflower oil, showing a significantly higher activity than that of the same catalyst produced by traditional methods. Biodiesel yield reached 96.9 % at 333 K with 5 % catalyst concentration and a methanol/oil molar ratio of 9:1.

#### 2.4. Bifunctional nanocatalysts

Base catalysts are well known for accelerating the alcoholysis reaction, whereas acid catalysts are tolerant to the impurity (FFA content) of the feedstocks. The proper combination of acid and base functionalities in a single nanocatalyst could gain relevance for the fast production of biodiesel in a two-step process from low-grade oils (containing high percentage of FFA). For example, biodiesel has been produced from cooking oil using 25 wt% tungstophosphoric Acid (TPA)/Nb<sub>2</sub>O<sub>5</sub> for the esterification of FFA, whereas 20 wt% ZnO/Na Y zeolite catalyst was used for the transesterification of the remaining feedstock.<sup>202</sup>

With that purpose, bifunctional nanocatalysts have been recently proposed as advanced solutions for biodiesel production from low-grade oils in a one-step reaction. These catalysts, comprising both acid and basic sites, could promote the esterification and transesterification at the same time. This technology could reduce the costs of biodiesel production not only by replacing a two-step reaction with a one-step, but also by avoiding the utilization of high-cost equipment.<sup>203</sup> A bifunctional Quintinite-3T nanocatalyst was reported as transesterification and esterification promoter for soy, canola, coffee and waste vegetable oils with variable amounts of FFAs (0–30 wt%).<sup>204</sup> The catalysts were easily prepared by a sol-gel method at 393 K for 24 h, followed by calcination at 773 K. This easy synthesis, combined with the natural availability of the reagents, made the catalysts economically cheap. The Quintinite-3T catalyst showed high activity even after five cycles, maintaining a yield of 96 % in 2 h at 75°C with 10 wt% catalyst amount and a methanol/oil molar ratio of 12:1.

Also Mo-Mn/g-Al<sub>2</sub>O<sub>3</sub>-15 wt% MgO has been reported as an efficient catalyst for the biodiesel production from waste cooking oil and methanol.<sup>205</sup> The catalyst was prepared by an impregnation method, using  $\gamma$ -Al<sub>2</sub>O<sub>3</sub>-MgO with small pore diameter (~60 Å) as support material. The maximum yield of 91.4% was reached in 4 h at 100°C using a methanol/oil molar ratio of 27:1 and 5 wt% catalyst.

### *2.5. Epoxidation nanocatalysts*

A recent overview by Danov *et al.*<sup>206</sup> summarizes the progress (past 15 years) in the selective epoxidation of vegetable oils and their derivatives, in particular unsaturated fatty acids (UFAs) and fatty acid methyl esters (FAMEs). Epoxidized vegetable oils (EVOs) have drawn much attention in recent years in the chemical industry owing to their environmental friendliness, biodegradability, renewability, high availability and nontoxic nature.<sup>206</sup> Four major types of catalysts have been extensively employed to produce epoxidized fatty acid compounds: homogeneous, heterogeneous, polyoxometalates and lipases. EVOs are currently produced industrially using a homogeneous catalytic conventional epoxidation process, in which unsaturated oils are converted using percarboxylic acids, such as peracetic or performic acid. However, this method suffers from several drawbacks such as relatively low selectivity for epoxides owing to oxirane ring opening, and corrosion problems caused by the strong acids in an oxidizing environment, among others. Thus, in view of the principles of green chemistry, the development of new catalytic systems for the selective epoxidation of vegetable oils and their derivatives remains a significant challenge that was partially addressed using heterogeneous catalysts.<sup>206</sup> Epoxidized fatty acids and epoxidized fatty acid methyl esters can be promising substitutes of EVOs because the starting materials for their production have lower viscosity and higher reactivity, which will significantly increase the productivity of the epoxidation process.<sup>206</sup>

### *3. Catalytic Production of High Density Fuels*

Despite the abundance of gasoline and diesel-powered motor cars, high consumption vehicles such as jets, rockets, heavy trucks and ships require high density diesel with high volumetric net heat of combustion (NHOC).<sup>207</sup> Commercially available high density fuels are derived from petroleum and contain a large amount of naphthalene (~35%), which is the main component responsible for the high density.<sup>208</sup> Most of the recent research on renewable jet fuels has focused on synthetic paraffinic kerosenes (SPKs), which are mainly composed of purely paraffinic or isoparaffinic hydrocarbons in the C<sub>10-14</sub> range, resulting in low densities.<sup>209</sup> For example, the commercial JP-8 jet fuel has densities from 0.825 to 0.850 g mL<sup>-1</sup>, with a NHOC of ~120 kBtu gal<sup>-1</sup>.<sup>210</sup> In contrast, a

normal renewable biodiesel has a density range from 0.73 to 0.76 g mL<sup>-1</sup>.<sup>211</sup> A possible solution to the low density of these fuels is to produce high density compounds, such as polycycloalkanes, from biomass or plastic waste for blending with SPKs or direct use as biofuel.

### 3.1. Biomass high density biofuels

The conversion of biomass to high density fuels usually consists of sequential steps of different processes including alkylations, oligomerizations, condensations and hydrogenations. In all the processes, the employment of catalysts plays a crucial role in terms of efficiency, selectivity and yield.<sup>212-214</sup> Figure 11 schematically summarizes the latest progress, discussed below, in the utilization of nanocatalysts to produce high density biofuels.

Terpenoids are renewable sources of naphthalenes, as they can be extracted from pine resins or generated through biosynthesis.<sup>215</sup> Specifically, naphthalenes have been bioderived from monoterpenes, sesquiterpenes and diterpenes. Harrison *et al.* prepared three new advanced biofuels from sesquiterpene feedstocks.<sup>216</sup> The high density biofuel was prepared by catalytic hydrogenation using a PtO<sub>2</sub> catalyst, starting from cedarwood oil as feedstock, which primarily consists of the sesquiterpenes thujopsene,  $\alpha$ -cedrene and  $\beta$ -cedrane. The hydrogenated cedarwood oil (HCWO) showed a density of 0.917 g mL<sup>-1</sup>, with a NHOC above 12 % higher than JP-8 commercial fuel.

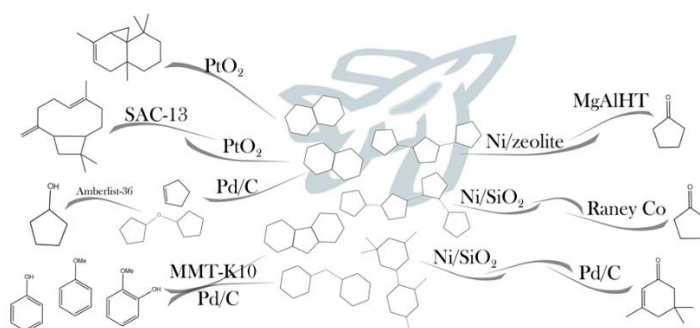


**Figure 11.** Illustration of recently developed nanocatalysts for the production of high density biofuels.

As demonstrated by Harvey *et al.*, the blending of multicyclic sesquiterpanes with SPK is a valid way to produce high density renewable diesel.<sup>217</sup> Sesquiterpanes were obtained from commercially available caryophyllene and limonene. Specifically, caryophyllane was heated with Nafion SAC-13 and sequentially hydrogenated over PtO<sub>2</sub>, whereas limonene was directly hydrogenated with PtO<sub>2</sub>. The SPK 5-methylundecane was prepared by catalytic (Zr/MAO) oligomerization of 1-hexene and by sequential hydrogenation over a Pd/C based catalyst. The resulting biofuel, composed by 65% sesquiterpanes and 35% 5-methylundecane, had a cetane number of 45.7, a density of 0.853 g mL<sup>-1</sup> and a volumetric NHOC similar to that of F-76 commercial fuel.

Interestingly, it should be mentioned that caryophyllane can be also produced in a biosynthetic way. Engineered *Escherichia coli* has been successfully employed as biocatalyst for the production of  $\beta$ -caryophyllane.<sup>218</sup> Sesquiterpenes were obtained by assembling a biosynthetic pathway in an engineered *E.coli* strain. The modified strain, named YJM59, was capable to produce 220 mg L<sup>-1</sup> of  $\beta$ -caryophyllene in flask culture. In fed batch fermentation, after 60 h, the YJM59 strain produced  $\beta$ -caryophyllene at a concentration of 1520 mg L<sup>-1</sup>.

Although terpene and sesquiterpene fuels are interesting because of their high density, lignin is more abundant than terpenoids, and therefore more economically available.<sup>219-222</sup> Chen *et al.* developed a three-step route to convert cyclopentanol, a platform lignocellulose compound, into jet fuel-range polycycloalkanes under solvent-free mild conditions.<sup>223</sup> As illustrated in Figure 12, cyclopentol was firstly dehydrated to cyclopentene over solid acids. In the second step, cyclopentene was converted to a mixture of polycycloalkenes by oligomerization/rearrangement catalyzed by Amberlyst-36 resin.

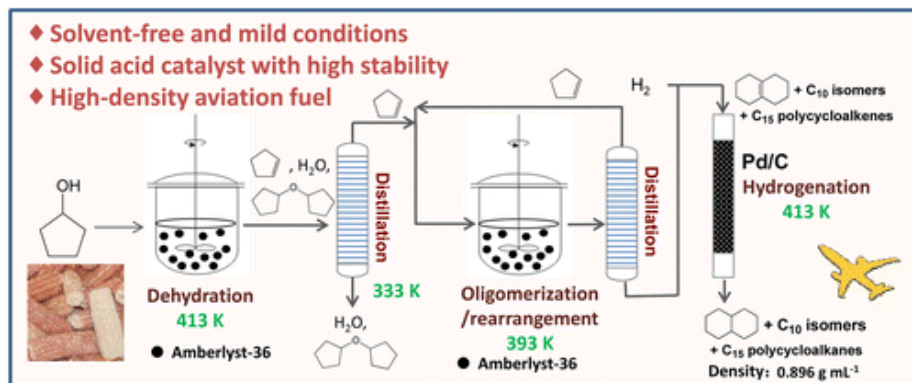


**Figure 12.** An illustration of the reaction route for the production of decaline from cyclopentanol. Taken from ref. 223. Copyright (2016), American Chemical Society.

The high activity and stability of the catalyst lead to the overall carbon yield of 62.2%. In the last step, the mixture of polycycloalkenes was further hydrogenated with Pd/C catalyst to a C<sub>10</sub> and C<sub>15</sub> mixture of polycycloalkenes. The so-produced biofuel showed a high density (0.896 g mL<sup>-1</sup>) and high content of decaline comparable to those of commercial JP-900. Another important lignocellulosic platform compound is cyclopentanone. In the literature, it has been reported that cyclopentanone can be produced by the aqueous-phase selective hydrogenation of furfural from hydrolysis of hemicellulose derived from forest residue and agriculture waste.<sup>224, 225</sup> This compound can be used as building block in the synthesis of jet fuel-range cycloalkanes. High density tri(cyclopentane), a polycycloalkane with three carbon rings, has been selectively synthesized from cyclopentanone in a dual-bed catalyst system.<sup>226</sup> In the first bed, the trimerization of cyclopentanone was obtained under solvent free conditions using MgAl-HT catalysts, obtaining up to 81.2 % carbon yield. The excellent performance of the catalyst was explained in terms of high surface area, combined with strong acidity and basicity. Furthermore, doping with noble metals such as Pt, Pd and Ru, significantly improved the catalytic activity. The best activity was obtained with the Pd-doped catalyst, which is highly active in the selective hydrogenation of C=C bond. In the second bed, condensation products of cyclopentanone were hydrodeoxygenated over a Ni/Hb zeolite catalyst. The overall reaction produced a yield of 80 % totri(cyclopentane) with density of 0.91 g mL<sup>-1</sup>, under mild reaction conditions (443 K, 0.1 MPa H<sub>2</sub>).

1-(3-cyclopentyl)cyclopentyl-2-cyclopentyl-cyclopentane has also been produced from cyclopentanone.<sup>227</sup> The procedure consisted of three steps. In the first step, 2-cyclopentylcyclopentanone was obtained through the reaction of cyclopentanone and H<sub>2</sub> under the catalysis of Raney metal and alkali hydroxides. With the best catalyst combination, Raney cobalt with KOH, the carbon yield of 83.3 % was obtained at 353 K. In the second step, solvent-free self-aldol condensation produced 2-cyclopentyl-5-(2-cyclopentylcyclopentylidene)-cyclopentanone with high carbon yield (95 %).

In the last step, 2-cyclopentyl-5-(2-cyclopentylcyclopentylidene)-cyclopentanone was hydrogenated over Ni/SiO<sub>2</sub> under solvent-free conditions, providing a carbon yield of 88.5 %. The catalyst, prepared by conventional deposition-precipitation (DP) method, was stable and no deactivation was noticed.<sup>228</sup> The obtained biofuel has a density of 0.943 g mL<sup>-1</sup> and a freezing point of 233 K. These characteristics indicate a possible application of the fuels as a substitute for the jet fuel blend J10.

In the acetone-butanol-ethanol fermentation of hemicellulose, isophorone is produced as a by-product.<sup>229</sup> Its cyclic chemical structure was exploited to produce high-density polycycloalkanes.<sup>230</sup> In detail, 1,1,3-trimethyl-5-(2,4,4-trimethylcyclohexyl) cyclohexane, was produced through three steps. Firstly, isophorone was selectively hydrogenated to 3,3,5-trimethylcyclohexanone using Pd/C as catalyst, achieving 99 % of carbon yield at room temperature in 1 h with 2 MPa H<sub>2</sub> pressure. In the second step, the self-aldol condensation of 3,3,5-trimethylcyclohexanone catalyzed with NaOH led to the production of 3,5,5-trimethyl-2-(3,3,5-trimethylcyclohexylidene) cyclohexanone. In the last step, Ni/SiO<sub>2</sub> catalyst was employed in the solvent-free hydrogenation of 3,5,5-trimethyl-2-(3,3,5-trimethylcyclohexylidene) cyclohexanone, to produce high density biofuel (0.858 g mL<sup>-1</sup>) with a carbon yield of 93.4 %. The biofuel can potentially blend with conventional fuels such as RP-1 and RG-1 for rocket propulsion.

Recently, lignin-derived phenols (phenol, anisole, guaiacol) were successfully converted into a low freezing point biofuel.<sup>231</sup> The simple process consisted of the sequential alkylation of the phenols, followed by hydrogenated intramolecular cyclization. The alkylation was performed at 383 K with benzyl ether and benzyl alcohol using Montmorillonite K10 (MMT-K10) as catalyst, leading to high conversion of anisole (32 %) and high selectivity to mono-alkylated product (68 %). The alkylation product was



hydrogenated in the presence of Pd/C and HZSM-5, producing 68.6% of perhydrofluorene and 31.4 % of dicyclohexylmethane after vacuum distillation. The biofuel has a density of 0.93 g mL<sup>-1</sup> and a freezing point of 233 K.

Handling the same lignin-derived phenols, Han *et al.* developed away to produce biofuels with freezing point down to 193 K.<sup>232</sup> The synthesis was carried out through an alkylation with furfural alcohols (furfuryl alcohol, 5-hydroxymethylfurfural) followed by hydrogenation. The alkylation with furfural alcohol was catalyzed with acid catalysts, as to generate furfuryl alcohol cations. Whereas FeCl<sub>3</sub> showed the best activity for the alkylation of anisole and guaiacol, AlCl<sub>3</sub> was most active for phenol. After hydrogenation over Pd/C and HZSM-5, the biofuel had density of 0.804 g mL<sup>-1</sup>, extremely close to the density of jet fuel blends J10.<sup>233</sup>

Although Pd/C catalyst is an extremely active catalyst for the hydrogenation of lignin model compounds, it is expensive.<sup>234, 235</sup> Non-noble metal catalysts based on Cu, Fe and Ni, have been proposed as valid cheaper alternatives.<sup>236, 237</sup> Recently, complete arene hydrogenation of phenolic compounds was obtained over a nanosized nickel catalyst.<sup>238</sup> The catalyst was prepared through borohydride reduction of Ni<sup>2+</sup> to Ni<sup>0</sup> with application of pyridine as a ligand and using ZSM-5 as support material. Pyridine was necessary for the formation of Ni particles of controlled size around 4 nm. The catalyst allowed the complete or near complete hydrogenation of the aromatic rings of phenols and its twelve derivatives at 453 K in autoclave.

### 3.2. Plastic derived high density fuels

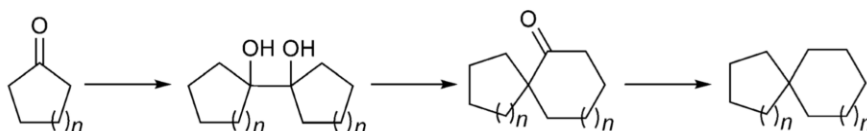
A green and captivating way to produce high density fuels could also be tracked to the recycling of plastic waste. Nowadays, approximately half of the plastic waste is disposed of, as it cannot be recovered. This issue causes several serious environmental problems such as ocean plastic pollution.<sup>239</sup> Since the direct combustion of plastics generates the release of harmful compounds, its catalytic conversion into valuable chemicals and fuels has attracted crucial interest.<sup>240</sup>

Zhang *et al.* developed an integrated technology of microwave-induced degradation followed by a hydro treating process.<sup>241</sup> Low-density polyethylene (LDPE)

was employed as a common model compound. In the first step, ZSM-5 catalyst was employed as a promoter of the microwave assisted degradation. At 650 K, the carbon yield of liquid organics achieved 66%, with a coke yield below 1 %. The sequential hydrotreating process using commercially available RANEYS nickel reached up to 95 wt% in 2 h at 523 K. The produced fuels showed a high content of cycloalkanes (53 %), which places the fuel in the navy fuel density range.

### 3.3. Other recent biomass-derived fuels

Renewable high density spiro-fuels have also been synthesized from lignocellulose-derived cyclic ketones for the first time, which show higher density, higher neat heat of combustion and lower freezing point compared with other biofuels synthesized from the same feedstock, and thus represent a new type of renewable high-density fuel attractive for practical applications (Scheme 2).<sup>242</sup>



**Scheme 2.** Reaction route for the synthesis of spirocycloalkanes from cyclic ketones.

Bio-oils, produced by the destructive distillation of cheap and renewable lignocellulosic biomass, contain high energy density oligomers in the water insoluble fraction that can be utilized for the production of diesel and valuable fine chemicals. Recently, kraft lignin from black liquor was converted into biodiesel in three steps.<sup>243</sup> First, a Ni catalyst promoted the reduction of ethers, carbonyls, and olefins using isopropanol as H-donor in mild conditions at 140°C and 8.5 bar for 16 h. In the second step, the lignin residue was treated with an organo catalyst aiming to achieve an esterified lignin residue soluble in light gas oil. Finally, the esterified lignin residue was hydro processed with commercial NiMo to produce the biofuel. The produced green fuel has average characteristics to qualify as EN590 road diesel.<sup>243</sup> More recently, an efficient

hydrodeoxygenation catalyst that combines highly dispersed palladium and ultra-fine molybdenum phosphate nanoparticles on silica was reported for the hydrodeoxygenation of phenol as a model substrate to cyclohexane under mild conditions in a batch reaction (100 % conversion, 97.5 % selectivity).<sup>244</sup> The catalyst also demonstrated are markable regeneration ability in long-term continuous flow tests. Importantly, the synthesized catalyst could perform an efficient hydrodeoxygenation of lignin, cellulose, and hemicellulose-derived oligomers into liquid alkanes with high efficiency and yields using wood- and bark-derived feedstocks. Detailed investigations into the nature of the catalyst pointed to a combination of hydrogenation activity (Pd) and high density of both Brønsted and Lewis acid sites, which are considered as key features for the observed efficient catalytic hydrodeoxygenation behaviour.<sup>244</sup>

A new vision of using carbon dioxide (CO<sub>2</sub>) catalytic processing of oleic acid into C<sub>8–15</sub> alkanes over a nano-nickel/zeolite catalyst has been very recently reported, as shown in Figure 13.<sup>245</sup> The proposed process employs an innovative catalytic reaction pathway for oleic acid transformation in a CO<sub>2</sub> atmosphere. C<sub>8–15</sub> yields could reach 73 mol% under CO<sub>2</sub> atmosphere, which is significantly larger than that obtained under hydrogen (H<sub>2</sub>) atmosphere (*ca.* 50 mol%). In the absence of an external H<sub>2</sub> source, products in the range of aviation fuel are generated where aromatization of propene (C<sub>3</sub>H<sub>6</sub>), oxidative dehydrogenation (ODH) involving CO<sub>2</sub> and propane (C<sub>3</sub>H<sub>8</sub>) and hydrogen transfer reactions are responsible for the liberation of hydrogen in oleic acid, achieving its rearrangement into the final alkane products.



**Figure 13.** A representation of the new protocol developed by Xing *et al.* Taken from ref. 244. Reproduced by permission of the Royal Society of Chemistry.

The reaction pathway under CO<sub>2</sub> atmosphere is significantly different from that under H<sub>2</sub>, as shown by the presence of 8-heptadecene,  $\gamma$ -stearo lactone, and 3-heptadecene as reaction intermediates, as well as a CO formation pathway.<sup>245</sup> Because of the highly dispersed Ni metal centres on the zeolite support in the catalyst, H<sub>2</sub> spill over is observed under H<sub>2</sub> atmosphere, which inhibits the production of short-chain alkanes and reveals the inherent disadvantage of using H<sub>2</sub>. CO<sub>2</sub> processing of oleic acid described in this manuscript can significantly contribute to future CO<sub>2</sub> utilization chemistries and provide an economic and promising approach for the production of sustainable alkane products within the range of aviation fuels.<sup>245</sup>

Last, but not least, an interesting recent dual catalysis approach enables the selective functionalization of unconventional feedstocks composed of complex fatty acid mixtures with highly unsaturated portions such as eicosapentaenoate (20:5) along with monounsaturated compounds, as shown in Figure 7.<sup>246</sup> The degree of unsaturation is unified by selective heterogeneous hydrogenation on Pd/ $\gamma$ -Al<sub>2</sub>O<sub>3</sub>, complemented by effective activation to a homogeneous carbonylation catalyst [(dtbpx)PdH(L)]<sup>+</sup> by addition of diprotonated diphosphine (dtbpxH<sub>2</sub>)(OTf)<sub>2</sub>. By this one-pot approach, neat 20:5 as a model substrate could be hydrogenated up to 80% to the monounsaturated analogue (20:1), and subsequently functionalized to the desired C<sub>21</sub>  $\alpha$ ,  $\omega$ -diester building block with a linear selectivity over 90%. This catalytic approach is demonstrated to be suitable for crude microalgae oil from *Phaeodactylum tricornutum* genetically engineered for this purpose, as well as tall oil, an abundant lignocellulosic waste material. Both substrates were fully converted with an overall selectivity to the linear  $\alpha$ ,  $\omega$ -diester of up to 75%.<sup>246</sup>

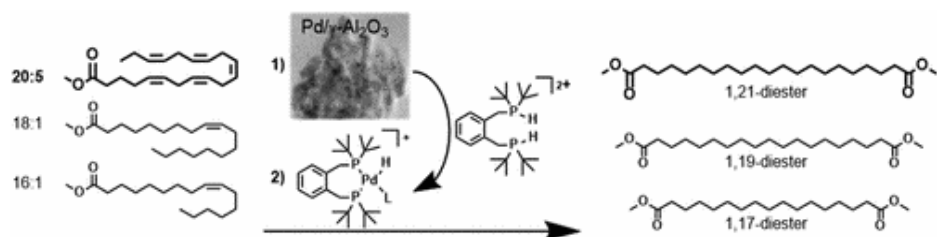


**Figure 14.** Selective functionalization of complex fatty. Taken from ref. 245. Copyright (2017), American Chemical Society.

In addition to these, other interesting molecules including alkyl levulinates and gamma-valerolactone (GVL) have also interesting potential as compounds in biofuel blends and solvents. In particular, alkyl levulinates can be produced from lignocellulosic feedstocks (C<sub>5</sub> sugars) and have been reported to be produced from furfuryl alcohol using alumina/SBA-15 heterogeneous catalysts.<sup>247</sup>

A 20 wt% Al<sub>2</sub>O<sub>3</sub>/SBA-15 catalyst exhibited the best activity in the alcoholysis of furfuryl alcohol with n-butanol, giving 94% selectivity toward n-butyl levulinate in a batch process, with results also transferable to a continuous flow process.

#### *4. Conclusions and Outlook*

Catalysts usually employed in the synthesis of biofuels are expensive or show other disadvantages such as difficult removal from the product, low stability and low selectivity. Nanotechnology has developed nanocatalysts with characteristics that can be considered intermediate between homogeneous and heterogeneous systems, combining the high activity of homogeneous catalysts, with the easy recoverability of heterogeneous solid materials. Among the different possible options to produce biofuels, the alcoholysis of oils has been frequently applied, especially for the synthesis of biodiesel. Most advanced nanocatalysts for the production of biodiesel are base nanocatalysts, acid nanocatalysts, and bifunctional nanocatalysts. Base nanocatalysts accelerate the reaction in mild reaction conditions, but need pure oils. In contrast, acid catalysts can catalyze the alcoholysis of low-grade feedstock, but time consuming processes are required. Bifunctional catalysts have been proposed as solutions for biodiesel production from low grade oils in a one-step reaction, catalyzing at the same time the transesterification and esterification reaction of oils and fats. Nanocatalysts have been successfully employed also for the production of high density biofuels. Notably, in addition to the utilization of biomass feedstocks such as terpenoids or lignin, high density biofuels have been prepared from plastic waste, offering additional possibilities to the conversion of waste-derived feedstocks into valuable products (biofuels) as part of the waste valorization concept.

1. Source: Web of Science, © 2019 Clarivate Analytics.
2. Stark, W. J.; Pratsinis, S. E., Aerosol flame reactors for manufacture of nanoparticles. *Powder Technology* **2002**, *126* (2), 103-108.
3. Sastry, M.; Swami, A.; Mandal, S.; Selvakannan, P. R., New approaches to the synthesis of anisotropic, core-shell and hollow metal nanostructures. *Journal of Materials Chemistry* **2005**, *15* (31), 3161-3174.
4. Wang, H. J.; Jeong, H. Y.; Imura, M.; Wang, L.; Radhakrishnan, L.; Fujita, N.; Castle, T.; Terasaki, O.; Yamauchi, Y., Shape- and Size-Controlled Synthesis in Hard Templates: Sophisticated Chemical Reduction for Mesoporous Monocrystalline Platinum Nanoparticles. *Journal of the American Chemical Society* **2011**, *133* (37), 14526-14529.
5. Sneed, B. T.; Brodsky, C. N.; Kuo, C. H.; Lamontagne, L. K.; Jiang, Y.; Wang, Y.; Tao, F.; Huang, W. X.; Tsung, C. K., Nanoscale-Phase-Separated Pd-Rh Boxes Synthesized via Metal Migration: An Archetype for Studying Lattice Strain and Composition Effects in Electrocatalysis. *Journal of the American Chemical Society* **2013**, *135* (39), 14691-14700.
6. Rafique, M.; Sadaf, I.; Rafique, M. S.; Tahir, M. B., A review on green synthesis of silver nanoparticles and their applications. *Artificial Cells Nanomedicine and Biotechnology* **2017**, *45* (7), 1272-1291.
7. Shanker, U.; Jassal, V.; Rani, M.; Kaith, B. S., Towards green synthesis of nanoparticles: From bio-assisted sources to benign solvents. A review. *International Journal of Environmental Analytical Chemistry* **2016**, *96* (9), 801-835.
8. Nabi, G.; Qurat ul, A.; Khalid, N. R.; Tahir, M. B.; Rafique, M.; Rizwan, M.; Hussain, S.; Iqbal, T.; Majid, A., A Review on Novel Eco-Friendly Green Approach to Synthesis TiO<sub>2</sub> Nanoparticles Using Different Extracts. *Journal of Inorganic and Organometallic Polymers and Materials* **2018**, *28* (4), 1552-1564.
9. El-Seedi, H. R.; El-Shabasy, R. M.; Khalifa, S. A. M.; Saeed, A.; Shah, A.; Shah, R.; Iftikhar, F. J.; Abdel-Daim, M. M.; Omri, A.; Hajrahand, N. H.; Sabir, J. S. M.; Zou, X. B.; Halabi, M. F.; Sarhan, W.; Guo, W. S., Metal nanoparticles fabricated by green chemistry using natural extracts: biosynthesis, mechanisms, and applications. *RSC Advances* **2019**, *9* (42), 24539-24559.
10. Sun, Y. G.; Xia, Y. N., Shape-controlled synthesis of gold and silver nanoparticles. *Science* **2002**, *298* (5601), 2176-2179.
11. Lance Kelly, K.; Coronado, E.; Zhao, L. L.; Schatz, G. C., The Optical Properties of Metal Nanoparticles: The Influence of Size, Shape, and Dielectric Environment. *Journal of Physical Chemistry B* **2002**, *107* (3), 668-677
12. Daniel, M. C.; Astruc, D., Gold nanoparticles: Assembly, supramolecular chemistry, quantum-size-related properties, and applications toward biology, catalysis, and nanotechnology. *Chemical Reviews* **2004**, *104* (1), 293-346.
13. Sharma, V. K.; Yngard, R. A.; Lin, Y., Silver nanoparticles: Green synthesis and their antimicrobial activities. *Advances in Colloid and Interface Science* **2009**, *145* (1-2), 83-96.
14. Blanco-Andujar, C.; Le Duc, T.; Thanh, N. T. K., Synthesis of nanoparticles for biomedical applications. *Annual Reports on the Progress of Chemistry, Section a: Inorganic Chemistry* **2010**, *106*, 553-568.
15. Mallat, T.; Baiker, A., Potential of Gold Nanoparticles for Oxidation in Fine Chemical Synthesis. In *Annual Review of Chemical and Biomolecular Engineering, Vol 3*, Prausnitz, J. M., Ed. 2012; Vol. 3, pp 11-28.
16. Mirzaei, H.; Darroudi, M., Zinc oxide nanoparticles: Biological synthesis and biomedical applications. *Ceramics International* **2017**, *43* (1), 907-914.
17. Ong, C. B.; Ng, L. Y.; Mohammad, A. W., A review of ZnO nanoparticles as solar photocatalysts: Synthesis, mechanisms and applications. *Renewable & Sustainable Energy Reviews* **2018**, *81*, 536-551.
18. Liu, L. C.; Corma, A., Metal Catalysts for Heterogeneous Catalysis: From Single Atoms to Nanoclusters and Nanoparticles. *Chemical Reviews* **2018**, *118* (10), 4981-5079.

19. Ambrosi, M.; Fratini, E.; Canton, P.; Dankesreiter, S.; Baglioni, P., Bottom-up/top-down synthesis of stable zirconium hydroxide nanophases. *Journal of Materials Chemistry* **2012**, *22* (44), 23497-23505.
20. Hill, L. E.; Gomes, C. L., Optimization of synthesis process of thermally-responsive poly-n-isopropylacrylamide nanoparticles for controlled release of antimicrobial hydrophobic compounds. *Materials Research Express* **2014**, *1* (4).
21. Glasnov, T. N.; Kappe, C. O., The Microwave-to-Flow Paradigm: Translating High-Temperature Batch Microwave Chemistry to Scalable Continuous-Flow Processes. *Chemistry-a European Journal* **2011**, *17* (43), 11956-11968.
22. Maddikeri, G. L.; Pandit, A. B.; Gogate, P. R., Intensification Approaches for Biodiesel Synthesis from Waste Cooking Oil: A Review. *Industrial & Engineering Chemistry Research* **2012**, *51* (45), 14610-14628.
23. Patil, D. M.; Akamanchi, K. G., Microwave assisted process intensification and kinetic modelling: Extraction of camptothecin from *Nothapodytes nimmoniana* plant. *Industrial Crops and Products* **2017**, *98*, 60-67.
24. Ding, H.; Ye, W.; Wang, Y. Q.; Wang, X. Q.; Li, L. J.; Liu, D.; Gui, J. Z.; Song, C. F.; Ji, N., Process intensification of transesterification for biodiesel production from palm oil: Microwave irradiation on transesterification reaction catalyzed by acidic imidazolium ionic liquids. *Energy* **2018**, *144*, 957-967.
25. Nuchter, M.; Ondruschka, B.; Bonrath, W.; Gum, A., Microwave assisted synthesis - a critical technology overview. *Green Chemistry* **2004**, *6* (3), 128-141.
26. Polshettiwar, V.; Varma, R. S., Microwave-assisted organic synthesis and transformations using benign reaction media. *Accounts of Chemical Research* **2008**, *41* (5), 629-639.
27. Xu, H.; Xing, S. J.; Zeng, L. P.; Xian, Y. Z.; Shi, G. Y.; Jin, L. T., Microwave-enhanced voltammetric detection of copper(II) at gold nanoparticles-modified platinum microelectrodes. *Journal of Electroanalytical Chemistry* **2009**, *625* (1), 53-59.
28. Anandam, S.; Selvamuthukumar, S., Optimization of microwave-assisted synthesis of cyclodextrin nanosponges using response surface methodology. *Journal of Porous Materials* **2014**, *21* (6), 1015-1023.
29. Rosa, R.; Ponzoni, C.; Veronesi, P.; Sora, I. N.; Felice, V.; Leonelli, C., Solution combustion synthesis of La-1 (-) xSrxFe1-yCuyO3 (+/-) (w) (x=0, 0.2; y=0, 0.2) perovskite nanoparticles: Conventional vs. microwaves ignition. *Ceramics International* **2015**, *41* (6), 7803-7810.
30. Horikoshi, S.; Abe, H.; Torigoe, K.; Abe, M.; Serpone, N., Access to small size distributions of nanoparticles by microwave-assisted synthesis. Formation of Ag nanoparticles in aqueous carboxymethylcellulose solutions in batch and continuous-flow reactors. *Nanoscale* **2010**, *2* (8), 1441-1447.
31. Sarkar, K. T.; Mailloux, J. R.; Oliner, A.; Salazar-Palma, M. S.; Dipak L., *History of Wireless*. Wiley & Sons, Inc. : 2006.
32. Hull, A. W., The effect of a uniform magnetic field on the motion of electrons between coaxial cylinders. *Physical Review* **1921**, *18* (1), 31-57.
33. Hackmann, W., Meters to microwaves - british development of active components for radar systems 1937 to 1944 - Callick,eb. *British Journal for the History of Science* **1993**, *26* (90), 376-377.
34. Antonio, d. I. H.; Loupy, A., *Microwaves in Organic Synthesis, Third Edition*. Wiley-VCH Verlag GmbH & Co.: Weinheim, 2013.
35. Schiffmann, R. F., Industrial microwave heating of food: principles and three case studies of its commercialization. *Case Studies in Novel Food Processing Technologies: Innovations in Processing, Packaging, and Predictive Modelling* **2010**, (197), 407-426.
36. Tamborrino, A.; Romaniello, R.; Caponio, F.; Squeo, G.; Leone, A., Combined industrial olive oil extraction plant using ultrasounds, microwave, and heat exchange: Impact on olive oil quality and yield. *Journal of Food Engineering* **2019**, *245*, 124-130.

37. Satoshi, H., Serpone, *Microwaves in Nanoparticle Synthesis*, Wiley-VCH Verlag GmbH & Co.: Weinheim, 2013.
38. Gedye, R.; Smith, F.; Westaway, K.; Ali, H.; Baldisera, L.; Laberge, L.; Rousell, J., THE USE OF MICROWAVE-OVENS FOR RAPID ORGANIC-SYNTHESIS. *Tetrahedron Letters* **1986**, 27 (3), 279-282.
39. Giguere, R. J.; Bray, T. L.; Duncan, S. M.; Majetich, G., APPLICATION OF COMMERCIAL MICROWAVE-OVENS TO ORGANIC-SYNTHESIS. *Tetrahedron Letters* **1986**, 27 (41), 4945-4948.
40. Kappe, C. O.; Stadler, A., Microwaves in Organic and Medicinal Chemistry. *Microwaves in Organic and Medicinal Chemistry* **2005**, 52, 1-409.
41. <https://www.anton-paar.com/za-en/products/group/microwave-synthesis-synthetic-chemistry/>.
42. <http://cem.com/en>.
43. <https://www.milestonesrl.com/>.
44. Richards, L. A., The use of triode vacuum tube rectifiers to supply constant voltage. *Review of Scientific Instruments* **1933**, 4 (9), 479-482.
45. Madore, C.; Matlosz, M.; Landolt, D., EXPERIMENTAL INVESTIGATION OF THE PRIMARY AND SECONDARY CURRENT DISTRIBUTION IN A ROTATING CYLINDER HULL CELL. *Journal of Applied Electrochemistry* **1992**, 22 (12), 1155-1160.
46. Mansuripur, M.; Zakharian, A. R., Maxwell's macroscopic equations, the energy-momentum postulates, and the Lorentz law of force. *Physical Review E* **2009**, 79 (2), 1-10.
47. Lagroye, I.; Anane, R.; Wetrting, B. A.; Moros, E. G.; Straube, W. L.; Laregina, M.; Niehoff, M.; Pickard, W. F.; Baty, J.; Roti, J. L. R., Measurement of DNA damage after acute exposure to pulsed-wave 2450 MHz microwaves in rat brain cells by two alkaline comet assay methods. *International Journal of Radiation Biology* **2004**, 80 (1), 11-20.
48. Lagroye, I.; Hook, G. J.; Wetrting, B. A.; Baty, J. D.; Moros, E. G.; Straube, W. L.; Roti, J. L. R., Measurements of alkali-labile DNA damage and protein-DNA crosslinks after 2450 MHz microwave and low-dose gamma irradiation in vitro. *Radiation Research* **2004**, 161 (2), 201-214.
49. Hilsun, C., Semiconductor microwave generators. *Journal of Physics D-Applied Physics* **1968**, 1 (3), 265-275.
50. Boot, H. A. H.; Randall, J. T., Historical notes on cavity magnetron. *Ieee Transactions on Electron Devices* **1976**, 23 (7), 724-729.
51. Bogdal, D.; Prociak, A., *Microwave-Enhanced Polymer Chemistry and Technology*. Blackwell Publishing: Oxford, 2007.
52. Kappe, C. O.; Dallinger, D.; Murphree, S. S., *Practical Microwave Synthesis for Organic Chemistry: Strategies, Instruments, and Protocols*. WILEY-VCH Verlag GmbH & Co. KGaA: Weinheim, 2009.
53. Liao, H.; Li, D.; Zhou, C.; Liu, T., Microporous Co/rGO nanocomposites: Strong and broadband microwave absorber with well-matched dielectric and magnetic loss. *Journal of Alloys and Compounds* **2019**, 782, 556-565.
54. Mingos, D. M. P.; Baghurst, D. R., Applications of microwave dielectric heating effects to synthetic problems in chemistry. *Chemical Society Reviews* **1991**, 20 (1), 1-47.
55. Peng, Z.; Hwang, J.-Y.; Mouris, J.; Hutcheon, R.; Huang, X., Microwave Penetration Depth in Materials with Non-zero Magnetic Susceptibility. *Isij International* **2010**, 50 (11), 1590-1596.
56. Kuhnert, N., Microwave-assisted reactions in organic synthesis - Are there any nonthermal microwave effects? *Angewandte Chemie-International Edition* **2002**, 41 (11), 1863-1866.



57. Herrero, M. A.; Kremsner, J. M.; Kappe, C. O., Nonthermal microwave effects revisited: On the importance of internal temperature monitoring and agitation in microwave chemistry. *Journal of Organic Chemistry* **2008**, *73* (1), 36-47.
58. Kappe, C. O.; Pieber, B.; Dallinger, D., Microwave Effects in Organic Synthesis: Myth or Reality? *Angewandte Chemie-International Edition* **2013**, *52* (4), 1088-1094.
59. Matli, P. R.; Shakoore, R. A.; Mohamed, A. M. A.; Gupta, M., Microwave Rapid Sintering of Al-Metal Matrix Composites: A Review on the Effect of Reinforcements, Microstructure and Mechanical Properties. *Metals* **2016**, *6* (7), 143.
60. Hou, J.; Li, H. Y.; Wang, L.; Zhang, P.; Zhou, T. Y.; Ding, H.; Ding, L., Rapid microwave-assisted synthesis of molecularly imprinted polymers on carbon quantum dots for fluorescent sensing of tetracycline in milk. *Talanta* **2016**, *146*, 34-40.
61. Guo, Y. F.; Li, J.; Yuan, Y. P.; Li, L.; Zhang, M. Y.; Zhou, C. Y.; Lin, Z. Q., A Rapid Microwave-Assisted Thermolysis Route to Highly Crystalline Carbon Nitrides for Efficient Hydrogen Generation. *Angewandte Chemie-International Edition* **2016**, *55* (47), 14693-14697.
62. Ferrari, A.; Hunt, J.; Stiegman, A.; Dudley, G. B., Microwave-Assisted Superheating and/or Microwave-Specific Superboiling (Nucleation-Limited Boiling) of Liquids Occurs under Certain Conditions but is Mitigated by Stirring. *Molecules* **2015**, *20* (12), 21672-21680.
63. Horikoshi, S.; Kamata, M.; Sumi, T.; Serpone, N., Selective heating of Pd/AC catalyst in heterogeneous systems for the microwave-assisted continuous hydrogen evolution from organic hydrides: Temperature distribution in the fixed-bed reactor. *International Journal of Hydrogen Energy* **2016**, *41* (28), 12029-12037.
64. Raner, K. D.; Strauss, C. R.; Trainor, R. W.; Thorn, J. S., A new microwave reactor for batchwise organic-synthesis. *Journal of Organic Chemistry* **1995**, *60* (8), 2456-2460.
65. Tsuzuki, T., Commercial scale production of inorganic nanoparticles. *International Journal of Nanotechnology* **2009**, *6* (5-6), 567-578.
66. Malinoski, F. J., The nanomedicines alliance: an industry perspective on nanomedicines. *Nanomedicine-Nanotechnology Biology and Medicine* **2014**, *10* (8), 1819-1820.
67. Foldbjerg, R.; Jiang, X. M.; Miclaus, T.; Chen, C. Y.; Autrup, H.; Beer, C., Silver nanoparticles - wolves in sheep's clothing? *Toxicology Research* **2015**, *4* (3), 563-575.
68. Zaytseva, O.; Neumann, G., Carbon nanomaterials: production, impact on plant development, agricultural and environmental applications. *Chemical and Biological Technologies in Agriculture* **2016**, *3* (17).
69. Gupta, R.; Xie, H., Nanoparticles in Daily Life: Applications, Toxicity and Regulations. *Journal of Environmental Pathology Toxicology and Oncology* **2018**, *37* (3), 209-230.
70. Foladori, G.; Invernizzi, N., A Critical Vision of Disruptive Nanotechnologies. *Perspectives on Global Development and Technology* **2018**, *17* (5-6), 614-631.
71. Somorjai, G. A.; Frei, H.; Park, J. Y., Advancing the Frontiers in Nanocatalysis, Biointerfaces, and Renewable Energy Conversion by Innovations of Surface Techniques. *Journal of the American Chemical Society* **2009**, *131* (46), 16589-16605.
72. Polshettiwar, V.; Asefa, T., Nanocatalysis Synthesis and Applications. John Wiley & Sons, Inc.: 2013.
73. Roldan Cuenya, B.; Behafarid, F., Nanocatalysis: size- and shape-dependent chemisorption and catalytic reactivity. *Surface Science Reports* **2015**, *70* (2), 135-187.
74. Yang, F.; Deng, D. H.; Pan, X. L.; Fu, Q.; Bao, X. H., Understanding nano effects in catalysis. *National Science Review* **2015**, *2* (2), 183-201.
75. Wang, S. B.; Boyjoo, Y.; Choueib, A.; Zhu, Z. H., Removal of dyes from aqueous solution using fly ash and red mud. *Water Research* **2005**, *39* (1), 129-138.

76. Crini, G., Non-conventional low-cost adsorbents for dye removal: A review. *Bioresource Technology* **2006**, *97* (9), 1061-1085.
77. Frumkin, H.; Hess, J.; Vindigni, S., Energy and Public Health: The Challenge of Peak Petroleum. *Public Health Reports* **2009**, *124* (1), 5-19.
78. Oregan, B.; Gratzel, M., A low-cost, high-efficiency solar-cell based on dye-sensitized colloidal TiO<sub>2</sub> films. *Nature* **1991**, *353* (6346), 737-740.
79. Fan, W. G.; Jewell, S.; She, Y. Y.; Leung, M. K. H., In situ deposition of Ag-Ag<sub>2</sub>S hybrid nanoparticles onto TiO<sub>2</sub> nanotube arrays towards fabrication of photoelectrodes with high visible light photoelectrochemical properties. *Physical Chemistry Chemical Physics* **2014**, *16* (2), 676-680.
80. Chiarello, G. L.; Zuliani, A.; Ceresoli, D.; Martinazzo, R.; Selli, E., Exploiting the Photonic Crystal Properties of TiO<sub>2</sub> Nanotube Arrays To Enhance Photocatalytic Hydrogen Production. *Acs Catalysis* **2016**, *6* (2), 1345-1353.
81. Tran, V. A.; Truong, T. T.; Phan, T. A. P.; Nguyen, T. N.; Huynh, T. V.; Agresti, A.; Pescetelli, S.; Le, T. K.; Di Carlo, A.; Lund, T.; Le, S. N.; Nguyen, P. T., Application of nitrogen-doped TiO<sub>2</sub> nano-tubes in dye-sensitized solar cells. *Applied Surface Science* **2017**, *399*, 515-522.
82. Ahmadi, M.; Motlagh, H. R.; Jaafarzadeh, N.; Mostoufi, A.; Saeedi, R.; Barzegar, G.; Jorfi, S., Enhanced photocatalytic degradation of tetracycline and real pharmaceutical wastewater using MWCNT/TiO<sub>2</sub> nanocomposite. *Journal of Environmental Management* **2017**, *186*, 55-63.
83. Yang, L.; Wang, W. H.; Zhang, H.; Wang, S. H.; Zhang, M.; He, G.; Lv, J. G.; Zhu, K. R.; Sun, Z. Q., Electrodeposited Cu<sub>2</sub>O on the {101} facets of TiO<sub>2</sub> nanosheet arrays and their enhanced photoelectrochemical performance. *Solar Energy Materials and Solar Cells* **2017**, *165*, 27-35.
84. Zhu, M. P.; Muhammad, Y.; Hu, P.; Wang, B. F.; Wu, Y.; Sun, X. D.; Tong, Z. F.; Zhao, Z. X., Enhanced interfacial contact of dopamine bridged melamine-graphene/TiO<sub>2</sub> nano-capsules for efficient photocatalytic degradation of gaseous formaldehyde. *Applied Catalysis B-Environmental* **2018**, *232*, 182-193.
85. Zhang, X. C.; Hu, W. Y.; Zhang, K. F.; Wang, J. N.; Sun, B. J.; Li, H. Z.; Qiao, P. Z.; Wang, L.; Zhou, W., Ti<sup>3+</sup> Self-Doped Black TiO<sub>2</sub> Nanotubes with Mesoporous Nanosheet Architecture as Efficient Solar-Driven Hydrogen Evolution Photocatalysts. *ACS Sustainable Chemistry & Engineering* **2017**, *5* (8), 6894-6901.
86. Fenoll, J.; Ruiz, E.; Hellin, P.; Flores, P.; Navarro, S., Heterogeneous photocatalytic oxidation of cyprodinil and fludioxonil in leaching water under solar irradiation. *Chemosphere* **2011**, *85* (8), 1262-1268.
87. Phuong Nguyen, T.; Rtimi, S.; Tuan Anh, N.; Minh Thanh, V., Physics, Electrochemistry, Photochemistry, and Photoelectrochemistry of Hybrid Nanoparticles. *Noble Metal-Metal Oxide Hybrid Nanoparticles: Fundamentals and Applications* **2019**, 95-123.
88. Huang, H. J.; Zhang, J.; Jiang, L.; Zang, Z. G., Preparation of cubic Cu<sub>2</sub>O nanoparticles wrapped by reduced graphene oxide for the efficient removal of rhodamine B. *Journal of Alloys and Compounds* **2017**, *718*, 112-115.
89. Devi, H. S.; Sofi, A. H.; Singh, T. D.; Shah, M. A., Facile Hydrothermal Synthesis of Cu and Al Oxide Nanoparticles for Photodegradation of Chlorpyrifos. *Journal of Nanoscience and Nanotechnology* **2019**, *19* (12), 7707-7713.
90. Liu, W.; Zhou, J.; Hu, Z., Nano-sized g-C<sub>3</sub>N<sub>4</sub> thin layer @ CeO<sub>2</sub> sphere core-shell photocatalyst combined with H<sub>2</sub>O<sub>2</sub> to degrade doxycycline in water under visible light irradiation. *Separation and Purification Technology* **2019**, 227.
91. Dutta, D. P.; Dagar, D., Efficient Selective Sorption of Cationic Organic Pollutant from Water and Its Photocatalytic Degradation by AlVO<sub>4</sub>/g-C<sub>3</sub>N<sub>4</sub> Nanocomposite. *Journal of Nanoscience and Nanotechnology* **2020**, *20* (4), 2179-2194.
92. Lu, Q. P.; Yu, Y. F.; Ma, Q. L.; Chen, B.; Zhang, H., 2D Transition-Metal-Dichalcogenide-Nanosheet-Based Composites for Photocatalytic and Electrocatalytic Hydrogen Evolution Reactions. *Advanced Materials* **2016**, *28* (10), 1917-1933.

93. Li, J.; Liu, E. Z.; Ma, Y. N.; Hu, X. Y.; Wan, J.; Sun, L.; Fan, J., Synthesis of MoS<sub>2</sub>/g-C<sub>3</sub>N<sub>4</sub> nanosheets as 2D heterojunction photocatalysts with enhanced visible light activity. *Applied Surface Science* **2016**, *364*, 694-702.
94. Zeng, B.; Zeng, W. J., Microwave-Assisted Ion-Exchange Synthesis and Enhanced Visible-Light Photoactivity of Graphene-CdS/CuS Nanoplates. *Journal of Nanoscience and Nanotechnology* **2020**, *20* (4), 2365-2371.
95. Feng, J.; Sun, Y.; Mu, J. L.; Chen, L. D.; Han, T. X.; Miao, H.; Liu, E. Z.; Fan, J.; Hu, X. Y., Microwave-assistant synthesis of Au/SnS<sub>2</sub> nanoflowers as improved visible-light responsive photocatalysts. *Materials Letters* **2019**, *236*, 534-537.
96. Shi, W. D.; Yan, Y.; Yan, X., Microwave-assisted synthesis of nano-scale BiVO<sub>4</sub> photocatalysts and their excellent visible-light-driven photocatalytic activity for the degradation of ciprofloxacin. *Chemical Engineering Journal* **2013**, *215*, 740-746.
97. Saha, S.; Pal, A.; Kundu, S.; Basu, S.; Pal, T., Photochemical Green Synthesis of Calcium-Alginate-Stabilized Ag and Au Nanoparticles and Their Catalytic Application to 4-Nitrophenol Reduction. *Langmuir* **2010**, *26* (4), 2885-2893.
98. Rafique, M.; Sadaf, I.; Tahira, M. B.; Rafique, M. S.; Nabi, G.; Iqbal, T.; Sughra, K., Novel and facile synthesis of silver nanoparticles using Albizia procera leaf extract for dye degradation and antibacterial applications. *Materials Science & Engineering C-Materials for Biological Applications* **2019**, *99*, 1313-1324.
99. Shylesh, S.; Schunemann, V.; Thiel, W. R., Magnetically Separable Nanocatalysts: Bridges between Homogeneous and Heterogeneous Catalysis. *Angewandte Chemie-International Edition* **2010**, *49* (20), 3428-3459.
100. Singh, S. K.; Iizuka, Y.; Xu, Q., Nickel-palladium nanoparticle catalyzed hydrogen generation from hydrous hydrazine for chemical hydrogen storage. *International Journal of Hydrogen Energy* **2011**, *36* (18), 11794-11801.
101. Kudr, J.; Haddad, Y.; Richtera, L.; Heger, Z.; Cernak, M.; Adam, V.; Zitka, O., Magnetic Nanoparticles: From Design and Synthesis to Real World Applications. *Nanomaterials* **2017**, *7* (9), 243.
102. Tsang, S. C.; Caps, V.; Paraskevas, I.; Chadwick, D.; Thompsett, D., Magnetically separable, carbon-supported nanocatalysts for the manufacture of fine chemicals. *Angewandte Chemie-International Edition* **2004**, *43* (42), 5645-5649.
103. Fel'dblyum, V. S.; Antonova, T. N.; Zefirov, N. S., Cyclization and dehydrocyclization of C-5 hydrocarbons over platinum nanocatalysts and in the presence of hydrogen sulfide. *Doklady Chemistry* **2009**, *424*, 27-30.
104. Polshettiwar, V.; Luque, R.; Fihri, A.; Zhu, H.; Bouhrara, M.; Bassett, J.-M., Magnetically Recoverable Nanocatalysts. *Chemical Reviews* **2011**, *111* (5), 3036-3075.
105. Liu, R.; Zhao, Q. S.; Li, Y.; Zhang, G. L.; Zhang, F. B.; Fan, X. B., Graphene Supported Pt/Ni Nanoparticles as Magnetically Separable Nanocatalysts. *Journal of Nanomaterials* **2013**.
106. Cao, S. W.; Tao, F.; Tang, Y.; Li, Y. T.; Yu, J. G., Size- and shape-dependent catalytic performances of oxidation and reduction reactions on nanocatalysts. *Chemical Society Reviews* **2016**, *45* (17), 4747-4765.
107. Iqbal, A.; Iqbal, K.; Li, B.; Gong, D.; Qin, W., Recent Advances in Iron Nanoparticles: Preparation, Properties, Biological and Environmental Application. *Journal of Nanoscience and Nanotechnology* **2017**, *17* (7), 4386-4409.
108. Wang, D.; Astruc, D., The recent development of efficient Earth-abundant transition-metal nanocatalysts. *Chemical Society Reviews* **2017**, *46* (3), 816-854.
109. Mayoral, E. P.; Soriano, E.; Calvino-Casilda, V.; Rojas-Cervantes, M. L.; Martin-Aranda, R. M., Silica-based nanocatalysts in the C-C and C-heteroatom bond forming cascade reactions for the synthesis of biologically active heterocyclic scaffolds. *Catalysis Today* **2017**, *285*, 65-88.

110. Shrestha, S.; Mustain, W. E., Platinum Nanoparticles Supported on N-Functionalized Mesoporous Carbon. *ECS Transactions* **2010**, *33*(1):293-302
111. Xu, X.; Li, Y.; Gong, Y. T.; Zhang, P. F.; Li, H. R.; Wang, Y., Synthesis of Palladium Nanoparticles Supported on Mesoporous N-Doped Carbon and Their Catalytic Ability for Biofuel Upgrade. *Journal of the American Chemical Society* **2012**, *134* (41), 16987-16990.
112. Shang, L.; Bian, T.; Zhang, B. H.; Zhang, D. H.; Wu, L. Z.; Tung, C. H.; Yin, Y. D.; Zhang, T. R., Graphene-Supported Ultrafine Metal Nanoparticles Encapsulated by Mesoporous Silica: Robust Catalysts for Oxidation and Reduction Reactions. *Angewandte Chemie-International Edition* **2014**, *53* (1), 250-254.
113. Braganca, L. F. F. P. G.; Avillez, R. R.; Moreira, C. R.; Pais da Silva, M. I., Synthesis and characterization of Co-Fe nanoparticles supported on mesoporous silicas. *Materials Chemistry and Physics* **2013**, *138* (1), 17-28.
114. Zienkiewicz-Strzalka, M.; Derylo-Marczewska, A.; Pikus, S., Bimetallic systems of mesoporous ordered silica supports and noble metals nanoparticles. *Microporous and Mesoporous Materials* **2016**, *227*, 228-241.
115. Srivastava, V., Mesoporous Silica Supported Ru Nanoparticles for Hydrogenation of CO<sub>2</sub> Molecule. *Letters in Organic Chemistry* **2017**, *14* (2), 74-79.
116. Moon, R. J.; Martini, A.; Nairn, J.; Simonsen, J.; Youngblood, J., Cellulose nanomaterials review: structure, properties and nanocomposites. *Chemical Society Reviews* **2011**, *40* (7), 3941-3994.
117. Patino-Ruiz, D.; Sanchez-Botero, L.; Hinestroza, J.; Herrera, A., Modification of Cotton Fibers with Magnetite and Magnetic Core-Shell Mesoporous Silica Nanoparticles. *Physica Status Solidi a-Applications and Materials Science* **2018**, *215* (19).
118. Kontturi, E.; Laaksonen, P.; Linder, M. B.; Nonappa; Groschel, A. H.; Rojas, O. J.; Ikkala, O., Advanced Materials through Assembly of Nanocelluloses. *Advanced Materials* **2018**, *30* (24).
119. Veisi, H.; Najafi, S.; Hemmati, S., Pd(II)/Pd(0) anchored to magnetic nanoparticles (Fe<sub>3</sub>O<sub>4</sub>) modified with biguanidine-chitosan polymer as a novel nanocatalyst for Suzuki-Miyaura coupling reactions. *International Journal of Biological Macromolecules* **2018**, *113*, 186-194.
120. Wei, X. R.; Zhang, Z. J.; Zhou, M. Y.; Zhang, A. J.; Wu, W. D.; Wu, Z. X., Solid-state nanocasting synthesis of ordered mesoporous CoN<sub>x</sub>-carbon catalysts for highly efficient hydrogenation of nitro compounds. *Nanoscale* **2018**, *10* (35), 16839-16847.
121. Turner, M.; Golovko, V. B.; Vaughan, O. P. H.; Abdulkin, P.; Berenguer-Murcia, A.; Tikhov, M. S.; Johnson, B. F. G.; Lambert, R. M., Selective oxidation with dioxygen by gold nanoparticle catalysts derived from 55-atom clusters. *Nature* **2008**, *454* (7207), 981-983.
122. Li, L.; Ji, W.; Au, C.-T., Gold Nanoparticles Supported on Mesoporous Silica and Their Catalytic Application. *Progress in Chemistry* **2009**, *21* (9), 1742-1749.
123. He, L.; Ni, J.; Sun, H.; Cao, Y., Gold Nanocatalysis for Green Synthesis of Fine Chemicals: Opportunities and Challenges. *Chinese Journal of Catalysis* **2009**, *30* (9), 958-964.
124. Biao, L. H.; Tan, S. N.; Meng, Q. H.; Gao, J.; Zhang, X. W.; Liu, Z. G.; Fu, Y. J., Green Synthesis, Characterization and Application of Proanthocyanidins-Functionalized Gold Nanoparticles. *Nanomaterials* **2018**, *8* (1).
125. Menegazzo, F.; Signoretto, M.; Fantinel, T.; Manzoli, M., Sol-immobilized vs deposited-precipitated Au nanoparticles supported on CeO<sub>2</sub> for furfural oxidative esterification. *Journal of Chemical Technology and Biotechnology* **2017**, *92* (9), 2196-2205.
126. Najafinejad, M. S.; Mohammadi, P.; Afsahi, M. M.; Sheibani, H., Biosynthesis of Au nanoparticles supported on Fe<sub>3</sub>O<sub>4</sub>@polyaniline as a heterogeneous and reusable magnetic nanocatalyst for reduction of the azo dyes at ambient temperature. *Materials Science & Engineering C-Materials for Biological Applications* **2019**, *98*, 19-29.

127. Kumari, M. M.; Philip, D., Facile one-pot synthesis of gold and silver nanocatalysts using edible coconut oil. *Spectrochimica Acta Part A-Molecular and Biomolecular Spectroscopy* **2013**, *111*, 154-160.
128. Ding, J.; Fan, M.; Zhong, Q.; Russell, A. G., Single-atom silver-manganese nanocatalysts based on atom-economy design for reaction temperature-controlled selective hydrogenation of bioresources-derivable diethyl oxalate to ethyl glycolate and acetaldehyde diethyl acetal. *Applied Catalysis B-Environmental* **2018**, *232*, 348-354.
129. Joseph, S.; Mathew, B., Microwave assisted facile green synthesis of silver and gold nanocatalysts using the leaf extract of *Aerva lanata*. *Spectrochimica Acta Part A-Molecular and Biomolecular Spectroscopy* **2015**, *136*, 1371-1379.
130. Veisi, H.; Dadres, N.; Mohammadi, P.; Hemmati, S., Green synthesis of silver nanoparticles based on oil-water interface method with essential oil of orange peel and its application as nanocatalyst for A3 coupling. *Materials science & engineering. C, Materials for biological applications* **2019**, *105*, 110031.
131. Ragauskas, A. J.; Williams, C. K.; Davison, B. H.; Britovsek, G.; Cairney, J.; Eckert, C. A.; Frederick, W. J.; Hallett, J. P.; Leak, D. J.; Liotta, C. L.; Mielenz, J. R.; Murphy, R.; Templer, R.; Tschaplinski, T., The Path Forward for Biofuels and Biomaterials. *Science* **2006**, *311* (5760), 484-489.
132. Marchetti, J. M.; Miguel, V. U.; Errazu, A. F., Possible methods for biodiesel production. *Renewable & Sustainable Energy Reviews* **2007**, *11* (6), 1300-1311.
133. Rodionova, M. V.; Poudyal, R. S.; Tiwari, I.; Voloshin, R. A.; Zharmukhamedov, S. K.; Nam, H. G.; Zayadan, B. K.; Bruce, B. D.; Hou, H. J. M.; Allakhverdiev, S. I., Biofuel production: Challenges and opportunities. *International Journal of Hydrogen Energy* **2017**, *42* (12), 8450-8461.
134. Marchetti, J. M., A summary of the available technologies for biodiesel production based on a comparison of different feedstock's properties. *Process Safety and Environmental Protection* **2012**, *90* (3), 157-163.
135. Avhad, M. R.; Marchetti, J. M., A review on recent advancement in catalytic materials for biodiesel production. *Renewable & Sustainable Energy Reviews* **2015**, *50*, 696-718.
136. Hansen, A. C.; Kyritsis, D. C.; Lee, C. F., Characteristics of biofuels and renewable fuel standards. In *Biomass to Biofuels: Strategies for Global Industries*, Vertes, A. A., Qureshi, N., Blaschek, H.P., Yukawa, H. (Eds.), Ed. John Wiley & Sons, Ltd.
137. Akia, M.; Yazdani, F.; Motae, E.; Han, D.; Arandiyani, H., A review on conversion of biomass to biofuel by nanocatalysts. *Biofuel Research Journal* **2014**, *1* (1), 16-25.
138. Pragma, N.; Pandey, K. K.; Sahoo, P. K., A review on harvesting, oil extraction and biofuels production technologies from microalgae. *Renewable & Sustainable Energy Reviews* **2013**, *24*, 159-171.
139. Azcan, N.; Yilmaz, O., Microwave assisted transesterification of waste frying oil and concentrate methyl ester content of biodiesel by molecular distillation. *Fuel* **2013**, *104*, 614-619.
140. Helwani, Z.; Aziz, N.; Bakar, M. Z. A.; Mukhtar, H.; Kim, J.; Othman, M. R., Conversion of *Jatropha curcas* oil into biodiesel using re-crystallized hydrotalcite. *Energy Conversion and Management* **2013**, *73*, 128-134.
141. Klaewkla, R.; Arend, M.; Hoelderich, W., A Review of Mass Transfer Controlling the Reaction Rate in Heterogeneous Catalytic Systems. Vol. Mass Transfer - Advanced Aspects.
142. Hill, J.; Nelson, E.; Tilman, D.; Polasky, S.; Tiffany, D., Environmental, economic, and energetic costs and benefits of biodiesel and ethanol biofuels. *Proceedings of the National Academy of Sciences of the United States of America* **2006**, *103* (30), 11206-11210.
143. Narasimharao, K.; Lee, A.; Wilson, K., Catalysts in production of biodiesel: A review. *Journal of Biobased Materials and Bioenergy* **2007**, *1* (1), 19-30.
144. Santos, A. L. F.; Martins, D. U.; Iha, O. K.; Ribeiro, R. A. M.; Quirino, R. L.; Suarez, P. A. Z., Agro-industrial residues as low-price feedstock for diesel-like fuel production by thermal cracking. *Bioresource Technology* **2010**, *101* (15), 6157-6162.

145. Sharma, R.; Chisti, Y.; Banerjee, U. C., Production, purification, characterization, and applications of lipases. *Biotechnology Advances* **2001**, *19* (8), 627-662.
146. Fu, J. Y.; Chen, L. G.; Lv, P. M.; Yang, L. M.; Yuan, Z. H., Free fatty acids esterification for biodiesel production using self-synthesized macroporous cation exchange resin as solid acid catalyst. *Fuel* **2015**, *154*, 1-8.
147. Cai, Z. Z.; Wang, Y.; Teng, Y. L.; Chong, K. M.; Wang, J. W.; Zhang, J. W.; Yang, D. P., A two-step biodiesel production process from waste cooking oil via recycling crude glycerol esterification catalyzed by alkali catalyst. *Fuel Processing Technology* **2015**, *137*, 186-193.
148. Boon-anuwat, N. N.; Kiatkittipong, W.; Aiouache, F.; Assabumrungrat, S., Process design of continuous biodiesel production by reactive distillation: Comparison between homogeneous and heterogeneous catalysts. *Chemical Engineering and Processing* **2015**, *92*, 33-44.
149. Gu, L.; Huang, W.; Tang, S. K.; Tian, S. J.; Zhang, X. W., A novel deep eutectic solvent for biodiesel preparation using a homogeneous base catalyst. *Chemical Engineering Journal* **2015**, *259*, 647-652.
150. Leca, M.; Tcacenco, L.; Micutz, M.; Staicu, T., Optimization of biodiesel production by transesterification of vegetable oils using lipases. *Romanian Biotechnological Letters* **2010**, *15* (5), 5618-5630.
151. Gui, M. M.; Lee, K. T.; Bhatia, S., Feasibility of edible oil vs. non-edible oil vs. waste edible oil as biodiesel feedstock. *Energy* **2008**, *33* (11), 1646-1653.
152. Rawat, I.; Kumar, R. R.; Mutanda, T.; Bux, F., Biodiesel from microalgae: A critical evaluation from laboratory to large scale production. *Applied Energy* **2013**, *103*, 444-467.
153. Ma, F. R.; Hanna, M. A., Biodiesel production: a review. *Bioresource Technology* **1999**, *70* (1), 1-15.
154. Bouaid, A.; Vazquez, R.; Martinez, M.; Aracil, J., Effect of free fatty acids contents on biodiesel quality. Pilot plant studies. *Fuel* **2016**, *174*, 54-62.
155. Feng, G.; Zhen, F., Biodiesel Production with Solid Catalysts. Vol. Biodiesel - Feedstocks and Processing Technologies. Biodiesel Production with Solid Catalysts, Biodiesel - Feedstocks and Processing Technologies, Margarita Stoytcheva and Gisela Montero, IntechOpen (2011), Available from: <https://www.intechopen.com/books/biodiesel-feedstocks-and-processing-technologies/biodiesel-production-with-solid-catalysts>
156. Zhao, X. B.; Qi, F.; Yuan, C. L.; Du, W.; Liu, D. H., Lipase-catalyzed process for biodiesel production: Enzyme immobilization, process simulation and optimization. *Renewable & Sustainable Energy Reviews* **2015**, *44*, 182-197.
157. Raita, M.; Arnthong, J.; Champreda, V.; Laosiripojana, N., Modification of magnetic nanoparticle lipase designs for biodiesel production from palm oil. *Fuel Processing Technology* **2015**, *134*, 189-197.
158. Polshettiwar, V.; Luque, R.; Fihri, A.; Zhu, H. B.; Bouhrara, M.; Bassett, J. M., Magnetically Recoverable Nanocatalysts. *Chemical Reviews* **2011**, *111* (5), 3036-3075.
159. Liu, C.; Lv, P. M.; Yuan, Z. H.; Yan, F.; Luo, W., The nanometer magnetic solid base catalyst for production of biodiesel. *Renewable Energy* **2010**, *35* (7), 1531-1536.
160. Taylor, H. S., A theory of the catalytic surface. *Proceedings of the Royal Society of London Series a-Containing Papers of a Mathematical and Physical Character* **1925**, *108* (745), 105-111.
161. Somorjai, G. A.; Park, J. Y., Evolution of the surface science of catalysis from single crystals to metal nanoparticles under pressure. *Journal of Chemical Physics* **2008**, *128* (18).
162. Somorjai, G. A.; Materer, N., Surface structures in ammonia synthesis. *Topics in Catalysis* **1994**, *1* (3-4), 215-231.
163. Bankovic-Ilic, I. B.; Miladinovic, M. R.; Stamenkovic, O. S.; Veljkovic, V. B., Application of nano CaO-based catalysts in biodiesel synthesis. *Renewable & Sustainable Energy Reviews* **2017**, *72*, 746-760.

164. Almerindo, G. I.; Probst, L. F. D.; Campos, C. E. M.; de Almeida, R. M.; Meneghetti, S. M. P.; Meneghetti, M. R.; Clacens, J. M.; Fajardo, H. V., Magnesium oxide prepared via metal-chitosan complexation method: Application as catalyst for transesterification of soybean oil and catalyst deactivation studies. *Journal of Power Sources* **2011**, *196* (19), 8057-8063.
165. Jeon, H.; Kim, D. J.; Kim, S. J.; Kim, J. H., Synthesis of mesoporous MgO catalyst templated by a PDMS-PEO comb-like copolymer for biodiesel production. *Fuel Processing Technology* **2013**, *116*, 325-331.
166. Dias, A. P. S.; Bernardo, J.; Felizardo, P.; Correia, M. J. N., Biodiesel production over thermal activated cerium modified Mg-Al hydrotalcites. *Energy* **2012**, *41* (1), 344-353.
167. Wang, S. H.; Wang, Y. B.; Dai, Y. M.; Jehng, J. M., Preparation and characterization of hydrotalcite-like compounds containing transition metal as a solid base catalyst for the transesterification. *Applied Catalysis a-General* **2012**, *439*, 135-141.
168. Narkhede, N.; Patel, A., Biodiesel Production by Esterification of Oleic Acid and Transesterification of Soybean Oil Using a New Solid Acid Catalyst Comprising 12-Tungstosilicic Acid and Zeolite H beta. *Industrial & Engineering Chemistry Research* **2013**, *52* (38), 13637-13644.
169. Costa, A. A.; Braga, P. R. S.; de Macedo, J. L.; Dias, J. A.; Dias, S. C. L., Structural effects of WO<sub>3</sub> incorporation on USY zeolite and application to free fatty acids esterification. *Microporous and Mesoporous Materials* **2012**, *147* (1), 142-148.
170. Zhang, Y.; Wong, W. T.; Yung, K. F., Biodiesel production via esterification of oleic acid catalyzed by chlorosulfonic acid modified zirconia. *Applied Energy* **2014**, *116*, 191-198.
171. Vieira, S. S.; Magriotis, Z. M.; Santos, N. A. V.; Saczk, A. A.; Hori, C. E.; Arroyo, P. A., Biodiesel production by free fatty acid esterification using lanthanum (La<sup>3+</sup>) and HZSM-5 based catalysts. *Bioresource Technology* **2013**, *133*, 248-255.
172. Laurent, S.; Forge, D.; Port, M.; Roch, A.; Robic, C.; Elst, L. V.; Muller, R. N., Magnetic iron oxide nanoparticles: Synthesis, stabilization, vectorization, physicochemical characterizations, and biological applications. *Chemical Reviews* **2008**, *108* (6), 2064-2110.
173. Shylesh, S.; Schunemann, V.; Thiel, W. R., Magnetically Separable Nanocatalysts: Bridges between Homogeneous and Heterogeneous Catalysis. *Angewandte Chemie-International Edition* **2010**, *49* (20), 3428-3459.
174. Gawande, M. B.; Luque, R.; Zboril, R., The Rise of Magnetically Recyclable Nanocatalysts. *Chemcatchem* **2014**, *6* (12), 3312-3313.
175. Guo, P. M.; Huang, F. H.; Zheng, M. M.; Li, W. L.; Huang, Q. D., Magnetic Solid Base Catalysts for the Production of Biodiesel. *Journal of the American Oil Chemists Society* **2012**, *89* (5), 925-933.
176. Xie, W. L.; Ma, N., Enzymatic transesterification of soybean oil by using immobilized lipase on magnetic nano-particles. *Biomass & Bioenergy* **2010**, *34* (6), 890-896.
177. Guldhe, A.; Singh, B.; Mutanda, T.; Pernaual, K.; Bux, F., Advances in synthesis of biodiesel via enzyme catalysis: Novel and sustainable approaches. *Renewable & Sustainable Energy Reviews* **2015**, *41*, 1447-1464.
178. Sharma, R. K.; Dutta, S.; Sharma, S.; Zboril, R.; Varma, R. S.; Gawande, M. B., Fe<sub>3</sub>O<sub>4</sub> (iron oxide)-supported nanocatalysts: synthesis, characterization and applications in coupling reactions. *Green Chemistry* **2016**, *18* (11), 3184-3209.
179. Joo, S. H.; Park, J. Y.; Tsung, C. K.; Yamada, Y.; Yang, P. D.; Somorjai, G. A., Thermally stable Pt/mesoporous silica core-shell nanocatalysts for high-temperature reactions. *Nature Materials* **2009**, *8* (2), 126-131.
180. Čejka, J.; Morris, R. E.; Nachtigall, P., *Zeolites in Catalysis: Properties and Applications*. RSC: 2017.
181. Van der Graaff, W. N. P.; Pidko, E. A.; Hensen, E. J. M., *Zeolite Catalysis for Biomass Conversion*. Vol. Zeolites in Sustainable Chemistry.

182. Schachter, Y.; Pines, H., Calcium-oxide-catalyzed reactions of hydrocarbons and of alcohols. *Journal of Catalysis* **1968**, *11* (2), 147-158.
183. Peterson, G. R.; Scarrarh, W. P., Rapeseed oil trans-esterification by heterogeneous catalysis. *Journal of the American Oil Chemists Society* **1984**, *61* (10), 1593-1597.
184. Kabashima, H.; Hattori, H., Cyanoethylation of alcohols over solid base catalysts. *Catalysis Today* **1998**, *44* (1-4), 277-283.
185. Ono, Y., Solid base catalysts for the synthesis of fine chemicals. *Journal of Catalysis* **2003**, *216* (1-2), 406-415.
186. Kumar, D.; Ali, A., Nanocrystalline Lithium Ion Impregnated Calcium Oxide As Heterogeneous Catalyst for Transesterification of High Moisture Containing Cotton Seed Oil. *Energy & Fuels* **2010**, *24*, 2091-2097.
187. Kaur, M.; Ali, A., Lithium ion impregnated calcium oxide as nano catalyst for the biodiesel production from karanja and jatropha oils. *Renewable Energy* **2011**, *36* (11), 2866-2871.
188. Wen, L. B.; Wang, Y.; Lu, D. L.; Hu, S. Y.; Han, H. Y., Preparation of KF/CaO nanocatalyst and its application in biodiesel production from Chinese tallow seed oil. *Fuel* **2010**, *89* (9), 2267-2271.
189. Hu, S. Y.; Guan, Y. P.; Wang, Y.; Han, H. Y., Nano-magnetic catalyst KF/CaO-Fe<sub>3</sub>O<sub>4</sub> for biodiesel production. *Applied Energy* **2011**, *88* (8), 2685-2690.
190. Kaur, M.; Ali, A., Potassium fluoride impregnated CaO/NiO: An efficient heterogeneous catalyst for transesterification of waste cottonseed oil. *European Journal of Lipid Science and Technology* **2014**, *116* (1), 80-88.
191. Kumar, D.; Ali, A., Transesterification of Low-Quality Triglycerides over a Zn/CaO Heterogeneous Catalyst: Kinetics and Reusability Studies. *Energy & Fuels* **2013**, *27* (7), 3758-3768.
192. Degirmenbasi, N.; Coskun, S.; Boz, N.; Kalyon, D. M., Biodiesel synthesis from canola oil via heterogeneous catalysis using functionalized CaO nanoparticles. *Fuel* **2015**, *153*, 620-627.
193. Kouzu, M.; Hidaka, J., Transesterification of vegetable oil into biodiesel catalyzed by CaO: A review. *Fuel* **2012**, *93* (1), 1-12.
194. Zhang, P. B.; Shi, M.; Liu, Y. L.; Fan, M. M.; Jiang, P. P.; Dong, Y. M., Sr doping magnetic CaO parcel ferrite improving catalytic activity on the synthesis of biodiesel by transesterification. *Fuel* **2016**, *186*, 787-791.
195. Deng, X.; Fang, Z.; Liu, Y. H.; Yu, C. L., Production of biodiesel from Jatropha oil catalyzed by nanosized solid basic catalyst. *Energy* **2011**, *36* (2), 777-784.
196. Xie, W. L.; Yang, X. L.; Fan, M. L., Novel solid base catalyst for biodiesel production: Mesoporous SBA-15 silica immobilized with 1,3-dicyclohexyl-2-octylguanidine. *Renewable Energy* **2015**, *80*, 230-237.
197. Canakci, M.; Van Gerpen, J., Biodiesel production from oils and fats with high free fatty acids. *Transactions of the Asae* **2001**, *44* (6), 1429-1436.
198. Zhang, Y.; Dube, M. A.; McLean, D. D.; Kates, M., Biodiesel production from waste cooking oil: 2. Economic assessment and sensitivity analysis. *Bioresource Technology* **2003**, *90* (3), 229-240.
199. Wang, H. W.; Covarrubias, J.; Prock, H.; Wu, X. R.; Wang, D. H.; Bossmann, S. H., Acid-Functionalized Magnetic Nanoparticle as Heterogeneous Catalysts for Biodiesel Synthesis. *Journal of Physical Chemistry C* **2015**, *119* (46), 26020-26028.
200. Borges, L. D.; Moura, N. N.; Costa, A. A.; Braga, P. R. S.; Dias, J. A.; Dias, S. C. L.; de Macedo, J. L.; Ghesti, G. F., Investigation of biodiesel production by HUSY and Ce/HUSY zeolites: Influence of structural and acidity parameters. *Applied Catalysis a-General* **2013**, *450*, 114-119.
201. Dehghani, S.; Haghghi, M., Sono-sulfated zirconia nanocatalyst supported on MCM-41 for biodiesel production from sunflower oil: Influence of ultrasound irradiation power on catalytic properties and performance. *Ultrasonics Sonochemistry* **2017**, *35*, 142-151.



202. Srilatha, K.; Devi, B. L. A. P.; Lingaiah, N.; Prasad, R. B. N.; Prasad, P. S. S., Biodiesel production from used cooking oil by two-step heterogeneous catalyzed process. *Bioresource Technology* **2012**, *119*, 306-311.
203. Shibasaki-Kitakawa, N.; Kanagawa, K.; Nakashima, K.; Yonemoto, T., Simultaneous production of high quality biodiesel and glycerin from *Jatropha* oil using ion-exchange resins as catalysts and adsorbent. *Bioresource Technology* **2013**, *142*, 732-736.
204. Kondamudi, N.; Mohapatra, S. K.; Misra, M., Quintinite as a bifunctional heterogeneous catalyst for biodiesel synthesis. *Applied Catalysis a-General* **2011**, *393* (1-2), 36-43.
205. Farooq, M.; Ramli, A.; Subbarao, D., Biodiesel production from waste cooking oil using bifunctional heterogeneous solid catalysts. *Journal of Cleaner Production* **2013**, *59*, 131-140.
206. Danov, S. M.; Kazantsev, O. A.; Esipovich, A. L.; Belousov, A. S.; Rogozhin, A. E.; Kanakov, E. A., Recent advances in the field of selective epoxidation of vegetable oils and their derivatives: a review and perspective. *Catalysis Science & Technology* **2017**, *7* (17), 3659-3675.
207. Wierzbicki, T. A.; Lee, I. C.; Gupta, A. K., Performance of synthetic jet fuels in a meso-scale heat recirculating combustor. *Applied Energy* **2014**, *118*, 41-47.
208. Sackett, W. M., Petroleum in the marine environment - An introduction. *Marine Technology Society Journal* **1984**, *18* (3), 2-3.
209. Corporan, E.; Edwards, T.; Shafer, L.; DeWitt, M. J.; Klingshirm, C.; Zabarnick, S.; West, Z.; Striebich, R.; Graham, J.; Klein, J., Chemical, Thermal Stability, Seal Swell, and Emissions Studies of Alternative Jet Fuels. *Energy & Fuels* **2011**, *25* (3), 955-966.
210. Hsieh, P. Y.; Widgren, J. A.; Fortin, T. J.; Bruno, T. J., Chemical and Thermophysical Characterization of an Algae-Based Hydrotreated Renewable Diesel Fuel. *Energy & Fuels* **2014**, *28* (5), 3192-3205.
211. Prak, D. J. L.; Cowart, J. S.; Hamilton, L. J.; Hoang, D. T.; Brown, E. K.; Trulove, P. C., Development of a Surrogate Mixture for Algal-Based Hydrotreated Renewable Diesel (vol 27, pg 954, 2013). *Energy & Fuels* **2013**, *27* (5), 2857-2857.
212. Huber, G. W.; Iborra, S.; Corma, A., Synthesis of transportation fuels from biomass: Chemistry, catalysts, and engineering. *Chemical Reviews* **2006**, *106* (9), 4044-4098.
213. Corma, A.; Iborra, S.; Velty, A., Chemical routes for the transformation of biomass into chemicals. *Chemical Reviews* **2007**, *107* (6), 2411-2502.
214. Xia, Q. N.; Chen, Z. J.; Shao, Y.; Gong, X. Q.; Wang, H. F.; Liu, X. H.; Parker, S. F.; Han, X.; Yang, S. H.; Wang, Y. Q., Direct hydrodeoxygenation of raw woody biomass into liquid alkanes. *Nature Communications* **2016**, *7*.
215. Fortman, J. L.; Chhabra, S.; Mukhopadhyay, A.; Chou, H.; Lee, T. S.; Steen, E.; Keasling, J. D., Biofuel alternatives to ethanol: pumping the microbial well. *Trends in Biotechnology* **2008**, *26* (7), 375-381.
216. Harrison, K. W.; Harvey, B. G., Renewable high density fuels containing tricyclic sesquiterpanes and alkyl diamondoids. *Sustainable Energy & Fuels* **2017**, *1* (3), 467-473.
217. Harvey, B. G.; Merriman, W. W.; Koontz, T. A., High-Density Renewable Diesel and Jet Fuels Prepared from Multicyclic Sesquiterpanes and a 1-Hexene-Derived Synthetic Paraffinic Kerosene. *Energy & Fuels* **2015**, *29* (4), 2431-2436.
218. Yang, J. M.; Li, Z. F.; Guo, L. Z.; Du, J.; Bae, H. J., Biosynthesis of beta-caryophyllene, a novel terpene-based high-density biofuel precursor, using engineered *Escherichia coli*. *Renewable Energy* **2016**, *99*, 216-223.
219. Alonso, D. M.; Bond, J. Q.; Dumesic, J. A., Catalytic conversion of biomass to biofuels. *Green Chemistry* **2010**, *12* (9), 1493-1513.
220. Climent, M. J.; Corma, A.; Iborra, S., Conversion of biomass platform molecules into fuel additives and liquid hydrocarbon fuels. *Green Chemistry* **2014**, *16* (2), 516-547.

221. Sacia, E. R.; Balakrishnan, M.; Deaner, M. H.; Goulas, K. A.; Toste, F. D.; Bell, A. T., Highly Selective Condensation of Biomass-Derived Methyl Ketones as a Source of Aviation Fuel. *Chemsuschem* **2015**, *8* (10), 1726-1736.
222. Deng, Q.; Xu, J. S.; Han, P. J.; Pan, L.; Wang, L.; Zhang, X. W.; Zou, J. J., Efficient synthesis of high-density aviation biofuel via solvent-free aldol condensation of cyclic ketones and furanic aldehydes. *Fuel Processing Technology* **2016**, *148*, 361-366.
223. Chen, F.; Li, N.; Yang, X. F.; Li, L.; Li, G. Y.; Li, S. S.; Wang, W. T.; Hu, Y. C.; Wang, A. Q.; Cong, Y.; Wang, X. D.; Zhang, T., Synthesis of High-Density Aviation Fuel with Cyclopentanone. *ACS Sustainable Chemistry & Engineering* **2016**, *4* (11), 6160-6166.
224. Guo, J. H.; Xu, G. Y.; Han, Z.; Zhang, Y.; Fu, Y.; Guo, Q. X., Selective Conversion of Furfural to Cyclopentanone with CuZnAl Catalysts. *ACS Sustainable Chemistry & Engineering* **2014**, *2* (10), 2259-2266.
225. Li, X. L.; Deng, J.; Shi, J.; Pan, T.; Yu, C. G.; Xu, H. J.; Fu, Y., Selective conversion of furfural to cyclopentanone or cyclopentanol using different preparation methods of Cu-Co catalysts. *Green Chemistry* **2015**, *17* (2), 1038-1046.
226. Sheng, X. R.; Li, G. Y.; Wang, W. T.; Cong, Y.; Wang, X. D.; Huber, G. W.; Li, N.; Wang, A. Q.; Zhang, T., Dual-Bed Catalyst System for the Direct Synthesis of High Density Aviation Fuel with Cyclopentanone from Lignocellulose. *Aiche Journal* **2016**, *62* (8), 2754-2761.
227. Wang, W.; Li, N.; Li, G. Y.; Li, S. S.; Wang, W. T.; Wang, A. Q.; Cong, Y.; Wang, X. D.; Zhang, T., Synthesis of Renewable High-Density Fuel with Cyclopentanone Derived from Hemicellulose. *Acs Sustainable Chemistry & Engineering* **2017**, *5* (2), 1812-1817.
228. He, J. Y.; Zhao, C.; Lercher, J. A., Ni-Catalyzed Cleavage of Aryl Ethers in the Aqueous Phase. *Journal of the American Chemical Society* **2012**, *134* (51), 20768-20775.
229. Kelkar, C. P.; Schutz, A. A., Efficient hydrotalcite-based catalyst for acetone condensation to alpha-isophorone - scale up aspects and process development. *Applied Clay Science* **1998**, *13* (5-6), 417-432.
230. Wang, W.; Liu, Y. T.; Li, N.; Li, G. Y.; Wang, W. T.; Wang, A. Q.; Wang, X. D.; Zhang, T., Synthesis of renewable high-density fuel with isophorone. *Scientific Reports* **2017**, *7*, 6111.
231. Nie, G. K.; Zhang, X. W.; Han, P. J.; Xie, J. J.; Pan, L.; Wang, L.; Zou, J. J., Lignin-derived multi-cyclic high density biofuel by alkylation and hydrogenated intramolecular cyclization. *Chemical Engineering Science* **2017**, *158*, 64-69.
232. Han, P. J.; Nie, G. K.; Xie, J. J.; E, X. T. F.; Pan, L.; Zhang, X. W.; Zou, J. J., Synthesis of high-density biofuel with excellent low-temperature properties from lignocellulose-derived feedstock. *Fuel Processing Technology* **2017**, *163*, 45-50.
233. Labeckas, G.; Slavinskas, S., Combustion phenomenon, performance and emissions of a diesel engine with aviation turbine JP-8 fuel and rapeseed biodiesel blends. *Energy Conversion and Management* **2015**, *105*, 216-229.
234. Yan, N.; Zhao, C.; Dyson, P. J.; Wang, C.; Liu, L. T.; Kou, Y., Selective Degradation of Wood Lignin over Noble-Metal Catalysts in a Two-Step Process. *Chemsuschem* **2008**, *1* (7), 626-629.
235. Ye, Y. Y.; Zhang, Y.; Fan, J.; Chang, J., Novel Method for Production of Phenolics by Combining Lignin Extraction with Lignin Depolymerization in Aqueous Ethanol. *Industrial & Engineering Chemistry Research* **2012**, *51* (1), 103-110.
236. Rensel, D. J.; Rouvimov, S.; Gin, M. E.; Hicks, J. C., Highly selective bimetallic FeMoP catalyst for C-O bond cleavage of aryl ethers. *Journal of Catalysis* **2013**, *305*, 256-263.
237. Barta, K.; Warner, G. R.; Beach, E. S.; Anastas, P. T., Depolymerization of organosolv lignin to aromatic compounds over Cu-doped porous metal oxides. *Green Chemistry* **2014**, *16* (1), 191-196.
238. Qi, S. C.; Zhang, L.; Einaga, H.; Kudo, S.; Norinaga, K.; Hayashi, J., Nano-sized nickel catalyst for deep hydrogenation of lignin monomers and first-principles insight into the catalyst preparation. *Journal of Materials Chemistry A* **2017**, *5* (8), 3948-3965.

239. Serrano, D. P.; Aguado, J.; Escola, J. M., Catalytic cracking of a polyolefin mixture over different acid solid catalysts. *Industrial & Engineering Chemistry Research* **2000**, *39* (5), 1177-1184.
240. Artetxe, M.; Lopez, G.; Amutio, M.; Elordi, G.; Bilbao, J.; Olazar, M., Cracking of High Density Polyethylene Pyrolysis Waxes on HZSM-5 Catalysts of Different Acidity. *Industrial & Engineering Chemistry Research* **2013**, *52* (31), 10637-10645.
241. Zhang, X. S.; Lei, H. W., Synthesis of high-density jet fuel from plastics via catalytically integral processes. *RSC Advances* **2016**, *6* (8), 6154-6163.
242. Xie, J.; Zhang, X.; Pan, L.; Nie, G.; Xiu-Tian-Feng, E.; Liu, Q.; Wang, P.; Li, Y.; Zou, J.-J., Renewable high-density spiro-fuels from lignocellulose-derived cyclic ketones. *Chemical Communications* **2017**, *53* (74), 10303-10305.
243. Duan, H.; Dong, J.; Gu, X.; Peng, Y.-K.; Chen, W.; Issariyakul, T.; Myers, W. K.; Li, M.-J.; Yi, N.; Kilpatrick, A. F. R.; Wang, Y.; Zheng, X.; Ji, S.; Wang, Q.; Feng, J.; Chen, D.; Li, Y.; Buffet, J.-C.; Liu, H.; Tsang, S. C. E.; O'Hare, D., Hydrodeoxygenation of water-insoluble bio-oil to alkanes using a highly dispersed Pd-Mo catalyst. *Nature Communications* **2017**, *8*, 591.
244. Lofstedt, J.; Dahlstrand, C.; Orebom, A.; Meuzelaar, G.; Sawadjoon, S.; Galkin, M. V.; Agback, P.; Wimby, M.; Corresa, E.; Mathieu, Y.; Sauvanaud, L.; Eriksson, S.; Corma, A.; Samec, J. S. M., Green Diesel from Kraft Lignin in Three Steps. *Chemsuschem* **2016**, *9* (12), 1392-1396.
245. Xing, S.; Lv, P.; Yuan, H.; Yang, L.; Wang, Z.; Yuan, Z.; Chen, Y., Insight into forced hydrogen re-arrangement and altered reaction pathways in a protocol for CO<sub>2</sub> catalytic processing of oleic acid into C-8-C-15 alkanes. *Green Chemistry* **2017**, *19* (17), 4157-4168.
246. Hess, S. K.; Schunck, N. S.; Goldbach, V.; Ewe, D.; Kroth, P. G.; Mecking, S., Valorization of Unconventional Lipids from Microalgae or Tall Oil via a Selective Dual Catalysis One-Pot Approach. *Journal of the American Chemical Society* **2017**, *139* (38), 13487-13491.
247. Enumula, S. S.; Koppadi, K. S.; Gurram, V. R. B.; Burri, D. R.; Kamaraju, S. R. R., Conversion of furfuryl alcohol to alkyl levulinate fuel additives over Al<sub>2</sub>O<sub>3</sub>/SBA-15 catalyst. *Sustainable Energy & Fuels* **2017**, *1* (3), 644-651





# **Hypothesis and Objectives**



## Hypothesis I

Last works on the development of photocatalytically active nanoparticles have demonstrated the possibility to achieve high performant materials *via* green synthetic paths. These compounds have been used in different reactions, such as water splitting, dehydrogenations or oxidations. A large numbers of research articles have also reported the degradation of pollutant dyes as an easily-measurable index of the photocatalytic activities as well as a good green chemistry reaction model.<sup>1</sup>

In recent years, copper sulphide ( $\text{Cu}_2\text{S}$ ) have been proposed as a green photocatalytic compound with p-type semi-conductor properties, low preparation costs and low toxicity characteristics. For example,  $\text{Cu}_2\text{S}$  nanoparticles have been used for the efficient degradation of methylene blue under UV-Vis light irradiation.<sup>2</sup> In addition, different composite compounds, such as  $\text{Cu}_2\text{S}/\text{ZnO}$ ,  $\text{Cu}_2\text{S}/\text{TiO}_2$  or  $\text{Cu}_2\text{S}/\text{carbon}$ , have been prepared in order to enhance the photocatalytic activity of copper sulphide.<sup>3-6</sup>

However, the utilization of non-renewable and/or highly toxic sulphur sources compounds as well as the long-term preparation procedures still entail practical and sustainable limits in the preparation of these types of materials. Furthermore, most of the active materials are design to operate under UV-Vis light irradiation, while the Sun mostly emits in the visible and IR regions.

## Objective I

**Microwave-assisted synthesis of a novel nano- $\text{Cu}_2\text{S}$  photocatalytically active compound for the efficient degradation of a pollutant dye under visible light irradiation.<sup>7</sup>**

Copper sulphide ( $\text{Cu}_2\text{S}$ ) carbon composite has been prepared using waste pig bristles as sulphur and carbon source. The novel compound has been prepared by a microwave-assisted hydrothermal treatment of a mixture of ethylene glycol, pig bristles and copper chloride. The synthesis have been carried out using a multimode microwave oven. The new material has been characterized by X-Ray diffraction (XRD),  $\text{N}_2$  physisorption, scanning electron microscopy (SEM-EDX) and UV-Vis spectroscopy. The

Cu<sub>2</sub>S-carbon composite has been employed as catalysts for the photodegradation of methyl red under LED visible light irradiation.

## Hypothesis II

The preparation of selective and active nanocatalysts for the synthesis of fine chemicals is an extremely captivating challenge. In the last years, several mesoporous materials have been studied as supporting materials for the stabilization of gold and silver nanoparticles. SBA-15 has particularly emerged due to its high surface area and stability under different reaction conditions as well as to the possibility of enhance Lewis acidic properties by incorporating Al.<sup>8</sup> The most innovative and highly efficient methods for supporting the nanoparticles include solvent-less ball milling techniques and fast microwave-assisted approaches.<sup>9, 10</sup>

Imidazonoles represent an important class of chemicals for the agrochemical and pharmaceutical industry. A large variety of imidazolones has been reported as herbicides, insecticides, antifungals, anti-inflammatories as well as antitumor agents while others have been tested as cardiotoxic, antioxidant, vasodilator and enhancing-memory drugs. Recently, the synthesis of imidazolones *via* the cycloisomerization of ureas, precisely propargylureas, has gained attention due to the large availability of starting materials and consequential low production costs.<sup>11</sup>

Unfortunately, these synthesis usually need the utilization of strong bases or expensive homogeneous metal catalysts (*e.g.*, Ag, Au and Ru systems) as well as toxic/hazardous chemicals. Alternatively, several substituted imidazolones have been recently prepared operating in toluene and employing silver and gold homogeneous catalysts avoiding the use of any strong bases and highly toxic chemicals.<sup>12, 13</sup> Nevertheless, the utilization of homogeneous catalysts implied the metal contamination in the final product and the high cost of production due to the impossible recovery of the catalysts. In addition, despite not highly toxic, toluene is still an undesirable (being also cancerogenic) solvent and its utilization should be limited as much as possible in industry.<sup>14</sup>



## Objective II

Innovative design of nanosilver and nanogold catalysts for the investigation of the low toxicity, fast and safe microwave-assisted cycloisomerizations of propargylic ureas.<sup>15</sup>

A sequence of Au/AlSBA-15 and Ag/AlSBA-15 compounds have been synthesized comparing mechanochemistry and microwave-assisted approaches. The heterogeneous systems have been employed for the fast, mild and environmentally friendly microwave-assisted cycloisomerization of propargylic ureas using a monomode microwave oven. Specifically, the synthesis were carried out varying the solvents, the reaction conditions and the type of catalysts. The results were also combined in order to carry out the microwave- assisted reaction using only water as solvent and promoter of the reaction.

## Hypothesis III

Biorefinery processes for the production of biofuels require the utilization of stable, cheap and efficient heterogeneous catalysts. The research over magnetically recoverable nanoparticles have received special attention due to easy separation of the catalysts from the reaction mixture. If on the one hand the most studied magnetically recoverable compounds are based on magnetite and maghemite or, more in general, ferrite compounds, on the other hand the research have proposed alternative materials, such as pure metallic nickel nanoparticles.<sup>16-18</sup>

Nickel nanoparticles have been demonstrated to show unique properties including high magnetism, high surface area, large surface energy, excellent chemical stability, low melting point, and low cost (due to large availability of the metal).<sup>19</sup> In the last decade, different techniques have been proposed as valid procedures for the preparation of Ni nanoparticles composites, including thermal decomposition, pulsed laser ablation, sputtering and metal vapor condensation.<sup>20, 21</sup>

However, the bibliography is quite limited respect the synthesis of pure metallic Ni magnetic nanoparticles. In addition, the few reports are generally based on the so-called polyol methods (or similar), which need the utilization of a toxic or hazardous

reducing agent (*e.g.* hydrazine or  $\text{NaBH}_4$ ) for the preparation of the nanoparticles.<sup>22-24</sup> Finally, low effort has been made for the microwave-assisted synthesis of biofuels using Ni nanoparticles as catalysts.

## Objective III

Development of a green microwave-assisted protocol for the preparation of magnetically recoverable nickel nanoparticles as active catalysts for the microwave-assisted synthesis of biofuels from lignin.<sup>25</sup>

Metallic nickel nanoparticles have been synthesized modifying a polyol method through a fast, simple and environmentally friendly procedure. Specifically, the magnetically recoverable nanoparticles have been synthesized hydrothermally heating a mixture of ethylene glycol, ethanol and nickel chloride. The procedure has been carried out in a monomode microwave oven. The mixture of ethylene glycol and ethanol have been proved to work as solvent as well as reducing agent. The parameter combinations for the occurrence of the precipitation of Ni nanoparticles were finely studied. The so-produced nanoparticles were characterized by XRD,  $\text{N}_2$  physisorption, SEM-EDX and transmission electron microscopy (TEM). The nanoparticles were successfully employed for the hydrogenolysis of benzyl phenyl ether (BPE), a lignin model compound, in a microwave-assisted reaction, using isopropanol as solvent and hydrogen donor.

1. Byrne, C.; Subramanian, G.; Pillai, S. C., Recent advances in photocatalysis for environmental applications. *Journal of Environmental Chemical Engineering* **2018**, *6* (3), 3531-3555.
2. Cao, Q.; Che, R. C.; Chen, N., Scalable synthesis of Cu<sub>2</sub>S double-superlattice nanoparticle systems with enhanced UV/visible-light-driven photocatalytic activity. *Applied Catalysis B-Environmental* **2015**, *162*, 187-195.
3. Zhang, J.; Yu, J. G.; Zhang, Y. M.; Li, Q.; Gong, J. R., Visible Light Photocatalytic H<sub>2</sub>-Production Activity of CuS/ZnS Porous Nanosheets Based on Photoinduced Interfacial Charge Transfer. *Nano Letters* **2011**, *11* (11), 4774-4779.
4. Li, D. M.; Cheng, L. Y.; Zhang, Y. D.; Zhang, Q. X.; Huang, X. M.; Luo, Y. H.; Meng, Q. B., Development of Cu<sub>2</sub>S/carbon composite electrode for CdS/CdSe quantum dot sensitized solar cell modules. *Solar Energy Materials and Solar Cells* **2014**, *120*, 454-461.
5. Zhang, L.; Zhao, Y.; Zhong, L. L.; Wang, Y.; Chai, S. N.; Yang, T.; Han, X. L., Cu<sub>2</sub>S-Cu-TiO<sub>2</sub> mesoporous carbon composites for the degradation of high concentration of methyl orange under visible light. *Applied Surface Science* **2017**, *422*, 1093-1101.
6. Tang, Y.; Zhang, D.; Pu, X.; Ge, B.; Li, Y.; Huang, Y., Snowflake-like Cu<sub>2</sub>S/Zn<sub>0.5</sub>Cd<sub>0.5</sub>S p-n heterojunction photocatalyst for enhanced visible light photocatalytic H<sub>2</sub> evolution activity. *Journal of the Taiwan Institute of Chemical Engineers* **2019**, *96*, 487-495.
7. Zuliani, A.; Munoz-Batista, M. J.; Luque, R., Microwave-assisted valorization of pig bristles: towards visible light photocatalytic chalcocite composites. *Green Chemistry* **2018**, *20*, 3001-3007.
8. Qiao, Y.; Said, N.; Rauser, M.; Yan, K.; Qin, F.; Theyssen, N.; Leitner, W., Preparation of SBA-15 supported Pt/Pd bimetallic catalysts using supercritical fluid reactive deposition: how do solvent effects during material synthesis affect catalytic properties? *Green Chemistry* **2017**, *19* (4), 977-986.
9. Balu, A. M.; Dallinger, D.; Obermayer, D.; Campelo, J. M.; Romero, A. A.; Carmona, D.; Balas, F.; Yohida, K.; Gai, P. L.; Vargas, C.; Kappe, C. O.; Luque, R., Insights into the microwave-assisted preparation of supported iron oxide nanoparticles on silica-type mesoporous materials. *Green Chemistry* **2012**, *14* (2), 393-402.
10. Ojeda, M.; Balu, A. M.; Barron, V.; Pineda, A.; Coleto, A. G.; Angel Romero, A.; Luque, R., Solventless mechanochemical synthesis of magnetic functionalized catalytically active mesoporous SBA-15 nanocomposites. *Journal of Materials Chemistry A* **2014**, *2* (2), 387-393.
11. Lauder, K.; Toscani, A.; Scalacci, N.; Castagnolo, D., Synthesis and Reactivity of Propargylamines in Organic Chemistry. *Chemical Reviews* **2017**, *117* (24), 14091-14200.
12. Peshkov, V. A.; Pereshivko, O. P.; Sharma, S.; Meganathan, T.; Parmar, V. S.; Ermolat'ev, D. S.; Van der Eycken, E. V., Tetrasubstituted 2-Imidazolones via Ag(I)-Catalyzed Cycloisomerization of Propargylic Ureas. *Journal of Organic Chemistry* **2011**, *76* (14), 5867-5872.
13. Pereshivko, O. P.; Peshkov, V. A.; Jacobs, J.; Van Meervelt, L.; Van der Eycken, E. V., Cationic Gold- and Silver-Catalyzed Cycloisomerizations of Propargylic Ureas: A Selective Entry to Oxazolidin-2-imines and Imidazolidin-2-ones. *Advanced Synthesis & Catalysis* **2013**, *355* (4), 781-789.
14. Tomatis, M.; Xu, H. H.; He, J.; Zhang, X. D., Recent Development of Catalysts for Removal of Volatile Organic Compounds in Flue Gas by Combustion: A Review. *Journal of Chemistry* **2016**.
15. Zuliani, A.; Ranjan, P.; Luque, R.; Van der Eycken, E. V., Heterogeneously Catalyzed Synthesis of Imidazolones via Cycloisomerizations of Propargylic Ureas Using Ag and Au/Al SBA-15 Systems. *ACS Sustainable Chemistry & Engineering* **2019**, *7* (5), 5568-5575.
16. Vigneswari, T.; Raji, P., Structural and magnetic properties of calcium doped nickel ferrite nanoparticles by co-precipitation method. *Journal of Molecular Structure* **2017**, *1127*, 515-521.
17. Duman, F.; Sahin, U.; Atabani, A. E., Harvesting of blooming microalgae using green synthesized magnetic maghemite (gamma-Fe<sub>2</sub>O<sub>3</sub>) nanoparticles for biofuel production. *Fuel* **2019**, *256*, 115935.

18. Polshettiwar, V.; Luque, R.; Fihri, A.; Zhu, H.; Bouhrara, M.; Bassett, J.-M., Magnetically Recoverable Nanocatalysts. *Chemical Reviews* **2011**, *111* (5), 3036-3075.
19. Wu, S. H.; Chen, D. H., Synthesis and characterization of nickel nanoparticles by hydrazine reduction in ethylene glycol. *Journal of Colloid and Interface Science* **2003**, *259* (2), 282-286.
20. Baskaya, G.; Yildiz, Y.; Savk, A.; Okyay, T. O.; Eris, S.; Sert, H.; Sen, F., Rapid, sensitive, and reusable detection of glucose by highly monodisperse nickel nanoparticles decorated functionalized multi-walled carbon nanotubes. *Biosensors & Bioelectronics* **2017**, *91*, 728-733.
21. Wu, M. S.; Jao, C. Y.; Chuang, F. Y.; Chen, F. Y., Carbon-encapsulated nickel-iron nanoparticles supported on nickel foam as a catalyst electrode for urea electrolysis. *Electrochimica Acta* **2017**, *227*, 210-216.
22. Logutenko, O. A.; Titkov, A. I.; Vorob'yov, A. M.; Balaev, D. A.; Shaikhutdinov, K. A.; Semenov, S. V.; Yukhin, Y. M.; Lyakhov, N. Z., Effect of molecular weight of sodium polyacrylates on the size and morphology of nickel nanoparticles synthesized by the modified polyol method and their magnetic properties. *European Polymer Journal* **2018**, *99*, 102-110.
23. Galhardo, T. S.; Goncalves, M.; Mandelli, D.; Carvalho, W. A., Glycerol valorization by base-free oxidation with air using platinum-nickel nanoparticles supported on activated carbon as catalyst prepared by a simple microwave polyol method. *Clean Technologies and Environmental Policy* **2018**, *20* (9), 2075-2088.
24. Mokrane, T.; Boudjahem, A. G.; Bettahar, M., Benzene hydrogenation over alumina-supported nickel nanoparticles prepared by polyol method. *RSC Advances* **2016**, *6* (64), 59858-59864.
25. Zuliani, A.; Balu, A. M.; Luque, R., Efficient and Environmentally Friendly Microwave-Assisted Synthesis of Catalytically Active Magnetic Metallic Ni Nanoparticles. *ACS Sustainable Chemistry & Engineering* **2017**, *5* (12), 11584-11587.



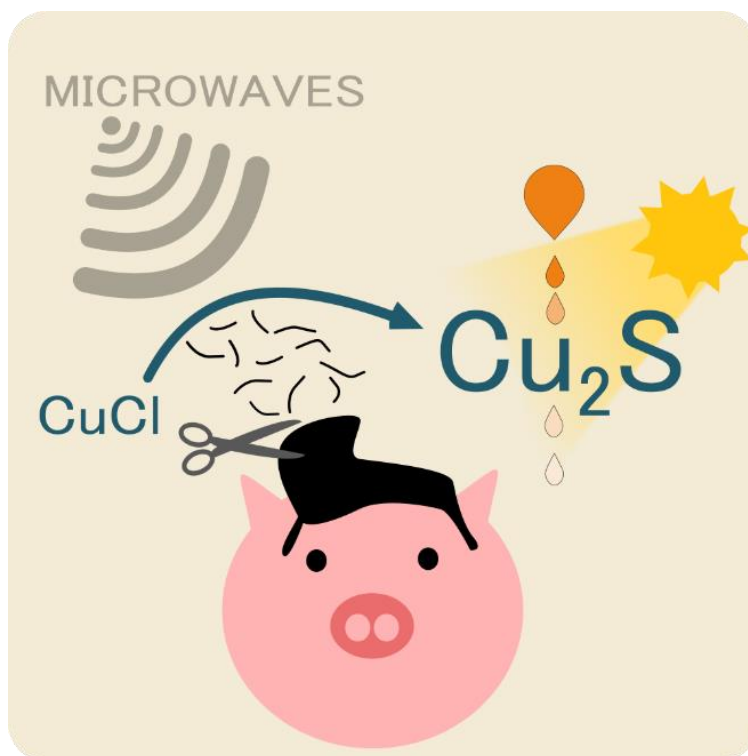
## Results and Discussion



## Microwave-assisted valorization of pig bristles: towards visible light photocatalytic chalcocite composites

Alessio Zuliani,<sup>a\*</sup> Mario J. Muñoz-Batista<sup>a</sup> and Rafael Luque<sup>a, b\*</sup>

*Green Chem.*, 2018, **20**, 3001-3007



<sup>a</sup> Departamento de Química Organica, Universidad de Cordoba, Edificio Marie-Curie (C-3), Ctra Nnal IV-A, Km 396, Cordoba, Spain

<sup>b</sup> Peoples' Friendship University of Russia (RUDN University), 6 Miklukho-Maklaya Street, 117198, Moscow, Russia

*Abstract: Waste valorization for the production of valuable materials is of great importance for a sustainable development. Herein, a new green methodology for the synthesis of photocatalytically active copper sulfide (Cu<sub>2</sub>S) carbon composites using pig bristles is reported. The catalyst was prepared via microwave-assisted methodology using ethylene glycol as solvent, pig bristles as sulfur and carbon source, and copper chloride as metal precursor. Cu<sub>2</sub>S carbon composites (denoted as pb-Cu<sub>2</sub>S, where “pb” states for “pig bristle”) were characterized by XRD, N<sub>2</sub> physisorption, EDX and UV-Vis spectroscopy. In order to validate the practical utilization of pig bristles- derived chemicals, the photocatalytic degradation of methyl red using pb-Cu<sub>2</sub>S was investigated under white, blue, green and red visible light irradiation.*

## 1. INTRODUCTION

Moving our society dependence away from petroleum to renewable biomass resources is one of the most important challenges for a future development of sustainable industries.<sup>1</sup> An extremely captivating challenge is the valorization of bio wastes for the production of valuable chemicals.<sup>2</sup> Considering EUROSTAT data (EU 28 countries), *ca.* 250 million pigs were slaughtered in the European Union in 2017.<sup>3</sup> Since each slaughtered pig delivers ~0.9 kg of pig bristles, approximately 225 k tons of wasted pig bristles are produced annually.<sup>4</sup> Despite such large quantities of waste products, research on new ways of valorization of pig bristles has not received the pulse to upsurge to date. Boiled (sanitized) pig bristles are exclusive commercial products currently employed in brushes factories. Therefore, as every commercially available product, boiled pig bristles could be easily collected and studied in laboratory scale aiming to provide potential roadmaps for the valorization of wasted pig bristles at industrial scale.

Only counted reports about the reutilization of wasted pig bristles are available in literature. Importantly, they are limited to the reutilization of pig bristles as sources of fodder food supplements (e.g. for the high content of keratin).<sup>4-7</sup>

Herein we report an unprecedented simple route for the valorization of pig bristles for the production of a high performance material as photocatalyst. Specifically,



the synthesis of Cu<sub>2</sub>S carbon nanocomposite (denoted as pb-Cu<sub>2</sub>S, where “pb” states for “pig bristle derived”) was accomplished using pig bristles as sulphur and carbon source.

Since biorefineries should be based on new, highly efficient and sustainable strategies for biomass conversion,<sup>1, 8-10</sup> we have also employed a microwave approach for the synthesis of pb-Cu<sub>2</sub>S.

Microwave-assisted reactions offer several advantages that include fast reaction time, the possibility to obtain higher yields, different selectivity as well as the potential to accomplish reactions/chemistries that generally do not take place under conventional heating conditions.<sup>11-15</sup> In addition, the unique characteristics of microwave assisted reactions are attracting lot of attentions for the valorization of biomass.<sup>16-20</sup>

Based on our experience in microwave chemistry, we have developed an environmentally friendly, simple and straightforward method for the valorization of pig bristles under microwave-assisted conditions.<sup>17, 18, 21-24</sup> A low-toxicity mixture of ethylene glycol, copper chloride and pig bristles, was treated in a microwave oven to directly obtain pb-Cu<sub>2</sub>S avoiding any calcination steps. Where appropriate, a small amount of sodium hydroxide was used to optimize the synthesis and favour the formation of copper sulphide in the form of the more photocatalytically active Chalcocite crystals. The material was characterized by XRD, N<sub>2</sub> physisorption, EDX and UV-Vis spectroscopy, demonstrating the formation of Cu<sub>2</sub>S carbon composites.

In order to validate the practical utilization of pig bristles- derived chemicals, pb-Cu<sub>2</sub>S was tested as photocatalyst.

Indeed, photochemistry is widely studied for harvesting the sunlight radiation with clean and green conversion to chemical power though different materials.<sup>25-27</sup> In detail, semiconductors with a specific band gap can resonate if irradiated with a light of a specific wavelength producing electrons and holes, consequently generating active hydroxyl radicals in solution.<sup>28</sup> These hydroxyl radicals can degrade organics by advanced oxidation processes (APOs).<sup>29</sup>

Considering that Cu<sub>2</sub>S is a p-type semiconductor with a narrow bulk band gap of 1.2 eV, the synthesized material could be a suitable photocatalyst under visible light irradiation.<sup>30</sup> The photocatalytic activity of pb-Cu<sub>2</sub>S was tested in the photodegradation

of a toxic and contaminant colorant. Truly the environmental impact caused by dye used in the textile industries is one of the most sensible: because of their toxicity and ability to reduce the uptake of light; dyes interfere with the photosynthesis of aquatic plants hence having a direct impact in the oxygen content of water sources. Therefore, the degradation of contaminant dyes is of remarkable importance. The photodegradation of methyl red dye (CI 13020) catalysed by pb-Cu<sub>2</sub>S, was investigated under visible light and, in order to deeply understand the activity of the catalyst in function of specific wavelength, under red, green, and blue light. Lighting emitting diodes (LEDs) were employed pointing to the design of an efficient photoreactor.<sup>31</sup>

## 2. EXPERIMENTAL SECTIONS

Copper (I) chloride (CuCl, 98.8%) was purchased from Panreac Quimica SLU, Barcelona, Spain. Ethylene glycol (HOCH<sub>2</sub>CH<sub>2</sub>OH, 99.9%), methyl red (4-Dimethylaminoazobenzene-2'-carboxylic acid), TiO<sub>2</sub> (Titanium (IV) oxide nanopowder, Aeroxide® P25), sodium hydroxide (NaOH) and ethanol (CH<sub>3</sub>CH<sub>2</sub>OH, 99.5%) were purchased from Sigma-Aldrich Inc., St. Louis, MO, USA. All reagents were used without any further purification.

### 2.1 Synthesis of pb-Cu<sub>2</sub>S with microwave assisted method

In a typical synthesis, pig bristle (1.5 g, cut in pieces of ~0.5 cm) and the metallic precursor CuCl (480 mg, 4.85 mmol) were added to ethylene glycol (20 mL) in a 50 mL Teflon microwave tube equipped with a stirrer. Eventually, different amount of NaOH (up to 100 mg, 2.5 mmol) were added to the mixture to favour the formation of the more photocatalytically active Chalcocite crystals. The mixture was sequentially stirred for 10 minutes at 700 rpm at room temperature. Successively, the tube was introduced into a Milestone Ethos D (Milestone Srl, Italy) microwave reactor. The tube was irradiated with microwaves at 500 W using a temperature ramp of 3 minutes and maintained at maximum 200°C for one additional minute. After the reaction, the mixture was cooled to room temperature naturally. The precipitate was filtrated and washed with 10 mL ethanol and 10 mL acetone and oven dried (100°C) for 24 h.

## 2.2 Synthesis of pb-Cu<sub>2</sub>S with conventional heating

To avoid any safety issue (please see below paragraph 2.3 for details) the synthesis of optimized pb-Cu<sub>2</sub>S under conventional heating was carried out in an oil bath. Pig bristle (1.5 g, cut in pieces of ~0.5 cm), sodium hydroxide and the metallic precursor CuCl (480 mg, 4.85 mmol) were added to ethylene glycol (20 mL) in a 250 mL round flask equipped with a stirring bar and a reflux. The mixture was heated in an oil bath for 6 h at 200°C. The precipitate was filtrated and washed with 10 mL ethanol and 10 mL acetone and oven dried (100°C) for 24 h.

## 2.3 IMPORTANT Warning notes about mixing ethylene glycol and NaOH

Despite no significant pressure increases nor safety issues (overtemperature, pressure, explosions, *etc.*) were never detected during all the experiments, an important note on the utilization of ethylene glycol mixed with NaOH should be stated. Indeed, during late 60's, a few incidents occurred in some industrial plants while operating with ethylene glycol and sodium hydroxide.<sup>32</sup> Even though the toxic problems were related to other components in the reactors (*e.g.* dioxins) and not to the mixture of EG and NaOH, some important safety procedures must be mentioned. As demonstrated by Milnes, an exothermic decomposition of ethylene glycol mixed with NaOH could start in the 230°C range and rapidly increases to 400°C, realising white vapour.<sup>33</sup> The exothermal reaction is related to the decomposition of sodium 2-hydroxyethoxide (NaOCH<sub>2</sub>CH<sub>2</sub>OH), which rapidly forms the vapour. It should be notice that the amount of sodium hydroxide should be quite high to form enough quantity of the sodium 2-hydroxyethoxide and cause a rapid vapour release. For example, in the cases of industrial incidents, the amount of ethylene glycol and NaOH was 3:1 in weight.<sup>32</sup> In order to operate in safe conditions and avoid any uncontrollable issue, all the reactions were made operating at maximum 200°C for maximum four minutes. In addition, the maximum weight ratio of ethylene glycol and NaOH was set to 180:1. In order to avoid any explosions, all the operation were made using a Teflon tube equipped with a safe vale (48 bar max pressure). All the reactions were carefully monitored, controlling both internal and external temperature, and setting safe temperature limits of 200°C as internal temperature limit and 60°C as external temperature limit. Due to the impossible control of the online internal temperature of an

autoclave and the absence of any safe valve, no reactions under conventional heating were carried out in closed containers.

## 2.4 Characterization

Powder X-ray diffraction (XRD) pattern of pb-Cu<sub>2</sub>S was recorded using a Bruker D8 DISCOVER A25 diffractometer (PanAnalytic/Philips, Lelyweg, Almelo, The Netherlands) using CuK $\alpha$  ( $\lambda=1.5418\text{\AA}$ ) radiation. Wide angle scanning patterns were collected over a  $2\theta$  range from  $10^\circ$  to  $80^\circ$  with a step size of  $0.018^\circ$  and counting time of 5 s per step.

Textural properties of the samples were determined by N<sub>2</sub> physisorption using a Micromeritics ASAP 2020 automated system (Micromeritics Instrument Corporation, Norcross, GA, USA) with the Brunauer-Emmet-Teller (BET) and the Barret-Joyner-Halenda (BJH) methods. The samples were outgassed for 24 h at  $100^\circ\text{C}$  under vacuum ( $P_0 = 10^{-2}$  Pa) and subsequently analysed.

Scanning electron microscopy images were recorded with a JEOL JSM-6300 scanning microscope (JEOL Ltd., Peabody, MA, USA) equipped with Energy-dispersive X-ray spectroscopy (EDX) at 15 kV at the Research Support Service Center (SCAI) from University of Cordoba.

## 2.5 Photocatalytic activity measurements

The photocatalytic activity of pb-Cu<sub>2</sub>S was evaluated in the degradation rate of methyl red (C.I. 13020) under visible-light irradiation. The experimental set up consisted in a 50 mL Pyrex glass tube irradiated by a commercially available LED lamp 6A. The distance between the lamp and the tube was set up to 2 cm. (see S.1 for a schematic illustration of the reactor). The mixture was irradiated with blue (peak centred at 465 nm), green (peak centred at 515 nm), red (peak centred at 630 nm) and white (as simultaneous irradiation of the three light) visible lights. Fig. 1 shows the emission spectrum of LED lamp: the three different colour components and the white light.

In a typical experiment, 10 mL ethanol solution of methyl red (50 ppm) was mixed with 5.0 mg of pb-Cu<sub>2</sub>S in a 50 mL Pyrex glass tube equipped with a stirrer. Before

irradiation, the mixture was sonicated for 30" in an US bath in order to achieve a good homogenization of the solution. After the photoreaction runs, samples of 0.35 mL were withdrawn from the solution at regular time intervals and diluted in 2 mL ethanol. Before UV-Vis absorption measurements, the solutions were filtrated to remove the catalyst. The quantitative determination of residue methyl red was conducted by measuring the absorption at a fixed wavelength. For comparison, the methyl red degradation was conducted under the same condition without any catalysts and employing commercially available Aeroxil®P25 TiO<sub>2</sub>. UV-visible (UV-vis) absorption spectra were recorded using a Lambda 365 UV-Vis Spectrophotometer (PerkinElmer, Waltham, MA, USA).

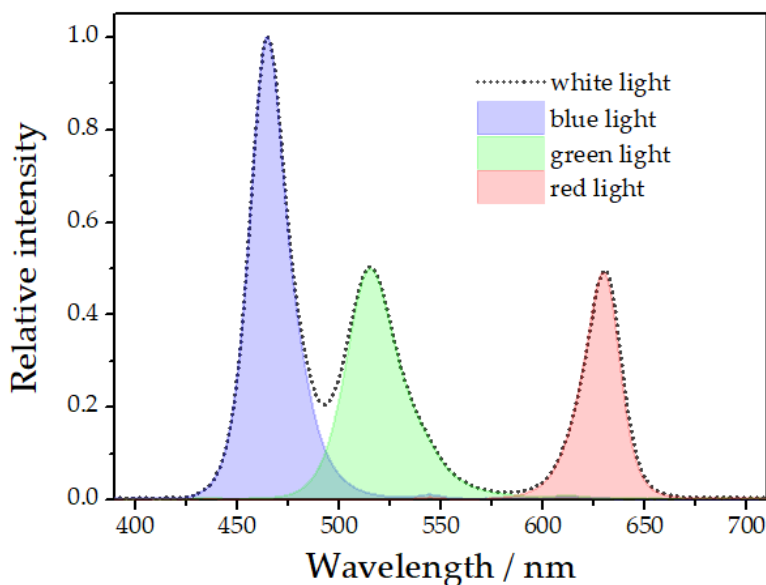


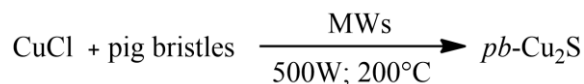
**Fig. 1** Emission spectra of the LED lamp and the three mayor light components used in the photocatalytic degradation of methyl red.

### 3. RESULTS AND DISCUSSION

#### 3.1 Formation of pb-Cu<sub>2</sub>S

A facile, fast and low toxicity one-pot route is herein reported for the synthesis of Cu<sub>2</sub>S carbon composites from wasted pig bristles. As illustrated in Scheme 1, the

preparation involved a simple microwave assisted heating step of a mixture of pig bristles, copper (I) chloride, ethylene glycol and, where appropriate, sodium hydroxide.



**Scheme 1** Reaction scheme for the synthesis of pb-Cu<sub>2</sub>S

The formation of pb-Cu<sub>2</sub>S could be explained in terms of thermo-degradation of pig bristles, which served as source of sulphur and carbon. As reported by Gonzalo *et al.*, pig bristles are mainly composed of keratin, an insoluble protein packed with cross-linked fibres by disulfide bonds.<sup>4</sup> The disulphide bonds are found in cysteine, while other amino acids containing sulfur are methionine and cysteic acid. In general, the total amount of sulphur contained in pig bristles could be quantified as *ca.* 5% wt.<sup>5, 34, 35</sup> Pig bristles started to decompose upon microwave irradiation at high temperature and sulphur, mainly in the form of ions, was released. Copper sulfide was then formed by combining S<sup>2-</sup> with Cu<sup>+</sup> and particles were self-aggregated to minimize the surface energy. During the aggregation step, the particles bind together with pig bristles residual carbon, as observed in SEM images.

Sodium hydroxide was employed in order to optimize the synthesis and accelerate the degradation of pig bristles and the formation of Chalcocite, which was found to be the most photocatalytically active crystalline form of copper sulfide. However, as shown in Fig.2, NaOH was not essential for the formation of Cu<sub>2</sub>S. The optimized sample was synthesized using 100 mg of NaOH (2.5 mmol). Based on previous experience, ethylene glycol was chosen for its ideal stabilising behaviour, low toxicity, high boiling point (198°C) and high viscosity under MW heating.<sup>24</sup> Aiming to make Cu<sub>2</sub>S, the molar amount of sulphur, therefore the amount of pig bristles (1.5 g equals to 2.34 mmol of S), and copper (4.85 mmol) was set up to an ideal 2:1. XRPD and SEM-EDX analysis confirmed the formation of copper sulfide carbon composites.

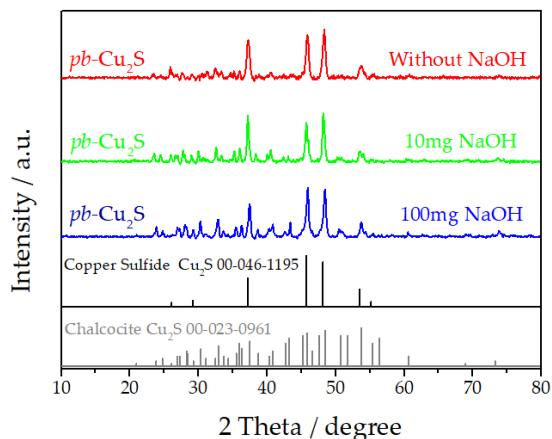
The synthesis of pb-Cu<sub>2</sub>S under conventional heating was carried out aiming to investigate the effect of MWs in the formation of the material. Due to safe issues

described in paragraph 2.3, conventional heating experiments were ran in an oil bath open vessel at 200°C. The formation of the first crystals of Cu<sub>2</sub>S was detected after 6 h of reaction by XRPD analysis. The pattern of the obtained material was compared with the material obtained in the microwave, confirming the efficiency of microwave heating for the crystallization of Cu<sub>2</sub>S. (for the XRD patterns comparison, please see S.2).

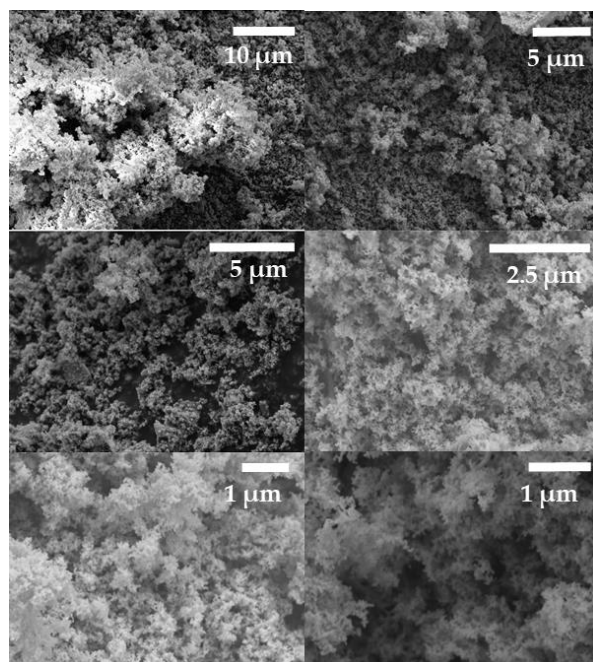
### 3.2 Morphology and Properties of pb-Cu<sub>2</sub>S

Fig.2 shows the XRPD pattern of the prepared pb-Cu<sub>2</sub>S. Cu<sub>2</sub>S was found in all the samples, while the crystalline form of Chalcocite was facilitated by the addition of different amount of NaOH (from 10 mg/0.25 mmol to 100 mg/2.5 mmol). Considering the pattern of the optimized sample, produced with 2.5 mmol of NaOH, the most intense diffraction peaks observed at 2 $\theta$  values of 23.85°, 26.90°, 28.15°, 30.25°, 32.85°, 37.45°, 45.95°, 47.45°, 53.75° and 73.82° could be index to (2 4 2), (1 8 0), (2 6 2), (0 9 1), (0 4 4), (1 11 1), (2 13 1), (6 6 2), (4 0 6) and (0 20 3) planes of Chalcocite Cu<sub>2</sub>S with orthorhombic structure (JCPDS 00-023-0961).<sup>36</sup> (For a complete list of the peaks and the assigned planes please see Table S.2)

The morphology of optimized pb-Cu<sub>2</sub>S was investigated by SEM and EDX spectrum. Fig.3 shows SEM images of the material. The material exhibited a structure that can be defined as coral-like homogeneous structure where fine granular particles were aggregated together. The structure rose from the fast degradation of the pig bristles, which left fine homogeneous carbon particles residues. The agglomeration of the carbon particles with the Chalcocite built the coral-like structure.



**Fig. 2** XRD pattern of pb-Cu<sub>2</sub>S produced with different amount of sodium hydroxide. All the samples showed copper sulfide, while the increasing of the content of NaOH facilitated the formation of Chalcocite, more photocatalytically active.



**Fig. 3** SEM images of pb-Cu<sub>2</sub>S.

SEM-EDX mapping results are summarized in Fig.4. Sulfur atomic content average was measured as ~13%, while copper content was determined to be ~31%. The atomic ratio about 2:1 between Copper and Sulfur was in line with XRPD analysis, which



demonstrated the formation of Chalcocite  $\text{Cu}_2\text{S}$ . The atomic content of carbon was determined to be  $\sim 50\%$ , or  $\sim 20\%$  weight. Except for oxygen, most likely absorbed as  $\text{CO}_2$ , no other elements were detected in EDX analysis, pointing to a high purity of the material. The closeness of EDX mapping results in different area demonstrated a good homogeneity of the sample. (For the complete results of EDX mapping, please see S.4)

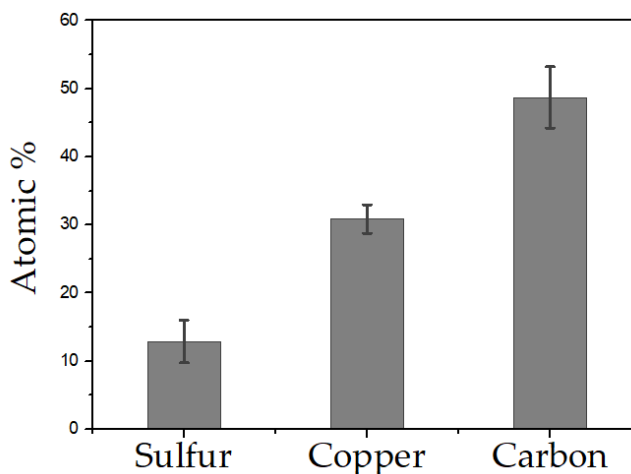


Fig. 4 SEM-EDX mapping results of pb- $\text{Cu}_2\text{S}$ .

Brunauer–Emmett–Teller (BET) physisorption was conducted to determine the specific surface area of pb- $\text{Cu}_2\text{S}$  carbon composite by nitrogen adsorption–desorption measurements. The BET surface area was found to be  $17\text{--}20\text{ m}^2/\text{g}$ , with isotherms clearly indicating a non-porous material, in good agreement with SEM analysis. (ESI, Figure S.5)

To investigate the optical behaviour of pb- $\text{Cu}_2\text{S}$ , UV-Vis absorption spectrum was recorded, and reported in the form of Kubelka-Munk, as shown in Fig.4 A. The spectrum exhibited an adsorption edge at *ca.*  $1050\text{ nm}$ , remarkably higher as compared to reported Chalcocite phases.<sup>30, 37</sup> This can be explained by the presence of carbon. The spectrum clearly showed that the pb- $\text{Cu}_2\text{S}$  could absorb visible light and hence pb- $\text{Cu}_2\text{S}$  can be a promising photocatalytic material. The optical band gap was obtained by the equation:<sup>38</sup>

$$(\alpha h\nu)^n = A(h\nu - E_g)$$

To determine the energy band gap,  $(\alpha h\nu)^2$  vs  $(h\nu)$  was plotted, as shown in Fig. 4 B (" $\alpha$ " was the absorption coefficient, " $h\nu$ " was the photon energy and " $A$ " was a constant, " $E_g$ " was the band gap and " $n$ " was either  $\frac{1}{2}$  for an indirect transition or 2 for a direct transition). The plot gave a straight line whose intercept on the energy axis resulted in the direct energy gap. Fig. 4 C shows the plot of  $(\alpha h\nu)^{1/2}$  vs  $(h\nu)$  used to calculate the indirect band gap. The band gap obtained for pb-Cu<sub>2</sub>S were 1.17 eV (direct) and 0.85 eV (indirect), remarkably reduced as compared to reported values for Chalcocite.<sup>39</sup>

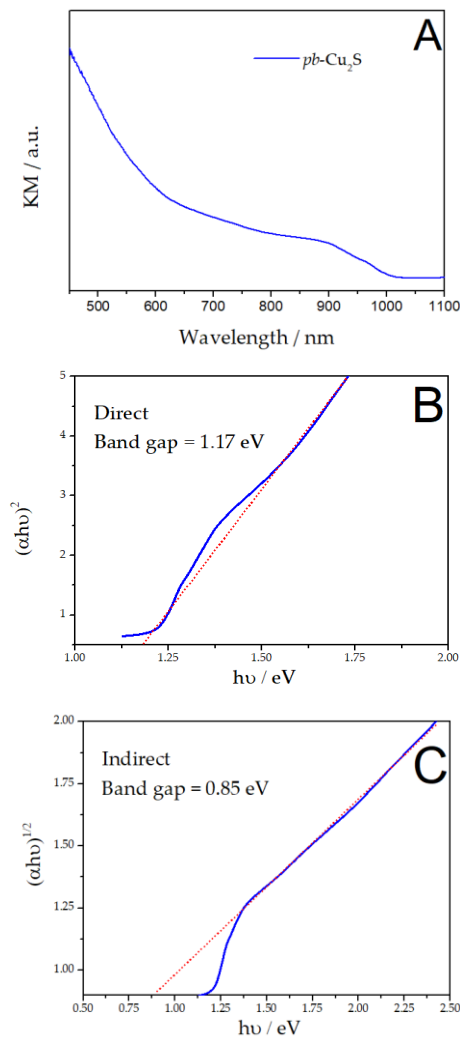


**Fig.4** Optical measurements of as-synthesized pb-Cu<sub>2</sub>S. (A) Kubelka Munk spectra. (B) Plot of  $(\alpha h\nu)^2$  vs photon energy  $h\nu$  for determination of direct band gap. (C) Plot of  $(\alpha h\nu)^{1/2}$  vs photon energy  $h\nu$  for determination of indirect band gap.

### 3.3 Photocatalytic activity measurements

The photocatalytic activity of pb-Cu<sub>2</sub>S was demonstrated in the photodegradation of a model organic dye. Methyl red (CI 13020), a commercially available dye used in industry, was chosen as model compound for pollutants removal. In fact, methyl red is an environmentally recalcitrant, possible carcinogen and toxic agent, and its degradation has important impact.

Despite all the materials showed photocatalytic properties, most active pb-Cu<sub>2</sub>S was in the form of Chalcocite (please see S.6 for a comparison of the photocatalytic activity of pb-copper sulfide and pb-Chalcocite).

Two different sets of blank experiments for the dye solution were performed. The activity of optimized pb-Cu<sub>2</sub>S was compared with the activity of commercial Aeroxil®P25 TiO<sub>2</sub> and with a blank run (to ascertain potential photobleaching of the dye) in the same reaction conditions. Results are shown in Fig.5 and clearly point out a remarkable dye degradation performance of pb-Cu<sub>2</sub>S under white LEDs irradiation (black line), particularly with a negligible degradation observed for P25 (dotted black line). pb-Cu<sub>2</sub>S could also provide certain photodegradation activity at different wavelengths (465, 515 and 630 nm).

To better understand the activity of the catalyst, the kinetic parameters were evaluated by pseudo first-order model:  $\ln(C_0/C_t) = kt$ .<sup>30</sup> Results are illustrated in Fig.6 while  $k$  and  $R^2$  data are given in table 1. The closeness of  $R^2$  to 1 indicated a good fitting of the data to pseudo-first order reaction.

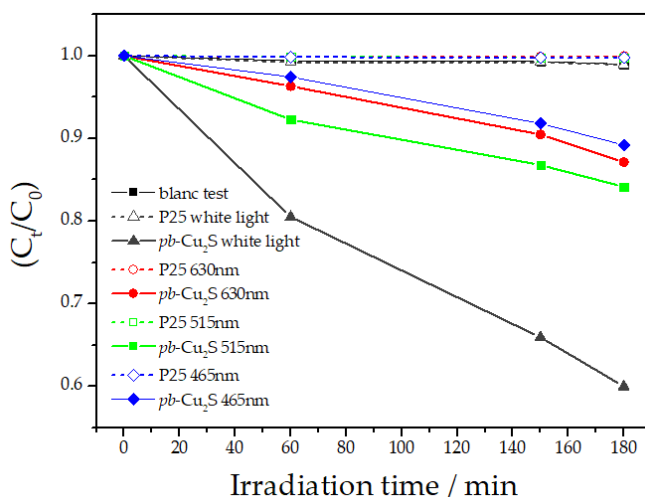


**Fig. 5** Photodegradation of methyl red catalysed by pb-Cu<sub>2</sub>S in function of time at different wavelength irradiation.

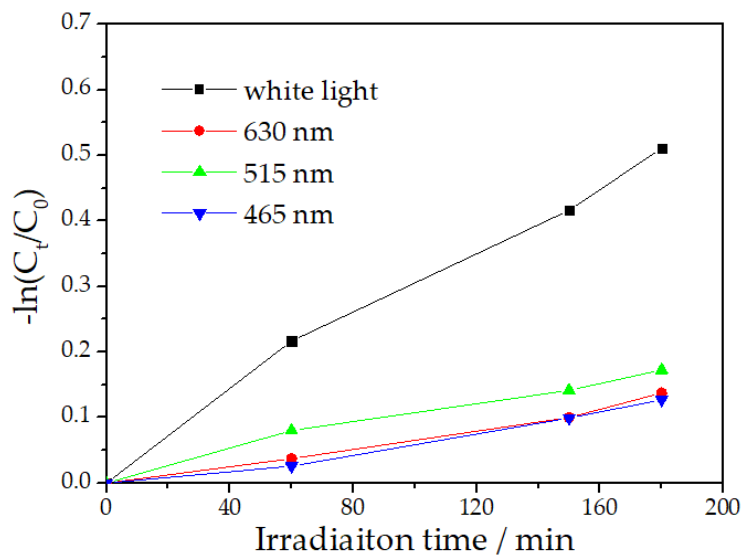


Fig. 6 Plot of  $-\ln(C_t/C_0)$  versus irradiation time.

Irradiation light	$k / \text{min}^{-1}$	$R^2$
White	0.00273	0.98924
630 nm	$7.42643 \times 10^{-4}$	0.98748
515 nm	$9.11448 \times 10^{-4}$	0.98115
465 nm	$6.31303 \times 10^{-4}$	0.98513

Table 1 k and  $R^2$  data.

#### 4. CONCLUSIONS

An unprecedented approach for the valorization of pig bristles to valuable photoactive materials has been developed. The use of environmentally friendly reagents and the utilization of microwaves provide an environmentally sound, facile, efficient and fast synthetic route. Pig bristles were used as sulphur and carbon source for the synthesis of copper sulfide carbon composite. The material was used as photocatalyst for the degradation of methyl red, with promising results that may pave the way to the utilisation of pb-Cu<sub>2</sub>S in a wide range of applications not limited to the field of photochemistry.

The new method successfully demonstrated, for the first time, the possibility to valorize wasted pig bristles. We believe the proposed eco friendly approach could act as springboard for the development of additional applications for wasted pig bristles that will be reported in due course.

#### Conflicts of interest

The authors declare no conflicts of interest.

#### Acknowledgements

The authors thank Pennellificio OMEGA S.p.A., Bologna (IT), and Mr. Massimo Rondelli for the free supply of pig bristles.

This project has received funding from the European Union's Horizon 2020 research and innovation programme under the Marie Skłodowska-Curie grant agreement No 721290. This publication reflects only the author's view, exempting the Community from any liability. Project website: <http://cosmic-etn.eu/>. M.J.M-B thanks MINECO for the award of postdoctoral JdC contract (FJCI-2016-29014). The publication has been prepared with support of RUDN University program 5-100.

1. A. J. Ragauskas, C. K. Williams, B. H. Davison, G. Britovsek, J. Cairney, C. A. Eckert, W. J. Frederick, J. P. Hallett, D. J. Leak, C. L. Liotta, J. R. Mielenz, R. Murphy, R. Templer and T. Tschaplinski, *Science*, 2006, **311**, 484-489.
2. C. Okkerse and H. van Bekkum, *Green Chemistry*, 1999, **1**, 107-114.

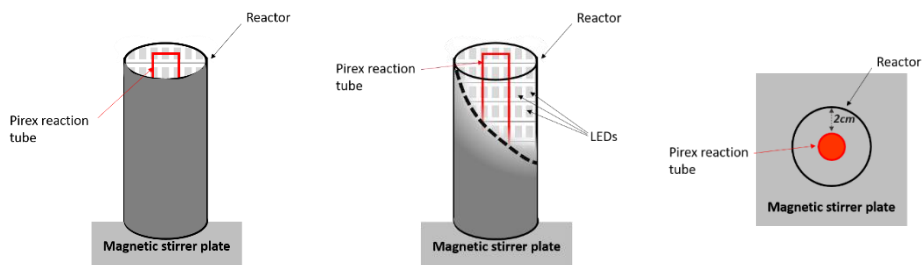
3. ©European Union 1995-2017, EUROSTAT 2017, [http://appsso.eurostat.ec.europa.eu/nui/show.do?dataset=apro\\_mt\\_lspig](http://appsso.eurostat.ec.europa.eu/nui/show.do?dataset=apro_mt_lspig)
4. M. Gonzalo, C. M. Jespersen, K. Jensen, S. Støier and L. Meinert, presented in part at the 62<sup>nd</sup> International Congress of Meat Science and Technology, Bangkok, Thailand, 2016.
5. W. Laba, W. Kopec, D. Chorazyk, A. Kancelista, M. Piegza and K. Malik, *International Biodeterioration & Biodegradation*, 2015, **100**, 116-123.
6. F. G. Gachango, K. S. Ekmann, J. Frorup and S. M. Pedersen, *Aquaculture*, 2017, **479**, 265-272.
7. W. Laba, D. Chorazyk, A. Pudlo, J. Trojan-Piegza, M. Piegza, A. Kancelista, A. Kurzawa, I. Zuk and W. Kopec, *Waste and Biomass Valorization*, 2017, **8**, 527-537.
8. J. J. Bozell, *Science*, 2010, **329**, 522-523.
9. J. J. Bozell and G. R. Petersen, *Green Chemistry*, 2010, **12**, 539-554.
10. *Trends in Biotechnology*, 2001, **19**, 172 - 177.
11. C. H. Deng, H. M. Hu, X. Q. Ge, C. L. Han and D. F. Zhao, *Asian Journal of Chemistry*, 2013, **25**, 5542-5544.
12. R. S. Varma, *Green Chemistry*, 2014, **16**, 2027-2041.
13. A. Makridis, I. Chatzitheodorou, K. Topouridou, M. P. Yavropoulou, M. Angelakeris and C. Dendrinou-Samara, *Materials Science & Engineering C-Materials for Biological Applications*, 2016, **63**, 663-670.
14. A. Mirzaei and G. Neri, *Sensors and Actuators B-Chemical*, 2016, **237**, 749-775.
15. M. Tsuji, *Chemistryselect*, 2017, **2**, 805-819.
16. C. O. Kappe and D. Dallinger, *Molecular Diversity*, 2009, **13**, 71-193.
17. A. Yopez, S. De, M. S. Climent, A. A. Romero and R. Luque, *Applied Sciences-Basel*, 2015, **5**, 532-543.
18. M. Francavilla, S. Intini, L. Luchetti and R. Luque, *Green Chemistry*, 2016, **18**, 5971-5977.
19. H. Z. Gao, C. P. Teng, D. H. Huang, W. Q. Xu, C. H. Zheng, Y. S. Chen, M. H. Liu, D. P. Yang, M. Lin, Z. B. Li and E. Y. Ye, *Materials Science & Engineering C-Materials for Biological Applications*, 2017, **80**, 616-623.
20. A. Jana, E. Scheer and S. Polarz, *Beilstein Journal of Nanotechnology*, 2017, **8**, 27.
21. A. M. Balu, J. M. Hidalgo, J. M. Campelo, D. Luna, R. Luque, J. M. Marinas and A. A. Romero, *Journal of Molecular Catalysis a-Chemical*, 2008, **293**, 17-24.
22. A. M. Balu, D. Dallinger, D. Obermayer, J. M. Campelo, A. A. Romero, D. Carmona, F. Balas, K. Yohida, P. L. Gai, C. Vargas, C. O. Kappe and R. Luque, *Green Chemistry*, 2012, **14**, 393-402.
23. J. M. Bermudez, M. Francavilla, E. G. Calvo, A. Arenillas, M. Franchi, J. A. Menendez and R. Luque, *Rsc Advances*, 2014, **4**, 38144-38151.
24. A. Zuliani, A. M. Balu and R. Luque, *Acs Sustainable Chemistry & Engineering*, 2017, **5**, 11584-11587.
25. D. Cambie, C. Bottecchia, N. J. W. Straathof, V. Hessel and T. Noel, *Chemical Reviews*, 2016, **116**, 10276-10341.
26. K. L. Skubi, T. R. Blum and T. P. Yoon, *Chemical Reviews*, 2016, **116**, 10035-10074.
27. G. L. Chiarello, A. Zuliani, D. Ceresoli, R. Martinazzo and E. Selli, *Acs Catalysis*, 2016, **6**, 1345-1353.
28. T. H. Han, H. G. Wang and X. M. Zheng, *Rsc Advances*, 2016, **6**, 7829-7837.
29. M. Cheng, G. M. Zeng, D. L. Huang, C. Lai, P. Xu, C. Zhang and Y. Liu, *Chemical Engineering Journal*, 2016, **284**, 582-598.

30. G. Mondal, P. Bera, A. Santra, S. Jana, T. N. Mandal, A. Mondal and S. I. Seok, *New Journal of Chemistry*, 2014, **38**, 4774-4782.
31. C. Casado, R. Timmers, A. Sergejevs, C. T. Clarke, D. W. E. Allsopp, C. R. Bowen, R. van Grieken and J. Marugan, *Chemical Engineering Journal*, 2017, **327**, 1043-1055.
32. F. Lees, *Lees' Loss Prevention in the Process Industries: Hazard Identification, Assessment and Control*, Butterworth-Heinemann, 2012.
33. M. H. Milnes, *Nature*, 1971, **232**, 395-&.
34. Z. P. Liu, S. Z. Yu and X. S. Xu, *Acta Pharmacologica Sinica*, 1988, **9**, 526-529.
35. W. Gumz, *INFLUENCE OF ORIGIN ON THE MINERAL-CONTENT OF PIG BRISTLES*, 1993.
36. W. R. Cook, L. Shiozawa and F. Augustine, *Journal of Applied Physics*, 1970, **41**, 3058-3036.
37. Y. Liu, Y. H. Deng, Z. K. Sun, J. Wei, G. F. Zheng, A. M. Asiri, S. B. Khan, M. M. Rahman and D. Y. Zhao, *Small*, 2013, **9**, 2702-2708.
38. C. Yang, H. Q. Fan, Y. X. Xi, J. Chen and Z. Li, *Applied Surface Science*, 2008, **254**, 2685-2689.
39. B. J. Mulder, *Physica Status Solidi a-Applied Research*, 1973, **18**, 633-638.



## Supporting Information

### S.1 Schematic illustration of the photoreactor employed for degradation of methyl red

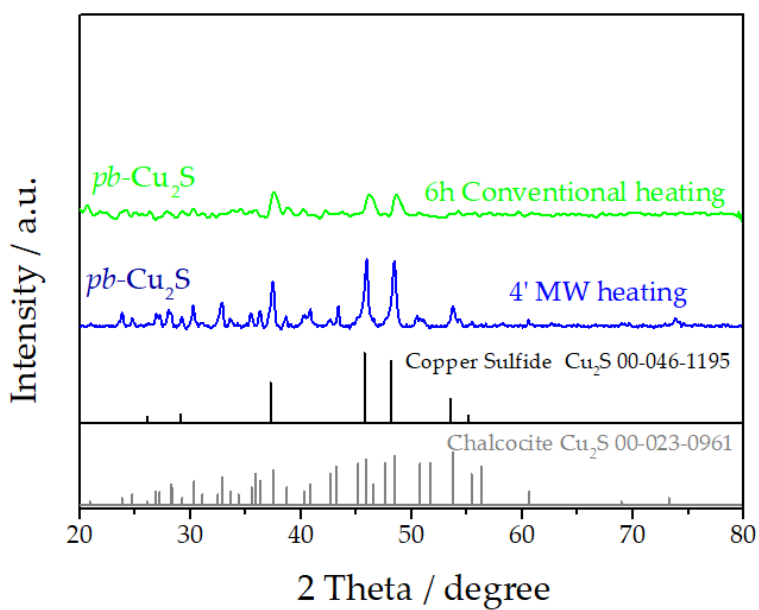


S.1 B Illustration of the photoreactor

S.1 B section of the photoreactor

S.1 C Top view of the reactor

### S.2 XRD patterns of *pb*-Cu<sub>2</sub>S produced by thermal and MWs heating with 100 mg NaOH



S.3 XRD peaks of *pb-Cu<sub>2</sub>S*

<b>pb-Cu<sub>2</sub>S</b>			<b>Chalcocite, 00-023-0961</b>					
	<b>Pos. [°2Th.]</b>	<b>Intensity</b>	<b>h</b>	<b>k</b>	<b>l</b>	<b>d</b>	<b>Pos. [°2Th.]</b>	<b>Intensity</b>
1	23,876	19,8	2	4	2	3,73	23,836	20
2	24,8053	10,57	3	0	2	3,59	24,78	16
3	27,309	13,81	4	2	0	3,27	27,25	25
4	28,1707	18,84	2	6	2	3,18	28,037	40
5	29,2486	14,15	2	4	3	3,05	29,258	20
6	30,2957	28,09	1	9	1	2,873	31,104	16
7	32,924	33,35	0	4	4	2,718	32,927	55
8	33,5561	9,13	2	2	4	2,659	33,679	25
9	35,4024	17,27	4	2	3	2,524	35,539	40
10	36,3388	22,3	4	3	3	2,469	36,358	45
11	37,4597	65,23	1	11	1	2,396	37,507	85
12	38,6774	14,92	1	7	4	2,325	38,697	40
13	40,8337	22,35	2	2	5	2,207	40,855	30
14	42,6074	8,52	4	4	4	2,117	42,675	12
15	43,3759	32,1	1	9	4	2,093	43,189	10
16	45,9566	100	2	13	1	1,977	45,863	100
17	48,463	92,33	2	14	0	1,876	48,486	90
18	50,7156	9,61	5	9	3	1,797	50,765	14
19	53,7104	28,73	4	0	6	1,704	53,751	35
20	58,2692	3,14	6	0	5	1,632	56,328	10
21	60,5742	5,51	4	8	6	1,526	60,634	25
23	69,3398	1,8	6	8	6	1,361	68,941	10
24	73,8131	9,77	0	20	3	1,291	73,263	20

S.3 SEM-EDX mapping results of *pb*-Cu<sub>2</sub>S

Element	Wt%	Wt% Sigma	Atomic %
C	20.01	0.62	49.84
O	4.73	0.21	8.85
S	12.73	0.19	11.88
Cu	62.52	0.55	29.43
Total:	100.00		100.00

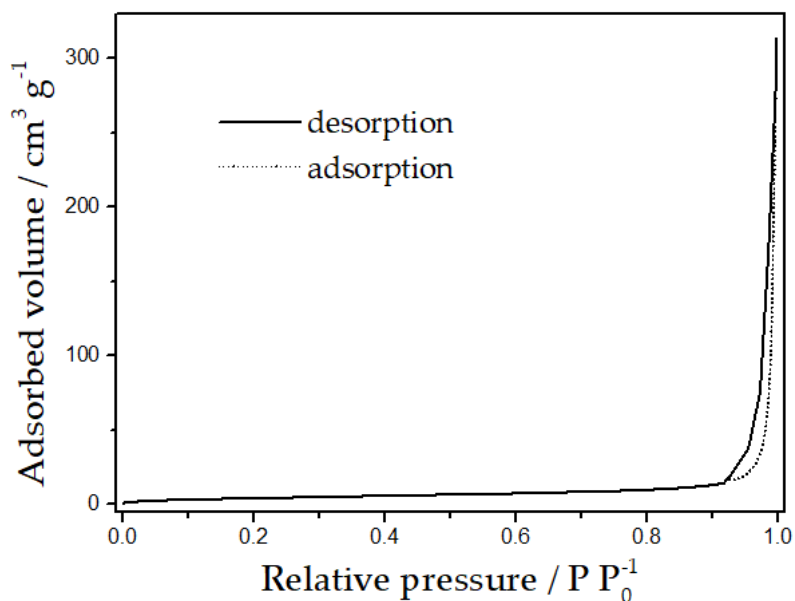
Element	Wt%	Wt% Sigma	Atomic %
C	20.73	0.66	51.31
O	4.51	0.23	8.38
S	11.58	0.19	10.74
Cu	63.19	0.59	29.57
Total:	100.00		100.00

Element	Wt%	Wt% Sigma	Atomic %
C	22.18	0.54	53.94
O	4.06	0.19	7.42
S	10.49	0.16	9.56
Cu	63.27	0.49	29.09
Total:	100.00		100.00

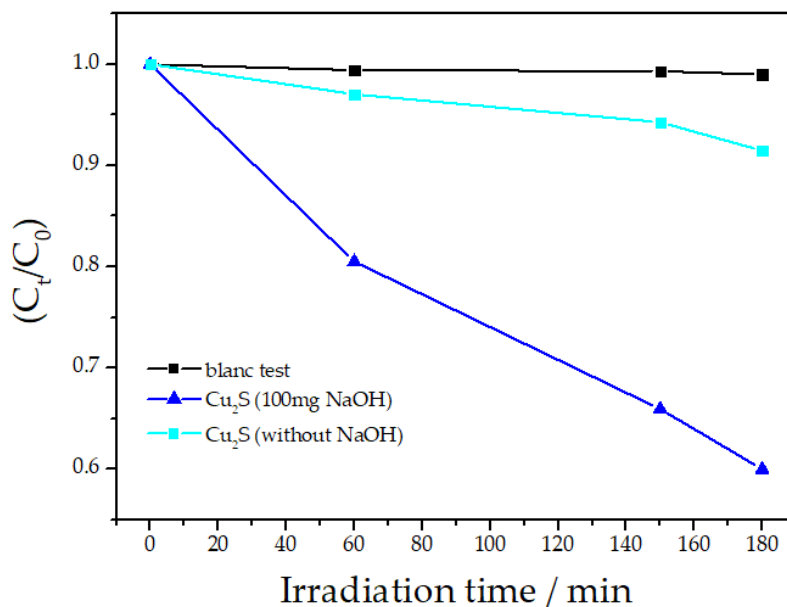
Element	Wt%	Wt% Sigma	Atomic %
C	15.53	0.75	42.74
O	3.14	0.22	6.49
S	16.51	0.27	17.03
Cu	64.82	0.65	33.74
Total:	100.00		100.00

Element	Wt%	Wt% Sigma	Atomic %
C	17.10	0.73	45.66
O	3.30	0.22	6.63
S	15.21	0.25	15.21
Cu	64.39	0.63	32.51
Total:	100.00		100.00

S.5 N<sub>2</sub> adsorption–desorption isotherm of *pb*-Cu<sub>2</sub>S



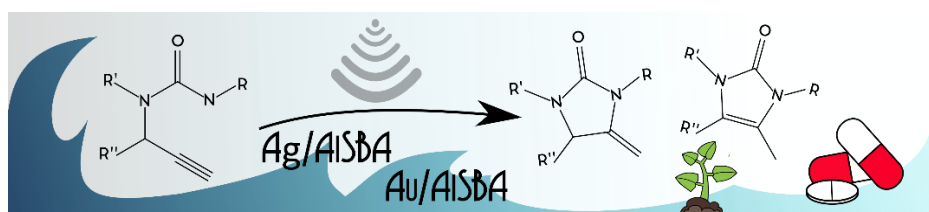
S.6 Photodegradation of methyl red catalysed by *pb*-Cu<sub>2</sub>S obtained with different amount of NaOH.



## Heterogeneously catalyzed synthesis of imidazolones *via* cycloisomerizations of propargylic ureas using Ag and Au/Al SBA-15 systems

Alessio Zuliani,<sup>a</sup> Prabhat Ranjan,<sup>b</sup> Rafael Luque<sup>a,c\*</sup> and Erik V. Van der Eycken<sup>b,c\*</sup>

*ACS Sustain. Chem Eng.*, 2019, 7 (5), 5568-5575



<sup>a</sup> Departamento de Química Organica, Universidad de Córdoba, Edificio Marie-Curie (C-3), Ctra Nnal IV-A, Km 396, Córdoba, Spain

<sup>b</sup> Laboratory for Organic & Microwave-Assisted Chemistry (LOMAC), Department of Chemistry, University of Leuven (KU Leuven), Celestijnenlaan 200F, B-3001 Leuven, Belgium

<sup>c</sup> Peoples' Friendship University of Russia (RUDN University), 6 Miklukho-Maklaya Street, 117198, Moscow, Russia

Adapted with permission from *ACS Sustain. Chem Eng.*, 2019, 7 (5), 5568-5575. Copyright 2019 American Chemical Society.

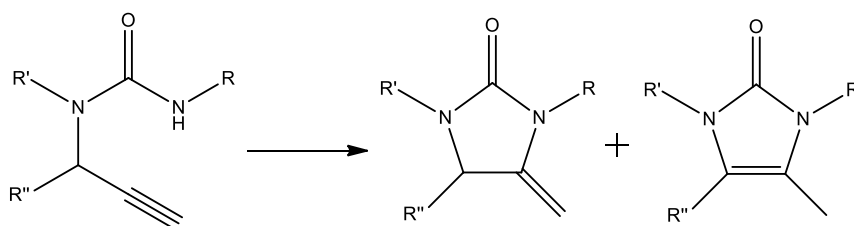
*Abstract: The synthesis of imidazolones through the cycloisomerization of ureas, specifically propargylureas, has gained attention due to the large availability of starting materials. However, this type of synthesis normally requires the utilization of strong bases such as NaOH, expensive homogeneous metal catalysts such as Ag, Au and Ru-based systems, or toxic and hazardous chemicals. Herein, a study of different synthetic routes for the preparation of imidazolones through the cycloisomerization of propargylic ureas under fast, mild and environmentally friendly conditions under heterogeneous catalysis was explored. Firstly, the synthesis were carried out under mild conditions using toluene and acetonitrile as solvents. Silver and gold nanoparticles supported on AISBA-15 were used as heterogeneous catalysts. The catalysts were prepared by mechanochemical and microwave-assisted techniques. Sequentially, a range of solvents were replaced by the greener ethanol. Finally, all obtained results were combined in order to carry out the reaction using only water as solvent and promoter of the reaction. Aiming to expedite the procedure, the synthesis were carried out under conventional and microwave irradiation.*

## INTRODUCTION

Imidazolones are well known compounds widely used in industries for the preparation of different chemicals, agrochemicals and pharmaceuticals. Indeed, due to the existence of tautomeric forms, they can easily interact with biopolymers and receptors present in living systems which account for the different biological activities.<sup>1</sup> Some substituted imidazolones were found to be herbicides, insecticidal, antifungal, anti-inflammatory and antitumor agents while others showed cardiotoxic, antioxidant, vasodilator and enhancing-memory properties.<sup>2-5</sup> For example, in 2008 Congiu *et al.* reported imidazole-2-one derivatives as active anti-tumoral against human cancer cells.<sup>6</sup> More recently, some other imidazolone derivatives were demonstrated to show high hypertensive activity by molecular modelling approaches.<sup>7</sup> Imidazolones have been also proved to be novel ligands for the synthesis of catalytically active complexes with transition metals. Tiow-Gan and co-workers reported the hydroamination of aminoalkenes with zirconium complexes supported on imidazolones.<sup>8</sup>

As a result, the preparation of substituted imidazolones is gaining more attention day by day. The most studied methods for the preparation of imidazolones include the

synthesis from acylouins and ureas,<sup>4</sup> the intramolecular cyclization of ureidoacetals, ureidoxazinanes and ureidoketones<sup>9</sup> or the transformations of imidazole derivatives such as imidazolidine-diones or imidazole-oxides.<sup>10</sup> During recent years, the synthesis of substituted imidazolones from ureas, specifically from propargylureas, as illustrated in Scheme 1, have gained more attention due to the large availability of the starting materials propargylureas and isocyanates.<sup>11</sup> In fact, diverse type of propargylamines can be synthesized in one-pot reactions through A-3 coupling of alkynes, amines and aldehydes, which are starting material of low economic impact. However, the cycloisomerization of propargylic ureas normally requires the utilization of strong bases, such as KOH or NaOH, or the use of highly toxic, hazardous and expensive chemicals, limiting the applicability in terms of safety, waste/by-products production and environmental impact.<sup>12,13</sup> The challenge of developing sustainable and low toxicity paths for the efficient cycloisomerization of propargylureas is therefore a captivating topic.



**Scheme 1.** General scheme of cycloisomerization of propargylic urea

In some previous works we have synthesized several substituted imidazolones starting from propargylic ureas, operating in toluene and employing silver and gold homogeneous catalysts avoiding the use of any strong bases and highly toxic chemicals.<sup>14,15</sup> The homogeneous catalytic conditions were selected as they offer better selectivity and high reactivity avoiding mass transfer limitations, which decrease the overall time of reaction. However, the utilization of homogeneous catalysts entails some inherent disadvantages including the metal contamination in the final product and the high cost of production due to the impossible recovery of the precious metals.<sup>16,17</sup> In addition, the U.S. Department of Health and Human Services Food and Drug

Administration classified toluene as Class 2 solvent and its utilization should be limited in pharmaceutical industry.<sup>18</sup>

Herein, in order to switch the reaction to greener conditions, different sustainable, environmentally friendly, low toxicity and efficient paths for the catalysed cycloisomerization of propargylic ureas were investigated. Initially, the study of the reaction was accomplished in toluene and acetonitrile, substituting gold and silver homogeneous catalysts with heterogeneous systems based on gold and silver nanoparticles supported on AISBA-15. In general, metal-nanoparticles supported on solids allow the exploitation of nanocatalysis, at the boundary between homogeneous and heterogeneous catalysis, with the simplified recovery of the material.<sup>17,19</sup> In the last years, different mesoporous materials have been studied as supports for the stabilization of gold and silver nanoparticles and mesoporous silica materials emerged due to the abundance of Si-OH bonds on the surface, which can stabilize the metal nanoparticles.<sup>20,21,22</sup> Specifically, SBA-15 emerged for its outstanding characteristics.<sup>23</sup> To the best of our knowledge, no report on similar works were found in the literature. The catalyst were prepared through environmentally friendly and highly innovative paths, including solventless ball milling techniques and fast microwave-assisted synthesis. Triphenylphosphine was used as mild additive to increase the reaction yield without any leaching effects. Sequentially the solvents were substitute with ethanol, which is classified as Class 3 solvent by the U.S. FDA (less toxic and of lower risk to human health).<sup>18</sup> Finally, a new methodology for the cycloisomerization of propargylic ureas using only water as solvent and synthesis promoter was developed. In order to sensibly accelerate all the reactions, the synthesis were carried out under conventional and microwave heating. In fact, microwave heating offer the possibility to perform experiments in an extremely effective, safe, rapid, and highly reproducible way.<sup>24,25</sup> The results indicated that heterogeneous catalyst in toluene promoted most N-cyclization reactions, while ethanol favored the cyclization of propargylic ureas characterized by more electron withdrawing groups. Finally, water-mediated reactions favoured the cyclization of propargylic ureas containing electron donor compounds in the structure.



## MATERIALS AND METHODS

**Materials.** Pluronic P123 (PEG-PPG-PEG), hydrochloric acid (HCl, 37%wt), aluminium isopropoxyde ( $(\text{Al}[\text{OCH}(\text{CH}_3)_2]_3)$ ,  $\geq 98\%$ ), tetraethyl orthosilicate (TEOS,  $\text{Si}(\text{OC}_2\text{H}_5)_4$ , 98%), silver nitrate ( $\text{AgNO}_3$ ,  $\geq 99.0\%$ ), gold bromide ( $\text{AuBr}_3$ , 99.9%), ethanol ( $\text{CH}_3\text{CH}_2\text{OH}$ , 99.8%), acetonitrile ( $\text{CH}_3\text{CN}$ , 99.8%), toluene ( $\text{C}_7\text{H}_8$ , 99.8%), triphenylphosphine ( $(\text{C}_6\text{H}_5)_3\text{P}$ , 99%), chloroform-d ( $\text{CDCl}_3$ , 99.96 atom % D), chloro(triphenylphosphine)gold(I) ( $[(\text{C}_6\text{H}_5)_3\text{P}]\text{AuCl}$ ,  $\geq 99.9\%$ ), silvertrifluoromethanesulfonate ( $\text{CF}_3\text{SO}_3\text{Ag}$ ,  $\geq 98.0\%$ ), 1,4-diazabicyclo[2.2.2]octane (DABCO,  $\text{C}_6\text{H}_{12}\text{N}_2$ ,  $\geq 99\%$ ), 4-(dimethylamino)pyridine (DMAP,  $\text{C}_7\text{H}_{10}\text{N}_2$ ,  $\geq 99\%$ ), triethylamine ( $(\text{C}_2\text{H}_5)_3\text{N}$ ,  $\geq 99.5\%$ ), N-methyl propargylamine ( $\text{HC}\equiv\text{CCH}_2\text{NHCH}_3$ , 95%), were purchased from Sigma-Aldrich Inc., St. Louis, MO, USA. All reagents were used without any further purification.

**General procedure for the synthesis of the catalysts.** AISBA-15 was synthesized according to a procedure reported in a previous work.<sup>26</sup> Briefly, 20 g of Pluronic P123 were dissolved under stirring in 750 mL of a 1.5 pH solution of distilled water and HCl at r.t.. After the complete dissolution of P123 (1 h), 2.10 g of Aluminium isopropoxyde were slowly added. Finally, 45 mL of tetraethyl orthosilicate (TEOS) were added drop-by-drop. The mixture was stirred at 35°C for 24 hours, and hydrothermally treated for 24 hours at 100°C. The precipitated white solid was filtrated and dried at r.t. for 12 hours. The template was removed by calcination under  $\text{N}_2$  flux at 600 °C for 8 h.

Silver nanoparticles were supported on the so-produced AISBA-15 by a ball milling technique developed in our laboratories.<sup>27</sup> In order to obtain 2 %wt metal charge, 160 mg of  $\text{AgNO}_3$  (0.9 mmol) were added to 5 g of AISBA-15 in a 125 mL ball milling bowl equipped with eighteen 5 mm  $\varnothing$  stainless steel balls. Sequentially the powders were grounded in a Retsch PM-100 planetary ball mill (350 rpm, 10 min). The resulting material was calcined at 450 °C for 4 h under synthetic air flux. The same procedure was applied for the production of 2 %wt gold nanoparticles supported on AISBA-15, using 226 mg of  $\text{AuBr}_3$  (0.5 mmol) mixed with 5 g of AISBA-15. The supported nanocatalysts produced by ball milling were denoted BM-2% $\text{Au}@$ AISBA-15 and BM-2% $\text{Ag}@$ AISBA-15.

Alternatively, silver and gold nanoparticles were supported on AISBA-15 though a microwave-assisted methodology.<sup>28</sup> Briefly, 200 mg of AISBA-15 were mixed together

with 6.3 mg of  $\text{AgNO}_3$  (0.04 mmol) in 2 mL of ethanol in a 10 mL Pirex microwave vial sealed with the proper cap. The mixture was stirred at 700 rpm for 15 minutes prior to MW heating. Subsequently, the vial was placed in a CEM microwave reactor and heated at  $150^\circ\text{C}$  for 3'. The rapid heating led to the quick precipitation of metallic silver well-distributed over AISBA-15. Finally, the mixture was filtered and washed with ethanol (10mL). The filtrated solid was recovered and dried overnight at  $100^\circ\text{C}$ . Similarly, gold nanoparticles were prepared using 9 mg of  $\text{AuBr}_3$  (0.02 mmol) and 200 mg AISBA-15. The supported nanocatalysts produced by microwave-assisted techniques were denoted MW-2%Au@AISBA-15 and MW-2%Ag@AISBA-15 respectively.

**General procedure for catalyzed cycloisomerization of propargylic ureas.** To accomplish the cycloisomerization reaction, the selected propargylic urea was mixed with appropriate solvent (dry in case of toluene, acetonitrile and ethanol) in a 10 mL screw cap vial or 10 mL Pirex microwave vial. Reaction vial was charged with the different catalysts and sealed with proper cap. The reaction mixture was stirred at 800 rpm for 10 minutes prior to reaction. The reaction was carried out in a preheated oil bath or in a CEM Microwave reactor. After completion, the reaction mixture was filtered through a micropore filter (Chromafil® 0-20/25MS, PTFE) and the filter was washed with EtOH (3 x 1 mL).

**Characterization of product.** All products were analysed by  $^1\text{H}$ -NMR and  $^{13}\text{C}$ -NMR and can be found in our previous reports.<sup>14,15</sup>

## RESULTS AND DISCUSSION

**Heterogeneous catalyzed reactions in toluene and acetonitrile.** The first studies were carried out in order to switch the catalysed cycloisomerization of propargyl ureas from homogeneous to heterogeneous conditions. Gold and silver nanoparticles supported on AISBA-15 (2 wt% metal load), which showed good activity in previous work for the synthesis of spiroindolenines, were selected as catalysts.<sup>28</sup> The catalysts were prepared by both mechanochemical methods and microwave-assisted synthesis. On the one hand, mechanochemistry emerged as a promising solventless technology where the kinetic energy is transferred to the milled material achieving the breaking of chemical

bonds and/or creating new surfaces by fractures.<sup>29</sup> In recent years, this method has allowed the simple, clean, versatile and highly reproducible preparation of advanced materials such as MOFs, supported nanometals and metal oxides for diverse applications in catalysis or related advanced technologies (*e.g.* electrochemistry).<sup>30-32</sup> The preparation of the catalysts via mechanochemistry involved two simple steps: the grinding of AISBA-15 with the metal precursors, and the sequential calcination at high temperature in order to perform the reduction of the metals, forming the nanoparticles strongly stick to the walls of AISBA-15.<sup>27</sup> On the other hand, microwave techniques show several advantages, including the reduction of reaction time, the possibility to obtain higher yields, different selectivities, and the potential to accomplish reactions/chemistries that don't take place under conventional heating conditions.<sup>33,34</sup> Furthermore, microwave-assisted methods have emerged for providing scaled-up processes without suffering thermal gradient effects, leading to an important advancement in the large-scale synthesis of nanomaterials.<sup>35</sup> In the present work, the catalysts were prepared by a unique easy step, were an homogeneous mixture of the metal precursors and AISBA-15 in ethanol, were quickly heated by microwave irradiation. This rapid heating allowed the fast and precipitation of the metal precursor, which were reduced by ethanol, forming the nanoparticles on the SBA surface.<sup>28</sup> Mesoporous silica SBA-15 was selected as supporting material for gold and silver nanoparticles because of the abundance of Si-OH bonds on the surface, which can stabilize nanoparticles.<sup>36</sup> In addition, SBA-15 features unique properties including large surface areas (up to 1000 m<sup>2</sup>/g), controllable thick walls, small pore sizes (4–30 nm), and high thermal and mechanical stability.<sup>37</sup> Lastly, aluminum can be easily inserted into the structure of SBA-15, forming AISBA-15 with enhanced Lewis-acidic, ion-exchanging, and catalytic properties.<sup>38</sup> The employed catalysts were fully characterized in previous reports. Specifically, XRD, SEM, TEM, XPS, surface area analysis and thermal stability analysis can be found in the literature.<sup>28</sup> As an example, Figure 1 depicts a TEM image of BM-2%Ag@AISBA-15 in which silver nanoparticles can be observed inside and outside the channels of AISBA-15.

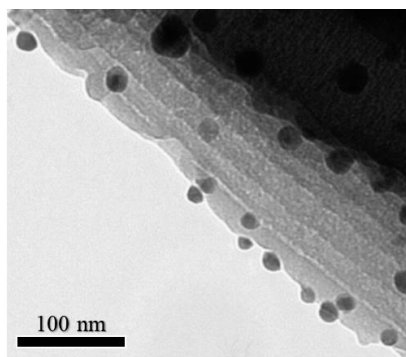
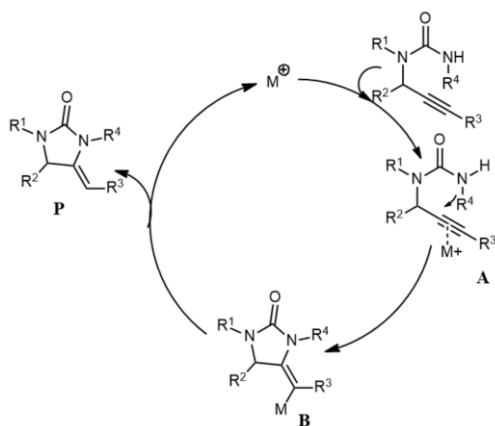


**Figure 1.** TEM of BM-2%Ag@AISBA-15. Reprinted with permission from ref. 28. Copyright 2016 American Chemical Society.

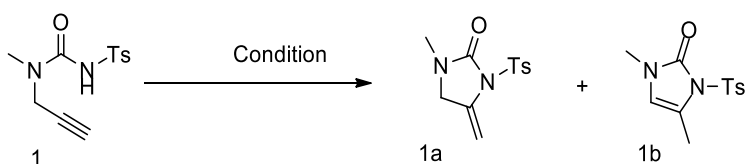
Initially, the experiments of cycloisomerization of propargylic urea were carried out using terminal propargylic urea **1** synthesized by tosyl isocyanate and N-methylpropargylamine (Table 1). Ball-milling synthesized catalysts BM-2 %Ag@AISBA-15 and BM-2%Au@AISBA-15 were firstly employed. The proposed general reaction mechanism is illustrated in Scheme 2.



**Scheme 2.** Plausible mechanism for formation of 2-imidazole.

The first aim consisted in the determination of the selectivities and in the comparison of these results with those reported using homogeneous catalysts. The cycloisomerization of propargylic ureas derived from tosyl isocyanate was selected as

model reaction, as illustrated in Scheme 3. As shown in Table 1, the reaction was first run with 18 mg of BM-2%Au@Al-SBA15 in toluene, obtaining 47% yield of imidazolidin-2-one 1a with 20 % of migrated double bond product imidazole-2-one 1b (Table 1, entry 1). The result was close to the previous reported in which the synthesis of imidazolidin-2-one was successfully promoted by PPh<sub>3</sub>AuCl (Table 1, entry 16) in homogeneous conditions.<sup>14</sup> Furthermore, the increasing of the amount of BM-2%Au@Al-SBA-15 employed improved the formation of 1a (Table 1, entry 2).



**Scheme 3.** Reaction scheme of cycloisomerization of propargylic ureas derived from tosyl isocyanate.

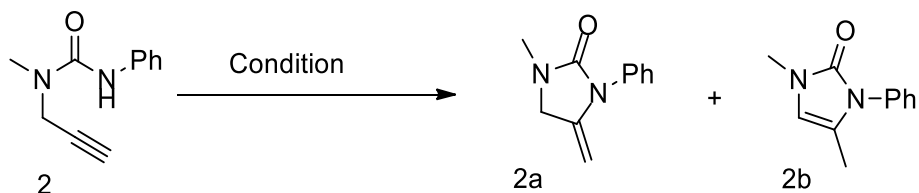
**Table 1. Optimization of the reaction illustrated in Scheme 3<sup>a</sup>**

Entry	Cat (mg)	Solvent	T (°C)	t (h)	% yield (a/b) <sup>f</sup>
1 <sup>b</sup>	Au (0.018)	Toluene	40	3	47/20
2 <sup>b</sup>	Au (0.035)	Toluene	40	3	78/20
3 <sup>b</sup>	Au (0.035)	Toluene	40	2	70/20
4 <sup>b</sup>	Au (0.035)	Toluene	40	1	20/0
5 <sup>b</sup>	Au (0.035)	Toluene	80	1	60/36
6 <sup>b</sup>	Au (0.035)	ACN	40	0.5	17/0
7 <sup>b</sup>	Au (0.035)	ACN	40	1	22/0
8 <sup>c</sup>	6 Ag (0.035)	Toluene	40	1	85/0
9 <sup>c</sup>	8 Ag (0.035)	Toluene	40	1	96/0
10 <sup>c</sup>	Ag (0.010)	Toluene	40	1	97/0
11 <sup>c</sup>	Ag (0.019)	Toluene	40	2	97/0
12 <sup>c</sup>	Ag (0.019)	Toluene	80	1	98/0
13 <sup>c</sup>	Ag (0.010)	ACN	40	2	87/0
14 <sup>c</sup>	Ag (0.010)	ACN	40	1	80
15 <sup>d</sup>	AgOTf (0.002)	ACN	80	4	66
16 <sup>e</sup>	AuPPh <sub>3</sub> Cl (2)	CDCl <sub>3</sub>	50	22	40/6
17	no cat.	ACN	80	8	-

<sup>a</sup> All reactions were run with **1** (72 μmol, 0.5 mL solvent) in a screw-cap vial. Bold text highlights the best conditions. <sup>b</sup>BM-2%Au@Al-SBA15. <sup>c</sup>BM-2%Ag@Al-SBA15. <sup>d</sup>AgOTf. <sup>e</sup>AuPPh<sub>3</sub>Cl. <sup>f</sup>Reaction yield.

The decrease of the reaction time resulted in a decrease of the yield with more selectivity to the formation of imidazolidin-2-one (Table 1, entries 3, 4). This can be explained in terms of kinetic vs. thermodynamic stability: kinetically favorable product 1a was dominating over thermodynamically stable 1b in short reaction time. The use of ACN as alternative solvent was not as effective as compared to toluene (Table 1, entries 6, 7). Sequentially, BM-2%Au@AISBA-15 was replaced by BM-2%Ag@AISBA-15 (Table 1, entries 8-14), a cheaper catalyst. Interesting, a smaller amount of BM-2%Ag@AISBA-15 was needed to obtain higher yields and selectivity, compared to gold catalyst (Table 1, entries 8, 9, 10). Indeed, 10 mg of catalyst and 1h of reaction were found to be the best conditions to obtain 97% yield of imidazolidin-2-one 1a with 0% production of migrated <sup>39</sup> double bond imidazole-2-one 1b (Table 1, entry 10 compared with 11). The above results showed the higher metallic character of Ag@AISBA-15 over Au@AISBA-15. In fact, XPS measurement of Au@AISBA-15 showed the existence of some Au<sup>3+</sup> (band at 85.7 & 89.4 eV) species with mostly Au(0) while XPS measurement of Ag@AISBA-15 exhibited mainly metallic silver not oxidic.<sup>28</sup> The switch to acetonitrile (ACN) provided good selectivity and excellent yields of 1a (Table 1, entry 13, 14). However, silver mirror was noticed inside the NMR tube, demonstrating the leaching of silver with acetonitrile.<sup>40</sup> As a consequence, ACN was considered inappropriate for the reaction. Positively, no silver mirror was observed in the NMR tube using toluene.

Sequentially, based on the optimized conditions of using 10 mg BM-2%Ag@AISBA-15 in toluene, the reaction was attempted using phenyl isocyanate (compound 2 in Scheme 4). As shown in Table 2, the high reaction yields and selectivities obtained with propargylic ureas 1 (Table 1) were never observed, despite increasing the reaction time up to 17 h nor the temperature up to 80°C (Table 2, entry 1, 2, 3 and 4).



**Scheme 4.** Cycloisomerization of propargylic ureas derived from phenyl isocyanate.

**Table 2. Optimization of the reaction illustrated in Scheme 4<sup>a</sup>**

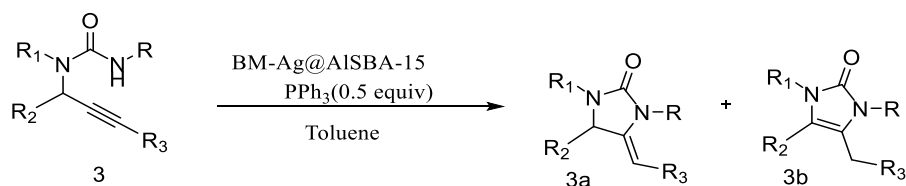
Entry	Additive (equiv.)	pK <sub>a</sub>	T (°C)	t (h)	% yield (a/b) <sup>b</sup>
1	/		40	1	0
2	/		40	3	0
3	/		40	17	0/17
4	/		80	17	0/41
5	PPh <sub>3</sub> (1 equiv)	7.6 <sup>c</sup>	40	3	0/70
6	PPh <sub>3</sub> (0.5 equiv)		80	3	0/86
7	PPh <sub>3</sub> (0.5 equiv)		80	2.5	0/86
8	DABCO(0.5 equiv)	8.2 <sup>c</sup>	80	3	0/10
9	DMAP(0.5 equiv)		80	3	10/0
10	Et <sub>3</sub> N(0.5 equiv)	10.7 <sup>d</sup>	80	3	0/0

<sup>a</sup>All reactions were run with **2** (72  $\mu$ mol, 0.5 mL toluene) in a screw-cap vial, BM-2%Ag@Al-SBA15 (0.01 g). <sup>b</sup>Reaction yield was determined by the NMR-integration method. <sup>c</sup>Basicity measurement in acetonitrile. <sup>d</sup>Determined in water for deprotonation of conjugate acid.

Aiming to increase the reaction yield, some additive were tested. Based on previous results, the effect of triphenylphosphine was investigated in combination with the new heterogeneous conditions.<sup>14</sup> Using 1 equivalent of triphenylphosphine and operating at 40°C, a major selectivity to imidazole-2-one was observed (Table 2, entry 5). This trial was repeated up to ten times by reusing the same catalyst, without noting any decrease of conversion. As triphenylphosphine is a well-known ligand for gold and silver, the possible leaching of BM-2%Ag@Al-SBA-15 was evaluated by hot filtration test after every cycle. To execute this test, the catalyst was removed from the reaction mixture after 30 min of ongoing stirring under the investigated reaction conditions (35% conversion). Fresh triphenylphosphine was subsequently introduced to avoid any loss and the reaction was continued for other 6 h. No appreciable conversion by NMR was observed, in good agreement with an identical Ag-loading in the catalyst before/after removal from the reaction mixture. These findings were a good indication about the heterogeneous nature of the reaction (please see ESI for additional details of leaching tests). The utilization of triphenylphosphine was subsequently tested at 80°C lowering the reaction time. Best condition led to the synthesis of product **2b** with 87% yield operating at 80°C for 2h 30' (Table 2, entry 7). In order to gain more insights, other Lewis bases were tested as additive (Table 2, entry 8, 9, 10). However, no improvement of the reaction yield was observed. These results may point to a unique and efficient electron-donating effect of the

phosphorus of triphenylphosphine, which upon coordination to Ag nanoparticles led to Ag species with an improved “metallic” character correlated to an improved reactivity for the investigated chemistry. This electron-donating effect is well documented in the literature for homogeneous catalysts and metals but firstly approached here as stabilizing effect for heterogeneous catalysts.<sup>41</sup>

With the new optimized conditions, the reaction was successively ran using other substituted propargylic ureas (compound 3 in Scheme 5), as shown in Table 3. The reaction was remarkably more efficient with nitro-phenyl isocyanate derived ureas as compared to aryl substituted ureas (Table 3, entries 1, 2 and 3). The observed low activity may be due to the free rotation of the benzyl group which can be responsible for steric hindrance.<sup>15</sup> The reaction with non-terminal alkynes under same optimized condition, resulted in less than 20% conversion. This was expected due to steric hindering substituent on the triple bond.<sup>42</sup> Sequentially, catalyst loading and reaction time were increased, resulting in 56% yield (Table 3, entry 6).



**Scheme 5.** General scheme for cycloisomerization of substituted propargylic ureas.

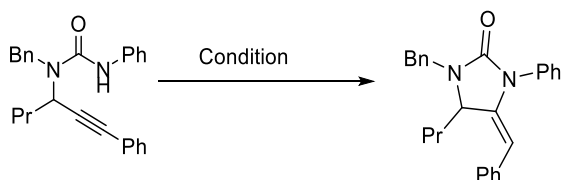
**Table 3. Optimization of the reaction illustrated in Scheme 5<sup>a</sup>**

Entry	R	R <sub>1</sub>	R <sub>2</sub>	R <sub>3</sub>	T (°C)	t (h)	% yield (a/b) <sup>b</sup>
1	<i>p</i> -NO <sub>2</sub> C <sub>6</sub> H <sub>5</sub>	Me	H	H	40	1	0/90
2	Bn	Me	H	H	40	6	0/10
3	Bn	Me	H	H	80	6	0/22
4	<i>p</i> -Tol	Me	H	H	80	3	0/73
5	Ph	Bn	Pr	Ph	80	3	0/14
6 <sup>c</sup>	Ph	Bn	Pr	Ph	80	4	0/56

<sup>a</sup>All reactions were run with 3 (72 μmol, 0.5 mL toluene) in a screw-cap vial using BM-2%Ag@AISBA15 (20 mg). Bn = Benzyl group. <sup>b</sup>Reaction yield was determined by the NMR-integration method. <sup>c</sup>Catalyst = 0.04 g, 1 mL toluene.



Due to the high load of the catalysts, these last reaction conditions (Table 3, entry 6) were selected for the comparison of nanocatalysts synthesized by ball milling and microwave-assisted techniques (Scheme 6 and Table 4).



**Scheme 6.** Cycloisomerization of substituted propargylic ureas.

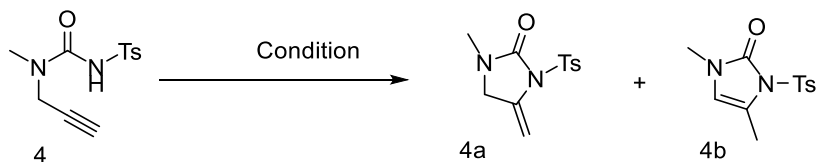
**Table 4. Cycloisomerization of propargylic urea comparing BM- and MW- 2%Ag@AISBA-15 and 2%Au@AISBA15, as well as microwave heating vs conventional heating**

Entry	Cat	% yield <sup>b</sup>
1	BM- 2%Ag@AISBA-15	56
2	MW- 2%Ag@AISBA-15	35
3	BM-2%Au@AISBA-15	<5
4	MW-2%Au@AISBA-15	<5

All reactions were run with **1** (72  $\mu$ mol, 1 mL toluene) in a screw-cap vial. <sup>b</sup>Reaction yield was determined by the NMR-integration method. Catalyst = BM/MW- 2%Ag@AISBA-15 (0.04 g), BM/MW-2%Au@AISBA-15 (0.07 g).

Gold nanocatalysts were found to be almost inactive for the reaction (Table 4, entries 3 and 4). Considering silver catalysts, ball-milling synthesized one was more active than MW-2%Ag@AISBA-15. Despite this lowest activity, it has to be highlighted that the microwave-assisted synthesis was much more favourable compared to the synthesis of nanocatalysts prepared by ball-milling. In fact, BM- catalysts needed longer time of preparation, resulting by the sum of the 10' of ball milling and the several hour of muffle treatment for the calcination. Instead, nanocatalysts prepared by microwave-assisted techniques were prepared only through a one easy reduction step of 5' irradiation in the microwave reactor. However, in order to obtain the higher yields, the ensuing trials were carried out using BM-2%Ag@AISBA-15.

**Switching to ethanol.** In order to accomplish the reaction in greener conditions, the synthesis was switched from toluene, which is classified as Class 3 solvent by U.S. FDA, to ethanol.<sup>18</sup> Following the same logical evolution accomplished in the first part of the research, the reactions were initially carried out without any additive, operating under conventional heating conditions, using propargyl urea 5 synthesized by tosyl isocyanate and N-methylpropargylamine (Scheme 7 and Table 5).



**Scheme 7.** Cycloisomerization of propargylic ureas derived from tosyl isocyanate in EtOH.

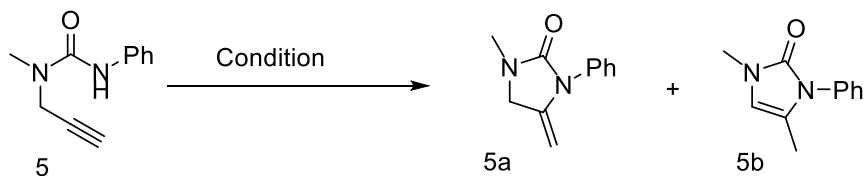
**Table 5. Optimization of the reaction illustrated in Scheme 7<sup>a</sup>**

Entry	Cat (mg)	T [°C]	t[h]	% yield (a/b) <sup>d</sup>
1 <sup>b</sup>	18 Au	80	14	27/32
2 <sup>b</sup>	35 Au	80	14	44/32
3 <sup>c</sup>	8 Ag	40	1	97/0
4 <sup>c</sup>	6 Ag	40	0.5	93/0
5 <sup>c</sup>	4 Ag	40	0.5	80/0
6 <sup>c</sup>	6 Ag	40	0.16	78/0

<sup>a</sup>All reactions were run with 4 (72  $\mu$ mol, 0.5 mL ethanol) in a screw-cap vial. <sup>b</sup>BM-2%Au@Al-SBA15. <sup>c</sup>BM-2%Ag@Al-SBA15.

<sup>d</sup>Reaction yield was determined by the NMR-integration method.

Best results were observed using 2 wt% BM-Ag@AISBA-15 catalysts and operating at 40° for 30 min. (Table 5, entry 4), finding the same results observed in toluene (Table 1, entry 10). In order to evaluate the effect of triphenylphosphine in ethanol, different trials were carried out. As summarized in Table 6, no cyclization occurred when triphenylphosphine was added.<sup>43,44</sup>



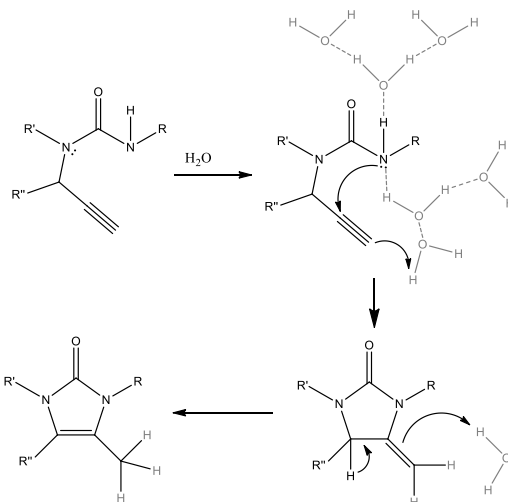
**Scheme 8.** Effect of polar solvent EtOH on cycloisomerization of propargylic ureas derived from phenyl isocyanate with  $\text{PPh}_3$  as an additive.

**Table 6. Optimization of the reaction illustrated in Scheme 8<sup>a</sup>**

Entry	R	T (°C)	t (h)	% yield (a/b)
1		40	6	-
2	$\text{PPh}_3(0.5 \text{ equiv})$	40	3	-
3	$\text{PPh}_3(0.5 \text{ equiv})$	80	3	-

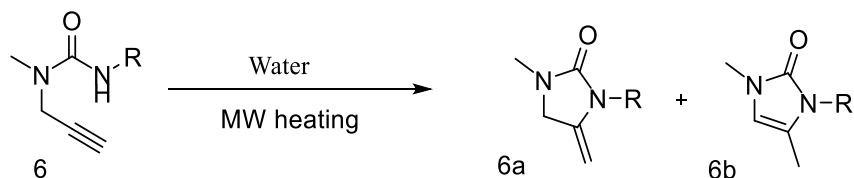
<sup>a</sup>All reactions were run with **5** (72  $\mu\text{mol}$ , 0.5 mL solvent) in a screw-cap vial with BM-2%Ag@Al-SBA15 (0.01 g).

**Developing the conditions for water-mediated reaction.** All obtained results were combined aiming to carry out the reaction in water. As AISBA-15 is instable in water, all the reactions were ran in microwave using only  $\text{H}_2\text{O}$  as solvent and promoter of the reaction. As reported by Mohan *et al.*,<sup>45</sup> water can act as mediator for the construction of different heterocycles. The possible mechanism is shown in Scheme 9.



**Scheme 9.** Possible mechanism for water-mediated formation of 2-imidazole.

As summarized in Table 7, different trails have been carried out, varying reaction time, temperature, and structure of propargylic ureas. Best results were obtained operating at 130°C for 20'. The outcomes clearly showed that water was favoring the cyclization of propargylic ureas containing electron donor compounds. As shown in Table 7 (entry 4), the best conditions allowed conditions allowed the preparation of substituted imizadolones in 72% yield with 20 min reaction time.



**Scheme 10.** Cycloisomerization of different propargylic ureas in water under microwave irradiation.

**Table 7. Optimization of the reaction illustrated in Scheme 10<sup>a</sup>**

Entry	R	T (°C)	t (h)	% yield (a/b) <sup>b</sup>
1	Ph	80	20	/
2	Ph	100	20	0/10
3	Ph	120	20	0/50
4	Ph	130	20	0/72
5	Ph	130	5	0/8
6	Ph	130	10	0/30
7	p-FC <sub>6</sub> H <sub>4</sub>	130	20	0/66
8	Bn	130	20	0/3
9	p-NO <sub>2</sub> C <sub>6</sub> H <sub>4</sub>	130	20	0/68

<sup>a</sup>All reactions were run with **6** (72 μmol, 0.5 mL water) in a screw-cap vial. <sup>b</sup>Reaction yield was determined by the NMR-integration method.

## CONCLUSIONS

In conclusion, the environmentally friendly paths for the cycloisomerization of propargylic ureas were explored. The syntheses were carried out in toluene, acetonitrile, ethanol, and water, using gold and silver heterogeneous catalysts produced by innovative ball-milling and microwave-assisted techniques. Several scopes were studied, highlighting the reaction mechanism in the selected different paths, where heterogeneous catalyst in toluene promoted N-cyclization reactions, ethanol favored the cyclization of propargylic

ureas characterized by more-electron-withdrawing groups and watermediated reactions favored the cyclization of propargylic ureas containing electron-donor compounds in the structure. In contrast to previous studies, the new developed paths offer the possibility to accomplish the cycloisomerization reaction in greener solvents using recoverable heterogeneous catalysts and avoiding the utilization of any strong base. In addition, all the reactions were carried out under conventional and microwave heating, emphasizing the possibility of using a microwave technique to reduce the reaction time.

#### ASSOCIATED CONTENT

##### *Supporting Information.*

The Supporting Information is available free of charge on the ACS Publications website at DOI: 10.1021/acssuschemeng.9b00198. General information regarding laboratory procedures, leaching determination by a hot-filtration experiment, reusability of catalyst, and synthesis of starting materials

#### AUTHOR INFORMATION

##### *Corresponding Authors*

\*R.L. e-mail: q62alsor@uco.es.

\*E.V.V.d.E e-mail: erik.vandereycken@kuleuven.be.

ORCID Rafael Luque: 0000-0003-4190-1916

##### *Author Contributions*

||A.Z. and P.R. contributed equally to this work.

##### *Notes*

The authors declare no competing financial interest.

## ACKNOWLEDGMENTS

This project has received funding from the European Union's Horizon 2020 research and innovation programme under the Marie Skłodowska-Curie grant agreement No 721290. This publication reflects only the author's view, exempting the Community from any liability. Project website: <http://cosmic-etn.eu/>. The publication has been prepared with support of RUDN University program 5-100.

- (1) Contreras, J. G.; Madariaga, S. T., Intramolecular proton transfer in tautomeric 2-imidazolone and 2-thioimidazolone. *J. Phys. Org. Chem.* **2003**, 16 (1), 47-52, DOI: 10.1002/poc.571.
- (2) Wu, C. H.; Hung, M. S.; Song, J. S.; Yeh, T. K.; Chou, M. C.; Chu, C. M.; Jan, J. J.; Hsieh, M. T.; Tseng, S. L.; Chang, C. P.; Hsieh, W. P.; Lin, Y.; Yeh, Y. N.; Chung, W. L.; Kuo, C. W.; Lin, C. Y.; Shy, H. S.; Chao, Y. S.; Shia, K. S., Discovery of 2-5-(4-Chloro-phenyl)-1-(2,4-dichloro-phenyl)-4-ethyl-1H-pyrazol-3-yl-1,5,5-trimethyl-1,5-dihydro-imidazol-4-thione (BPR-890) via an Active Metabolite. A Novel, Potent and Selective Cannabinoid-1 Receptor Inverse Agonist with High Antiobesity Efficacy in DIO Mice. *J. Med. Chem.* **2009**, 52 (14), 4496-4510, DOI: 10.1021/jm900471u.
- (3) Narasimhan, B.; Sharma, D.; Kumar, P., Biological importance of imidazole nucleus in the new millennium. *Med. Chem. Res.* **2011**, 20 (8), 1119-1140, DOI: 10.1007/s00044-010-9472-5.
- (4) Antonova, M. M.; Baranov, V. V.; Kravchenko, A. N., Methods for the synthesis of 1-substituted 1H-imidazol-2(3H)-ones. *Chem. Heterocycl. Comp.* **2015**, 51 (5), 395-420, DOI: 10.1007/s10593-015-1716-3.
- (5) Wani, M. Y.; Ahmad, A.; Shiekh, R. A.; Al-Ghamdi, K. J.; Sobral, A., Imidazole clubbed 1,3,4-oxadiazole derivatives as potential antifungal agents. *Bioorgan. Med. Chem.* **2015**, 23 (15), 4172-4180, DOI: 10.1016/j.bmc.2015.06.053.
- (6) Congiu, C.; Cocco, M. T.; Onnis, V., Design, synthesis, and in vitro antitumor activity of new 1,4-diarylimidazole-2-ones and their 2-thione analogues. *Bioorgan. Med. Chem. Lett.* **2008**, 18 (3), 989-993, DOI: 10.1016/j.bmcl.2007.12.023.
- (7) Aksoydan, B.; Kantarcioglu, I.; Erol, I.; Salmas, R. E.; Durdagi, S., Structure-Based Design of hERG-Neutral Antihypertensive Oxazolone and Imidazolone Derivatives (vol 78, pg 240 2017). *J. Mol. Graph. Model.* **2017**, 77, 240-240, DOI: 10.1016/j.jmgm.2017.08.004.
- (8) Hu, Y. C.; Liang, C. F.; Tsai, J. H.; Yap, G. P. A.; Chang, Y. T.; Ong, T. G., Zirconium Complexes Supported by Imidazolones: Synthesis, Characterization, and Application of Precatalysts for the Hydroamination of Aminoalkenes. *Organometallics* **2010**, 29 (15), 3357-3361, DOI: 10.1021/om100296m.
- (9) Cheng, J. F.; Kaiho, C.; Chen, M.; Arrhenius, T.; Nadzan, A., A traceless solid-phase synthesis of 2-imidazolones. *Tetrahedron Lett.* **2002**, 43 (26), 4571-4573, DOI: 10.1016/S0040-4039(02)00897-3.
- (10) Dandepally, S. R.; Elgoummadi, R.; Williams, A. L., Schwartz reagent mediated synthesis of thiazolones and imidazolones from thiazolidine-2,4-diones and imidazolidine-2,4-diones. *Tetrahedron Lett.* **2013**, 54 (8), 925-928, DOI: 10.1016/j.tetlet.2012.12.015.
- (11) Lauder, K.; Toscani, A.; Scalacci, N.; Castagnolo, D., Synthesis and Reactivity of Propargylamines in Organic Chemistry. *Chem. Rev.* **2017**, 117 (24), 14091-14200, DOI: 10.1021/acs.chemrev.7b00343.
- (12) Wen, J. J.; Zhu, Y.; Zhan, Z. P., The Synthesis of Aromatic Heterocycles from Propargylic Compounds. *Asian J. Org. Chem.* **2012**, 1 (2), 108-129, DOI: 10.1002/ajoc.201200053.
- (13) F. Huguenot, C. Delalande and M. Vidal, Metal-free 5-exo-dig cyclization of propargyl urea using TBAF. *Tetrahedron Lett.* **2014**, 55, 4632-4635, DOI: 10.1016/j.tetlet.2014.06.098.
- (14) Pereshivko, O. P.; Peshkov, V. A.; Jacobs, J.; Van Meervelt, L.; Van der Eycken, E. V., Cationic Gold- and Silver-Catalyzed Cycloisomerizations of Propargylic Ureas: A Selective Entry to Oxazolidin-2-imines and Imidazolidin-2-ones. *Adv. Synt. Catal.* **2013**, 355 (4), 781-789, DOI: 10.1002/adsc.201200905.
- (15) Peshkov, V. A.; Pereshivko, O. P.; Sharma, S.; Meganathan, T.; Parmar, V. S.; Ermolat'ev, D. S.; Van der Eycken, E. V., Tetrasubstituted 2-Imidazolones via Ag(I)-Catalyzed Cycloisomerization of Propargylic Ureas. *J. Org. Chem.* **2011**, 76 (14), 5867-5872, DOI: 10.1021/jo200789t.
- (16) Shylesh, S.; Schunemann, V.; Thiel, W. R., Magnetically Separable Nanocatalysts: Bridges between Homogeneous and Heterogeneous Catalysis. *Angew. Chem. Int. Edit.* **2010**, 49 (20), 3428-3459, DOI: 10.1002/anie.200905684.
- (17) Astruc, D.; Lu, F.; Aranzaes, J. R., Nanoparticles as recyclable catalysts: The frontier between homogeneous and heterogeneous catalysis. *Angew. Chem. Int. Edit.* **2005**, 44 (48), 7852-7872, DOI: 10.1002/anie.200500766.

- (18) <https://www.fda.gov/>
- (19) Gawande, M. B.; Branco, P. S.; Varma, R. S., Nano-magnetite (Fe<sub>3</sub>O<sub>4</sub>) as a support for recyclable catalysts in the development of sustainable methodologies. *Chem. Soc. Rev.* **2013**, 42 (8), 3371-3393, DOI: 10.1039/C3CS35480F.
- (20) Abis, L.; Armelao, L.; Dell'Amico, D. B.; Calderazzo, F.; Garbassi, F.; Merigo, A.; Quadrelli, E. A., Gold molecular precursors and gold-silica interactions. *J. Chem. Soc. Dalton* **2001**, (18), 2704-2709, DOI: 10.1039/B103414F.
- (21) Gawande, M. B.; Monga, Y.; Zboril, R.; Sharma, R. K., Silica-decorated magnetic nanocomposites for catalytic applications. *Coord. Chem. Rev.* **2015**, 288, 118-143, DOI: 10.1016/j.ccr.2015.01.001.
- (22) Deng, X. H.; Chen, K.; Tuysuz, H., Protocol for the Nanocasting Method: Preparation of Ordered Mesoporous Metal Oxides. *Chem. Mat.* **2017**, 29 (1), 40-52, DOI: 10.1021/acs.chemmater.6b02645.
- (23) Vinu, A.; Murugesan, V.; Bohlmann, W.; Hartmann, M., An optimized procedure for the synthesis of AISBA-15 with large pore diameter and high aluminum content. *J. Phys. Chem. B* **2004**, 108 (31), 11496-11505, DOI: 10.1021/jp048411f.
- (24) Kappe, C. O.; Pieber, B.; Dallinger, D., Microwave Effects in Organic Synthesis: Myth or Reality? *Angew. Chem. Int. Edit.* **2013**, 52 (4), 1088-1094, DOI: 10.1002/anie.201204103.
- (25) Gawande, M. B.; Shelke, S. N.; Zboril, R.; Varma, R. S., Microwave-Assisted Chemistry: Synthetic Applications for Rapid Assembly of Nanomaterials and Organics. *Accounts Chem. Res.* **2014**, 47 (4), 1338-1348, DOI: 10.1021/ar400309b.
- (26) Pineda, A.; Balu, A. M.; Campelo, J. M.; Romero, A. A.; Carmona, D.; Balas, F.; Santamaria, J.; Luque, R., A Dry Milling Approach for the Synthesis of Highly Active Nanoparticles Supported on Porous Materials. *ChemSuschem* **2011**, 4 (11), 1561-1565, DOI: 10.1002/cssc.201100265.
- (27) Campelo, J. M.; Conesa, T. D.; Gracia, M. J.; Jurado, M. J.; Luque, R.; Marinas, J. M.; Romero, A. A., Microwave facile preparation of highly active and dispersed SBA-12 supported metal nanoparticles. *Green Chem.* **2008**, 10 (8), 853-858, DOI: 10.1039/B801754A.
- (28) Schroder, F.; Sharma, U. K.; Mertens, M.; Devred, F.; Debecker, D. P.; Luque, R.; Van der Eycken, E. V., Silver-Nanoparticle-Catalyzed Dearomatization of Indoles toward 3-Spiroindolenines via a 5-exo-dig Spirocyclization. *ACS Catal.* **2016**, 6 (12), 8156-8161, DOI: 10.1021/acscatal.6b02443.
- (29) James, S. L.; Adams, C. J.; Bolm, C.; Braga, D.; Collier, P.; Friscic, T.; Grepioni, F.; Harris, K. D. M.; Hyett, G.; Jones, W.; Krebs, A.; Mack, J.; Maini, L.; Orpen, A. G.; Parkin, I. P.; Shearouse, W. C.; Steed, J. W.; Waddell, D. C., Mechanochemistry: opportunities for new and cleaner synthesis. *Chem. Soc. Rev.* **2012**, 41 (1), 413-447, DOI: 10.1039/c1cs15171a.
- (30) Matoga, D.; Oszejca, M.; Molenda, M., Ground to conduct: mechanochemical synthesis of a metal-organic framework with high proton conductivity. *Chem. Comm.* **2015**, 51 (36), 7637-7640, DOI: 10.1039/C5CC01789K.
- (31) Paseta, L.; Potier, G.; Sorribas, S.; Coronas, J., Solventless Synthesis of MOFs at High Pressure. *ACS Sust. Chem. Eng.* **2016**, 4 (7), 3780-3785, DOI: 10.1021/acssuschemeng.6b00473.
- (32) Muralidharan, N.; Brock, C. N.; Cohn, A. P.; Schauben, D.; Carter, R. E.; Oakes, L.; Walker, D. G.; Pint, C. L., Tunable Mechanochemistry of Lithium Battery Electrodes. *ACS Nano* **2017**, 11 (6), 6243-6251, DOI: 10.1021/acsnano.7b02404.
- (33) Horikoshi, S.; Serpone, N., *Microwaves in Nanoparticle Synthesis: Fundamentals and Applications*. Wiley-VCH **2013**.
- (34) Mirzaei, A.; Neri, G., Microwave-assisted synthesis of metal oxide nanostructures for gas sensing application: A review. *Sensors Actuat. B-Chem.* **2016**, 237, 749-775, DOI: 10.1016/j.snb.2016.06.114.
- (35) Panda, A. B.; Glaspell, G.; El-Shall M. S., Microwave Synthesis of Highly Aligned Ultra Narrow Semiconductor Rods and Wires. *JACS* **2006**, 128, 2790-2791, DOI: 10.1021/ja058148b.



- (36) Rajabi, F.; Fayyaz, F.; Luque, R., Cytosine-functionalized SBA-15 mesoporous nanomaterials: Synthesis, characterization and catalytic applications. *Micropor. Mesopor. Mat.* **2017**, 253, 64-70, DOI: 10.1016/j.micromeso.2017.06.043.
- (37) Zhao, D. Y.; Feng, J. L.; Huo, Q. S.; Melosh, N.; Fredrickson, G. H.; Chmelka, B. F.; Stucky, G. D., Triblock copolymer syntheses of mesoporous silica with periodic 50 to 300 angstrom pores. *Science* **1998**, 279 (5350), 548-552, DOI: 10.1126/science.279.5350.548.
- (38) Han, Y.; Xiao, F. S.; Wu, S.; Sun, Y. Y.; Meng, X. J.; Li, D. S.; Lin, S.; Deng, F.; Ai, X. J., A novel method for incorporation of heteroatoms into the framework of ordered mesoporous silica materials synthesized in strong acidic media. *J. Phys. Chem. B* **2001**, 105 (33), 7963-7966, DOI: 10.1021/jp011204k.
- (39) Akin, S. T.; Liu, X.; Duncan, M. A., Laser synthesis and spectroscopy of acetonitrile/silver nanoparticles. *Chem. Phys. Lett.* **2015**, 640, 161-164, DOI: 10.1016/j.cplett.2015.10.022.
- (40) Manahan, S. E.; Iwamoto, R. T., Complexes of copper(I) and silver(I) with acetonitrile in water lower alcohols acetone and nitroethane. *J. Electroanal. Chem.* **1967**, 14 (2), 213-217, DOI: 10.1016/0022-0728(67)80073-1.
- (41) Zhou, Z.; He, C.; Yang, L.; Wang, Y. F.; Liu, T.; Duan, C. Y., Alkyne Activation by a Porous Silver Coordination Polymer for Heterogeneous Catalysis of Carbon Dioxide Cycloaddition. *ACS Catal.* **2017**, 7 (3), 2248-2256, DOI: 10.1021/acscatal.6b03404.
- (42) Schroder, F.; Ojeda, M.; Erdmann, N.; Jacobs, J.; Luque, R.; Noel, T.; Van Meervelt, L.; Van der Eyckend, J.; Van der Eycken, E. V., Supported gold nanoparticles as efficient and reusable heterogeneous catalyst for cycloisomerization reactions. *Green Chem.* **2015**, 17 (6), 3314-3318, DOI: 10.1039/C5GC00430F.
- (43) Bantreil, X.; Bourderioux, A.; Mateo, P.; Hagerman, C. E.; Selkti, M.; Brachet, E.; Belmont, P., Phosphine-Triggered Selectivity Switch in Silver-Catalyzed o-Alkynylbenzohydroxamic Acid Cycloisomerizations. *Org. Lett.* **2016**, 18 (19), 4814-4817, DOI: 10.1021/acs.orglett.6b02235.
- (44) Parker, E.; Leconte, N.; Godet, T.; Belmont, P., Silver-catalyzed furoquinolines synthesis: from nitrogen effects to the use of silver imidazolate polymer as a new and robust silver catalyst. *Chem. Comm.* **2011**, 47 (1), 343-345, DOI: 10.1039/C0CC02623A.
- (45) Mohan, D. C.; Rao, S. N.; Adimurthy, S., Synthesis of Imidazo 1,2-a pyridines: "Water-Mediated" Hydroamination and Silver-Catalyzed Aminoxygenation. *J. Org. Chem.* **2013**, 78 (3), 1266-1272, DOI: 10.1021/jo3025303.

## Supporting Information

### General information

All components as well as reagents and solvents were used as received without further purification, unless stated otherwise. Reagents and solvents were bought from Sigma Aldrich and TCI and if applicable, kept under argon atmosphere. Technical solvents were bought from VWR International and Biosolve, and were used as received. Product isolation was performed using silica (60, F254, Merck™), and TLC analysis was performed using Silica on aluminum foils TLC plates (F254, Supelco Sigma-Aldrich™) with visualization under ultraviolet light (254 nm and 365 nm) or appropriate TLC staining. IR spectra were recorded on Bruker Alpha FT-IR spectrometer. <sup>1</sup>H (400MHz or 600 MHz), <sup>13</sup>C (100MHz) spectra were recorded on ambient temperature using a Bruker-Avance 400 or Mercury 400. <sup>1</sup>H NMR spectra are reported in parts per million (ppm) downfield relative to CDCl<sub>3</sub> (7.26 ppm) and all <sup>13</sup>C NMR spectra are reported in ppm relative to CDCl<sub>3</sub> (77.2 ppm). NMR spectra uses the following abbreviations to describe the multiplicity: s = singlet, d = doublet, t = triplet, q = quartet, p = pentet, h = hextet, hept = heptet, m = multiplet, dd = double doublet, td = triple doublet. Known products were characterized by comparing to the corresponding <sup>1</sup>H NMR and <sup>13</sup>C NMR from literature.

### Leaching Determination by Hot-Filtration Experiment

The hot-filtration test was executed in order to determine the possible metal leaching from the support. In the case of metal leaching, a further conversion after removal of the catalyst should have been observed. In order to perform the test, best reaction conditions were selected (Table 2, entry 5). After 30 min. of reaction, the catalyst was removed under hot condition to avoid any redepositing of Ag. The solution was transferred in new reaction vial with a new stirring bar and left under stirring. As no further conversion was observed, the heterogeneity of reaction was confirmed.

### Reusability of Catalyst:

The reaction (Table 2, entry 5) was performed up to 10 times under optimized condition without observing any loss of catalytic activity. After each cycle, the catalyst was washed with ethanol and dried under vacuum oven at 50 °C for 12 h. The same results were observed by using or not PPh<sub>3</sub>.

**Synthesis of starting materials:**

Appropriate isocyanates were added in solution of N-methyl propargylamine in DCM. After 1-2 h of stirring, 10 mL of pentane were added in the solution and the white precipitate was filtered.

Crude NMR to confirm 1: <sup>1</sup>H NMR (300 MHz, Chloroform-d) δ 7.96 (d, *J* = 8.3 Hz, 2H), 7.33 (d, *J* = 8.0 Hz, 3H), 4.05 (d, *J* = 2.6 Hz, 2H), 2.97 (d, *J* = 8.3 Hz, 3H), 2.44 (s, 3H), 2.30 (s, 1H).

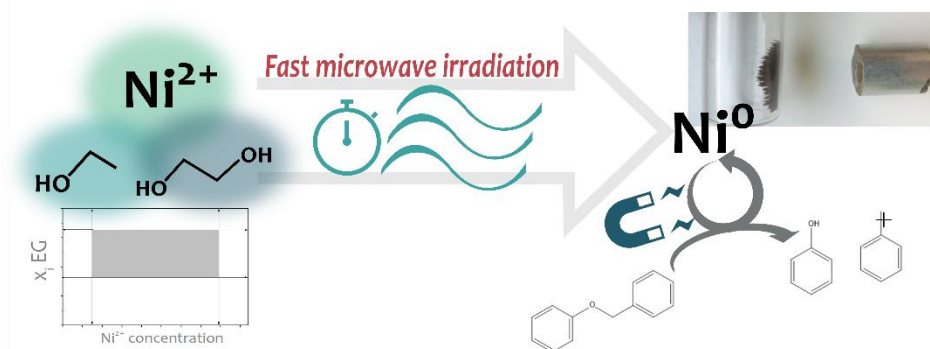
Non-terminal alkyne (Table 3, entry 6) was synthesis by A-3 coupling by previous reported method.



## Efficient and environmentally friendly microwave-assisted synthesis of catalytically active magnetic metallic Ni nanoparticles

Alessio Zuliani,<sup>a</sup> Alina M. Balu<sup>a</sup> and Rafael Luque<sup>a\*</sup>

*ACS Sustain. Chem Eng.*, 2017, 5 (12), 11584-11587



<sup>a</sup> Departamento de Química Orgánica, Universidad de Córdoba, Edificio Marie-Curie (C-3), Ctra Nnal IV-A, Km 396, Córdoba, Spain

Adapted with permission from *ACS Sustain. Chem Eng.*, 2017, 5 (12), 11584-11587. Copyright 2017 American Chemical Society.

*Abstract: Pure magnetic metallic nickel was synthesized by a simple and fast microwave-assisted method using a monomode microwave reactor. Nickel chloride was employed as metal precursor, while an environmental-friendly mixture of ethylene glycol and ethanol was simultaneously used as solvent and reducing agent. The parameters combination, for the occurrence of the reaction, of the mixture molar fraction and the metal precursor concentration was developed. The influence of the temperature and the time of the irradiation was investigated. The best performance (71% yield) was achieved at 250°C in 5 minutes of microwave irradiation. The phase and the morphology of the metal were analyzed by X-ray diffraction (XRD), scanning emission microscopy (SEM) and transmission electron microscopy (TEM) while the surface area was determined by nitrogen physisorption. The material exhibited a strong magnetic behavior. The metallic Nickel showed high catalytic activity for the hydrogenolysis of benzyl phenyl ether, a lignin model compound, in a microwave-assisted environmental-friendly reaction.*

## INTRODUCTION

Magnetic nanostructured materials have attracted significant interest due to their technical application in several fields including optoelectronics, magnetics, catalysis, biologic engineering, information storage and photovoltaic technology.<sup>1-3</sup> Nickel nanoparticles are particularly emerging for their unique characteristics such as high magnetism, high surface area, large surface energy, excellent chemical stability, low melting point, resource-richness, and low cost.<sup>4,5</sup> Several techniques for the synthesis of Nickel materials, including thermal decomposition, pulsed laser ablation, sputtering and metal vapor condensation have been extensively reported in literature.<sup>6-9</sup> However, only a few reports on the synthesis of pure Ni magnetic nanoparticles are available.<sup>10-12</sup>

Microwave-assisted reactions emerged as alternative reaction media to conduct catalytic processes and importantly in nanomaterials synthesis due to associated advantages of the technique that include the possibility to obtain higher yields, different selectivities, as well as the potential to accomplish reactions/chemistries that generally do not take place under conventional heating conditions.<sup>13-15</sup>

Based on our experience in microwave chemistry for the design of nanomaterials and nanoparticle systems,<sup>16-20</sup> herein we disclose a simple, efficient and environmentally friendly unprecedented synthesis of magnetic metallic Nickel (denoted as MMN) under microwave-assisted conditions, employing a mixture of ethylene glycol (EG) and ethanol, and NiCl<sub>2</sub> as metal precursor. The so-produced Nickel nanoparticles were used as heterogeneous catalyst for the hydrogenolysis of benzyl phenyl ether (BPE), a commonly used lignin model compound.<sup>21,22</sup>

## RESULTS AND DISCUSSION

PXRD pattern of MMN is shown in Figure 1. The peaks at 44,5°, 51,9° and 76,4° can be respectively indexed to the (111), (200) and (220) diffraction planes, from a face-centered cubic structure (*Fm3m*) of pure metallic Nickel. No other distinctive diffraction peaks indicate high purity and crystallinity of the samples. The XRD pattern showed a strong diffraction peak at (111) and the ratio of intensity of the (111) to (200) peak is 3.068.

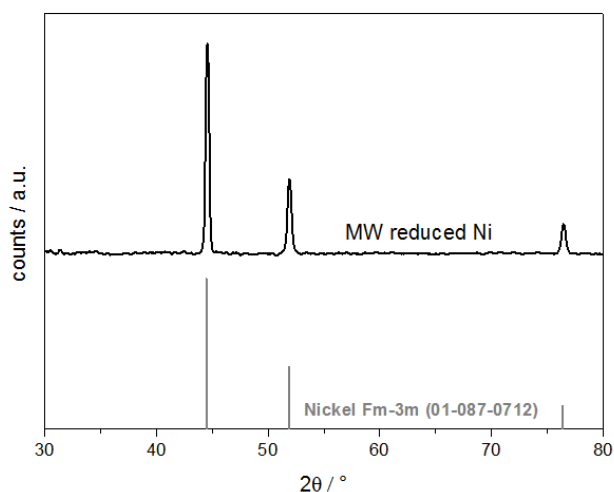


**Figure 1.** Powder X-ray diffraction of the MMN.

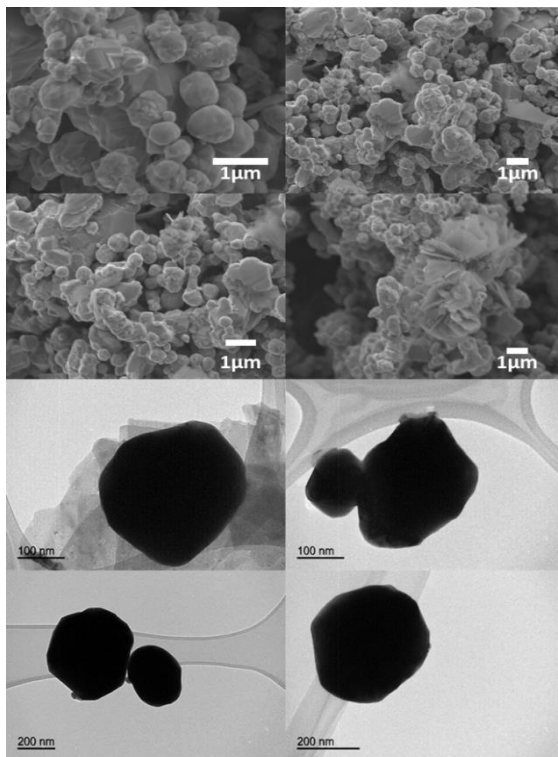


**Figure 2.** SEM and TEM images of the MMN.

Figure 2 shows SEM and TEM images of the Nickel nanoparticles synthesized. No specific description of the shape and the size of the particles was possible to define; nevertheless, most of the particles were in the form of spheres of approximately 200-500 nm of diameter. EDS analysis showed no relevant material adsorbed on the surface (95,65%wt Ni, Table S1).

The nitrogen absorption/desorption and pore size distribution revealed a non-porous material with a surface area of  $<5 \text{ m}^2/\text{g}$ . The magnetic mass susceptibility of the precipitate was determined to be  $442 \times 10^{-6} \text{ m}^3 \text{ Kg}^{-1}$  at room temperature, close to that of pure maghemite (*ca.*  $500 \times 10^{-6} \text{ m}^3 \text{ Kg}^{-1}$ ).<sup>23</sup> These findings indicate that a strong magnetic phase (Figure S1) could be created for metallic nickel under the proposed microwave reaction conditions, truly unprecedented in previous literature work.

The formation of the MMN was found to be a process depending on different variables. Specifically, the concentration of  $\text{NiCl}_2$  (therefore  $\text{Ni}^{2+}$  concentration), the molar



fraction of the ethylene glycol-ethanol solution, the irradiation time and the temperature were investigated. Table 1 summarizes the most relevant experiments (for a more detailed list of the experiments, see Table S2). The optimum yield (71%) was obtained with 0.031 molar concentration of NiCl<sub>2</sub>, in a mixture of 2.5 mL of 0.904 molar fraction of EG-EtOH, at 250°C with an irradiation time of 5 minutes.

The formation of the metallic precipitate was observed at a concentration of Ni<sup>2+</sup> ions up to 0.182 mol L<sup>-1</sup> and an EG molar fraction between 0.85 and 0.97.

**Table 1 Most significant trials varying different reaction parameters**

[Ni <sup>2+</sup> ] (mol L <sup>-1</sup> )	time (min)	T (°C)	EG (X <sub>i</sub> )	yield (%)
<b>Increasing reaction time</b>				
0.031	<b>20</b>	200	0.904	24
0.031	<b>30</b>	200	0.904	22
0.031	<b>60</b>	200	0.904	30
<b>Varying mixture composition</b>				
0.031	5	200	<b>0.846</b>	20
0.031	5	200	<b>0.865</b>	9
<b>Increasing reaction temperature</b>				
0.031	5	<b>220</b>	0.904	26
0.031	5	<b>230</b>	0.904	34
0.031	5	<b>240</b>	0.904	44
0.031	5	<b>250</b>	0.904	71
<b>Increasing metal precursor concentration</b>				
<b>0.072</b>	20	210	0.904	8
<b>0.110</b>	20	210	0.904	6
<b>0.182</b>	20	210	0.904	4

The yield of the reaction was strongly dependent on temperature, but less influenced by the reaction time. The minimum values of temperature and time for the formation of the metal precipitate were 180°C and 5 minutes irradiation, respectively.

As this work was aiming to a fast and simple reaction (with time found as low-influencing parameter), one-hour of irradiation was chosen as a limit. The upper limit of 250°C was forced by a safe pressure limit. Figure 3 represents the combination of the

parameter of  $\text{Ni}^{2+}$  ion concentration and solution composition for the formation of MMN. After extensive optimization, the MMN was obtained if the parameters matched a point inside the grey rectangle.

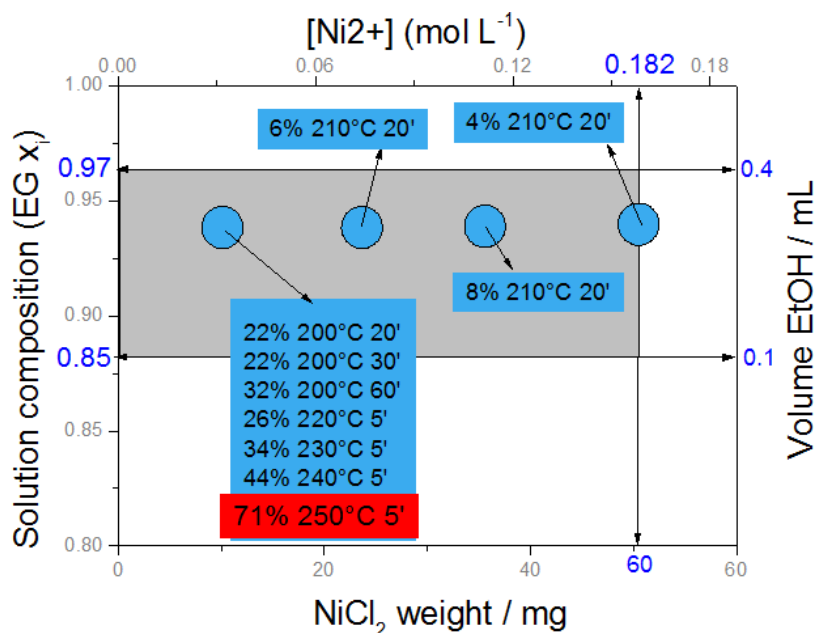
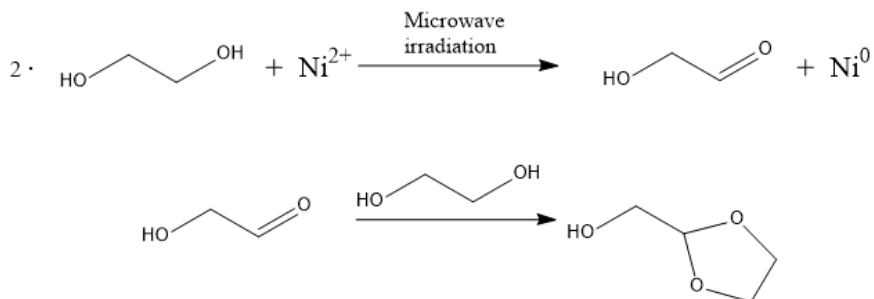


**Figure 3.** Schematic representation of the occurrence of the reaction depending on the nickel ion concentration and mixture composition. Best results are in the blue boxes where the yield, the reaction temperature and the time of reaction are reported.

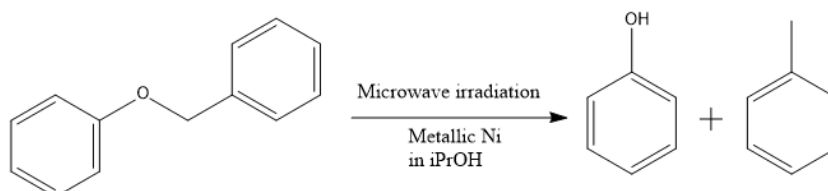
The reduction of  $\text{N}^{i2+}$  could be attributed to the action of EG as a reducing agent. Miller *et al.* proposed a reaction mechanism for the oxidation of different terminal diols employing an oxoammonium salt as oxidizing agent: the diol is oxidized to the corresponding aldehyde, which is immediately converted by protection of the aldehyde group with the same diol.<sup>24</sup> The overall reduction reaction is illustrated in Scheme 1.



**Scheme 1.** Proposed reaction scheme of the reduction of Nickel via microwave-assisted synthesis.

GC-MS analysis of the solution after the production of MMN demonstrate the presence of 1,3-Dioxolane-2-methanol (Figure S2), confirming the purposed mechanism. As the reaction was found to be possible at specific temperature and pressure, ethanol was likely increasing the penetration depth of the MWs irradiation, and lowering the bubble point of the mixture, therefore increasing vapor pressure. A simulation made with PRO/II software (Invensys System Inc.) at 70 psi showed a decreasing of the bubble point down to 185-220°C considering the EG molar fraction between 0.85-0.97, instead of 260°C of the pure EG. Similar results were obtained substituting EtOH with water and isopropanol, where still the MMN was successfully produced. Without this condition, the production of MMN would have requested hardly condition to occur, primarily the addition of other chemicals and longer time.<sup>25-27</sup>

Catalytic test of the hydrogenolysis of BPE, described in Scheme 2, were performed under microwave irradiation at 230°C employing isopropanol as green solvent and H donor.



**Scheme 2.** Hydrogenolysis of Benzyl Phenyl Ether.

Blank runs, in the absence of catalyst, showed no BPE hydrogenolysis under the investigated conditions. Best results were obtained after 45 mins of irradiation, for which a conversion of BPE of 24%, compared to the conversion of 43% obtained with commercial 5% Pd/C. The nanoparticles were stable and reusable under the investigated conditions, allowing a conversion of BPE of 21% after 5 cycles of 45 mins of irradiation each one. Despite the palladium catalyst exhibiting higher catalytic activity, the MMN possess extremely competitive characteristic such as easy and rapid synthesis being cost competitive due to reduced reagents costs (Pd vs Ni). For a detailed list of the results, please see Table S3.

## CONCLUSIONS

Pure metallic Nickel was prepared under a simple microwave-assisted hydrothermal method using a specific combination of NiCl<sub>2</sub>, ethylene glycol, and ethanol. The ethylene glycol acted as both solvent and reducing agent. The temperature was the most influencing factor for the yield of the reaction, while the reaction time was found to be less relevant under the investigated conditions. Owing to its simplicity, low-toxicity, and efficient features, this new methodology could track ways to large-scale production of Ni nanoparticles as a possible alternative to maghemite/magnetite nanoparticles. In fact, even though  $\gamma$ -Fe<sub>2</sub>O<sub>3</sub> is nowadays widely used in industry, its production is still long and quite toxic.<sup>28</sup> Furthermore, this work is a first example of employing the metallic nickel produced with the microwave-assisted technique in the hydrogenolysis of BPE. The observed results offer potential in a large number of green and fast hydrogenolyses as well as hydrogenation reactions that will be reported in due course.

## ASSOCIATED CONTENT

### *Supporting Information.*

The Supporting Information is available free of charge on the ACS Publications website at DOI: 10.1021/acssuschemeng.7b02945. Additional materials characterizations and detailed experimental section (PDF)

## AUTHOR INFORMATION

### *Corresponding Authors*

\*R.L. e-mail: q62alsor@uco.es.

ORCID Rafael Luque: 0000-0003-4190-1916

### *Notes*

The authors declare no competing financial interest.

## ACKNOWLEDGMENTS

This project has received funding from the European Union's Horizon 2020 research and innovation Programme under the Marie Skłodowska-Curie grant agreement No 721290. This publication reflects only the author's view, exempting the Community from any liability. Project website: <http://cosmic-etn.eu/>

- (1) Laurent, S.; Forge, D.; Port, M.; Roch, A.; Robic, C.; Elst, L. V.; Muller, R. N., Magnetic Iron Oxide Nanoparticles: Synthesis, Stabilization, Vectorization, Physicochemical Characterizations, and Biological Applications. *Chemical Reviews* **2008**, *108* (6), 2064-2110. DOI: 10.1021/cr068445e
- (2) Liu, Z. L.; Miao, F.; Hua, W.; Zhao, F., Fe<sub>3</sub>O<sub>4</sub> Nanoparticles: Microwave-assisted Synthesis and Mechanism. *Materials Letters* **2012**, *67* (1), 358-361. DOI: 10.1016/j.matlet.2011.09.095
- (3) Molina, M.; Asadian-Birjand, M.; Balach, J.; Bergueiro, J.; Miceli, E.; Calderon, M., Stimuli-responsive Nanogel Composites and their Application in Nanomedicine. *Chemical Society Reviews* **2015**, *44* (17), 6161-6186. DOI: 10.1039/C5CS00199D
- (4) Liu, Y. Y.; Jiang, H. L.; Zhu, Y. H.; Yang, X. L.; Li, C. Z., Transition Metals (Fe, Co, and Ni) Encapsulated in Nitrogen-doped Carbon Nanotubes as Bi-functional Catalysts for Oxygen Electrode Reactions. *Journal of Materials Chemistry A* **2016**, *4* (5), 1694-1701. DOI: 10.1039/C5TA10551J
- (5) Yao, Y. J.; Chen, H.; Lian, C.; Wei, F. Y.; Zhang, D. W.; Wu, G. D.; Chen, B. J.; Wang, S. B., Fe, Co, Ni Nanocrystals Encapsulated in Nitrogen-doped Carbon Nanotubes as Fenton-like Catalysts for Organic Pollutant Removal. *Journal of Hazardous Materials* **2016**, *314*, 129-139. DOI: 10.1016/j.jhazmat.2016.03.089
- (6) Ghatak, A.; Khan, S.; Roy, R.; Bhar, S., Chemoselective and Ligand-free Synthesis of Diaryl Ethers in Aqueous Medium Using Recyclable Alumina-supported Nickel Nanoparticles. *Tetrahedron Letters* **2014**, *55* (51), 7082-7088. DOI: 10.1016/j.tetlet.2014.10.144
- (7) Long, F.; Zhang, Z. H.; Wang, J.; Yan, L.; Zhou, B. W., Cobalt-nickel Bimetallic Nanoparticles Decorated Graphene Sensitized Imprinted Electrochemical Sensor for Determination of Octylphenol. *Electrochimica Acta* **2015**, *168*, 337-345. DOI: 10.1016/j.electacta.2015.04.054
- (8) El-Nagar, G. A.; Derr, I.; Fetyan, A.; Roth, C., One-pot synthesis of a high performance chitosan-nickel oxyhydroxide nanocomposite for glucose fuel cell and electro-sensing applications. *Applied Catalysis B-Environmental* **2017**, *204*, 185-199. DOI: 10.1016/j.apcatb.2016.11.031
- (9) Ramezanalizadeh, H.; Manteghi, F., Mixed Cobalt/Nickel Metal-Organic Framework, an Efficient Catalyst for One-pot Synthesis of Substituted Imidazoles. *Monatshefte Fur Chemie* **2017**, *148* (2), 347-355. DOI: 10.1007/s00706-016-1776-9
- (10) Barakat, N. A. M.; Kim, B.; Kim, H. Y., Production of Smooth and Pure Nickel Metal Nanofibers by the Electrospinning Technique: Nanofibers Possess Splendid Magnetic Properties. *Journal of Physical Chemistry C* **2009**, *113* (2), 531-536. DOI: 10.1021/jp805692r
- (11) Donegan, K. P.; Godsell, J. F.; Tobin, J. M.; O'Byrne, J. P.; Otway, D. J.; Morris, M. A.; Roy, S.; Holmes, J. D., Microwave-assisted Synthesis of Icosahedral Nickel Nanocrystals. *Crystengcomm* **2011**, *13* (6), 2023-2028. DOI: 10.1039/C0CE00759E
- (12) Guo, H.; Pu, B. X.; Chen, H. Y.; Yang, J.; Zhou, Y. J.; Bismark, B.; Li, H. D.; Niu, X. B., Surfactant-assisted Solvothermal Synthesis of Pure Nickel Submicron Spheres with Microwave-absorbing Properties. *Nanoscale Research Letters* **2016**, *11*, 16. DOI: 10.1186/s11671-016-1562-y
- (13) Kappe, C. O.; Dallinger, D., Controlled Microwave Heating in Modern Organic Synthesis: Highlights from the 2004-2008 Literature. *Molecular Diversity* **2009**, *13* (2), 71-193. DOI: 10.1007/s11030-009-9138-8
- (14) Satoshi Horikoshi, N. S., *Microwaves in Nanoparticles Synthesis: Fundamentals and Application*. Wiley-VCH: Weinheim, 2013.
- (15) Mirzaei, A.; Neri, G., Microwave-assisted Synthesis of Metal Oxide Nanostructures for Gas Sensing Application: A review. *Sensors and Actuators B-Chemical* **2016**, *237*, 749-775. DOI: 10.1016/j.snb.2016.06.114
- (16) Balu, A. M.; Hidalgo, J. M.; Campelo, J. M.; Luna, D.; Luque, R.; Marinas, J. M.; Romero, A. A., Microwave Oxidation of Alkenes and Alcohols Using Highly Active and Stable Mesoporous Organotitanium Silicates. *Journal of Molecular Catalysis a-Chemical* **2008**, *293* (1-2), 17-24. DOI: 10.1016/j.molcata.2008.06.016
- (17) Balu, A. M.; Dallinger, D.; Obermayer, D.; Campelo, J. M.; Romero, A. A.; Carmona, D.; Balas, F.; Yohida, K.; Gai, P. L.; Vargas, C.; Kappe, C. O.; Luque, R., Insights into the Microwave-assisted Preparation of

- Supported Iron Oxide Nanoparticles on Silica-type Mesoporous Materials. *Green Chemistry* **2012**, *14* (2), 393-402. DOI: 10.1039/C1GC16119A
- (18) Bermudez, J. M.; Francavilla, M.; Calvo, E. G.; Arenillas, A.; Franchi, M.; Menendez, J. A.; Luque, R., Microwave-induced Low Temperature Pyrolysis of Macroalgae for Unprecedented Hydrogen-enriched Syngas Production. *Rsc Advances* **2014**, *4* (72), 38144-38151. DOI: 10.1039/C4RA05372A
- (19) Yopez, A.; De, S.; Climent, M. S.; Romero, A. A.; Luque, R., Microwave-Assisted Conversion of Levulinic Acid to gamma-Valerolactone Using Low-Loaded Supported Iron Oxide Nanoparticles on Porous Silicates. *Applied Sciences-Basel* **2015**, *5* (3), 532-543. DOI: 10.3390/app5030532
- (20) Francavilla, M.; Intini, S.; Luchetti, L.; Luque, R., Tunable Microwave-assisted Aqueous Conversion of Seaweed-derived Agarose for the Selective Production of 5-hydroxymethyl Furfural/Levulinic Acid. *Green Chemistry* **2016**, *18* (22), 5971-5977. DOI: 10.1039/C6GC02072K
- (21) Park, H. W.; Park, S.; Park, D. R.; Choi, J. H.; Song, I. K., Catalytic Decomposition of Benzyl Phenyl Ether to Aromatics over Cesium-exchanged Heteropolyacid Catalyst. *Korean Journal of Chemical Engineering* **2011**, *28* (5), 1177-1180. DOI: 10.1007/s11814-010-0491-1
- (22) Yoon, J. S.; Lee, Y.; Ryu, J.; Kim, Y. A.; Park, E. D.; Choi, J. W.; Ha, J. M.; Suh, D. J.; Lee, H., Production of High Carbon Number Hydrocarbon Fuels from a Lignin-derived Alpha-O-4 Phenolic Dimer, Benzyl Phenyl Ether, via Isomerization of Ether to Alcohols on High-surface-area silica-alumina Aerogel Catalysts. *Applied Catalysis B-Environmental* **2013**, *142*, 668-676. DOI: 10.1016/j.apcatb.2013.05.039
- (23) Ojeda, M.; Balu, A. M.; Barron, V.; Pineda, A.; Coletto, A. G.; Romero, A. A.; Luque, R., Solventless Mechanochemical Synthesis of Magnetic Functionalized Catalytically Active Mesoporous SBA-15 Nanocomposites. *Journal of Materials Chemistry A* **2014**, *2* (2), 387-393. DOI: 10.1039/C3TA13564K
- (24) Miller, S. A.; Bobbitt, J. M.; Leadbeater, N. E., Oxidation of Terminal Diols using an Oxoammonium Salt: a Systematic Study. *Organic & Biomolecular Chemistry* **2017**, *15* (13), 2817-2822. DOI: 10.1039/C7OB00039A
- (25) Fievet, F.; Lagier, J. P.; Blin, B.; Beaudoin, B.; Figlarz, M., Homogeneous and Heterogeneous Nucleations in the Polyol Process for the Preparation of Micron and Sub-micron Size Metal Particles. *Solid State Ionics* **1989**, *32-3*, 198-205. DOI: 10.1016/0167-2738(89)90222-1
- (26) Chen, D.; Tang, K. B.; Shen, G. Z.; Sheng, J.; Fang, Z.; Liu, X. M.; Zheng, H. G.; Qian, Y. T., Microwave-assisted Synthesis of Metal Sulfides in Ethylene Glycol. *Materials Chemistry and Physics* **2003**, *82* (1), 206-209. DOI: 10.1016/S0254-0584(03)00206-2
- (27) Takahashi, K.; Yokoyama, S.; Matsumoto, T.; Huaman, J. L. C.; Kaneko, H.; Piquemal, J. Y.; Miyamura, H.; Balachandran, J., Towards a Designed Synthesis of Metallic Nanoparticles in Polyols - Elucidation of the Redox Scheme in a Cobalt-ethylene Glycol System. *New Journal of Chemistry* **2016**, *40* (10), 8632-8642. DOI: 10.1039/C6NJ01738J
- (28) Serna, C.J, Morales, M.P. Maghemite ( $\gamma$ -Fe<sub>2</sub>O<sub>3</sub>): A Versatile Magnetic Colloidal Material. In *Surface and Colloid Science*, E. Matijevic, M. Borkovec Eds., Kluwer Academic/Plenum Publishers: New York, 2004.

## Supporting Information

### S0 - Experimental Section

All the reagents were purchased from Sigma-Aldrich Inc, and were used without any further purification.

PXRD patterns were recorded using a Bruker D8 DISCOVER A25 diffractometer with a slit of  $0.018^\circ$  from  $2\theta=10^\circ$  to  $80^\circ$  and counting time of 5 s per step using  $\text{CuK}\alpha$  radiation. Textural properties of the samples were determined by  $\text{N}_2$  physisorption using a Micromeritics ASAP 2020 automated system with the Brunauer-Emmet-Teller (BET) and the Barret-Joyner-Halenda (BJH) methods. The samples were outgassed for 24 h at  $130^\circ\text{C}$  under vacuum ( $P_0 = 10^{-2}$  Pa) and subsequently analysed. SEM images were recorded with a JEOL JSM-6300 scanning microscope equipped with Energy-dispersive X-ray spectroscopy (EDS) at 20 kV. TEM images were recorded with JEOL 1200, at the Research Support Service Center (SCAI) from University of Cordoba. Prior to the recording, samples were prepared by suspension in EtOH, assisted by sonication and followed by deposition on a copper grid. The magnetic susceptibility was evaluated at room temperature and at low frequency (470 Hz), employing a Bartington MS-2 instrument. The reaction products were identified using GC (7890A)-MS (5975D inert MSD with Triple-Axis Detector) Agilent equipped with a capillary column HP-5MS (60 m x 0.32 mm), at the Research Support Service Center (SCAI) from University of Cordoba. Helium was used as a carrier gas. Quantitatively analysis were determined using GC (Agilent 7890 A) employing a FID and a PetroITM DH column (100 m x 0.25 mm x 0.50  $\mu\text{m}$ ). The carrier gas used was  $\text{N}_2$ .

CEM-Discover (CEM Corporation Matthews, NC, USA) microwave reactor was employed to perform the synthesis of the MMN and the hydrogenolysis of BFE. For the synthesis of MMN, the metallic precursor  $\text{NiCl}_2$ , EtOH and EG were added in a 10 mL microwave tube at room temperature. The mixture was irradiated with microwaves at different times between 5-60 mins in the  $180\text{-}250^\circ\text{C}$  temperature range using a temp. ramp of 1 minute. The precipitate was recovered with a magnet, washed with ethanol (5 mL) and acetone (5 mL) and oven dried ( $100^\circ\text{C}$ ). For the hydrogenolysis of BFE, BFE (25 mg) were added to isopropanol (0,5 mL) and catalysts (7% wt). The reaction was irradiated



with microwaves at different times between 5-45 mins at 230°C using a temp. ramp of 1 minute.

**Table S1 - EDS analysis of the surface of MWs metallic Nickel**

Element	Wt%	Wt% Sigma	Atomic %
C	3.72	0.17	15.69
O	0.45	0.04	1.41
Cl	0.19	0.02	0.27
Ni	95.65	0.17	82.63
Total:	100.00		100.00

**Figure S1 - Image of the magnetic metallic Nickel precipitate**

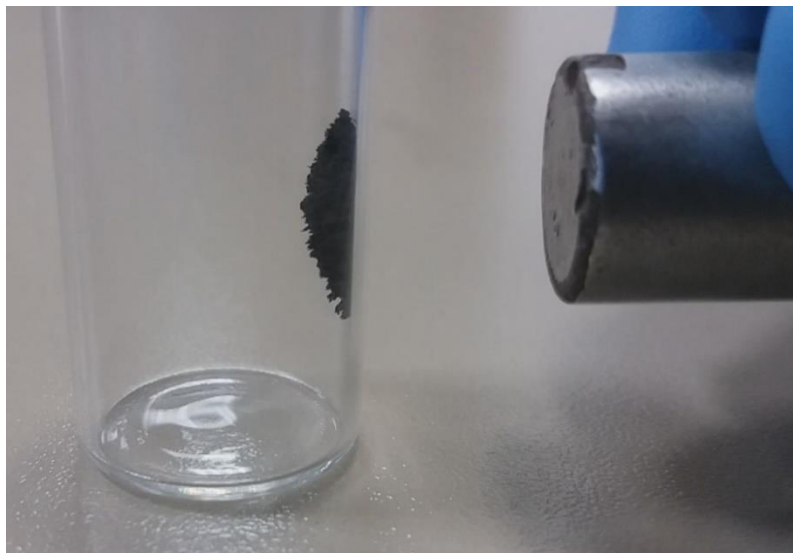


Table S2 - Most relevant trials

[Ni <sup>2+</sup> ] (mol L <sup>-1</sup> )	Reaction time (min)	Temperature (°C)	Mixture composition (EG X <sub>i</sub> )	yield (%)
<b>Increasing reaction time</b>				
0,031	<b>1</b>	200	0,904	0
0,031	<b>3</b>	200	0,904	0
0,031	<b>5</b>	200	0,904	undetectable*
0,031	<b>10</b>	200	0,904	undetectable*
0,031	<b>30</b>	200	0,904	22
0,031	<b>20</b>	200	0,904	24
0,031	<b>60</b>	200	0,904	30
<b>Varying mixture composition</b>				
0,031	5	150	<b>0,000</b>	0
0,031	5	150	<b>0,610</b>	0
0,031	5	200	<b>0,807</b>	0
0,031	5	200	<b>0,846</b>	20
0,031	5	200	<b>0,865</b>	9
0,031	5	200	<b>0,884</b>	undetectable*
0,031	5	200	<b>0,904</b>	undetectable*
0,309	5	200	<b>0,923</b>	undetectable*
0,031	5	200	<b>0,962</b>	undetectable*
0,031	5	200	<b>0,970</b>	undetectable*
0,031	5	200	<b>0,981</b>	0
0,031	5	200	<b>1,000</b>	0
0,031	5	230	<b>1,000</b>	0
<b>Increasing reaction temperature</b>				
0,031	5	<b>150</b>	0,904	0
0,310	5	<b>170</b>	0,904	0
0,031	5	<b>180</b>	0,904	undetectable*
0,031	5	<b>200</b>	0,904	undetectable*
0,031	5	<b>220</b>	0,904	26
0,031	5	<b>230</b>	0,904	34
0,031	5	<b>240</b>	0,904	44
0,031	5	<b>250</b>	0,904	71
<b>Increasing metal precursor concentration</b>				
<b>0,008</b>	20	210	0,904	undetectable*
<b>0,017</b>	20	210	0,904	undetectable*
<b>0,023</b>	20	210	0,904	undetectable*
<b>0,031</b>	20	210	0,904	undetectable*
<b>0,072</b>	20	210	0,904	8
<b>0,110</b>	20	210	0,904	6
<b>0,182</b>	20	210	0,904	4
<b>0,312</b>	20	210	0,904	0
<b>0,471</b>	20	210	0,904	0
<b>0,772</b>	20	230	0,904	0

\*the precipitate consisted of a fine magnetic powder, which was impossible to properly weight

Figure S2 - GC-MS analysis of 1,3-Dioxolane-2-methanol

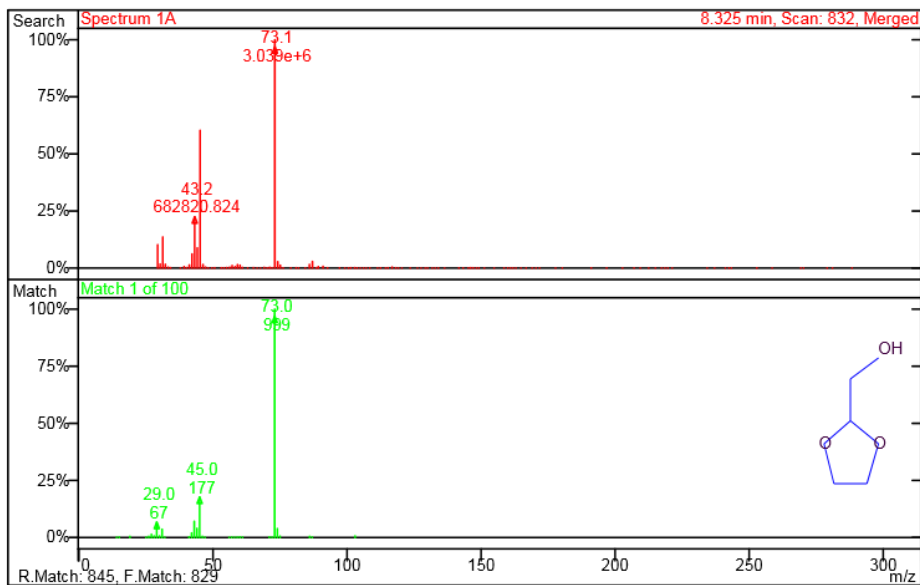


Table S3 - BPE hydrogenolysis with MWs Metallic Ni and commercially available 5% Pd/C

Catalyst	Time (min)	BFE conversion (%)	Toluene selectivity (%)	Phenol selectivity (%)
MMN	5	2	12	40
MMN	15	12	18	46
MMN	30	17	19	44
<b>MMN</b>	<b>45</b>	<b>24</b>	<b>15</b>	<b>44</b>
<b>5%Pd/C</b>	<b>45</b>	<b>43</b>	<b>24</b>	<b>56</b>
<b>MMN*</b>	<b>45</b>	<b>21</b>	<b>22</b>	<b>43</b>

\* reused 5 cycles





## **Conclusions and perspectives**



Despite each article presents a conclusion section, it is possible to combine the obtained results in order to track general outcomes and perspectives of the PhD Thesis:

- Microwave-assisted technique has been demonstrated to be more efficient than conventional heating methods for the preparation of nanoparticles, specifically metallic Ni nanoparticles as well as Cu<sub>2</sub>S nanocomposites. In fact, the microwave-assisted synthesis has been proved to reduce the reaction time and improve some morphological characteristics of the nanoparticles (*e.g.*, reduced size dimension and homogeneity of the composites samples). The successful exploitation of the reported procedures could lead to the preparation of similar compounds (*e.g.*, metallic Co or other Chalcogenides compounds) with captivating applications.
- As well established in the bibliography, the utilization of ethylene glycol has been confirmed to be highly useful to achieve uniform heating and therefore good-size distribution of the nanodimensional systems due to the high microwave adsorption properties. Also, the high viscosity characteristics of ethylene glycol have been demonstrated to slow down the deposition of the materials in the formation of the composites (*i.e.* Cu<sub>2</sub>S-carbon). These achievements could be useful in the microwave-assisted preparation of other composites materials where the different densities entail limits.
- Thanks to the microwave selective heating of the metallic centres of the nanocatalysts, it has been possible to enhance the yields of selected reactions, including the cycloisomerization of propargylic ureas and the hydrogenolysis of benzyl phenyl ether, by using low microwave adsorption solvents (*e.g.*, acetonitrile and toluene).
- The microwave-assisted preparation of supported gold and silver nanoparticles has been proved to be extremely rapid if carried out in a microwave oven. However, compared to a solvent less mechanochemistry approach, the microwave-assisted technique produces materials having slightly less catalytic activity in the cycloisomerization of propargyl ureas. These results specifically

highlight that in some reactions is better to support the metallic centres external to the SBA-15 channels, *i.e.* *via* mechanochemical approach, while in others the presence of metals inside the porous channel may be a winning strategy. Consequently, the morphological characteristics of the nanoparticles synthesized by microwave-assisted approaches should always be considered when designing catalysts for specific reactions.

- The microwave-heating of water has been proved to promote the reaction of cycloisomerization of propargyl ureas having electron-donor compounds in the structure. The exploitation of this phenomenon could lead to the efficient promotion of other similar reactions avoiding the use of catalysts and organic solvents.
- In general, the microwave-assisted synthesis of nanoparticles has been demonstrated to be still poorly developed to be efficiently scaled up. However, the effort in the development of easy, highly reproducible, fast and low toxicity procedures as well as the shifting to multimode microwave oven, *i.e.* Ethos Microwave from Milestones Srl, from monomode ovens, *i.e.* Discovery Microwave from CEM Corp., may track possible pilot scale up of the synthesis (multigram quantities).





# Summary



## English

### MICROWAVE-ASSISTED SYNTHESIS OF NANOCATALYSTS IN BATCH CONDITIONS

The development of intensified processes for the preparation of novel catalytically active nanodimensional materials is a captivating challenge getting more attention day-by-day.<sup>1, 2</sup> In fact, nanoparticle systems offer the possibility of combining the high activity of homogenous catalysts with the better recoverability of heterogeneous ones, opening to unlimited application in the chemical industry. The microwave-assisted technique – recognized as one of the most innovative methods for process intensification – makes it possible to both synthesize and test new nanocatalysts exploiting the unique characteristics of microwave heating. These characteristics include reduced reaction times, minimized (or suppressed) side reactions, highly reproducibility, enhanced yields and selectivity as well as selective heating and magnetic loss heating.<sup>3-5</sup>

The PhD thesis presented has been developed thanks to the experience of the research group FQM-383 (NanoVal) in nanoscale chemistry, heterogeneous catalysis and waste/biomass valorization. More in details, the research studies of the PhD thesis demonstrated the potentiality of microwave-assisted techniques for the development of efficient nanocatalytic systems specifically designed for photochemical applications, fine chemical synthesis and biofuel production.<sup>6-10</sup>

Most important results obtained during the PhD Thesis have been described in three research articles. In addition, a comprehensive minireview has been included in the introduction section in order to highlight the primary importance of nanocatalysts for the production of biofuels.

The first research article, “Microwave-assisted valorization of pig bristles: towards visible light photocatalytic chalcocite composites”, discloses the preparation of nano-Cu<sub>2</sub>S carbon composites *via* a fast and low-toxicity microwave-assisted method.<sup>11</sup> The synthesis was carried out employing ethylene glycol as solvent, copper chloride as metal precursor and waste pig bristles as sulfur and carbon source, avoiding the use of any toxic sulfur precursor (*e.g.* H<sub>2</sub>S, thiourea). The high microwave adsorption and high viscosity of ethylene glycol allowed for the preparation of homogeneous Cu<sub>2</sub>S carbon

composites within a few minutes (4 minutes at 200°C operating in a multimode microwave oven). By contrast, conventional heating needed longer reaction times and formed inhomogeneous, low-active Cu<sub>2</sub>S carbon material. The so-produced composite has been characterized by X-ray diffraction (XRD), nitrogen physisorption (BET model), scanning electron microscopy/energy dispersive X-ray spectroscopy (SEM-EDX) and UV-Vis spectroscopy. Cu<sub>2</sub>S carbon composite has been successfully used for the photo degradation of methyl red, a common pollutant dye, under visible LED light irradiation, leading to ca. 40% of degradation within 3 hours.

In the second research article, “Heterogeneously Catalyzed Synthesis of Imidazolones *via* Cycloisomerizations of Propargylic Ureas Using Ag and Au/Al SBA-15 Systems”, a study of environmentally friendly paths for the cycloisomerization of propargylic ureas has been explored.<sup>12</sup> Specifically, different nanogold and nanosilver catalysts have been prepared by supporting the metal nanoparticles over mesoporous silica (SBA-15) through mechanochemistry and microwave-assisted approaches. The catalysts have been used as heterogeneous systems in the microwave assisted synthesis of a library of imidazolones *via* a sequential study aimed to shift the reaction to greener operative conditions. The employed systems avoided the utilization of strong bases, such as NaOH, or expensive homogeneous metal catalysts. The best conditions have been combined in order to catalyse the cycloisomerization of propargyl ureas using only water as solvent and promoter of the reaction. The results demonstrated that the selected solvent highly influenced the reactions, where toluene promoted N-cyclization reactions, ethanol favoured the cyclization of propargylic ureas characterized by more electron withdrawing groups and water favoured the cyclization of propargylic ureas containing electron donor compounds in the structure.

The third research article, “Efficient and Environmentally Friendly Microwave-Assisted Synthesis of Catalytically Active Magnetic Metallic Ni Nanoparticles” describes the preparation of pure magnetic metallic nickel by a simple and fast microwave-assisted method using a monomode microwave reactor (CEM Discover, CEM Corp.).<sup>13</sup> The synthesis has been carried out using nickel chloride as metal precursor and a mixture of ethylene glycol and ethanol (or isopropanol) as solvent and reducing agent. A fine study carried out varying the molar ratio of ethylene glycol and ethanol in function of the reaction temperature has highlighted the reaction conditions where the reduction of

nickel occurred. The best performance (71% yield) has been achieved operating at 250°C for 5 minutes under microwave irradiation. The mechanism of reaction for oxidation of ethylene glycol and reduction of Ni<sup>2+</sup> has been demonstrated by gas chromatography–mass spectrometry (GC-MS) analysis, while the behaviour of the mixture and its bubble point in function of the recorder pressure has been simulated by PRO/II software (Schneider Electric Group). The nanoparticles have been analysed by X-ray diffraction (XRD), scanning emission microscopy (SEM), transmission electron microscopy (TEM) and magnetic mass susceptibility. The surface area has been determined by nitrogen physisorption (BET model). The nanoparticles have showed good activity in the hydrogenolysis of benzyl phenyl ether (BPE), a lignin model compound, with a maximum conversion of 24%, and reusability up to 5 cycles without sensible loss of activity.



## Spanish

### SÍNTESIS DE NANOPARTÍCULAS ASISTIDA POR MICROONDAS EN CONDICIONES BATCH

El desarrollo de procesos destinados a la preparación de nuevos materiales con dimensiones nanométricas y, a su vez, catalíticamente activos, es un desafío fascinante que llama cada vez más la atención<sup>1, 2</sup>. De hecho, los sistemas compuestos de nanopartículas ofrecen la posibilidad de combinar la alta actividad de los catalizadores homogéneos con la mejor capacidad de recuperación de los heterogéneos, ofreciendo de esta manera un número ilimitado de aplicaciones en la industria química. La técnica asistida por microondas, reconocida como uno de los métodos más innovadores para la intensificación de procesos, permite sintetizar y probar nuevos nanocatalizadores que exploten las características únicas del calentamiento por microondas. Estas características incluyen tiempos de reacción reducidos, reacciones secundarias minimizadas (o suprimidas), alta reproducibilidad, rendimientos y selectividad mejorados, así como calentamiento selectivo y calentamiento por pérdida magnética.<sup>3-5</sup>

La presente tesis doctoral se ha desarrollado gracias a la experiencia del grupo de investigación FQM-383 (NanoVal) en química a nanoescala, catálisis heterogénea y valorización de residuos/biomasa. Más en detalle, los estudios de investigación de la tesis doctoral demostraron la potencialidad de las técnicas asistidas por microondas para el desarrollo de sistemas nanocatalíticos eficientes diseñados específicamente para aplicaciones fotoquímicas, síntesis química fina y producción de biocombustibles.<sup>6-10</sup>

Los resultados más importantes obtenidos durante la tesis doctoral se han descrito en tres artículos de investigación. Además, en la sección de introducción, un apartado va dedicado a resaltar la gran importancia de los nanocatalizadores en la producción de biocombustibles.

El primer artículo de investigación, "Microwave-assisted valorization of pig bristles: towards visible light photocatalytic chalcocite composites", describe la preparación de compuestos nano-Cu<sub>2</sub>S de carbono mediante un método asistido por microondas rápido y de baja toxicidad.<sup>11</sup> La síntesis se llevó a cabo empleando etilenglicol como disolvente, cloruro de cobre como precursor de metal y pelos de cerdo de desecho

como fuente de azufre y carbono, evitando el uso de cualquier precursor de azufre tóxico (por ejemplo, H<sub>2</sub>S, tiourea). La alta adsorción por microondas y la alta viscosidad del etilenglicol permitieron la preparación de compuestos de carbono Cu<sub>2</sub>S homogéneos en pocos minutos (4 minutos a 200 ° C trabajando en un horno de microondas multimodo). Por el contrario, el calentamiento convencional necesitó tiempos de reacción más largos, dando como resultado un material de carbono Cu<sub>2</sub>S poco homogéneo y poco activo. El compuesto así producido se ha caracterizado por difracción de rayos X (XRD), fisisorción de nitrógeno (modelo BET), microscopía electrónica de barrido / espectroscopía de rayos X dispersiva de energía (SEM-EDX) y espectroscopía UV-Vis. El compuesto de carbono Cu<sub>2</sub>S se ha utilizado con éxito para la foto degradación del rojo de metilo, un colorante contaminante común, bajo irradiación de luz LED visible, que conduce a ca. 40% de degradación en 3 horas.

En el segundo artículo de investigación, “Heterogeneously Catalyzed Synthesis of Imidazolones *via* Cycloisomerizations of Propargylic Ureas Using Ag and Au/Al SBA-15 Systems”, se han estudiado diversos caminos ecológicos para la cicloisomerización de ureas propargílicas<sup>12</sup>. Específicamente, diferentes nanocatalizadores de oro y plata se han preparado soportando las nanopartículas metálicas sobre sílice mesoporosa (AISBA-15) utilizando mecanoquímica y radiación microondas. Los catalizadores se han utilizado como sistemas heterogéneos en la síntesis asistida por microondas de una biblioteca de imidazolonas a través de un estudio secuencial destinado a cambiar la reacción a condiciones operativas más ecológicas. Los sistemas empleados evitaron la utilización de bases fuertes, como NaOH, o catalizadores metálicos homogéneos y caros. Las mejores condiciones se han combinado para catalizar la cicloisomerización de las propargilureas utilizando solo agua como disolvente y promotor de la reacción. Los resultados demostraron que el disolvente seleccionado tiene una gran influencia en las reacciones, en concreto el tolueno promovió las reacciones de N-ciclación, el etanol favoreció la ciclación de las ureas propargílicas caracterizadas por más grupos de extracción de electrones y el agua favoreció la ciclación de la urea propargílica que contiene compuestos donadores de electrones en la estructura.

El tercer artículo de investigación, “Efficient and Environmentally Friendly Microwave-Assisted Synthesis of Catalytically Active Magnetic Metallic Ni Nanoparticles” describe la preparación de níquel metálico y magnético mediante un método simple y



rápido asistido por microondas utilizando un reactor monomodo (CEM Discover, CEM Corp .) <sup>13</sup> La síntesis se ha llevado a cabo utilizando cloruro de níquel como precursor metálico y una mezcla de etilenglicol y etanol (o isopropanol) como disolvente y agente reductor. Un buen estudio llevado a cabo variando la relación molar de etilenglicol y etanol en función de la temperatura de reacción ha llevado a las condiciones de reacción donde se produjo la reducción de níquel. El mejor rendimiento (71%) se ha logrado operando a 250 ° C durante 5 minutos bajo irradiación de microondas. El mecanismo de reacción para la oxidación de etilenglicol y la reducción de Ni<sup>2+</sup> se ha demostrado mediante el análisis de cromatografía de gases-espectrometría de masas (GC-MS), mientras que el comportamiento de la mezcla y su punto de burbuja en función de la presión del registrador se ha simulado con PRO/II software (Grupo Schneider Electric). Las nanopartículas han sido analizadas por difracción de rayos X (XRD), microscopía de emisión de barrido (SEM), microscopía electrónica de transmisión (TEM) y susceptibilidad de masa magnética. El área superficial ha sido determinada por la fisisorción de nitrógeno (modelo BET). Las nanopartículas han mostrado una buena actividad en la hidrogenólisis del bencil fenil éter (BPE), un compuesto modelo de lignina, con una conversión máxima del 24%, y reutilización de hasta 5 ciclos sin aparente pérdida de actividad.

## Summary

1. Chen, M. N.; Mo, L. P.; Cui, Z. S.; Zhang, Z. H., Magnetic nanocatalysts: Synthesis and application in multicomponent reactions. *Current Opinion in Green and Sustainable Chemistry* **2019**, *15*, 27-37.
2. Qin, L.; Zeng, G. M.; Lai, C.; Huang, D. L.; Zhang, C.; Cheng, M.; Yi, H.; Liu, X. G.; Zhou, C. Y.; Xiong, W. P.; Huang, F. L.; Cao, W. C., Synthetic strategies and application of gold-based nanocatalysts for nitroaromatics reduction. *Science of the Total Environment* **2019**, *652*, 93-116.
3. Gawande, M. B.; Shelke, S. N.; Zboril, R.; Varma, R. S., Microwave-Assisted Chemistry: Synthetic Applications for Rapid Assembly of Nanomaterials and Organics. *Accounts of Chemical Research* **2014**, *47* (4), 1338-1348.
4. Kappe, C. O., My Twenty Years in Microwave Chemistry: From Kitchen Ovens to Microwaves that aren't Microwaves. *Chemical Record* **2019**, *19* (1), 15-39.
5. Lau, C. C.; Bayazit, M. K.; Reardon, P. J. T.; Tang, J. W., Microwave Intensified Synthesis: Batch and Flow Chemistry. *Chemical Record* **2019**, *19* (1), 172-187.
6. Campelo, J. M.; Luna, D.; Luque, R.; Marinas, J. M.; Romero, A. A., Sustainable Preparation of Supported Metal Nanoparticles and Their Applications in Catalysis. *Chemsuschem* **2009**, *2* (1), 18-45.
7. Colmenares, J. C.; Luque, R., Heterogeneous photocatalytic nanomaterials: prospects and challenges in selective transformations of biomass-derived compounds. *Chemical Society Reviews* **2014**, *43* (3), 765-778.
8. Raheem, A.; Prinsen, P.; Vuppaladadiyam, A. K.; Zhao, M.; Luque, R., A review on sustainable microalgae based biofuel and bioenergy production: Recent developments. *Journal of Cleaner Production* **2018**, *181*, 42-59.
9. Fang, R. Q.; Tian, P. L.; Yang, X. F.; Luque, R.; Li, Y. W., Encapsulation of ultrafine metal-oxide nanoparticles within mesopores for biomass-derived catalytic applications. *Chemical Science* **2018**, *9* (7), 1854-1859.
10. Cerdan, K.; Ouyang, W. Y.; Colmenares, J. C.; Munoz-Batista, M. J.; Luque, R.; Balu, A. M., Facile mechanochemical modification of g-C<sub>3</sub>N<sub>4</sub> for selective photo-oxidation of benzyl alcohol. *Chemical Engineering Science* **2019**, *194*, 78-84.
11. Zuliani, A.; Munoz-Batista, M. J.; Luque, R., Microwave-assisted valorization of pig bristles: towards visible light photocatalytic chalcocite composites. *Green Chemistry* **2018**, *20* (13), 3001-3007.
12. Zuliani, A.; Ranjan, P.; Luque, R.; Van der Eycken, E. V., Heterogeneously Catalyzed Synthesis of Imidazolones via Cycloisomerizations of Propargylic Ureas Using Ag and Au/Al SBA-15 Systems. *Acs Sustainable Chemistry & Engineering* **2019**, *7* (5), 5568-5575.
13. Zuliani, A.; Balu, A. M.; Luque, R., Efficient and Environmentally Friendly Microwave-Assisted Synthesis of Catalytically Active Magnetic Metallic Ni Nanoparticles. *Acs Sustainable Chemistry & Engineering* **2017**, *5* (12), 11584-11587.



# **Index of Quality**



Data taken from InCites Journal Citation Reports dataset, updated the 20<sup>th</sup> of June 2019. ©2019 Clarivate.

Journal	Green Chemistry	
Publisher	Royal Society of Chemistry	
Title	Microwave-assisted valorization of pig bristles: towards visible light photocatalytic chalcocite composites	
Authors	A. Zuliani, M.J. Muñoz-Batista, R. Luque	
DOI	10.1039/C8GC00669E	
Citation	<b>Green Chem.</b> , 2018, 20, 3001-3007	
Journal Impact Factor 2018	9.405	
Thematic Area	Chemistry, multidisciplinary	Green & Sustainable Science & Technology
Position	20/172 (Q1)	2/35 (Q1)

Journal	ACS Sustainable Chemistry & Engineering	
Publisher	American Chemical Society	
Title	Heterogeneously Catalyzed Synthesis of Imidazolones <i>via</i> Cycloisomerizations of Propargylic Ureas Using Ag and Au/Al SBA-15 Systems	
Authors	A. Zuliani, P. Ranjan, R. Luque, E. V. Van der Eycken	
DOI	10.1021/acssuschemeng.9b00198	
Citation	<b>ACS Sustain. Chem Eng.</b> , 2019, 7 (5), 5568-5575	
Journal Impact Factor 2018	6.970	
Thematic Area	Chemistry, multidisciplinary	Green & Sustainable Science & Technology
Position	26/172 (Q1)	5/35 (Q1)

Journal	ACS Sustainable Chemistry & Engineering	
Publisher	American Chemical Society	
Title	Efficient and Environmentally Friendly Microwave-Assisted Synthesis of Catalytically Active Magnetic Metallic Ni Nanoparticles	
Authors	A. Zuliani, A. M. Balu, R. Luque	
DOI	10.1021/acssuschemeng.7b02945	
Citation	<b>ACS Sustain. Chem Eng.</b> , 2017, 5 (12), 11584-11587	
Journal Impact Factor 2018	6.970	
Thematic Area	Chemistry, multidisciplinary	Green & Sustainable Science & Technology
Position	26/172 (Q1)	5/35 (Q1)







# Achievements



## Publications

1. Zuliani, A.; Balu, A. M.; Luque, R., Efficient and Environmentally Friendly Microwave-Assisted Synthesis of Catalytically Active Magnetic Metallic Ni Nanoparticles. *Acs Sustainable Chemistry & Engineering* **2017**, *5* (12), 11584-11587.
2. Zuliani, A.; Ivars, F.; Luque, R., Advances in Nanocatalyst Design for Biofuel Production. *Chemcatchem* **2018**, *10* (9), 1968-1981.
3. Zuliani, A.; Munoz-Batista, M. J.; Luque, R., Microwave-assisted valorization of pig bristles: towards visible light photocatalytic chalcocite composites. *Green Chemistry* **2018**, *20* (13), 3001-3007.
4. Ivars-Barcelo, F.; Zuliani, A.; Fallah, M.; Mashkour, M.; Rahimnejad, M.; Luque, R., Novel Applications of Microbial Fuel Cells in Sensors and Biosensors. *Applied Sciences-Basel* **2018**, *8* (7).
5. Cova, C. M.; Zuliani, A.; Munoz-Batista, M. J.; Luque, R., A Sustainable Approach for the Synthesis of Catalytically Active Peroxidase-Mimic ZnS Catalysts. *Acs Sustainable Chemistry & Engineering* **2019**, *7* (1), 1300-1307.
6. Cova, C. M.; Zuliani, A.; Santiago, A. R. P.; Caballero, A.; Munoz-Batista, M. J.; Luque, R., Microwave-assisted preparation of Ag/Ag<sub>2</sub>S carbon hybrid structures from pig bristles as efficient HER catalysts. *Journal of Materials Chemistry A* **2018**, *6* (43), 21516-21523.
7. Ferlin, F.; Giannoni, T.; Zuliani, A.; Piermatti, O.; Luque, R.; Vaccaro, L., Sustainable Protocol for the Reduction of Nitroarenes by Heterogeneous Au@SBA-15 with NaBH<sub>4</sub> under Flow Conditions. *Chemsuschem* **2019**, *12* (13), 3178-3184.
8. Zuliani, A.; Ranjan, P.; Luque, R.; Van der Eycken, E. V., Heterogeneously Catalyzed Synthesis of Imidazolones via Cycloisomerizations of Propargylic Ureas Using Ag and Au/AlSBA-15 Systems. *Acs Sustainable Chemistry & Engineering* **2019**, *7* (5), 5568-5575.
9. Martina, K.; Calsolaro, F.; Zuliani, A.; Berlier, G.; Chavez-Rivas, F.; Moran, M. J.; Luque, R.; Cravotto, G., Sonochemically-Promoted Preparation of Silica-Anchored Cyclodextrin Derivatives for Efficient Copper Catalysis. *Molecules* **2019**, *24* (13).
10. Cova, C. M.; Zuliani, A.; Muñoz-Batista, M. J.; Luque, R. Efficient scrap waste automotive converter Ru-based catalysts for the continuous-flow selective hydrogenation of cinnamaldehyde. *Green Chemistry* **2019**, *21*, 4712-4722.

## ***Other dissemination/communication activities***

1. **Other manuscript published:** A.Zuliani, R.Luque, chapter titled "Producing Fuels and Fine Chemicals from Biomass using Nanomagnetic Materials" for a book titled "Nanocatalysis: Applications and Technologies", edited by Taylor and Francis Group 2018
2. **Article in a no-peer review journal:** A. Zuliani, P. Ranjan, R. Luque and E. V. Van der Eycken, Designing sustainable microwave reactions, AMPERE Newsletter, 96 (2018)
3. **Infographic** on the COSMIC website and COSMIC social media, "COSMIC Project", 12<sup>th</sup> April 2017
4. **Infographic** on the COSMIC website and COSMIC social media, "Interesting conferences", 1<sup>st</sup> June 2017
5. **Blog** on the COSMIC website and COSMIC social media "Biorefinery: a glance at the past through present knowledge, for a COSMIC future", 8<sup>th</sup> January 2018
6. **Blog** on the COSMIC website and COSMIC social media (in two parts) "Arduino Device for Temperature Recording: A Cheap and Smart Solution for Our Lab Research!", June-July 2018

## ***Congress participation***

1. COSMIC Summer School, Leuven (BE) 4-8 September 2017
2. Doctoral School, Jaen (ES) 9-11 May 2018
3. IUPAC Summer School, Venice (IT) 7-14 July 2018
4. Green Extraction of Natural Products Conference, Bari (IT) 12-13 November 2018
5. NanoUCO Conference, Cordoba (ES) 21-22 January 2019
6. 23<sup>rd</sup> Annual Green Chemistry & Engineering Conference and 9<sup>th</sup> International Conference on Green and Sustainable Chemistry, Washington (USA) 11-13 June 2019
7. SECAT Conference, Cordoba (ES), 24-26 June 2019
8. UCRA Conference, Zaragoza (ES), 16-18 September 2019

## **Secondments**

1. KU Leuven, Leuven (BE), 1<sup>st</sup> of June 2018 – 31<sup>st</sup> of July 2018: “Utilisation of designed nanomaterials in C–H and C≡C bond activation”. Supervisors: E. V. Van der Eycken, W. De Borggraeve
2. University of Turin, Turin (IT), 1<sup>st</sup> of September 2018 – 3<sup>rd</sup> of December 2018: “Integration of microwaves with ultrasound for the synthesis of new nanomaterials”. Supervisors: G. Cravotto, K. Martina
3. Microinnova GmbH, Graz (AU), 23<sup>rd</sup> of January 2019 – 16<sup>th</sup> February 2019: “Scale-up of nanomaterial synthesis in flow”. Supervisors: D. Kirschneck, W. Linhart





# Acknowledgments

## *Acknowledgments*



Finally, the end of this great and unique adventure of three years has come. Firstly, I would like to thank my Supervisors Prof. Rafa and Prof. Alina. Thank you to have selected me as PhD candidate for this exceptional project. And thanks a lot to have guided me throughout the research. Your wisdom and your immense knowledge have given me the spirit to perform good investigation activities and learn a lot. Furthermore, your motivation and your patience have incredibly helped me also when things were going through a complicated direction. I'd like to especially thank you for your help beside work activities, you have been really more than is possible to imagine. THANK YOU!

Apart from my Supervisors, I'd like to express the gratitude to all the COSMIC team and to the European Commission for the Marie Skłodowska-Curie fellowship. Above all, I'd like to thank my Supervisors during the Secondments. Thank you, Prof. Katia and Prof. Giancarlo, to have made the experience of the Secondment in Turin an opportunity to grow from a scientific and human point of view. You have been incredible. Thank you to have been more than just Supervisors. And thanks a lot to all the people from your research group, especially to Federica, Maria-Jess, Janet, Riccardo, Pietro, Andreea, Luisa and Giorgio. I'd like also to thank Prof. Erick V. Van Der Eycken to have host me in KU Leuven and thank to the LOMAC research group, especially Prabhat and Upendra. I'd like to thank Dr. Dirk Kirschneck from Microinnova Engineering GmbH for the stage in his Company. Beside the Secondments, I'd like to express my thankfulness to all the people of COSMIC from the Supervisors to my early stage researchers colleagues. Thank you Ekim, your friendship will last for all my life, you're simply the best. Thank you, Roberta, it has been a pleasure to meet you since the first COSMIC interview in Leuven. You are a great ESR representative and a really great friend. Thank you, Maria-Jesus, for your support and friendship to me and to Camilla, I wish you the best and I wish we will meet in Caceres one day. Thank you Vidmantas, Prabhat and Ana Luisa, we had a really good time in Cordoba during your Secondments. Thank you, Heidy, Luca, Mohammed, Dwayne, Fabio C., Tilen, Gerardo, Fabio G. and Claire: I wish you all the best for your future!

I am also pleased to say thank you to all the people from Nanoval research group, especially Prof. Antonio. Thank you for your infinite patience helping me in the laboratory. Also, thanks to the post-docs that I met during this Project: Alfonso, Pepijn, Maria, Alain and Antonio. A special thanks to Araceli: thank you a lot for your support. Also, I'd like to thank Mario for his collaboration: I wish you the best career in Granada.

## Acknowledgments

Between all the predoctoral students, I'd like to especially thank Loles, Esther and Layla, more than just colleague: you are all great friends. I'd like to thank also all the other people from Nanoval: Sole, Kenneth, Paolma, Ana, Simona, Noelia Weiyi, Daily, and Paulette. Thank a lot also to the visiting students, post-docs and professors, and in particular to Gabriel, Viki and Bruna. The time we spent together was great. I look forward to meeting you again! A special thank also to Somayeh and Farveh, for the fun time together and for your delicious food. Thank also to Behgam Bingjie, Valeria, Yantao, Deyang, Adriano, Sandra, Bai, Gang, Clemente and Prasaanth. Thank a lot also to the laboratory technician, Pablo and Maria. And thanks a lot to the secretary of the Department Rafa, you are a really patience and comprehensive person. I'd like to thank also all the collaborator at the University of Cordoba, and in particular Manuel and the people form the SCAI, especially Isabel and Macarena.

I'd like also to thank Cordoba, a unique city in the World. Thanks to all the amazing people and friends I met here. And thanks to my family and to my friends from Italy, you have been always with me despite the distance.

With no doubts, everything I've done during my PhD couldn't have been done if I hadn't met great "*magistri*" during my life. In order, thanks to my grandpa Idio, master of everything, thanks to my Prof. Giorgio Miccinesi, my Commander Daniele Martinuzzi, my "*voga veneta*" teacher, Mr. Lino Farnea, my university Supervisors Prof. Gian Luca Chiarello and Prof. Elena Selli and my bosses Mrs. Cinzia Brignoli and Mr. Gianluca Frattarola.

Lastly, but more importantly, I am grateful to my wife, Camilla. You are my life. You, our little angel and our Gioele, are the reasons why I wake up everyday with my hearth full of gratitude to God. Thank you for your "Yes" that 23<sup>rd</sup> of December 2017, that has always been a "yes" to be together dealing with everyday troubles and challenges. Thank you to have never let me feel alone. Thank you to be always on my side. Thank you to let me feel free and happy.



## *Acknowledgments*



# **Annex I: Materials and Methods**



## Characterization

### **XRD**

X-ray powder diffraction (XRD) is one of the most important techniques for the analysis of solid crystals. It's a powerful non-destructive analysis that gives information about the crystalline nature, the chemical composition and the physical properties of a material. It is based on the analysis of the diffraction pattern of a sample hit by an X-ray bundle, as a function of the incidence angle, the polarization and the incident energy.

**Interaction between X-Ray and crystals:** the atoms (neutral or ionized) of a crystal are arranged in a long-range orderly periodic array, defined by the repetition of the unit cell (the basic repeating unit), as shown in Figure 1-A. The unit cell is defined by the crystal system (shape) and the lattice parameters (size). The energy minimization in the atomic structure (and therefore in the unit cell) defines the symmetry and the symmetry elements of the crystal structure (cubic, tetragonal, hexagonal, rhombohedral, orthorhombic, monoclinic, triclinic). On the other hand, the planes between atoms are described by the Miller indices (hkl), as illustrated in Figure 1-B. The vector normal to (hkl) is denoted as  $d_{hkl}$ . When X-ray irradiation (having a wavelength similar to the distance between atoms) hits a crystal, the scattering of X-rays from atoms generates a diffraction pattern. Clearly, when the atoms are not arranged in periodic arrays with long-range order, no diffraction is possible (amorphous material). The constructive diffraction generated from the scattering of X-Ray and the planes of atoms is related to the diffraction angle  $2\theta$  thanks to the Bragg's equation ( $n$  is an integer number, while  $\lambda$  is the X-Ray wavelength, normally fixed), as shown in Figure 1-C:

$$n\lambda = 2d_{hkl}\sin\theta$$

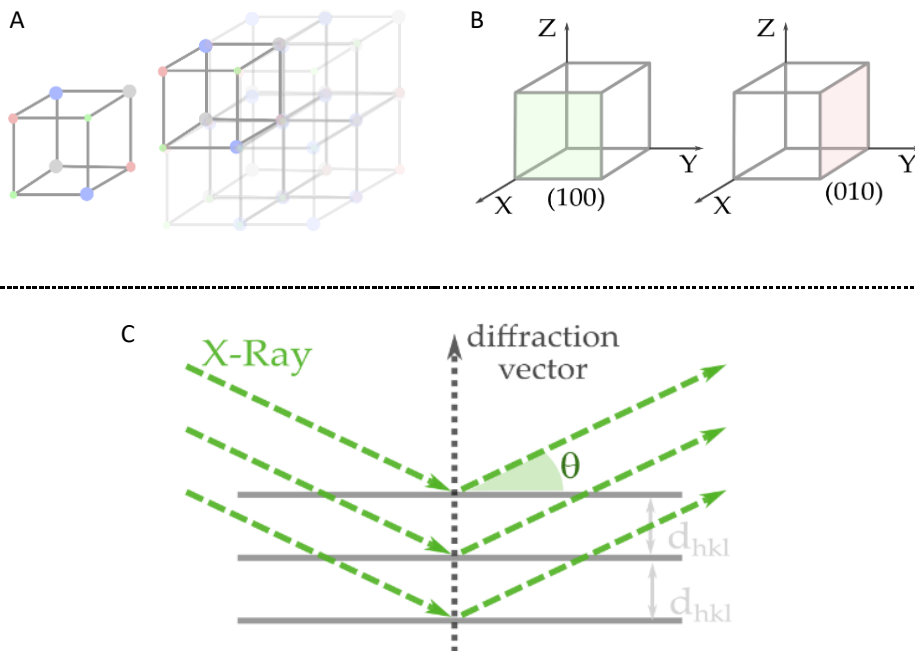


**Figure 1.** A) A-Unit cell (left) and crystal structure (right); B) Examples of Miller indices in a cubic crystals; C) Bragg's law for X-Ray diffraction.

When the X-Ray hits the crystal, the rays are scattered in a sphere around the sample and each cone along the sphere corresponds to a single Bragg angle  $2\theta$ , as shown in Figure 2-A. In this PhD thesis, the XRD patterns were recorded using a Bragg-Brentano diffractometer. In the Bragg-Brentano geometry, the diffraction vector is always normal to the surface of the sample while the incident angle ( $\omega$ ) is defined between the X-Ray source and the sample. The linear diffraction pattern is formed as the detector scans through an arc that intersects each Debye ring at a single point, giving the appearance of a discrete diffraction peak, which intensity depends on the arrangement of atoms in the entire crystal (Figure 2-B). Each peak could be assigned to a different plane. The diffraction angle,  $2\theta$ , is defined between the incident beam and the detector (Figure 2-C).



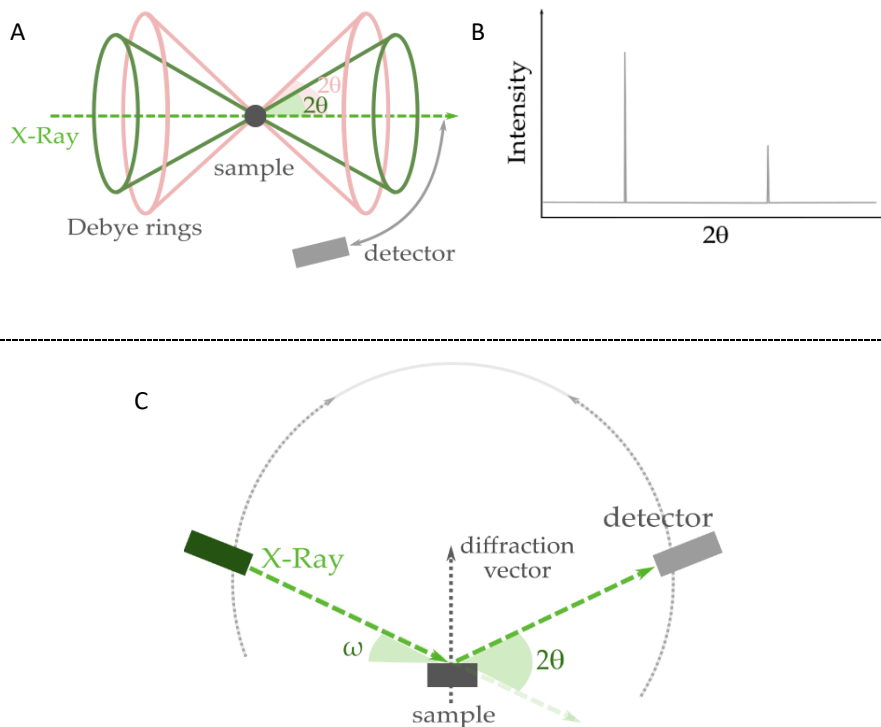


**Figure 2.** A) Debye cones generated by X-Ray scattering; B) Example of a linear diffraction pattern; C) Scheme of a Bragg-Brentano diffractometer.

A single crystal specimen in a Bragg-Brentano diffractometer would produce only one family of peaks in the diffraction pattern, while polycrystalline sample should contain thousands of crystallites, therefore all possible diffraction peaks could be observed. More in details, XRD analysis found its basis in the random orientation of crystals (and the crystal lattice) in the space. The experimental patterns are sequentially analysed and investigated in order to demine the position and relative intensity of the peaks to match experimental data to the reference patterns in the database.

**Experimental methodology:** The powder X-ray diffraction (XRD) patterns were recorded using a Bruker D8 DISCOVER A25 diffractometer (PANalytical/Philips, Lelyweg, Netherlands) using  $\text{CuK}\alpha$  ( $\lambda = 1.5418 \text{ \AA}$ ) radiation. Wide angle scanning patterns were obtained over a  $2\theta$  range from  $10^\circ$  to  $80^\circ$  with a step size of  $0.018^\circ$  and a counting time of 5 s per step. The data were analysed using Xpert High Score Plus software (PANalytical PANalytical/Philips, Lelyweg, Almelo, the Netherlands).

## Surface area and porosity measurements (BET)

The Brunauer-Emmet-Teller (BET) analysis is a useful technique for the determination of the surface area and porosity of a sample. It is based on the physical adsorption (and desorption) of a gas on a solid surface at its condensation temperature

**Gas-solid interaction.** Due to their intrinsic characteristics (low enthalpy of adsorption; no disruptive changes; no activation energy; reversibility), gas physical adsorption processes can be exploited for the determination of surface area and porosity of a sample. In fact, around eighty years ago, Brunauer, Emmett and Teller firstly described a model for the quantification of the physio-adsorbed gas on a surface. The model is based on Van der Waals gas-solid interactions, and it states that at fixed temperature, varying the gas pressure, it is possible to measure the molar quantity of a physio-adsorbed gas. More in details, the BET model is based on a sequence of hypothesis including: localized adsorption of the gas; equivalently of surface sites; absence of lateral interactions between successively adsorbed gas molecules as well as absence of interactions between layers; absence of limits in the number of adsorbed layers and assumption of liquid nature of the adsorbed molecules from the second layers onwards. When these hypothesis are satisfied, it is possible to calculate the volume occupied by a monolayer of the gas adsorbed ( $V$ ) divided by the gas volume corresponding to the monolayer formation ( $V_m$ ):

$$\frac{V}{V_m} = \frac{C \frac{p}{p^\circ}}{\left(1 - \frac{p}{p^\circ}\right) \cdot \left[1 + (C - 1) \frac{p}{p^\circ}\right]}$$

Where  $p$  is the measured pressure,  $p^\circ$  is the gas saturation pressure and  $C$  is a gas-surface interaction constant.

Linearizing the previous equation, it is possible to calculate:

$$\frac{p}{V(p - p^\circ)} = \frac{1}{V_m C} + \frac{(C - 1) p}{V_m C p^\circ}$$

By plotting  $\frac{p}{V(p - p^\circ)}$  vs  $\frac{p}{p^\circ}$ , a straight line can be obtained, from which it is possible to determine  $C$  and  $V_m$ .  $V_m$  is the parameter used to determine the specific surface area while

$C$  gives information about the gas behavior. When  $C \gg 1$ , the gas-solid affinity is greater than the gas-gas one and  $V_m$  has physical meaning. When  $C \ll 1$ ,  $V_m$  has no physical meaning. Furthermore, BET analysis can be considered acceptable when  $p/(p^\circ)$  is comprised between 0.05 and 0.35 (for lower relative pressures, BET underestimates the adsorption).

Knowing  $V_m$ , it is possible to estimate the value of the surface area of one sample, using the expression reported in the equation below:

$$S = \frac{V_m N_{Av} A}{22.414} \cdot 10^{-19}$$

Where  $A = 16.2 \text{ \AA}^2$  when nitrogen is used (it is the surface area occupied by a  $N_2$  molecule). By dividing  $A$  with the mass of the substance (reported in grams), the specific surface area value can be obtained.

Normally, the measure is carried out at  $\sim 77 \text{ K}$  and  $1 \text{ atm}$  pressure. The volume of the adsorbed gas is reported at standard temperature and pressure conditions ( $0 \text{ }^\circ\text{C}$  and  $760 \text{ torr}$ ), while the pressure is expressed as relative pressure, (actual pressure divided by the vapor pressure  $p^\circ$  of the adsorbing gas). The BET analysis give as results isotherms having six different possible forms. The six types of isotherms are characteristics of microporous (type I), non porous or macroporous (type II, III and IV), or mesoporous (type IV and V) materials (Figure 3). According to IUPAC the classes of porous materials are divided as follow: microporous, having the pore diameters  $< 2 \text{ nm}$ ; mesoporous, having pore diameter  $2\text{-}50 \text{ nm}$  and microporous, with pore diameter  $> 50 \text{ nm}$ .

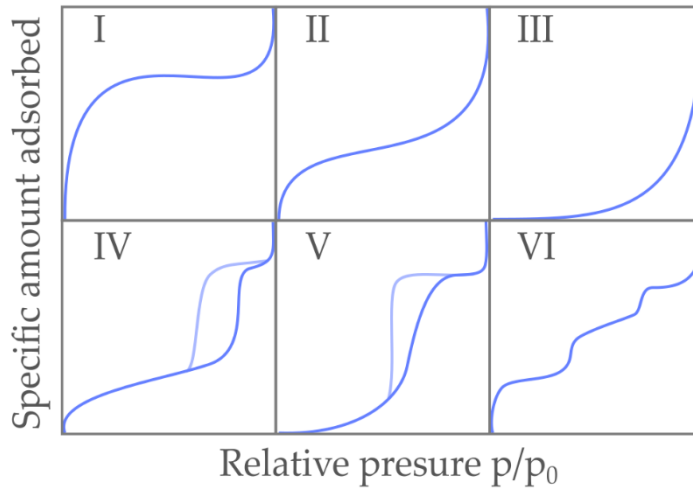


**Figure 3.** Different types of isotherms.

The shape of the hysteresis can also give information related to the type of pores (Figure 4):

- *H1 loop*: porous agglomerates with narrow distribution of pore size.
- *H2 loop*: often attributed to differences in the adsorption and desorption mechanism happening in the presence of pores with a particular shape. They show narrow necks and wide bodies, and hence they are called “ink-bottle pores” or “bottle-neck pores”.
- *H3 loop*: aggregates of plate-like particles, forming slit-shaped pores.
- *H4 loop*: attributed to slit-like pores (when the isotherm is of type I, there is microporosity).

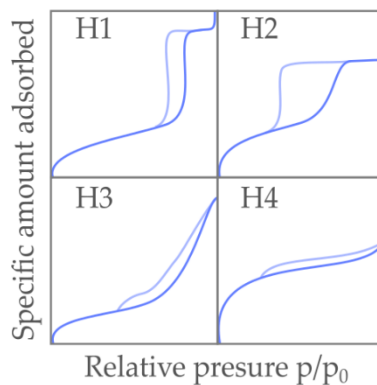


**Figure 4.** Shapes of hysteresis loop.

**Experimental methodology:** BET superficial areas BET and pore volumes were calculated by N<sub>2</sub> adsorption/desorption isotherms (conducted at 77 K) using an automotive analyzer, Micromeritics ASAP 2000 (Micromeritics Instrument Corp., Norcross, USA). The distribution of pore volume was calculated using the part relative to the adsorption of the N<sub>2</sub> adsorption/desorption isotherm, according to Barret, Joyner and Halenda' method (BJH).

### ***SEM-EDS and TEM***

Scanning Electron Microscopy (SEM) and Transmission electron microscopes (TEM) images give information related to the surface morphology and composition of an analysed material. The EM (electron microscopy) techniques use a bundle of electrons accelerated in vacuum, having high energy, hitting the sample and generating signals. Reflexes (SEM) or transmitted (TEM) electrons bundles are channelled in a cathode tube where they bump into another bundle of electrons, generating an image. When equipped with X-Ray detector (EDX or EDS, Energy Dispersive X-ray Analysis), it is possible to acquire spectra of elemental composition of selected point the surface of the analysed material.

**Interaction between electron beam and analysed sample:** in a EM microscope, the electron beam is firstly generated by accelerating and focusing electrons through a sequence of lenses and apertures. Sequentially, the electron beam hits the sample, which

is mounted in a vacuum chamber (in order to avoid, as much as possible, interferences with gases and volatile particles), generating a multitude of signals (electrons and photons), as shown in Figure 5. Many of them, are produced as consequence of the interaction of the beam inside the material (*e.g.* secondary electrons and X-Ray). The volume inside the sample in which interactions occur while interacting with the electron beam depends on several factors including the atomic number of the material (the higher atomic number the lower the interaction volume), the accelerating voltage (the higher the voltage, the higher the larger the interaction volume) and the angle of incidence for the electron beam (the greater the angle, the smaller the interaction volume). Different detectors collect the signal which is consecutively converted into images. The maximum resolution obtainable in a EM microscope is determined by different factors (*e.g.* the electron spot size or the interaction volume). On the other side, TEM images are recorder with the electrons passing through an ultrathin sample. TEM images give structural information at the highest possible resolution. As it goes through objects it can also give you information about internal structures, which SEM cannot provide.

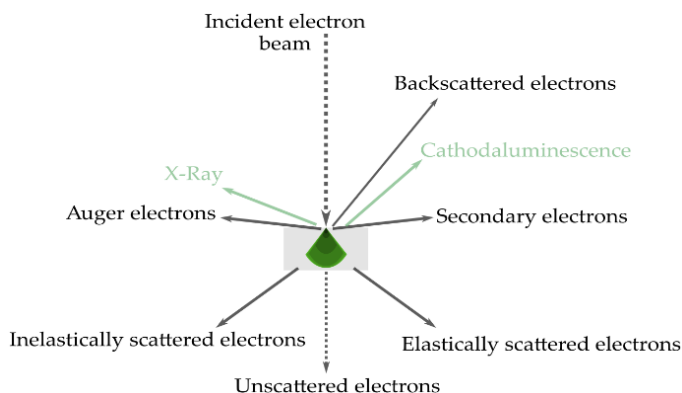


**Figure 5.** Electron beam- solid interaction.

TEM images are collected with transmitted electrons while SEM images are collected by sweeping the electron beam across the sample and recording the electrons that bounce back Figure 6.

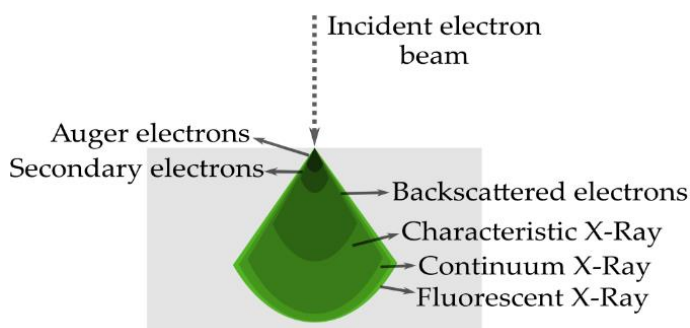


**Figure 6.** Interaction of electrons with the irradiated surface.

**Experimental methodology:** SEM images were recorded with a JEOL JSM-6300 scanning microscope (JEOL Ltd, Peabody, MA, USA) equipped with energy-dispersive X-ray spectroscopy (EDX) at 15 kV, while TEM images were recorded with JEOL 1200 (JEOL Ltd, Peabody, MA, USA), at the Research Support Service Centre (SCAI) at the University of Cordoba.

### **GC and GC-MS**

Gas chromatography (GC) and Gas chromatography–mass spectrometry (GC-MS) are analytical methods used to separate complex mixtures, to quantify analytes, and to determine trace levels of organic contamination. Specifically, GC is the separation technique for small and volatile molecules (*e.g.* benzenes, alcohols and aromatics, and simple molecules such as steroids, fatty acids and hormones). GC analysis can be applied towards the study of liquid, gaseous and solid samples. When combined with MS, in the so-called GC-MS, it is possible to determine the  $m/z$  ratios of the separated analysed samples.

**Gas separation processes.** In a GC equipment, the sample is firstly volatilized. The vaporized sample (the gas phase) is sequentially separated in its various components using a capillary column packed with a stationary (solid) phase. The compounds are propelled by an inert carrier gas such as argon, helium or nitrogen. As the components become separated, they elute from the column at different times, which is generally

referred to as their retention times. Once the components leave the GC column, they are ionized using electron or chemical ionization sources. In the case of GC-FID, an hydrogen/air flame oxidises organic molecules and produces electrically charged particles (ions) which are collected and produce an electrical signal which is then measured. In the case of GC-MS, the mass spectrometer ionize the molecules that are then accelerated through the instrument's mass analyser, which quite often is a quadrupole or ion trap. Ions are therefore separated based on their different mass-to-charge ( $m/z$ ) ratios. The signal produced by the GC and GC-MS equipment, is a spectrum giving relative abundance vs elution time. Peak are proportional to the quantity of the corresponding compound and can give information related to yield and selectivity of a reaction when an opportune standard (internal or external). In the case of GC-MS spectra, each peak correspond to a function of their  $m/z$  ratios (giving a mass spectrum). Using computer libraries of mass spectra for different compounds, it is possible to identify and quantitate unknown compounds and analytes.

**Experimental methodology:** GC-MS analysis were carried out using a GC (7890A)-MS (5975D inert MSD with Triple-Axis Detector) Agilent (Agilent Technologies Inc., CA, USA) equipped with a capillary column HP-5MS (60 m x 0.32 mm), at the Research Support Service Centre (SCAI) from the University of Cordoba. Helium was used as a carrier gas. Quantitatively analysis were determined using GC (Agilent 7890 A) employing a FID and a Petrol™ DH column (100 m×0.25 mm×0.50 μm). Nitrogen was used as carrier gas.

## **UV-Vis**

The UV/Vis spectroscopy (*ca.* 190-700 nm) is an instrumental technique for the qualitative and quantitative determination of different compounds including transition metals, conjugates organic compounds and biological molecules.

**Adsorbing the light.** The adsorption of visible or UV radiations by a molecule (M) can be considered as a two steps process. In the first step, the electrons adsorbs the radiation and are excited ( $M+h\nu$  gives  $M^*$ ). Specifically, considering organic compounds,



the electrons are promoted from the molecular orbitals of fundamental states to the ones of the excited states. In the case of inorganic compounds (in general ions and complexes of ions belonging to the first two series of transition metals), the absorbance of UV-Vis radiation implies transition between filled and empty d orbitals. Those transitions are possible if the molecule/compound is irradiated with a radiation whose energy equals to the difference between the states and (in case of organic molecules) if the transition gives rise to a strong change of the symmetry of the molecular orbitals. The absorption of UV-Vis light irradiation is limited to organic compounds possessing chromophores in their structures (functional groups having valence electrons that can be excited with relatively little energy). In the second step,  $M^*$  (having a short life  $10^{-8}$  to  $10^{-9}$  s) relaxes and goes back to the initial state, by thermal emission,  $M^*$  decomposition (photoreaction) or through emission of radiation (fluorescent or phosphorescent). If the emission of the radiation is detected and elaborated, it is possible to obtain UV-vis absorption spectra. The absorption spectrum of a molecule containing chromophores is generally complex due to the fact that the overlapping of the transitions of the vibro-rotational levels give a combination of overlapped lines. As a result, the spectra UV/Vis appear as a continuous absorption band. In the case of semiconductor material, the UV-Vis spectrum can be used to calculate the band gaps by plotting the graph between  $\alpha h\nu^2$  vs photon energy ( $h\nu$ ) (direct band gap) or  $\alpha h\nu^{1/2}$  vs photon energy ( $h\nu$ ) (indirect band gap).

**Experimental methodology:** UV visible (UV-vis) absorption spectra were recorded using a Lambda 365 UV-Vis spectrophotometer (PerkinElmer, Waltham, MA, USA).

## **NMR**

The Nuclear Magnetic Resonance Spectroscopy (NMR) is an analytical technique for the determination of the molecular structure of a sample as well as its content and its purity. NMR spectra can be used to match against libraries or to directly determine the basic chemical structure of a compound.

**Recording the spectra.** NMR technique can be used only with nuclei having a spin quantum number ( $I$ ) greater than zero. Those nuclei can be imagined as small

magnets that, after rotation, generate a magnetic dipole, which module is the magnetic nuclear  $\mu$ . Without applying an external magnetic field, the nuclei are randomly oriented. Oppositely, when an external magnetic field is applied, the nuclei tend to align to it. Regarding the chemical analysis, the most important nuclei are  $^1\text{H}$  and  $^{13}\text{C}$ , having  $I$  equal to  $\frac{1}{2}$ . The number of possible rotations which a nuclei can adapt depends on  $I$ , and equals to  $2I+1$ . As a result, the nuclei having  $I=1/2$  have two possible orientations, associated to two different energy levels (specifically, the orientation having direction parallel to the magnetic field will be associated to the lower energy level, which will be the most populated). The energy difference between the spin states depends on the applied magnetic field and on the nuclear magnetic moment. More in details, Larmor's frequency gives the energy necessary to promote a transition from two energy levels:

$$\nu = \mu B_0 / h I$$

$\nu$  is the frequency,  $\mu$  the magnetic nuclear moment,  $B_0$  the intensity of the magnetic field,  $h$  Planck's constant and  $I$  the spin quantum number. The higher the magnetic field, the higher the difference between the energy levels, the higher the frequency necessary to promote the transition between the energy levels.

An NMR experiment consists in applying a radiation that will promote the transition from a low energy level to a higher energy level in the nuclei. The energetical difference between the spin orientations depends on the specific position assumed by the atom in the molecule. This because each nucleus is subjected to the effect of the magnetic field on the neighbour nuclei. These energetical differences are detectable and recordable, giving important information of the positions of the nuclei in the molecule.

The experiment is practically carried out by putting a solution of the sample in a small glass tube between the poles of a magnet. The sample is sequentially irradiated with the radiofrequencies in the desired interval (*e.g.* covering the frequencies of the  $^1\text{H}$  adsorption) keeping a constant magnetic field, in order to let the protons adsorb at their single frequencies. The interpretation of the frequencies produces an interferogram that is difficult to comprehend. However, thanks to the Fourier transformation, it is possible to transform it into a spectrum showing the adsorption vs the applied frequencies. Firstly, the nuclei are irradiated with extremely short pulses of radiation ( $\mu\text{s}$ ). Sequentially, the excited nuclei go back to the fundamental state emitting the radiation they have adsorbed and the pulse cannot be repeated until the fundamental state is enough populated

(otherwise no radiation will be adsorbed). The process of returning to fundamental state is known as “relaxation” and can happen through different mechanisms. In the FT-NMR the pulses are frequently repeated (0,1-1 s) depending on the relaxation time of the nuclei, in order to record an elevated number of spectra, which can be summed in a few minutes. This technique functions well with low sensitive nuclei (low nuclear magnetic moment) and which are low abundant in nature (*i.e.*  $^{13}\text{C}$ ). An NMR spectrum is a graph reporting the intensity of the peaks vs the frequencies. The frequency is conventionally reported decreasing from left to right. The position of a peak is normally reported compared with a standard peak (*e.g.* tetramethylsilane, TMS) whose protons are all equivalent and resonate at high field compared with most of organic compounds. In order to better analyse the spectrum, the ppm ( $\delta$ ) are normally used. ppm can be obtained by dividing the band position respect to TMS ( $\nu - \nu_{\text{TMS}}$ ), *i.e.* the chemical shift, with the absolute frequency of the spectrum ( $\nu$ ) and by multiply by  $10^6$ . The chemical shifts are consequences of the fact that each nucleus, in a different environment, experiences different local magnetic fields, derived from the electron circulation in the neighbour bonds. Consequently, it is necessary to apply a different magnetic field to discriminate the different nuclei (different nuclei have different resonance frequencies). In an organic molecule, nuclei that are chemically close each other (max distance three chemical bonds) can give spin coupling effect, in which the adsorption bands, are splitted into multiple bands due to the interaction with neighbour nuclei. The distance between the band is called coupling constant (J). Remarkably, the coupling constant is generally smaller than chemical shift and is independent from the applied magnetic field.

**Experimental methodology:**  $^1\text{H}$  (400MHz or 600 MHz),  $^{13}\text{C}$  (100MHz) NMR spectra were recorded using a Bruker-Avance 400 or Mercury 400 (Bruker, MA, US).  $^1\text{H}$  NMR spectra were reported in parts per million (ppm) downfield relative to  $\text{CDCl}_3$  (7.26 ppm) and all  $^{13}\text{C}$  NMR spectra were reported in ppm relative to  $\text{CDCl}_3$  (77.2 ppm).

## Microwave-assisted methods

Microwave assisted techniques are based on the principles of microwave heating described in the introduction chapter. Microwave ovens for R&D purposes can be divided

into monomode (or single mode) and multimode reactor types. Monomode reactors have small compact cavities, in which microwave irradiation is directly focused on one single vessel containing the reaction mixture (where the electric and magnetic components have the highest intensities) (Figure 4-A). As a result, a high microwave field density is provided, resulting in exceedingly fast heating rates. As a drawback, the maximum applicable reaction volume in monomode reactors is normally 20 mL (only one sample per run), which makes them an ideal tool for optimizing chemical reactions on a small scale. On the contrary, multimode reactors have larger cavities in which the microwave field is distributed in a chaotic manner. In common multimode reactors the waves are reflected from the cavity walls and multiple modes of the electromagnetic waves interact with the cavity load (Figure 4-B). The homogeneity grade of distribution of the emitted radiation depends on the rate of stirring and rotation of the sample holders. Due to their larger size, these instruments can host different rotor types. In multimode microwave ovens it is possible to run parallel reactions in a scale range from a 300  $\mu$ L scale up to multigram synthesis in 100 mL reaction vessels (some models can host up to 25 vessels per run).

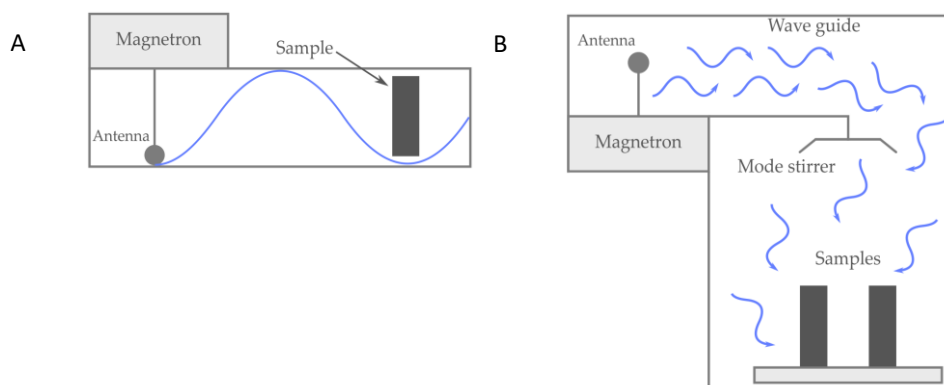


**Figure 4.** A) Monomode microwave oven; B) Multimode microwave oven.

**Experimental methodology:** Experiment in monomode microwave were carried out in a Discover CEM reactor (CEM Corp., Matthews, NC, USA). For experiment in multimode microwave, an Ethos One reactor (Milestones Srl, Bergamo, Italy) was chosen.

## Pro II software

PRO II / Software (previously Invensys System Inc., now Schneider Electric, Rueil-Malmaison, France) is a useful steady-state process simulator (process simulation) for process design and operational analysis for process engineer. It is possible to use the software to simulate the VLE (vapour liquid equilibrium) and the boiling points of mixture of compounds using different models (*e.g.* UNIFAC or UNIQUAC). For the estimation of the boiling point of the mixture of ethylene glycol and ethanol, the molecule were drawn with UNIFAC structures and fluxed in a flash drum.

## Photocatalytic activity

The Lambert-Beer's equation give information about the absorption of a solution respect to the concentration of the analysed specie:

$$A = \varepsilon cl$$

$A$  is the absorption,  $\varepsilon$  is the molar attenuation coefficient or absorptivity of the attenuating species,  $c$  is the concentration of the attenuating species and  $l$  the optical path length. If a sample adsorb radiation, the intensity of the incident light will be attenuated.  $A$  is directly proportional to the optical path length thanks to the molar attenuation coefficient, which depends on the specie and the incident wavelength. It is possible to plot the  $A$  vs the incident wavelength, obtaining a UV-vis spectrum of the analysed sample. In the case of the degradation of methyl red, it was possible to determine the grade of degradation by measuring the adsorption of the solution at fixed wavelength in function of the reaction time.

**Experimental methodology:** UV-visible (UV-vis) absorption values were recorded using a Lambda 365 UV-Vis spectrophotometer at fixed 405 nm (PerkinElmer, Waltham, MA, USA).





## **Annex II: Articles Permissions**





## Advances in Nanocatalyst Design for Biofuel Production

Alessio Zuliani,<sup>[a]</sup> Francisco Ivars,<sup>\*(b)</sup> and Rafael Luque<sup>\*(a)</sup>



**JOHN WILEY AND SONS LICENSE  
TERMS AND CONDITIONS**

Sep 27, 2019

This Agreement between Mr. Alessio Zuliani ("You") and John Wiley and Sons ("John Wiley and Sons") consists of your license details and the terms and conditions provided by John Wiley and Sons and Copyright Clearance Center.

License Number	4677050887126
License date	Sep 27, 2019
Licensed Content Publisher	John Wiley and Sons
Licensed Content Publication	ChemCatChem
Licensed Content Title	Advances in Nanocatalyst Design for Biofuel Production
Licensed Content Author	Rafael Luque, Francisco Ivars, Alessio Zuliani
Licensed Content Date	Feb 9, 2018
Licensed Content Volume	10
Licensed Content Issue	9
Licensed Content Pages	14
Type of use	Dissertation/Thesis
Requestor type	Author of this Wiley article
Format	Print and electronic
Portion	Full article
Will you be translating?	No
Title of your thesis / dissertation	MICROWAVE-ASSISTED SYNTHESIS OF NANOCATALYSTS IN BATCH CONDITIONS.
Expected completion date	Dec 2019
Expected size (number of pages)	250
Requestor Location	Mr. Alessio Zuliani Calle Sevilla 2A  Cordoba, 14003 Spain Attn: Mr. Alessio Zuliani
Publisher Tax ID	EU826007151
Total	0.00 USD

[Terms and Conditions](#)

**TERMS AND CONDITIONS**

This copyrighted material is owned by or exclusively licensed to John Wiley & Sons, Inc. or one of its group companies (each a "Wiley Company") or handled on behalf of a society with which a Wiley Company has exclusive publishing rights in relation to a particular work (collectively "WILEY"). By clicking "accept" in connection with completing this licensing transaction, you agree that the following terms and conditions apply to this transaction (along with the billing and payment terms and conditions established by the Copyright Clearance Center Inc., ("CCC's Billing and Payment terms and conditions"), at the time that you opened your RightsLink account (these are available at any time at <http://myaccount.copyright.com>).

### Terms and Conditions

- The materials you have requested permission to reproduce or reuse (the "Wiley Materials") are protected by copyright.
- You are hereby granted a personal, non-exclusive, non-sub licensable (on a stand-alone basis), non-transferable, worldwide, limited license to reproduce the Wiley Materials for the purpose specified in the licensing process. This license, **and any CONTENT (PDF or image file) purchased as part of your order**, is for a one-time use only and limited to any maximum distribution number specified in the license. The first instance of republication or reuse granted by this license must be completed within two years of the date of the grant of this license (although copies prepared before the end date may be distributed thereafter). The Wiley Materials shall not be used in any other manner or for any other purpose, beyond what is granted in the license. Permission is granted subject to an appropriate acknowledgement given to the author, title of the material/book/journal and the publisher. You shall also duplicate the copyright notice that appears in the Wiley publication in your use of the Wiley Material. Permission is also granted on the understanding that nowhere in the text is a previously published source acknowledged for all or part of this Wiley Material. Any third party content is expressly excluded from this permission.
- With respect to the Wiley Materials, all rights are reserved. Except as expressly granted by the terms of the license, no part of the Wiley Materials may be copied, modified, adapted (except for minor reformatting required by the new Publication), translated, reproduced, transferred or distributed, in any form or by any means, and no derivative works may be made based on the Wiley Materials without the prior permission of the respective copyright owner. **For STM Signatory Publishers clearing permission under the terms of the [STM Permissions Guidelines](#) only, the terms of the license are extended to include subsequent editions and for editions in other languages, provided such editions are for the work as a whole in situ and does not involve the separate exploitation of the permitted figures or extracts**. You may not alter, remove or suppress in any manner any copyright, trademark or other notices displayed by the Wiley Materials. You may not license, rent, sell, loan, lease, pledge, offer as security, transfer or assign the Wiley Materials on a stand-alone basis, or any of the rights granted to you hereunder to any other person.
- The Wiley Materials and all of the intellectual property rights therein shall at all times remain the exclusive property of John Wiley & Sons Inc, the Wiley Companies, or their respective licensors, and your interest therein is only that of having possession of and the right to reproduce the Wiley Materials pursuant to Section 2 herein during the continuance of this Agreement. You agree that you own no right, title or interest in or to the Wiley Materials or any of the intellectual property rights therein. You shall have no rights hereunder other than the license as provided for above in Section 2. No right, license or interest to any trademark, trade name, service mark or other branding ("Marks") of WILEY or its licensors is granted hereunder, and you agree that you shall not assert any such right, license or interest with respect thereto
- NEITHER WILEY NOR ITS LICENSORS MAKES ANY WARRANTY OR REPRESENTATION OF ANY KIND TO YOU OR ANY THIRD PARTY, EXPRESS, IMPLIED OR STATUTORY, WITH RESPECT TO THE MATERIALS OR THE ACCURACY OF ANY INFORMATION CONTAINED IN THE MATERIALS, INCLUDING, WITHOUT LIMITATION, ANY IMPLIED WARRANTY OF MERCHANTABILITY, ACCURACY, SATISFACTORY

QUALITY, FITNESS FOR A PARTICULAR PURPOSE, USABILITY, INTEGRATION OR NON-INFRINGEMENT AND ALL SUCH WARRANTIES ARE HEREBY EXCLUDED BY WILEY AND ITS LICENSORS AND WAIVED BY YOU.

- WILEY shall have the right to terminate this Agreement immediately upon breach of this Agreement by you.
- You shall indemnify, defend and hold harmless WILEY, its Licensors and their respective directors, officers, agents and employees, from and against any actual or threatened claims, demands, causes of action or proceedings arising from any breach of this Agreement by you.
- IN NO EVENT SHALL WILEY OR ITS LICENSORS BE LIABLE TO YOU OR ANY OTHER PARTY OR ANY OTHER PERSON OR ENTITY FOR ANY SPECIAL, CONSEQUENTIAL, INCIDENTAL, INDIRECT, EXEMPLARY OR PUNITIVE DAMAGES, HOWEVER CAUSED, ARISING OUT OF OR IN CONNECTION WITH THE DOWNLOADING, PROVISIONING, VIEWING OR USE OF THE MATERIALS REGARDLESS OF THE FORM OF ACTION, WHETHER FOR BREACH OF CONTRACT, BREACH OF WARRANTY, TORT, NEGLIGENCE, INFRINGEMENT OR OTHERWISE (INCLUDING, WITHOUT LIMITATION, DAMAGES BASED ON LOSS OF PROFITS, DATA, FILES, USE, BUSINESS OPPORTUNITY OR CLAIMS OF THIRD PARTIES), AND WHETHER OR NOT THE PARTY HAS BEEN ADVISED OF THE POSSIBILITY OF SUCH DAMAGES. THIS LIMITATION SHALL APPLY NOTWITHSTANDING ANY FAILURE OF ESSENTIAL PURPOSE OF ANY LIMITED REMEDY PROVIDED HEREIN.
- Should any provision of this Agreement be held by a court of competent jurisdiction to be illegal, invalid, or unenforceable, that provision shall be deemed amended to achieve as nearly as possible the same economic effect as the original provision, and the legality, validity and enforceability of the remaining provisions of this Agreement shall not be affected or impaired thereby.
- The failure of either party to enforce any term or condition of this Agreement shall not constitute a waiver of either party's right to enforce each and every term and condition of this Agreement. No breach under this agreement shall be deemed waived or excused by either party unless such waiver or consent is in writing signed by the party granting such waiver or consent. The waiver by or consent of a party to a breach of any provision of this Agreement shall not operate or be construed as a waiver of or consent to any other or subsequent breach by such other party.
- This Agreement may not be assigned (including by operation of law or otherwise) by you without WILEY's prior written consent.
- Any fee required for this permission shall be non-refundable after thirty (30) days from receipt by the CCC.
- These terms and conditions together with CCC's Billing and Payment terms and conditions (which are incorporated herein) form the entire agreement between you and WILEY concerning this licensing transaction and (in the absence of fraud) supersedes all prior agreements and representations of the parties, oral or written. This Agreement may not be amended except in writing signed by both parties. This Agreement shall be binding upon and inure to the benefit of the parties' successors, legal representatives,

and authorized assigns.

- In the event of any conflict between your obligations established by these terms and conditions and those established by CCC's Billing and Payment terms and conditions, these terms and conditions shall prevail.
- WILEY expressly reserves all rights not specifically granted in the combination of (i) the license details provided by you and accepted in the course of this licensing transaction, (ii) these terms and conditions and (iii) CCC's Billing and Payment terms and conditions.
- This Agreement will be void if the Type of Use, Format, Circulation, or Requestor Type was misrepresented during the licensing process.
- This Agreement shall be governed by and construed in accordance with the laws of the State of New York, USA, without regards to such state's conflict of law rules. Any legal action, suit or proceeding arising out of or relating to these Terms and Conditions or the breach thereof shall be instituted in a court of competent jurisdiction in New York County in the State of New York in the United States of America and each party hereby consents and submits to the personal jurisdiction of such court, waives any objection to venue in such court and consents to service of process by registered or certified mail, return receipt requested, at the last known address of such party.

#### **WILEY OPEN ACCESS TERMS AND CONDITIONS**

Wiley Publishes Open Access Articles in fully Open Access Journals and in Subscription journals offering Online Open. Although most of the fully Open Access journals publish open access articles under the terms of the Creative Commons Attribution (CC BY) License only, the subscription journals and a few of the Open Access Journals offer a choice of Creative Commons Licenses. The license type is clearly identified on the article.

##### **The Creative Commons Attribution License**

The [Creative Commons Attribution License \(CC-BY\)](#) allows users to copy, distribute and transmit an article, adapt the article and make commercial use of the article. The CC-BY license permits commercial and non-

##### **Creative Commons Attribution Non-Commercial License**

The [Creative Commons Attribution Non-Commercial \(CC-BY-NC\) License](#) permits use, distribution and reproduction in any medium, provided the original work is properly cited and is not used for commercial purposes.(see below)

##### **Creative Commons Attribution-Non-Commercial-NoDerivs License**

The [Creative Commons Attribution Non-Commercial-NoDerivs License \(CC-BY-NC-ND\)](#) permits use, distribution and reproduction in any medium, provided the original work is properly cited, is not used for commercial purposes and no modifications or adaptations are made. (see below)

##### **Use by commercial "for-profit" organizations**

Use of Wiley Open Access articles for commercial, promotional, or marketing purposes requires further explicit permission from Wiley and will be subject to a fee.

Further details can be found on Wiley Online Library <http://olabout.wiley.com/WileyCDA/Section/id-410895.html>

#### **Other Terms and Conditions:**

v1.10 Last updated September 2015

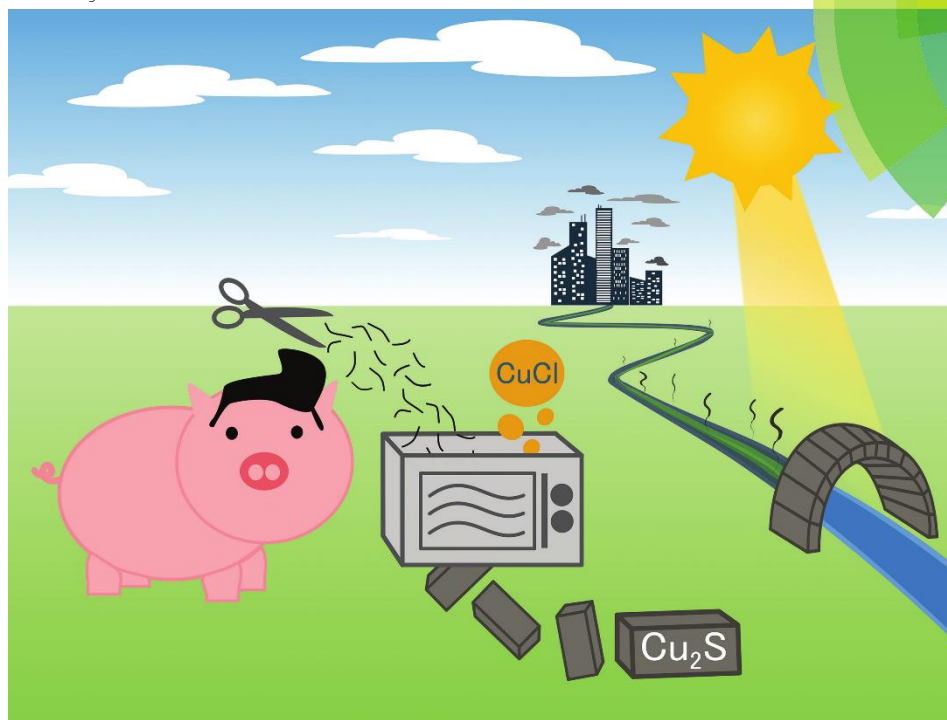
Questions? [customercare@copyright.com](mailto:customercare@copyright.com) or +1-855-239-3415 (toll free in the US) or +1-978-646-2777.



Volume 20 | Number 13 | 7 July 2018 | Pages 2923–3148

# Green Chemistry

Cutting-edge research for a greener sustainable future  
rsc.li/greenchem




ISSN 1463-9262



**PAPER**

Alessio Zuliani, Rafael Luque et al.  
Microwave-assisted valorization of pig bristles: towards visible light photocatalytic chalcocite composites

Gmail - Permission Request Form: Alessio Zuliani <https://mail.google.com/mail/u/0?ik=875999074&view=pt&search=a..>

 **Alessio Zuliani <zuliani.alessio@gmail.com>**

---

**Permission Request Form: Alessio Zuliani**  
2 messaggi

---

**noreply@rsc.org** <noreply@rsc.org> 1 ottobre 2019 13:12  
A: [contracts-copyright@rsc.org](mailto:contracts-copyright@rsc.org)  
Cc: [zuliani.alessio@gmail.com](mailto:zuliani.alessio@gmail.com)

Name : Alessio Zuliani  
Address :

Calle Sevilla 2A  
14003  
Cordoba  
Spain

Tel : +34617621831  
Fax :  
Email : [zuliani.alessio@gmail.com](mailto:zuliani.alessio@gmail.com)

I am preparing the following work for publication:

Article/Chapter Title : PhD thesis  
Journal/Book Title : MICROWAVE-ASSISTED SYNTHESIS OF NANOCATALYSTS IN BATCH CONDITIONS  
Editor/Author(s) : Alessio Zuliani  
Publisher : Universidad de Cordoba

I would very much appreciate your permission to use the following material:

Journal/Book Title : Green Chemistry  
Editor/Author(s) : Alessio Zuliani, Mario J. Muñoz-Batista, Rafael Luque  
Volume Number : 20  
Year of Publication : 2018  
Description of Material : Microwave-assisted valorization of pig bristles: towards visible light photocatalytic chalcocite composites  
Page(s) : 3001-3007

Any Additional Comments :

I would like to use the paper for my PhD thesis

---

**CONTRACTS-COPYRIGHT (shared)** <Contracts-Copyright@rsc.org> 1 ottobre 2019 14:14  
A: "[zuliani.alessio@gmail.com](mailto:zuliani.alessio@gmail.com)" <[zuliani.alessio@gmail.com](mailto:zuliani.alessio@gmail.com)>

Dear Alessio

The Royal Society of Chemistry (RSC) hereby grants permission for the use of your paper(s) specified below in the printed and microfilm version of your thesis. You may also make available the PDF version of your paper(s) that the RSC sent to the corresponding author(s) of your paper(s) upon publication of the paper(s) in the following ways: in your thesis via any website that your university may have for the deposition of theses, via your university's Intranet or via your own personal website. We are however unable to grant you permission to

I di 3 01/10/2019, 14:22



Gmail - Permission Request Form: Alessio Zuliani

<https://mail.google.com/mail/u/0/?ik=875999074&view=pt&search=a..>

include the PDF version of the paper(s) on its own in your institutional repository. The Royal Society of Chemistry is a signatory to the STM Guidelines on Permissions (available on request).

Please note that if the material specified below or any part of it appears with credit or acknowledgement to a third party then you must also secure permission from that third party before reproducing that material.

Please ensure that the thesis states the following:

Reproduced by permission of The Royal Society of Chemistry

and include a link to the paper on the Royal Society of Chemistry's website.

Please ensure that your co-authors are aware that you are including the paper in your thesis.

Regards

Gill Cockhead

Contracts & Copyright Executive

Gill Cockhead

Contracts & Copyright Executive

Royal Society of Chemistry,

Thomas Graham House,

Science Park, Milton Road,

Cambridge, CB4 0WF, UK

Tel +44 (0) 1223 432134

[Testo tra virgolette nascosto]

[Testo tra virgolette nascosto]

This communication is from The Royal Society of Chemistry, a company incorporated in England by Royal Charter (registered number RC000524) and a charity registered in England and Wales (charity number 207890). Registered office: Burlington House, Piccadilly, London W1J 0BA. Telephone: +44 (0) 20 7437 8656.

The content of this communication (including any attachments) is confidential, and may be privileged or contain copyright material. It may not be relied upon or disclosed to any person other than the intended recipient(s) without the consent of The Royal Society of Chemistry. If you are not the intended recipient(s), please (1) notify us immediately by replying to this email, (2) delete all copies from your system, and (3) note that disclosure, distribution, copying or use of this communication is strictly prohibited.

Any advice given by The Royal Society of Chemistry has been carefully formulated but is based on the information available to it. The Royal Society of Chemistry cannot be held responsible for accuracy or completeness of this communication or any attachment. Any views or opinions presented in this email are solely those of the author and do not represent those of The Royal Society of Chemistry. The views expressed in this communication are personal to the sender and unless specifically stated, this e-mail does not constitute any part of an offer or contract. The Royal Society of Chemistry shall not be liable for any resulting damage or loss as a result of the use of this email and/or attachments, or for the consequences of any actions taken on the basis of the information provided. The Royal Society of Chemistry does not warrant that its emails or attachments are Virus-free; The Royal Society of Chemistry has taken reasonable precautions to ensure that no viruses are contained in this email, but does not accept any responsibility once this email has been transmitted. Please rely on your own screening of electronic communication.

2 di 3

01/10/2019, 14:22

Gmail - Permission Request Form: Alessio Zuliani

https://mail.google.com/mail/u/0?ik=875999074&view=pt&search=a..

More information on The Royal Society of Chemistry can be found on our website: [www.rsc.org](http://www.rsc.org)

This communication is from The Royal Society of Chemistry, a company incorporated in England by Royal Charter (registered number RC000524) and a charity registered in England and Wales (charity number 207890). Registered office: Burlington House, Piccadilly, London W1J 0BA. Telephone: +44 (0) 20 7437 8656.

The content of this communication (including any attachments) is confidential, and may be privileged or contain copyright material. It may not be relied upon or disclosed to any person other than the intended recipient(s) without the consent of The Royal Society of Chemistry. If you are not the intended recipient(s), please (1) notify us immediately by replying to this email, (2) delete all copies from your system, and (3) note that disclosure, distribution, copying or use of this communication is strictly prohibited.

Any advice given by The Royal Society of Chemistry has been carefully formulated but is based on the information available to it. The Royal Society of Chemistry cannot be held responsible for accuracy or completeness of this communication or any attachment. Any views or opinions presented in this email are solely those of the author and do not represent those of The Royal Society of Chemistry. The views expressed in this communication are personal to the sender and unless specifically stated, this e-mail does not constitute any part of an offer or contract. The Royal Society of Chemistry shall not be liable for any resulting damage or loss as a result of the use of this email and/or attachments, or for the consequences of any actions taken on the basis of the information provided. The Royal Society of Chemistry does not warrant that its emails or attachments are Virus-free; The Royal Society of Chemistry has taken reasonable precautions to ensure that no viruses are contained in this email, but does not accept any responsibility once this email has been transmitted. Please rely on your own screening of electronic communication.

More information on The Royal Society of Chemistry can be found on our website: [www.rsc.org](http://www.rsc.org)

## Heterogeneously Catalyzed Synthesis of Imidazolones via Cycloisomerizations of Propargylic Ureas Using Ag and Au/Al SBA-15 Systems

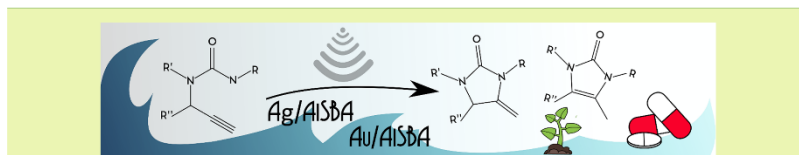
Alessio Zuliani,<sup>†,||</sup> Prabhat Ranjan,<sup>‡,||</sup> Rafael Luque,<sup>\*,†,§</sup> and Erik V. Van der Eycken<sup>\*,‡,§</sup>

<sup>†</sup>Departamento de Química Orgánica, Universidad de Córdoba, Edificio Marie-Curie (C-3), Ctra Nnal IV-A, Km 396, Córdoba, Spain

<sup>‡</sup>Laboratory for Organic & Microwave-Assisted Chemistry (LOMAC), Department of Chemistry, University of Leuven (KU Leuven), Celestijnenlaan 200F, B-3001 Leuven, Belgium

<sup>§</sup>Peoples' Friendship University of Russia (RUDN University), 6 Miklukho-Maklaya Street, 117198, Moscow, Russia

### Supporting Information



**ABSTRACT:** The synthesis of imidazolones through the cycloisomerization of ureas, specifically propargylureas, has gained attention due to the large availability of starting materials. However, this type of synthesis normally requires the utilization of strong bases, such as NaOH, expensive homogeneous metal catalysts, such as Ag-, Au-, and Ru-based systems, or toxic and hazardous chemicals. Herein, a study of different synthetic routes for the preparation of imidazolones through the cycloisomerization of propargylic ureas under fast, mild, and environmentally friendly conditions with heterogeneous catalysis was undertaken. First, the synthesis were carried out under mild conditions using toluene and acetonitrile as solvents. Silver and gold nanoparticles supported on AISBA-15 were used as heterogeneous catalysts. The catalysts were prepared by mechanochemical and microwave-assisted techniques. Sequentially, a range of solvents was replaced by the greener ethanol. Finally, all obtained results were combined in order to carry out the reaction using only water as solvent and promoter of the reaction. Aiming to expedite the procedure, the synthesis were carried out under conventional and microwave irradiation.

**KEYWORDS:** *Heterogeneous catalysis, Microwave chemistry, Isomerization, Mesoporous materials, Amides*

### INTRODUCTION

Imidazolones are well-known compounds widely used in industry for the preparation of different chemicals, agrochemicals, and pharmaceuticals. Indeed, due to the existence of tautomeric forms, they can easily interact with biopolymers and receptors present in living systems, which accounts for the different biological activities.<sup>1</sup> Some substituted imidazolones were found to be herbicides, insecticidal, antifungal, anti-inflammatory, and antitumor agents, while others showed cardiotoxic, antioxidant, vasodilator, and memory-enhancing properties.<sup>2–5</sup> For example, in 2008 Congiu et al. reported imidazole-2-one derivatives as active antitumoral against human cancer cells.<sup>6</sup> More recently, some other imidazolone derivatives were demonstrated to show high hypertensive activity by molecular modeling approaches.<sup>7</sup> Imidazolones have been also proved to be novel ligands for the synthesis of catalytically active complexes with transition metals. Ong and co-workers reported the hydroamination of aminoalkenes with zirconium complexes supported on imidazolones.<sup>8</sup>


As a result, the preparation of substituted imidazolones is gaining more attention day by day. The most studied methods for the preparation of imidazolones include the synthesis from acylloins and ureas;<sup>1</sup> the intramolecular cyclization of ureidoacetals, ureidoxazinanes, and ureido ketones,<sup>9</sup> or the transformations of imidazole derivatives such as imidazolidinediones or imidazole oxides.<sup>10</sup> During recent years, the synthesis of substituted imidazolones from ureas, specifically from propargylureas, as illustrated in Scheme 1, have gained more attention due to the large availability of the starting materials propargylureas and isocyanates.<sup>11</sup> In fact, diverse types of propargylamines can be synthesized in one-pot reactions through A-3 coupling of alkynes, amines, and aldehydes, which are starting material of low economic impact. However, the cycloisomerization of propargylic ureas normally requires the

Received: January 11, 2019


Revised: February 5, 2019


Published: February 8, 2019

Rightslink® by Copyright Clearance Center https://s100.copyright.com/AppDispatchService



# RightsLink®

[Home](#)
[Account Info](#)
[Help](#)




**Title:** Heterogeneously Catalyzed Synthesis of Imidazolones via Cycloisomerizations of Propargylic Ureas Using Ag and Au/Al SBA-15 Systems

**Author:** Alessio Zuliani, Prabhat Ranjan, Rafael Luque, et al

**Publication:** ACS Sustainable Chemistry & Engineering

**Publisher:** American Chemical Society

**Date:** Mar 1, 2019

Copyright © 2019, American Chemical Society

Logged in as:  
Alessio Zuliani  
Account #:  
3001525139

[LOGOUT](#)

**PERMISSION/LICENSE IS GRANTED FOR YOUR ORDER AT NO CHARGE**

This type of permission/license, instead of the standard Terms & Conditions, is sent to you because no fee is being charged for your order. Please note the following:

- Permission is granted for your request in both print and electronic formats, and translations.
- If figures and/or tables were requested, they may be adapted or used in part.
- Please print this page for your records and send a copy of it to your publisher/graduate school.
- Appropriate credit for the requested material should be given as follows: "Reprinted (adapted) with permission from (COMPLETE REFERENCE CITATION). Copyright (YEAR) American Chemical Society." Insert appropriate information in place of the capitalized words.
- One-time permission is granted only for the use specified in your request. No additional uses are granted (such as derivative works or other editions). For any other uses, please submit a new request.

[BACK](#)
[CLOSE WINDOW](#)

Copyright © 2019 [Copyright Clearance Center, Inc.](#) All Rights Reserved. [Privacy statement.](#) [Terms and Conditions.](#) Comments? We would like to hear from you. E-mail us at [customercare@copyright.com](mailto:customercare@copyright.com)

1 di 1

01/10/2019, 14:30

## Efficient and Environmentally Friendly Microwave-Assisted Synthesis of Catalytically Active Magnetic Metallic Ni Nanoparticles

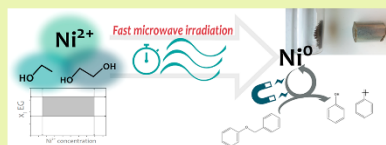
Alessio Zuliani, Alina M. Balu, and Rafael Luque\*<sup>✉</sup>

Departamento de Química Orgánica, Universidad de Córdoba, Edificio Marie-Curie (C-3), Ctra Nal IV, Km 396, Córdoba, Spain

## Supporting Information

**ABSTRACT:** Pure magnetic metallic nickel was synthesized by a simple and fast microwave-assisted method using a monomode microwave reactor. Nickel chloride was employed as metal precursor, while an environmental-friendly mixture of ethylene glycol and ethanol was simultaneously used as solvent and reducing agent. The parameters combination, for the occurrence of the reaction, of the mixture molar fraction, and the metal precursor concentration was developed. The influence of the temperature and the time of the irradiation was investigated. The best performance (71% yield) was achieved at 250 °C in 5 min of microwave irradiation. The phase and the morphology of the metal were analyzed by X-ray diffraction, scanning emission microscopy, and transmission electron microscopy, while the surface area was determined by nitrogen physisorption. The material exhibited a strong magnetic behavior. The metallic nickel showed high catalytic activity for the hydrogenolysis of benzyl phenyl ether, a lignin model compound, in a microwave-assisted environmental-friendly reaction.

**KEYWORDS:** Microwave chemistry, Nickel, Magnetic nanoparticles, Heterogeneous catalysis, Benzyl phenyl ether



## INTRODUCTION

Magnetic nanostructured materials have attracted significant interest due to their technical application in several fields including optoelectronics, magnetics, catalysis, biologic engineering, information storage, and photovoltaic technology.<sup>1–3</sup> Nickel nanoparticles are particularly emerging because of their unique characteristics such as high magnetism, high surface area, large surface energy, excellent chemical stability, low melting point, resource-richness, and low cost.<sup>4,5</sup> Several techniques for the synthesis of nickel materials, including thermal decomposition, pulsed laser ablation, sputtering, and metal vapor condensation have been extensively reported in the literature.<sup>6–9</sup> However, only a few reports on the synthesis of pure Ni magnetic nanoparticles are available.<sup>10–12</sup>

Microwave-assisted reactions have emerged as alternative reaction media to conduct catalytic processes especially in nanomaterials synthesis. The advantages of this technique include the possibility to obtain higher yields, different selectivities, and the potential to accomplish reactions/chemistries that generally do not take place under conventional heating conditions.<sup>13–15</sup>

On the basis of our experience in microwave chemistry for the design of nanomaterials and nanoparticle systems,<sup>16–20</sup> herein we disclose a simple, efficient, and environmentally friendly unprecedented synthesis of magnetic metallic nickel (denoted as MMN) under microwave-assisted conditions, employing a mixture of ethylene glycol (EG) and ethanol, and NiCl<sub>2</sub> as metal precursor. The so-produced nickel nanoparticles were used as a heterogeneous catalyst for the

hydrogenolysis of benzyl phenyl ether (BPE), a commonly used lignin model compound.<sup>21,22</sup>

## RESULTS AND DISCUSSION

The powder X-ray diffraction (PXRD) pattern of MMN is shown in Figure 1. The peaks at 44.5°, 51.9°, and 76.4° can be

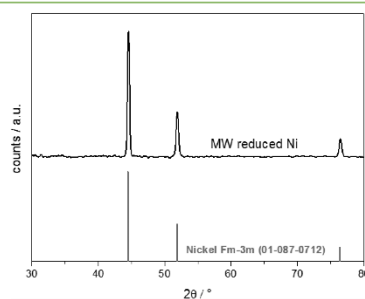



Figure 1. Powder X-ray diffraction of the MMN.

Received: August 24, 2017


Revised: October 6, 2017


Published: October 27, 2017

Rightslink® by Copyright Clearance Center https://s100.copyright.com/AppDispatchService



# RightsLink®

[Home](#)
[Account Info](#)
[Help](#)




**Title:** Efficient and Environmentally Friendly Microwave-Assisted Synthesis of Catalytically Active Magnetic Metallic Ni Nanoparticles

**Author:** Alessio Zuliani, Alina M. Balu, Rafael Luque

**Publication:** ACS Sustainable Chemistry & Engineering

**Publisher:** American Chemical Society

**Date:** Dec 1, 2017

Copyright © 2017, American Chemical Society

Logged in as:  
Alessio Zuliani  
Account #:  
3001525139

[LOGOUT](#)

**PERMISSION/LICENSE IS GRANTED FOR YOUR ORDER AT NO CHARGE**

This type of permission/license, instead of the standard Terms & Conditions, is sent to you because no fee is being charged for your order. Please note the following:

- Permission is granted for your request in both print and electronic formats, and translations.
- If figures and/or tables were requested, they may be adapted or used in part.
- Please print this page for your records and send a copy of it to your publisher/graduate school.
- Appropriate credit for the requested material should be given as follows: "Reprinted (adapted) with permission from (COMPLETE REFERENCE CITATION). Copyright (YEAR) American Chemical Society." Insert appropriate information in place of the capitalized words.
- One-time permission is granted only for the use specified in your request. No additional uses are granted (such as derivative works or other editions). For any other uses, please submit a new request.

[BACK](#)
[CLOSE WINDOW](#)

Copyright © 2019 Copyright Clearance Center, Inc. All Rights Reserved. [Privacy statement](#). [Terms and Conditions](#). Comments? We would like to hear from you. E-mail us at [customercare@copyright.com](mailto:customercare@copyright.com)

1 di 1

01/10/2019, 14:35



